DESIGN OF RECONFIGURABLE MICROSTRIP ANTENNAS FOR WIDEBAND APPLICATIONS

Thesis Submitted in fulfilment of the Requirements for the Degree of

DOCTOR OF PHILOSOPHY

IN

PHYSICS AND MATERIAL SCIENCE

BY

ACHYUT SHARMA

DEPARTMENT OF PHYSICS AND MATERIAL SCIENCE

JAYPEE UNIVERSITY OF INFORMATION TECHNOLOGY

WAKNAGHAT, SOLAN (173234), HIMACHAL PRADESH

INDIA

JULY 2025

JAYPEE UNIVERSITY OF INFORMATION TECHNOLOGY
(Established by H. P. state Legislative vide Act No. 14 of 2002)
Waknaghat P. O. Dumehar Bani, Kandaghat, Distt. Solan – 173234 (H. P.) INDIA
Website: www.juit.ac.in
Phone No. (91) 01792 -257999(30 lines)
Fax: (91)01792 245362

DECLARATION BY THE SCHOLAR

I hereby declare that the work reported in the Ph.D. thesis entitled **"Design of Reconfigurable Microstrip Antennas for Wideband Application"** submitted at **Jaypee University of Information Technology, Waknaghat, Solan (H.P.) India** is an authentic record of my work carried out under the supervision of **Prof. Sunil Kumar Khah** and **Dr. Sanyog Rawat**. I have not submitted this work elsewhere for any other degree or diploma. I am fully responsible for the contents of my Ph.D. thesis.

Mr. Achyut Sharma

Enrollment No. 186906

Department of Physics and Material Science
Jaypee University of Information Technology
Waknaghat, Solan, H.P. India-173234

JAYPEE UNIVERSITY OF INFORMATION TECHNOLOGY
WAKNAGHAT, P.O. - WAKNAGHAT
TEHSIL - KANDAGHAT, DISTRICT - SOLAN (H.P.)
PIN - 173234 (INDIA) Phone Number : +91-1792-257999
(Established by H.P. State Legislature Vide Act No. 14 of 2002)

Date: 16/7/25

Certification by the Supervisors

This is to certify that the work reported in the Ph.D. thesis entitled "**Design of Reconfigurable Microstrip Antennas for Wideband Applications**" submitted by **Achyut Sharma** (Enrolment No. 186906) in the fulfillment for the award of degree of Doctor of Philosophy in Physics and Materials Science at Jaypee University of Information Technology, Waknaghat, Solan (H.P.) India is a bonafide record of his original work carried out under our supervision. This work has not been submitted partially or wholly to any other University or Institute for the award of any other degree or diploma.

Prof. Sunil Kumar Khah

Department of Physics & Material Science
Jaypee University of Information Technology
Waknaghat, Solan, Himachal Pradesh-173234, India

Dr. Sanyog Rawat

Associate Professor
Department of Electronics & Communication Engineering
Central University of Rajasthan
Bandar Sindri, Ajmer, Rajasthan-305817, India

Acknowledgement

*The expedition of my Ph.D. has come to a close thanks to the serendipitous gift of **Lord Shiva** and my soul is filled with gratitude to each individual who has lent a helping hand in the form of support, belief, and efforts to complete my journey to this moment.*

*I would like to express my sincerest gratitude and deepest appreciation to my supervisor **Prof. Sunil Kumar Khah**, Department of PMS, JUIT Waknaghat and co-supervisor **Prof. Sanyog Rawat**, Department of ECE, C.U. Rajasthan, for their encouragement, guidance, advice and constant support during my PhD study. This thesis would not have been possible without their invaluable technical insight and continual guidance. Also, I am grateful to **Prof. P.B. Barman**, (HOD, Department of Physics and Material Science) for his support, cooperation and providing desired facilities within the department to carryout experimentation.*

*I pay my sincere thanks to **Mr. Jai Prakash Gaur** (JUIT Founder), JUIT administration, **Prof. (Dr.) Rajendra Kumar Sharma** (Vice Chancellor), **Prof. (Dr.) Sudhir Kumar** (Dean, Research and Internationalization), **Brigadier R. K. Sharm**a (Registrar) and the JUIT administrations for providing essential amenities, research funding and infrastructure for pursuing the research work.*

*I would like to express my sincere gratitude to **Dr. Surajit Hazra**, **Dr. Sanjiv Kumar Tiwari**, and **Dr. Saurabh Srivastava,** members of my Doctoral Progress Monitoring Committee (DPMC) for their invaluable assistance, insightful comments, and innovative recommendations during this work. Also, I'd like to thank the faculty of the Department of Physics and Material Science for their help and collaboration during my work. I am also grateful to Laboratory and Library Staff of the University for their support and sharing their lifelong experiences that enlighten me during the chaotic moments of my journey.*

I treasure every time I spent at JUIT, and I owe a debt of gratitude to my friends for making it possible. I would like to convey my heartfelt gratitude to Mayank Gupta, Dr. Sumit Singh Dhanda, Dr. Ratnadeep Roy, Dr. Ashwini Yadav, Vinod Sharma, Amit Chourasiya, Dr. Archek Praveen, Dr. Sandesh Reddy, Dr.Tapan Nahar, Dr. Pallav Rawal, Dr. Jonny Dhiman, Dr. Ratish, Dr.

Deepak Sharma, Dr. Rahul, Dr. Anjali, Dr. Manju Rana, Dr. Neeru Singla, Dr. Rajesh Yadav, Dr. Rajat, Sunny, Kalpana, Sweta Singh, Kamesh, Praduman, Rekha, Shivani, Aisha, Vishal, Neha and Ph.D friends of the JUIT, who are not just my superiors or colleagues, but also friends who have been by my side through rough and tough times. Their support during my journey of research strengthens me to complete my work with great enthusiasm.

Finally, I take this opportunity to thank my family – my mother, who was my first teacher and established the foundations of my education, my sister Aditi Sharma and my maternal uncles, who always helped and supported me. Last but not least, my heartfelt thanks go to my wife, Vartika for her love, support, and understanding throughout this long journey, which was not easy but exciting, that is for sure, for both of us. Thanks for believing in me, encouraging me when I was down and allowing me the space to reach this far. More than for anything else, I thank you for taking all my responsibilities on your shoulders and looking after our lovely baby, Bhavya Sharma.

In the end I also thankful and pay regards to those persons whom I am not able to mention here, although they are not forgotten and will always value for their role in this voyage.

Achyut Sharma

TABLE OF CONTENTS

LIST OF ABBREVIATIONS

2D	Two Dimensional
3D	Three Dimensional
AR	Axial Ratio
AUT	Antenna Under Test
BW	Bandwidth
CP	Circular Polarization
CPW	Co-planar Waveguide
CST	Computer Simulation Technology
DGS	Defected Ground Structure
EBG	Electronic Band Gap
EM	Electromagnetic
FBW	Fractional Bandwidth
FCC	Federal Communication Commission
FDTD	Finite Difference Time Difference
FET	Field Effect Transistor
FSS	Frequency Selective Surface
GPS	Global Positioning System
GSM	Global System for Mobile Communication
IEEE	Institute of Electrical and Electronics Engineers

ISM	Industrial, Scientific and Medical
LP	Linear Polarization
LHCP	Left Hand Circular Polarization
LTE	Long Term Evolution
MEMS	Microelectromechanical System
MIMO	Multiple Input Multiple Outpu
PCB	Printed Circuit Board
RF	Radio Frequency
RHCP	Right Hand Circular Polarization
SAR	Specific Absorption Rate
SRR	Split Ring Resonator
UWB	Ultra Wideband
VNA	Vector Network Analyzer
vs.	Versus
VSWR	Voltage Standing Wave Ratio
Wi-Fi	Wireless Fidelity
WiMAX	Worldwide Interoperability for Microwave Access
WLAN	Wireless Local Area Network

LIST OF FIGURES

LIST OF TABLES

LIST OF PUBLICATIONS

1 **A. Sharma**, S. Khah and S. Rawat, "Design of slot loaded Y- Shaped Antenna for WLAN/Wi-Max Bands", *Scientia Iranica,* vol. 31, no. 17, pp. 1556 – 1566, 2022, doi.10.24200/SCI.2022.59299.6163

2 **A. Sharma**, S. Khah and S. Rawat, "Annular rings antenna for WiMAX and WLAN application with frequency and polarization diversity", *Evergreen journal of Novel carbon resource sciences and green asia strategy*, vol. 11, no. 4, pp. 3156 – 3163, 2024, doi: 10.5109/7326953

3 J. Dhiman, **A. Sharma** and S. Khah, "Shared Aperture Microstrip Patch Antenna Array for L and S-Bands", Progress in Electromagnetics Research Letters, vol. 86, pp. 91–95, 2019, doi: 10.2582/PIERL19052905

4 **Achyut Sharma**, Sunil Khah and Sanyog Rawat, "An open annular ring antenna for WiMAX /WLAN band with frequency, polarization and pattern diversity", accepted in Physica Scripta, doi: https://doi.org/10.1088/1402-4896/aded45

CONFERENCES/ WORKSHOP

1 **A. Sharma**, J. Dhiman, S. Rawat and S. Khah, "A frequency reconfigurable X-shaped antenna for WiMAX/WLAN band", 2022 Int. Conf. for Advancement in Technology (ICONAT) Goa, 2022.

2 Attended International conference on Transforming Lives Through Adoption of SDGS: Role of Higher Education Institutions (TLASH -2024) at GD Goenka University, Gurugram From May 30 – 31, 2024.

3 Attended one week faculty development program on **Antenna Trends** at MNIT Jaipur from July 1 – 5, 2019.

ABSTRACT

In wireless communication systems, antennas are pivotal element for transmitting and receiving signals as electromagnetic waves. Conventionally, antenna geometry is optimized for particular frequencies, polarizations or radiation patterns. Nonetheless, the recent development and deployment of multiple wireless standards has enabled the faster connectivity and large volume of data exchanged between portable devices and owes to the exponential growth of wireless communication in recent times. The abovesaid motivates the antenna researcher to investigate and develop novel, compact, multiband, multimode and feature rich devices that are suitable for adapting in fast changing requirements for communication standards in the next and currently developing generation of wireless communications known as 5G, hence influences the hardware design process including antenna and front end in portable gadgets.

Reconfigurable antennas have drawn a lot of research attention in next generation wireless communication systems due to their dynamic adaptability in changing environment conditions or system requirements and greatly enhances its usability and versatility. On the account of adaptive design, reconfigurable antennas are preferred over multiple fixed performance antennas, as they ensures miniaturization, boosted bandwidths, affordability, simplifies system integration etc., and enables multiple wireless services in single device. The reconfiguration can be achieved by altering the electrical current on antenna's structure through several techniques like geometric variation, electrical switches or tuners, modification in material characteristics and optical switches.

But the use of these techniques results in non-uniform /inconsistent performances of RA under variable frequencies, patterns and polarizations and also engagement of numerous feeding and impedance matching networks and regulating mechanisms raises its volume with govern complications. The RA ideas are established with the intention of circumventing complex feed network, lossy biasing arrangements and avoid the use of multiple antennas for multi-functionality, thus facilitating the miniaturization of antenna system configuration with even results for all probable changeable states. Reconfigurable antennas are broadly classified in single characteristic tunable antenna and hybrid reconfigurable antennas. Here, two or more tunable antenna characteristics are integrated simultaneously in single antenna element without much affecting their individual operations. As the communication environment become more complex nowadays, so hybrid antennas are preferred as they bring versatility to antenna

systems in various wireless scenarios. In this context, novel PIN diodes loaded hybrid reconfigurable antennas with wide performance range are proposed in this thesis.

The first chapter of this thesis proposed a Y – shaped patch antenna with DGS for WiMAX and WLAN band application. Here, initially designed UWB antenna is modified into triple band (One WiMAX and two WLAN bands) antenna by incorporating two hook shaped slits of optimized dimensions at suitable position on the ground element. The prototyped antenna structure realized the wide band impedance of 24 % with omnidirectional radiation pattern at lowest frequency and bidirectional radiation pattern at other remaining frequencies.

The remaining two chapters in this thesis, discussed the compound (hybrid) reconfigurable antenna designs by integrating two or more functionalities in single element antenna by utilizing electrical switching elements. By integration, we mean that a portion of antenna is shared among other antenna elements to achieve the desired reconfigurable functionality. This strategy might be suitable in designing multimode wireless terminals with modest antenna footprints. The optimization procedure (parametric study) including a study of relevant design parameters is also presented.

The frequency and polarization reconfigurable antenna have many advantages like efficient spectrum utilization by frequency reuse, minimizing multipath fading with increased system capacity and can be utilized in emerging wireless communication system like cognitive radio (CR) etc. In chapter 2, a circular rings antenna with integrated frequency agility and polarization diversity is discussed. Here, circular polarization was realized by extruding a horizontal slit below one ring on the ground plane. While the loading or unloading of an arc on another ring via PIN diodes changes current distribution on suggested structure, which provides the swapping between linear and circular polarization state in WLAN band, this also changes the effective electrical length which in turn gives the frequency reconfiguration between WiMAX and WLAN band.

Pattern reconfigurable antennas are preferred for a variety of uses including RADAR, remote sensing, mobile and satellite communication and etc. As they enhance the antenna performances by steering antenna beam in desired direction and improving the signal-to-noise (SNR) in noisy environment. Chapter 3 reported a multi-functional reconfigurable antenna concepts that integrate frequency tunability, polarization diversity and pattern reconfigurability with very few switching elements. Here, initially designed UWB antenna is modified into

frequency – polarization – pattern reconfigurable antenna via loading or unloading of stubs on ground plane via PIN diodes. The antenna can reconfigure between dual (WiMAX, WLAN) and single (WLAN) band, polarization switching between circular and linear state in WLAN band with 0.13 GHz ARBW and pattern reconfiguration of WLAN band between -55° to -90° for different states of PIN diodes.

The electromagnetic simulator is used to foresee the performance of reported antennas with experimental validation of prototyped in the measurement lab. To verify the idea and design performance, the described antennas are correlated with other antennas that have been presented for comparable uses. The demonstrated antenna concepts and outcomes can be used as design thoughts when creating new reconfigurable antenna (or antenna array) designs for upcoming communication systems for different frequency bands, provided that appropriate switching/tuning gears are available in the desired operating bands.

CHAPTER 1

INTRODUCTION

INTRODUCTION

1.1 Background

The substantial growth of wireless communication technology over the last few years has changed people's life activities in all sorts of useful ways. The recent advances in wireless systems not only revolutionized the telecommunication industry, but also brought significant changes in healthcare, medical diagnosis medication, automotive production and industrial remote monitoring systems, etc. The development in emerging technologies have led to the development of different wireless standards (technologies) like Bluetooth, global positioning systems (‘GPS’), wireless fidelity (‘Wi-Fi’), worldwide interoperability for microwave access (‘WiMAX’), wireless local area network (‘WLAN’), universal mobile telecommunication service (‘UMTS’), Cognitive Radio etc. These technologies are expected to progress in future to cater the increased number of end users, their needs and to decongest the spectrum. The deployment of emerging communication technologies requires innovative and versatile devices equipped with the new standards of mobile communication, capable of supporting the large amount of data exchange between devices at very high speed with low latency. The devices require antenna and associated radio frequency (RF) circuitry with specific characteristics to support the multiple service.

In wireless communication networks, antennas are a critical and indispensable component for receiving or transmitting the signal. Antenna is a time invariant device and it transforms the electrical signals into electromagnetic (EM) waves to radiate (transmit) or receive the information [1]. Recently, the emergence of the wireless communication industry has led antenna designers to develop new antenna designs for numerous target applications such as sensing, navigation, imaging, short/long range communication, mobile application, biomedical application, etc. Broadly antennas are divided into many categories on the basis of antenna structure, operating principle or feeding mechanism, including monopoles / dipoles, loop antennas, slot/ horn antennas, microstrip patch antennas, log periodic, helical, dielectric/lens and waveguide based antennas have been explored in the literature [2–9]. The inherent merits and demerits of each antenna type helps to determine their suitability for any particular applications.

The rapid surge in wireless communication has led to the demand of a physically, economically viable and technically compatible antenna that can support multiple wireless standards with simultaneous miniaturization of mobile units. The microstrip antennas [10] are widely used for this purpose, as they offer multiple advantages like low profile, planar, conformal, light weight, easy to fabricate, efficient radiation, easy integration with other microwave devices over the conventional antennas. Nowadays, the majority of antennas used in wireless platforms or communication systems have static or fixed antenna characteristics (frequency, polarization and radiation pattern) and may be utilized for single services only. However, the usage of multiple static antennas in a single device for supporting multiple standards can enhance the productivity and ease of communication leading to a number of issues like increased system size, interference among adjacent antenna elements, control complexity and huge installation cost. Thus, fixed characteristics of static antennas limit the overall performance of the transceiving system. Futuristic wireless communication techniques requires a smart and multifunctional antenna systems that can adapt their characteristics accordingly to changing system requirements [11–14].

Furthermore, because wireless-based services across different segments are changing so quickly, it becomes more difficult to deliver more services without increasing the system complexity, number of antenna elements, and device size. The current and future communication technologies will redefine connectivity and present new technologies in order to manage enormous data needs, rapid connectivity, seamless communications and data services. Owing to the demands of existing and imminent wireless systems, it is crucial to conceptualize, design and develop antennas having flexible and manageable features. Due to their adaptability for changing conditions, the antennas with reconfigurable frequency, radiation, and polarization characteristics become a promising and practical solution [15–16]. They can help overcome the limits imposed by many single-functional or fixed (static) performance antennas and also improves system efficiency with enhanced functionalities. Also, the additional functionalities offered by reconfigurable antennas can be used in variety of applications like spectrum sensing, security, throughput maximization and managing multipath interference [17–23].

1.2 Overview of the Reconfigurable Antennas

Reconfigurable antennas have gained much attention after Schaubert patented the first frequency and polarization agile antenna design [24] in 1983. From IEEE Standard Definitions [1] of 2014 release, reconfigurable antenna is defined as an antenna 'capable of changing its performance characteristics (resonant frequency, radiation pattern, and polarization) by mechanically or electrically changing its architecture'. The working mechanism involves a controlled and reversible distribution of surface current or electric field on radiating structure with the help of active or passive components that produces the reversible antenna characteristics [15], [25]. Thus, a reconfigurable antenna is a one-of-a-kind device that can acquire the radiation performance of a multi-antenna system by utilizing dynamically adjustable geometry. In this situation, antenna design optimization for specific requirements should attempt to improve system effectiveness and power efficiency by removing superfluous additional radiating components.

1.2.1 Classification of Reconfigurable Antennas

Based on the number of integrated reconfigurable parameters, the reconfigurable antennas are broadly classified in two types (i) Reconfigurable antenna with single tunable parameter (ii) Hybrid or Compound or Multi-parameter Reconfigurable antenna as presented in figure 1.1. On the basis of tunable properties, antennas are termed as frequency reconfigurable, pattern reconfigurable and polarization reconfigurable antenna.

In compound reconfigurable antennas, two or more antenna characteristics are integrated and controlled simultaneously without affecting their individual operations. These antennas are classified as 'frequency – polarization', 'frequency – pattern', 'polarization – pattern' and 'frequency – pattern – polarization' reconfigurable antennas. The conceptual presentation of basic three reconfigurability types are presented in below figure 1.2.

(a) Frequency Reconfigurable Antennas: The antenna geometry exhibits the capability of tuning its operating frequencies either by smooth transition or discretely within the control range is termed as frequency reconfigurable antenna. The basic principle for frequency reconfigurability involves the change in effective electrical length of antenna by different tactics like impedance loading, switching, material property tuning, etc. [27–29]. The dynamic frequency switching attribute gives frequency selectivity to these antennas for filtering out interference.

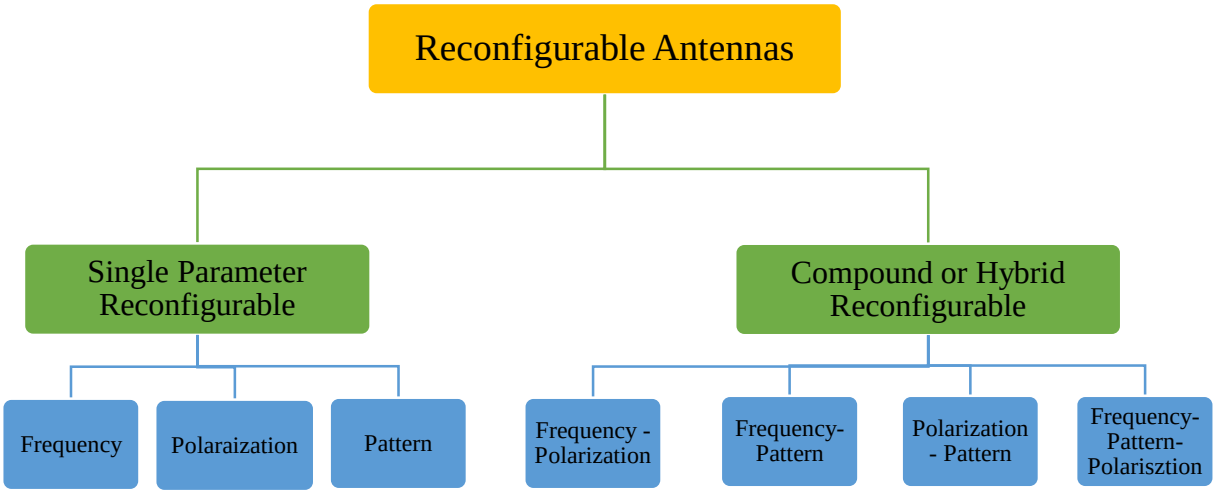

Figure 1.1 Classification of reconfigurable antennas

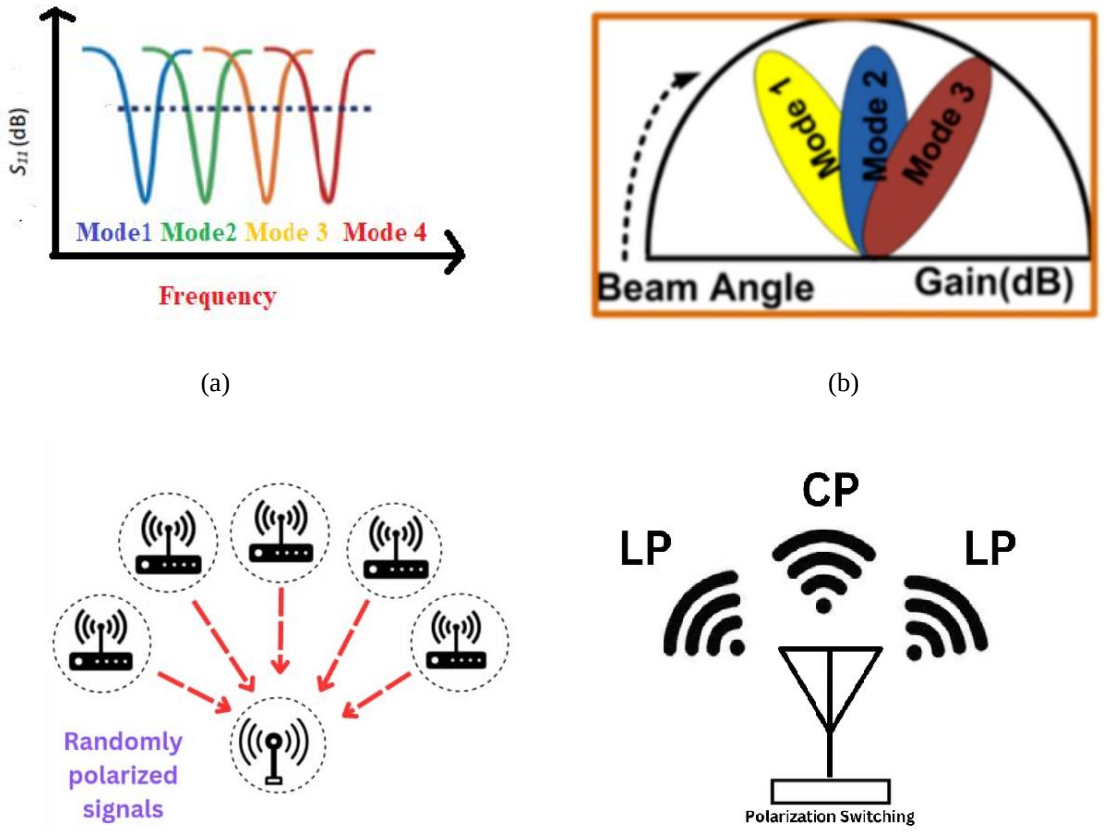

Figure 1.2 Reconfiguration categories [26] (a) frequency reconfiguration (b) pattern reconfiguration (c) polarization reconfiguration

(b) Polarization Reconfigurable Antennas: The orientation of the E – field vector or current flow direction on the radiating structure determines the polarization state of the radiated wave in the far-field of the antenna. Any alteration on antenna structure, material property and feed configuration have changed the direction of current flow or electric field vector on antenna structure provides the polarization reconfigurability. The polarization reconfiguration involves the switching between in different states of linear polarization like vertical or horizontal or any other orientation, left hand or right hand in circular polarization and in between linear and circular polarization [30]. The polarization reconfiguration gives the immunity against interfering signals, minimizes the polarization miss-match loss and boosts the signal reception for portable devices.

(c) Pattern Reconfigurable Antenna: An antenna that can change its radiation pattern in terms of shapes, beam direction, beamwidths etc. over a frequency range in any direction is categorized as pattern reconfigurable antenna [31-32]. The purposefully alteration in charge distribution on radiating geometry by movable structures, switchable parasitic elements and reactive loading provides reconfiguration in radiation pattern. Beam steering and null scanning are accomplished with the pattern reconfigurable antennas. The gain of antenna can be maximized by directing the maximum radiation in intended direction and retain a steadfast link with portable gadgets.

(d) Compound or Hybrid Reconfigurable Antenna: Here, multiple reconfigurable characteristics are integrated in a single antenna geometry and controlled by different means with minimal or no disturbances on the other characteristics. Thus, individual control of multiple parameters in a single entity makes it very effective in a fast changing communication atmosphere. Also, they present a viable substitutes for minimizing complexities of diversity methods [15], [33].

1.3 Overview of Design Methods for Reconfiguration Operations

The antenna with a single reconfigurable characteristic can be realized by a number of design methods. The design methods for realizing reconfigurability in microstrip antennas are divided into following electrical, optical, physical and material reconfigurations categories of [34– 35], which are further sub-divided in various types as depicted in figure 1.3.

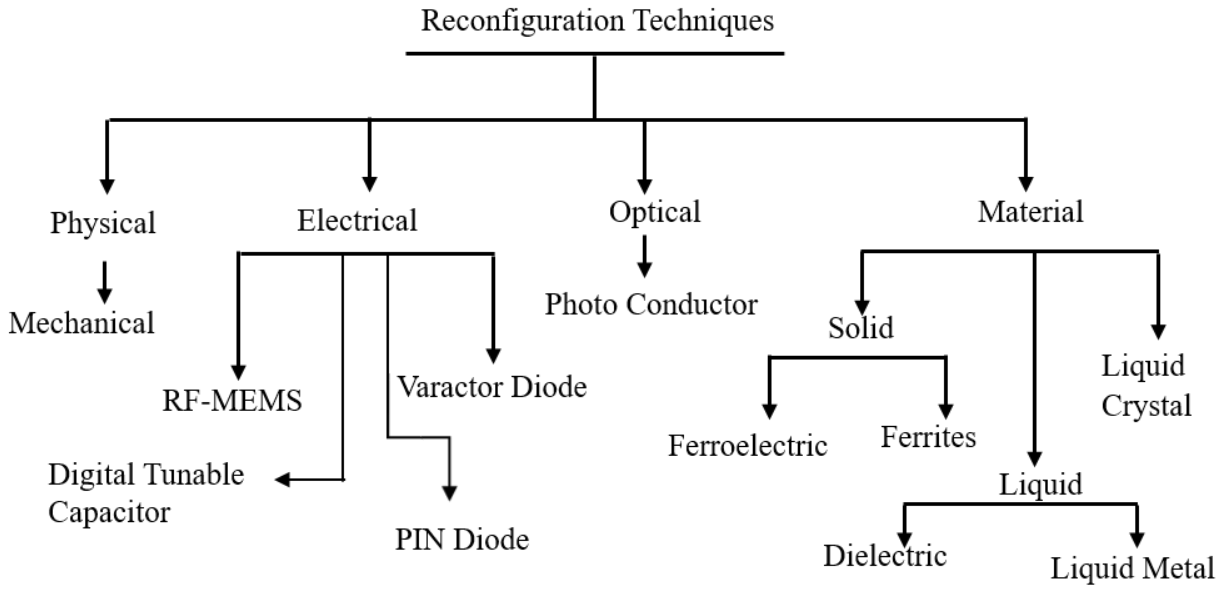

Figure 1.3 Classification of antenna reconfiguration techniques [34]

The implementation of compound reconfiguration in a single antenna requires careful design strategies so that they do not hinder each other during antenna operations. Generally two design approaches are used for achieving the multi – parameter reconfiguration characteristics. The first method involves the integration of multiple reconfigurable elements by utilizing different methods. The second method involves the reconfigurable aperture or pixel antennas to achieve the hybrid reconfiguration in a single entity. Here, the radiating surface is divided into small sections or pixels and RF switches are used for interconnection between adjacent pixels [36]. The activation of suitable RF switches reshaped the radiating surface into various configurations for realizing the compound reconfiguration.

The physical method involves the movement or mechanical adjustment of radiating elements in antenna structure for various reconfiguration operations. In electric tuning, different kinds of switches like p-i-n diodes, radio frequency microelectromechanical systems (‘RF–MEMS’) and varactor diodes are utilized in electrical tuning methods to redirect the surface current for realization of different reconfiguration characteristics. In optical switching, photoconductive switches utilize the light signals for reconfiguration operation, thus eliminating the need of electrical wires. Finally smart materials such as ferrites, ferroelectric, liquid metal, liquid dielectrics and liquid crystals [37–38] are utilized to achieve different reconfiguration operations. The advantages and disadvantages [39] of these approaches are summarized in Table 1.1.

Table 1.1 Advantages and disadvantages of the reconfiguration methods

S. No.	Techniques	Advantages	Disadvantages
1	Electrical	• Fast Tuning Speed • Low Cost • Compatible for Integration	• Insertion Loss • Requires DC lines • Reduced Antenna Efficiency
2	Physical	• No biasing lines • High Power Handling capacity • Low Losses • Continuous Tuning • Suitable for high frequency	• Very slow Response time • Bulky & Complicated Structure • Small life cycle due to wear-and-tear
3	Optical	• No biasing lines	• Bulky • Complex switch activation • Slower switching compared to electrical
4	Material	• Antenna miniaturization due to high value of permittivity and permeability	• Complex biasing network • High DC power consumption • Low Antenna efficiency

1.3.1 Components for Electrical Tuning

In reconfigurable operation modes, the interface amid radiating and reconfiguration element is very critical to obtain the best impedance matching with anticipated pattern attributes. The antenna design must contain a reconfigurable element with controllable attributes to regulate

its operating conditions of governing surface current dispersal for pattern and impedance matching aspects, so it needs to be applied to the antenna geometry with care.

The electrical tuning is widely used reconfiguration methods in comparison to other techniques owing to easy access and many advantages of tuning components make it attractive for real implementations. The electrical tuning components including PIN diodes, varactor diodes, digital tunable capacitor (DTC) and RF-MEMS switches are of low cost, very high switching speed, easy access, compatible and easy integration and having very good electrical characteristics. Depending upon the design complexity, besides advantages they also have various disadvantages like inclusion of extra circuit elements, DC power network and biasing lines may disturb the beam pattern which reduces the antenna proficiency by adding losses to the antenna system. A comparative study on advantages and disadvantages of different electrical tuning component [16], [34], [39] is presented in Table 1.2.

Table 1.2 Comparison of different electrical switching elements

Characteristics	**PIN diode**	**RF-MEMS**	**Varactor**
Operation	• ON state (Forward DC bias) • OFF state (Reverse DC bias)	• ON and OFF state controlled by mechanical movements	• Variable capacitor by biasing DC voltages
Function	Discrete Switching	Discrete Switching	Continuous Switching
Biasing DC voltage	Low (around 1V)	High (20 – 100 V)	Moderate (0 – 30 V)
Tuning Speed	Fast (nsec scale)	Low (μsec scale)	Fast (nsec scale)
Power Consumption (mWatt)	Low (5 -100)	Extremely Low (< 0.1)	Moderate (around 250)
Loss	Low	Extremely Low	Moderate
Cost	Extremely Low	High	Low
Reliability	Excellent	Poor	Excellent

The RF tunable components such as PIN diodes, DTC and RF-MEMS produces the discrete frequency response, while the reverse biasing of varactor diodes generates the continuous frequency switching within the tunable range. As each electrical tuning component has unique features makes them suitable for distinct applications. The PIN diodes are generally used for designing reconfigurable antennas below 10 GHz frequency band, because of low cost, high reliability, faster switching speed and minimal insertion loss features. While above 10 GHz, losses in PIN diodes increases drastically and isolation deterioration at the same time restricts the use of PIN diodes at higher frequency. The RF-MEMS utilizes the mechanical force (microelectromechanical movement) to achieve the short or open circuit effect so that performance can be maintained throughout a wide frequency range, thus making it a good substitute for PIN diodes in high frequency applications. Although RF-MEMS are expensive and need high DC biasing voltages during operation, they are used in reconfigurable antenna designs for Ku bands. The digital tunable capacitor can adjust their capacitance via altering properties of the material between plates via electronic signal, which results in fast and fine adjustment of resonant frequency within the wider band. Apart from PIN diode and MEMS switch, another element i.e. varactor diode can be used for electrical tuning. The varactor diode achieves smooth tuning through steady variation of capacitance by changing the bias voltage in continuous manner unlike discrete tuning obtained from remaining switching elements. This capability is particularly useful for applications like beam steering, frequency sweeping, beamwidth shaping, and other similar tasks. Although many reconfigurable antenna designs have been implemented by utilizing electrical tuning methods, still there is much scope for us to explore.

1.4 Applications of Reconfigurable Antennas

The reconfigurable antennas with multiple functionalities found their utilization in present and emerging wireless communication systems. An overview of various prospective applications are presented below.

1.4.1 Frequency Reconfigurable Antennas

A number of single or multi band antennas [40–44] are incorporated in a single device to handle a variety of communication protocols for access to the different wireless services and thus occupy a huge chunk in space constrained portable devices as shown in figure 1.4(a). The

frequency switching antenna is particularly suited in substituting multiple static antennas, since it would reduce the overall size of the system and fulfill several requirements to meet compactness and portability [28], [45–46]. Apart from this, they can also be used for replacing the conventional wideband antennas that cover all frequency channels in multi-channel communication systems.

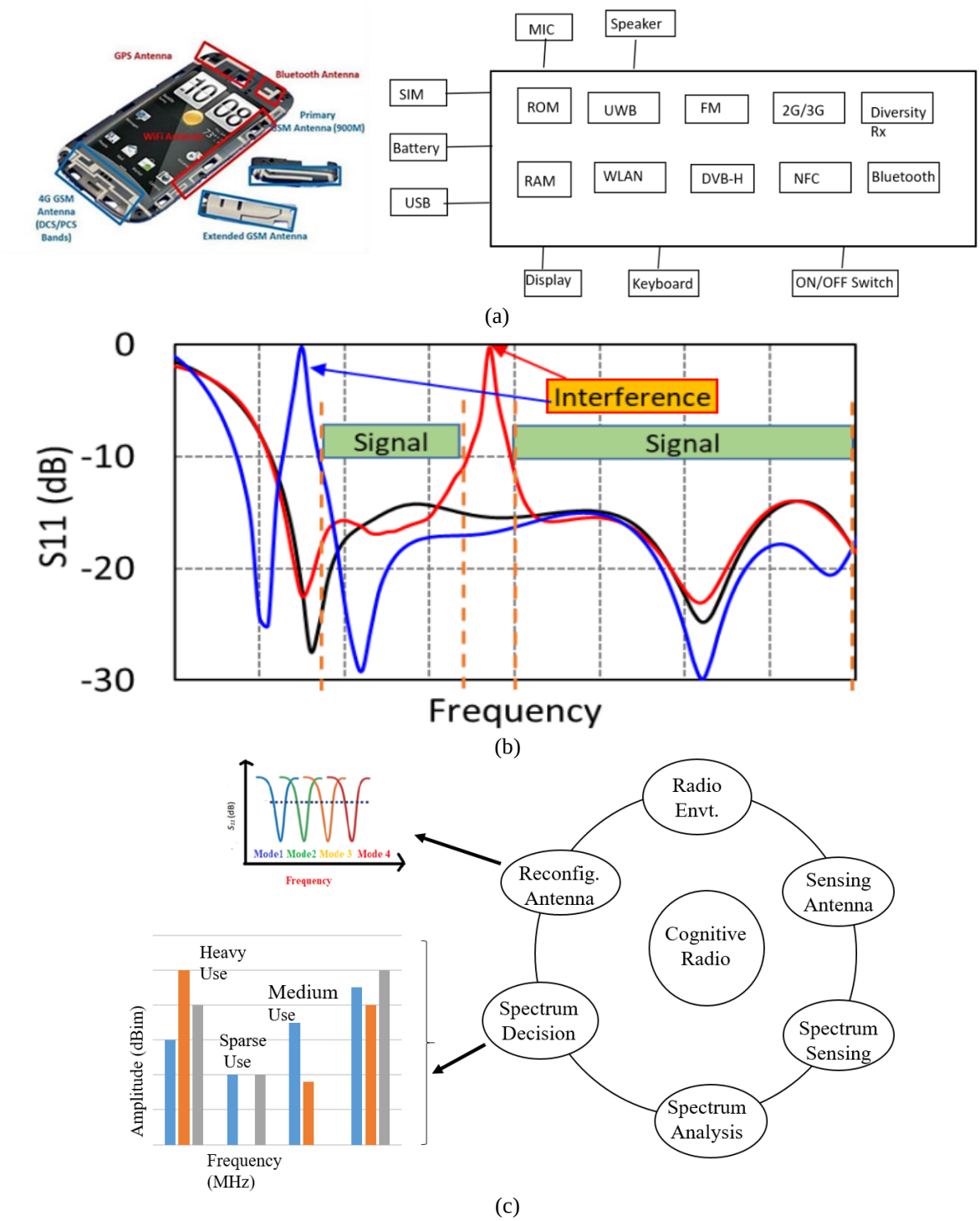

Figure1.4 Applications of frequency reconfigurable antennas (a) multiple antennas in portable devices [45], [53] (b) interference rejection (c) cognitive radio (CR) platform for spectrum sensing [54]

Figure 1.4(b) illustrates how the frequency agile antennas may also be used for interference rejection. By purposefully making band notches in the antenna's frequency response, the interference signals from nearby bands are reduced or eliminated. Filtering is necessary to prevent congestion in wideband applications where several communication channels overlap. This approach lessens the requirement for extra filters that are employed at different phases of a communication system [47–49].

In addition to above, frequency reconfigurable antenna plays a vital role in recently developed cognitive radio systems. The CR transceivers decide the spectrum allocation and adjust the frequency channel to operate within a free or unused band based on the current spectrum allocation, usage, and available (white spaces) channel behaviour. This allows them to conduct concurrent communications and enhance radio operating performance. Figure 1.4 (c) illustrates how frequency reconfigurable antennas may change the frequency spectrum to suit the system's requirements. Over its operational band, the CR system is significantly enhanced by the antenna's frequency tunability function [50–52].

1.4.2 Pattern Reconfigurable Antennas

In order to meet the constantly changing needs of various wireless applications, such as radar systems, cellular and satellite communication, tracing and remote sensing, vehicle-to-vehicle communication, on-the-go communication, and so forth, pattern reconfigurable antennas can change the radiation pattern characteristics [55–57]. The ability of pattern reconfigurable antennas to steer or scan the main beam or null spot in the desired direction is their most alluring feature.

Beam-steering antenna can redirect the high gain radiation beam towards desired direction for sustaining a robust line-of-sight communication link among immoveable and moveable portable equipment as depicted in figure 1.5(a), thus provide a wide coverage with increased data transmission rate [11], [60–61]. Similarly figure 1.5 (b) illustrates the interference [58] avoidance by redirecting the null position towards irrelevant angle. Moreover, in-band interferences are notoriously hard to filter out using traditional techniques for out-of-band interference suppression [62], but they can be effectively suppressed or filtered out by combining these two properties. In this case, the antenna is rotated to evade interference by pointing the null against the interference direction and the highest gain pattern towards the incoming signal. Figure 1.5(c) illustrates a satellite and terrestrial communications network

application scenario for outdoor networking of moving vehicles [59]. The moving vehicles are able to preserve a continual communication hookup with each other thanks to the roof-mounted pattern reconfigurable antennas with directing beam scanning function. Increased efficiency and high signal-to-noise (SNR) would result from switching high directed beams.

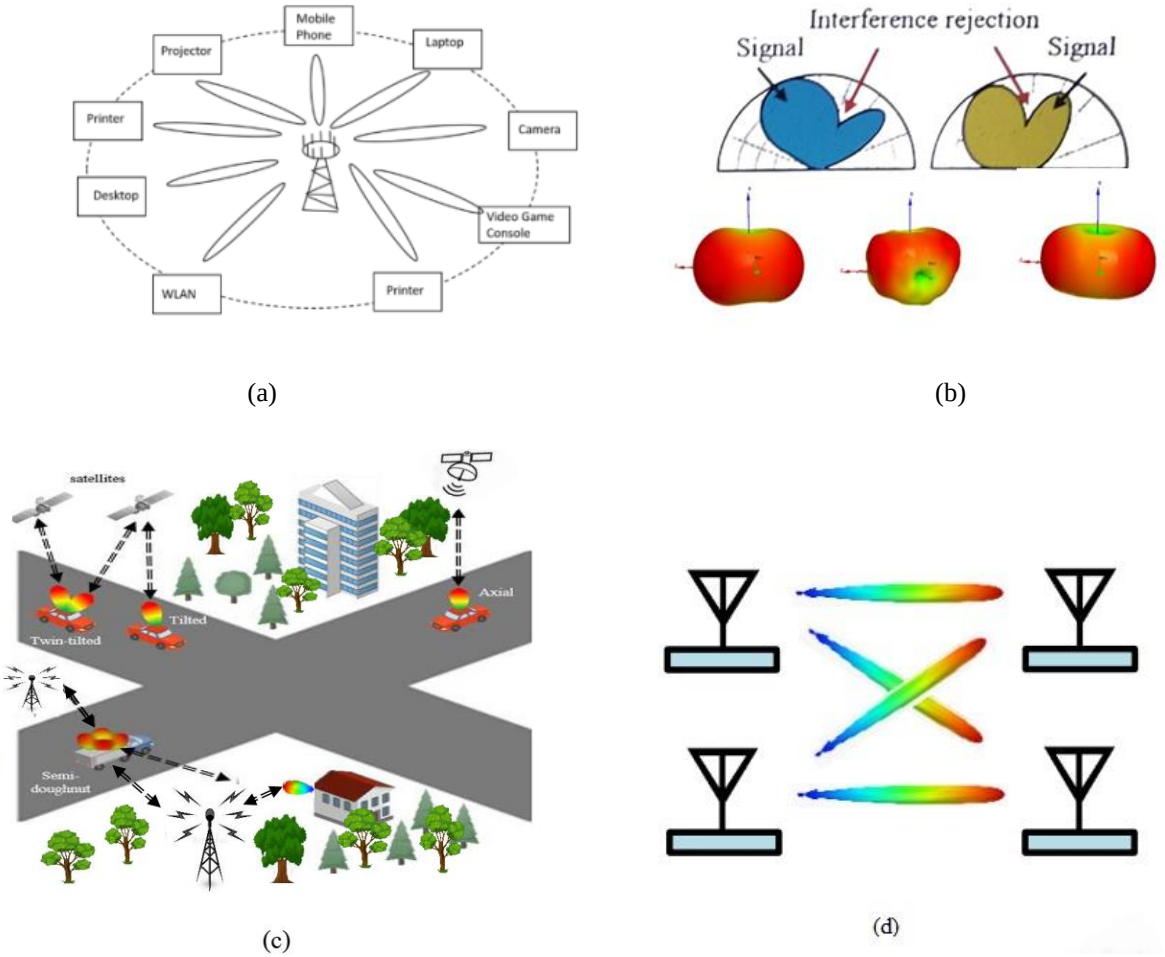

Figure 1.5 Applications of pattern reconfigurable antenna designs (a) beam-scanning (b) 3D pattern of null scanning [58], © 2013 IEEE (c) outdoor networking scenario [59], © 2017 IEEE (d) adaptive MIMO system with beam-steering antennas

Another intriguing use of pattern reconfigurability is the adaptive MIMO system. Here, as schematically shown in figure 1.5(d), pattern reconfigurable antennas are used in place of the MIMO system's static antennas. The MIMO system's spatial variety and antenna pattern diversity offer an extra degree of flexibility to reduce spatial correlation between signals and increase connection capacity [63–66].

Nowadays, portable wireless communication devices are becoming increasingly popular. The excessive radiation exposure from the device will have a negative impact on the individual's health. Portable devices that use pattern reconfigurable antennas can reduce the specific absorption rate (SAR) by rerouting the radiation that is released away from the user's body.

1.4.3 Polarization Reconfigurable Antennas

The movement of mobile devices changes the orientation or polarization of the radiated signal. The polarization mismatch between communicating devices results in signal loss. A very interesting idea to overcome the aforementioned transmitter-receiver restriction is the polarization agile antenna.

Polarization reconfigurable antennas are a natural choice in a linearly polarized system, where line of sight path is crucial for signal gathering [67–68]. The fading loss due to multipath can be minimized with the help of polarization reconfigurable antennas. Dual transmission channels that are appropriate for frequency reuse can be obtained by using reconfigurable antennas that have swapped two orthogonal polarization modes. Because of poor correlation between two orthogonal polarizations in non-LOS settings, it can be used as a diversity technique in non-LOS communications.

The indoor wireless sensor networks [69] comprises a receiving antenna engulfed by multiple wireless sensors as depicted in figure 1.6(a). If random polarized signals from sensors are incident on a single polarized receiving antenna, a polarization mismatch will occur on it. Similarly in body centric wireless communication [70] as shown in figure 1.6(b), the polarization mismatch will happen again due to random positioning of implanted devices. The losses due to polarization mismatch can be easily mitigated by employing a polarization reconfigurable antenna at receiver's end.

Additionally Numerous applications, including satellite and radar applications, mobile earth stations, ground systems for satellite monitoring and tracking, etc., can make advantage of polarization reconfiguration [71–72]. Additionally, they improve the systems' performance and connection capacity by offering polarization diversity in MIMO systems.

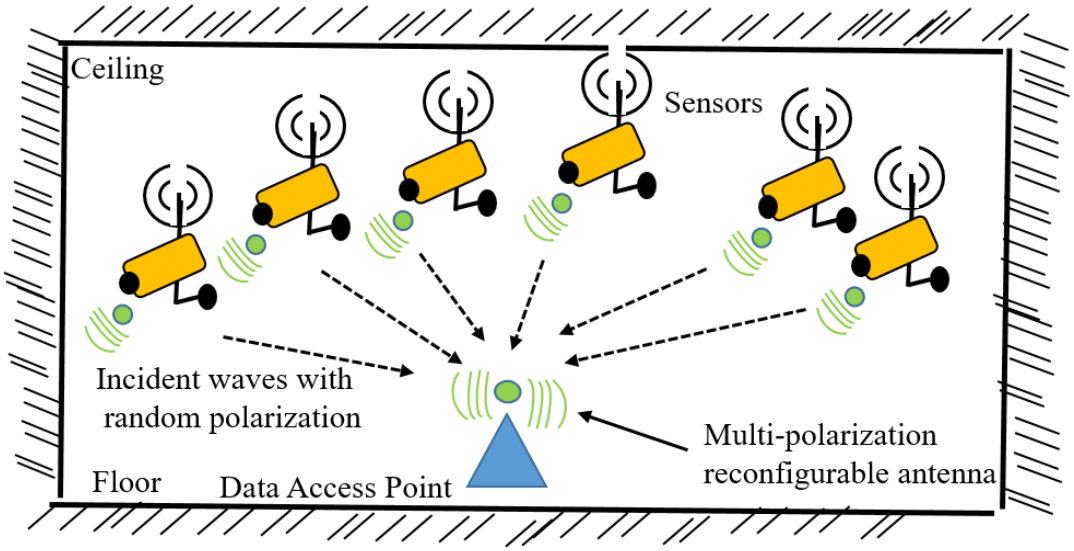

(a)

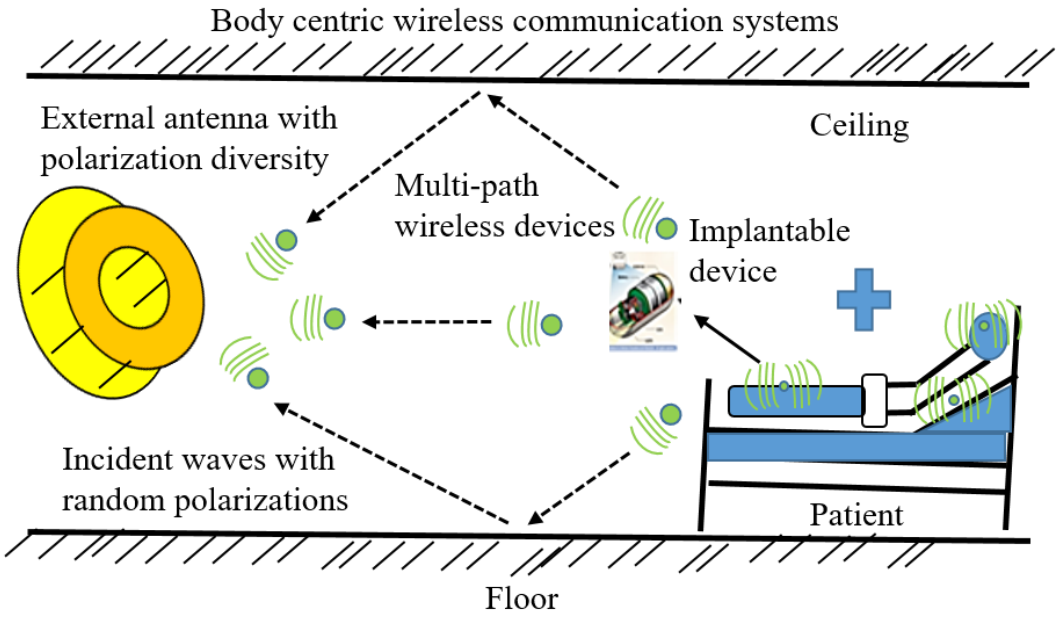

(b)

Figure 1.6 Polarization reconfigurable antenna (a) wireless sensor network [69], © 2017 IEEE (b) body centric wireless communication system [70], © IEEE

1.4.4 Hybrid Reconfigurable Antenna

Incorporation of certain combinations of reconfigurable characteristics in hybrid reconfigurable antennas are of particular interest, because they provide flexibility with enhanced performances. An example of integrating frequency and pattern together in antenna design can improve the spectral efficiency significantly by concurrently shifting the frequency to less congested spectrum and enhancing the link budget by redirecting the beam in different directions [15],

[73]. Thus, interference reduction is done by frequency selectivity while link budget enhancement is obtained through the use of highly focused beams, both at the same time. The strong interference rejection capability with higher signal-to-interference (SIR) ratio is provided by the combined out-of-band and in-band interference suppression by frequency and polarization reconfigurability [74], respectively. The polarization and pattern diversity are integrated and studied simultaneously in an adaptive MIMO system. Allowing a transition between available pattern and polarization reconfiguration can increase the system's overall capacity [34], [65]. By diverting radiation away from the device and rerouting the frequency to the proper band, compound reconfigurability in personal communication devices also lowers the SAR value while conserving battery life. Due to their numerous reconfigurable features, compound reconfigurable antennas have a lot of promise and can be applied to a variety of situations.

1.5 Advantages of Reconfigurable Antennas

The dynamic capability and flexibility of reconfigurable antennas, which also improve system performance, give them numerous advantages over fixed performance antenna (FPA) types [26], [39]. Some advantages are listed below:

1) Reconfigurable antennas are adaptable to work as a single element or an array of multiple elements to have reconfigurable integrated multi-functionality.
2) Multiple communication protocols are supported by reconfigurable antennas to access the wireless services makes the antenna system economical and space efficient with better selectivity
3) Replacement of multiple static antennas by single RA reduces the complexity in antenna and associated feed circuitry resulting in energy efficient and easy integration with other microwave devices.
4) System performances are improved in terms of robust interference rejection capability, enhanced communication link efficiency, increased speed and data capacity by employing reconfigurable antennas.
5) In next generation communication, reconfigurable antennas must be able to learn from and adjust to varying scenarios possess the flexibility to learn from and adaptable to changing scenarios through automatic controller unit.

1.6 Challenges, Motivation and Research Objectives

The recent advancements in next generation wireless communication, identification and sensing technologies has fostered the research activities in adaptive devices or reconfigurable antennas to achieve high performance designs with very good flexibility in functionalities. Although extensive research work has been undertaken on the reconfigurable antennas, but numerous limitations still exist in reconfigurable antenna designs, which challenges the antenna engineers to see them new research opportunities. In order to achieve reconfigurability, some geometries incorporate impedance matching networks, whereas many reconfigurable design techniques rely on multiple feeds or extended excitation networks with radiating components. The antennas physically enlarge with more external circuitry, and their performance is hampered by certain losses in the external feed network. Limited reconfigurability range, asymmetrical beam-steering, and inconsistent reconfigurable performances between states are further issues that diminish the usefulness of reconfigurable antennas. Although several thoughtful methods have been employed to tackle these problems, they seem to be hindered by high-profiles, intricate design, and reconfigurability processes.

Besides these challenges, the adaptive devices or reconfigurable antennas have a very promising future in next generation wireless communication technology. As they have many attractive attributes like adaptability in different application scenarios, support multiple communication protocols, multi-functionality, improved antenna performances etc. that attracts more researchers to put efforts in this areas continually. Implementing reconfigurable characteristics in an antenna design is motivated by the need to address the various issues like extensive demand, miniaturization at low frequency and increasing requirement of minimizing the number of antennas. It also provides extra features that improve the antenna systems performance by assisting in the regulation of the device's polarization and radiation pattern. This thesis offers innovative reconfigurable antenna concepts and designs to overcome the reconfigurable design difficulties.

The primary aim of the research project is to design and develop reconfigurable microstrip antennas for wideband applications. The aim is achieved in the following three steps, these steps have emerged as the three objectives of our thesis.

1) Create a compact, planar multi-band microstrip antenna

2) Generation of frequency – polarization reconfigurable characteristics in compact, planar microstrip antenna
3) Design a compact, planar wide-band antenna with frequency–polarization–pattern reconfiguration characteristics

1.7 Original Contribution

The first contribution of this Ph.D. thesis is in the design of a planar antenna structure with slits on the ground plane. This antenna is capable of producing three wideband resonating frequencies (Wi-Fi, WiMAX and WLAN) for radio communication below 6 GHz band.

The integration of multiple reconfigurable characteristics in a single antenna design has significant advantages with a wide range of capabilities. Furthermore, two antenna designs with multiple tuning properties are developed by combining multiple reconfigurable elements using electrical tuning devices in this research. The first antenna is developed by combining an arc of suitable length on a truncated ring in annular rings antenna design via PIN diodes. The antenna reconfigures in between from circularly polarized single WLAN band antenna to linearly polarized dual WiMAX & WLAN band antenna, by controlling the switching state of PIN diodes.

In process of work, we have realized a novel wideband antenna design with simultaneous frequency-pattern-polarization reconfigurable characteristics by using a combining reconfigurable elements method. The design is composed of truncated ring with tunable stubs of asymmetric lengths on a partial ground plane. With independent tuning, the antenna switched its frequency response from single (WLAN) to dual (WiMAX & WLAN) band, maximum beam scanning range upto ± 35° between radiation patterns and polarization switching between linear and circular state in WLAN band with ARBW of 0.16 GHz.

1.8 Research Methodology

The universal research methodology to carry out the research work is presented as flow – diagram in figure 1.7. Normally we start with a design idea and basic antenna layout. Now the antenna design is evaluated on comparative literature surveys of similar kind and helped to finalize the design idea.

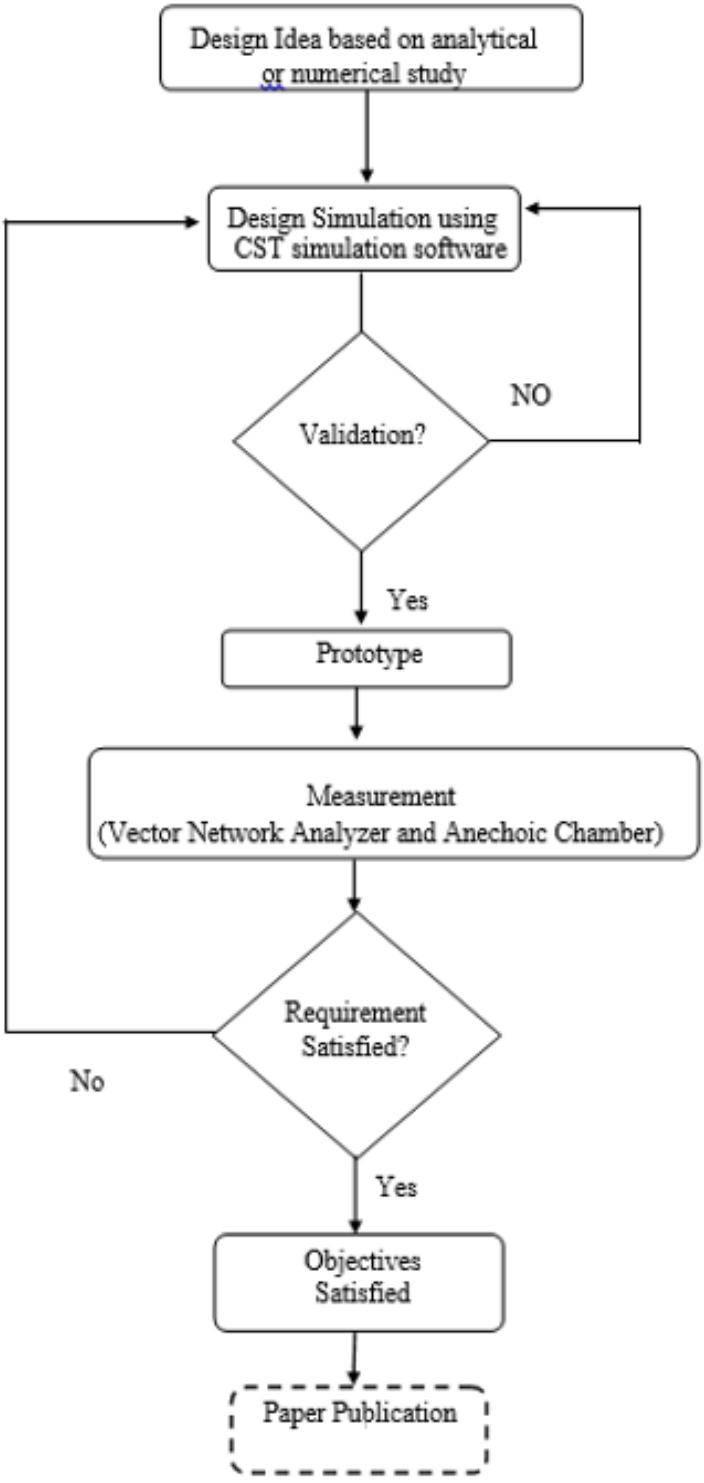

Figure 1.7 Flow chart for antenna designing

In the next step, the simulation model was simulated using full wave 'CST-MWS' ('Computer Simulation Technology–Microwave Studio'). The parametric operations and corresponding modifications are performed on designs until the desired results are obtained. After expected

results, the antenna design is fabricated on substrate by photolithography process and lumped elements are soldered on antenna PCB (printed circuit board), if any.

1.8.1 Software / Simulation / Programming Language / Tools used

CST software has been used for antenna simulation and optimization, as it is a convenient tool for 3D electromagnetic modelling of microwave and RF components. It provides the rapid and accurate analysis of RF devices, including filters, circulators, resonators, power dividers, couplers, antennas, and single- or multi-layer structures, as well as electromagnetic compliance impacts [75]. There are several steps involved in the production of microstrip antennas. Computer-aided antenna geometry design is the initial step. The design's negative was embossed on a transparent sheet to create the mask. The copper coated FR-4 sheet is cleaned and dried with acetone. So no dirt or other contaminants are on the surface, as their presence on the surface may disturb the etched pattern and ultimately the resonant frequency. Now, a negative mask is applied to the copper-clad substrate with photo-resist laminate. The exposed photoresist solidifies and turns dark blue, while unexposed photoresist is light blue and dissolves in the developer solution of sodium carbonate. A 'ferric chloride' ('$FeCl_3$') solution is then used to chemically remove the produced copper-clad substrate. Except for the glued photo resist, the copper particles break down in '$FeCl_3$'. The treated substrate is cleaned to get rid of any leftover etchant before it is truly dried. Sodium hydroxide is used to dissolve the damaged photo-resist. An SMA (Sub Miniature version) connection is connected to a microstrip antenna. Fabrication facilities of the RF fabrication lab at Swami Keshawanand Institute of Technology (SKIT) Jaipur were used to fabricate the antenna.

1.8.2 Measurement

The measurement for S – parameter, VSWR, resonant frequency and input impedance is carried out with Agilent N5234A VNA (vector network analyzer) at Govt. Mahila Engineering College, Ajmer and JUIT Waknaghat. Also, radiation pattern, axial ratio and gain of the prototypes are measured in the anechoic chamber available at Govt. Mahila Engineering College, Ajmer.

The anechoic chamber setup is presented in figure 1.8. The fabricated antenna or antenna under test (AUT) is mounted on the top of a computer controlled turntable with 360° rotation. The standard gain horn (SGH) is kept fixed and placed 5 meter away from the turntable. The AUT

and SGH antennas are connected to VNA through RF cables and via control cables to a personal computer loaded with Labview software. The desired frequency signal is generated with a sweep generator and the corresponding radiation pattern for the antenna is recorded by changing elevation angle from 0° to 360°. In axial ratio measurement, AUT antenna is rotated in azimuthal plane from -90° to +90° and SGH is kept fixed [76]. The axial ratio of AUT is obtained by subtracting the highest and minimum values of the received signal levels for a specific frequency. At frequencies when the axial ratio value is less than 3 dB, the AUT is regarded as a circularly polarized antenna.

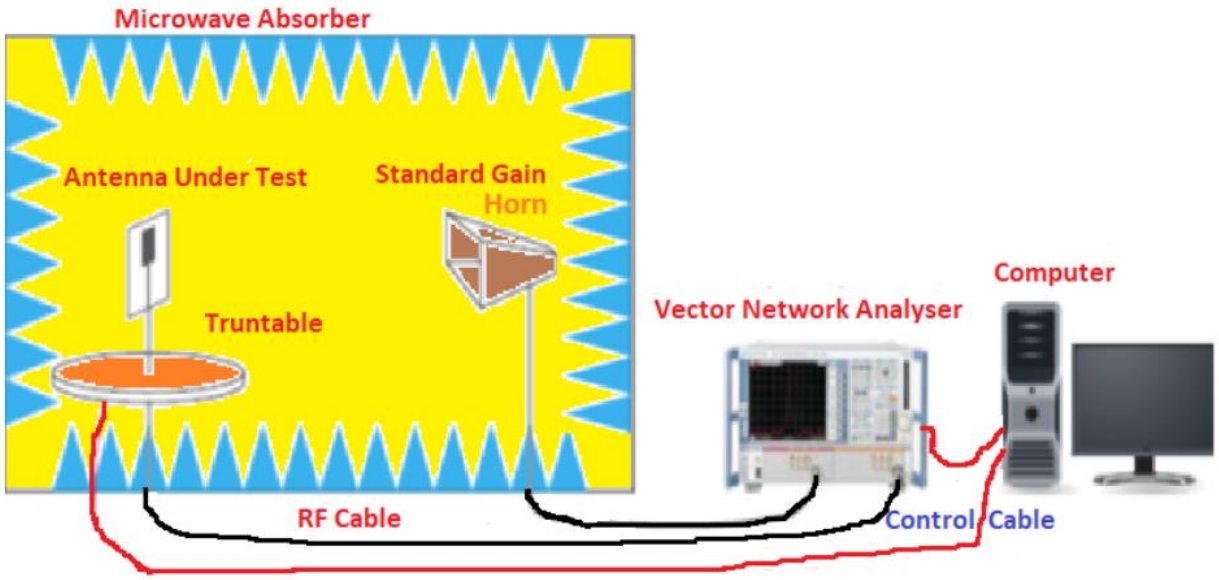

Figure 1.8 Antenna measurement setup

The FRIIS transmission equation is used to calculate the gain measurement at each frequency [3]. The equations is given as:

$$\frac{P_{AUT}}{P_T}\ (dB) = G_{AUT}(dB) + G_T(dB) + 20\ log_{10}\left(\frac{\lambda}{4\pi R}\right) \qquad (1.1)$$

Where,

P_T = Transmitted power of reference antenna

P_{AUT} = Received power at AUT

G_T = Gain of reference Antenna

G_{AUT} = Gain of AUT

λ = Wavelength of transmitted signal

R = Distance in reference antenna and AUT

$\frac{P_{AUT}}{P_T}$ = Maximum measured value of S_{21} of AUT by VNA

The connecting cables between AUT, reference antenna and VNA have introduced some losses in the measurement setup, known as cable losses. These losses must considered in the calculation of AUT gain as:

$$G_{AUT}\,(dB) = S_{21}(dB) - G_T(dB) - 20log_{10}\left(\frac{\lambda}{4\pi R}\right) - cable\ losses\ (dB) \quad (1.2)$$

Where, Gain (G_T) of reference antenna is taken from the datasheet of a SGH antenna and cable losses are measured with the help of VNA.

1.9 Organization of Thesis

The primary aim of this project work is to design reconfigurable microstrip antenna for wideband applications, so the suggested antenna design may be used in next generation wireless applications. The above mentioned requirement is achieved in three steps. First, we started work to design a multi-band antenna, which is further optimized to be frequency-polarization reconfigurable and ultimately frequency-polarization-pattern reconfigurable antenna with simple control circuitry. This dissertation's research is divided into six chapters, which are outlined below:

The **Chapter 1** presents a brief overview on reconfigurable antennas, kinds of reconfiguration, their application, advantages, design challenges and motivation with objectives for the research project on one of the emerging technologies in recent years.

The **Chapter 2** briefly reviewed the previously and currently developed different antenna designs, techniques with their associated circuitry for achieving the single (frequency, polarization, pattern) or multi-parameter reconfigurable characteristics, also potential and constraint of each design method.

Chapter 3 illustrates the process of designing and developing a Y – shaped antenna with defected ground structure (DGS) for multi-band operation in short radio communication. The design steps, operation principles are also presented in this chapter. The simulated results are

validated from measurement of prototyped antenna. The performance comparison of suggested antennas with other similar structures and in last a comprehensive summary is include.

In **Chapter 4**, a frequency-polarization reconfigurable annular rings antenna design is presented with a minimum count of p-i-n diodes. The architecture details orderly explains the working mechanism, which is further cemented by corresponding simulated and measured results at each step. The chapter concludes with a general review after comparing the antenna's performance with that of more contemporary, comparable reconfigurable antennas.

A new frequency-pattern-polarization reconfigurable antenna design with a truncated annular ring and asymmetric I-shaped stubs on a partial ground plane is presented in **Chapter 5**. This chapter describes the design process used to create the suggested antenna, tuning techniques, and performance outcomes.

The thesis is finally concluded in **Chapter 6** with recommendations for further study on hybrid reconfigurable antennas. This thesis concludes with a reference section comprising documented work in related subjects.

CHAPTER 2

LITERATURE REVIEW

LITERATURE REVIEW

2.1 Overview

In this chapter, a wide review on reconfigurable antenna designs with critics' perspective have been carried out. The reconfigurable antennas are capable of customizing their operations by altering the geometry via different means and provides the same or more throughput as multiple antenna systems. Generally, the tuning mechanism can be classified as continuous and discrete, which are further subdivided into electronic, mechanical, optical and material types, on the basis of current distribution control on antenna structure. Significant amounts of research have been done to explore the reconfigurable patch antennas by modifying antenna structures with radio frequency lumped elements, modifying substrate characteristics with tunable constituents and employing metamaterial based structures. Besides existing technologies, additional design ideas like altering radiator configuration or slot shape/ slot transition, using multiple radiators or switchable radiators, adding parasitic elements, parasitic layer/ multilayer configuration, dual feed structures, monopole and loop combination etc. are also suggested by antenna engineers for realizing the reconfigurable antenna designs. The upcoming sections are dedicated to the types of reconfigurable antennas and different approaches of their implementation with much emphasis on electrical tuning using RF switches.

2.2 Review of recent development in reconfigurable antennas

Wireless technologies are constantly developing for next-generation wireless communication, which will enable connectivity for billions of devices with high data communication speeds (giga-bit-per-second), low latency, and high reliability. This could lead to applications such as tele-surgery, fully automated industries, driverless autonomous cars, and many more [77]. Hence, a mobile device must be compatible with different wireless standards for maintaining smooth services. Microstrip antennas are used extensively due to their small size, low profile, light weight, affordability although they give low radiation efficiency, limited bandwidth and gain etc. For any portable or small communication system, incorporating several fixed performance antennas to satisfy different needs is a major difficulty. In order to meet these requirements, antenna designers had to create flexible, adaptive antennas that worked well with wireless devices [78–83]. A number of investigations have been conducted to study planar

adaptable antennas for altering the antenna structure via a variety of methods like changing substrate properties using tunable materials, using RF lumped elements, etc. [84 –165].

2.2.1 Frequency Reconfigurable Antennas

In frequency reconfigurable antennas, the resonating frequency bands can tune either in discrete or continuous manner without significant changes in radiation pattern and polarization state. Here, a wide selection of frequency bands are offered by a single device and can be used in such systems that support multiple communication protocols to access different wireless services. The mobile terminals are the direct application of frequency reconfigurable antennas. The basic mechanism involves the alteration in effective electrical length of antenna structure by applying different methods such as switching (electrical or optical), reactive loading, metamaterial and tuning material [84–101] produces the variation in operating frequency bands or central resonance frequencies. The frequency agility can be realized in various radiator types like patches, monopoles, dipoles, slot antennas, vivaldi, dielectric resonator antennas (DRA) and PIFA (planar inverted F – antennas) etc. by utilizing electrical tuning components to achieve a reliable system performance. The PIN diode is preferred over the RF-MEMS and DTC as they are inexpensive, consistent, lightning-fast swapping speed and high capacity to handle power.

A frequency reconfigurable antenna design [84] comprises of inverted-F antenna with PIN diodes between radiators for coarse tuning between 1.85 – 1.99 GH, 1.92 -2.18 GHz and 5.15 - 5.825 GHz, also varactor diodes on antenna's shorting line gives the fine tuning within the resonating bands is suggested by Lim et al. In [85], Jung et al. utilized a combination of switching (PIN diode) and reactive (varactor diode) tuning elements in meander monopole radiator to achieve the coarse tuning of frequency bands between 2 GHz and 5 GHz band and fine tuning within the resonating frequencies respectively. An annular slot antenna with RF-MEMS [86] for switchable resonant frequencies is prototyped by Cetiner et al. Here, the radiating annular slot with two RF-MEMS actuator and microstrip feed line with single RF-MEMS actuator is fabricated on two layers, which are bonded together. The activation or deactivation of the MEMS actuator within antenna geometry produces the switching between 2.4 GHz and 5.2 GHz. A center fed circular patch antenna surrounded by four sector shaped patches with four pairs of varactor diodes across the gap are realized for frequency reconfiguration by Ge et al. [88]. The antenna can be continuously tuned to different resonant

frequencies in the frequency range from 1.64 – 2.12 GHz with a stable radiation pattern by varying the capacitance of the varactor diode through reverse biasing. Rhee et al. [89] designed a folded unipole (or biconical unipole) antenna with gasket (ground) and a single PIN diode for aircraft communication. The antenna is a V-type travelling antenna for the ON state of the diode and radiates from 30-300 MHz & 960 – 1150 MHz, otherwise the antenna acts as a unipole antenna with resonating bands from 300 – 400 MHz & 1120-1250 MHz band. A coaxial fed square patch antenna with optical loaded stub [90] for frequency reconfiguration through photoconductive switch is suggested by Pendharker et al., the illumination of photoconductive switch via laser turned it ON, so stub is loaded on the patch thus switching the resonant frequency. The four dielectric resonators with PIN diodes located on the feed line midway between each pair of resonators are realized by Danesh et al. [91] for frequency reconfiguration in LTE/WWAN and WLAN bands. The antenna exhibits frequency reconfiguration between 1.89, 2.14, 2.53 and 2.77 GHz resonant frequencies for all diodes switched ON simultaneously and switching OFF one diode alternatively. A double sided printed bow-tie shaped antenna [92] for frequency reconfiguration is realized by Li et al., the switching of embedded six PIN diodes on bow-tie arm changes the effective electrical length of antenna results in frequency switching in between 2.2 – 2.53 GHz, 2.91 – 3.71 GHz and 4.51 – 6 GHz band with same radiation pattern. A low profile monopolar antenna [93] with varactor controlled shorting rods and symmetric slot for frequency reconfiguration between two bands is developed by Nguyen et al. The equivalent magnetic-current loop through center fed patch with shorting post gives the lower resonating frequency (0.76 – 1.04 GHz) band, while four symmetrical slots on patch are responsible for higher resonating frequency (1.50 – 1.87 GHz) band by creating another magnetic-current loop. A CPW fed flexible [94] circular patch with strips for spiral shaped structure is prototyped by Idris et al. for frequency reconfiguration. The antenna can switch between five frequency bands i.e. .19–4.48, 5.98–6.4, 3.42–4.0, 5.4–5.68, and 6.8–7.0 GHz with the help of a dual pair of PIN diodes. Wright et al. [95] developed a multilayer antenna pixelated, which is composed of fiberglass composite, Rohacell foam, graphite fiber and conductive epoxy with RF-MEMS for frequency diversity. The foam has the conducting pixel, whose connection or disconnection generates reconfiguration between 1.16 GHz, 1.28 GHz and 1.6 GHz resonant frequencies respectively. Tawk et al. [96] developed a novel software controlled monopole antenna for frequency diversity. Here, antenna is comprised of three meandered radiating elements joined at two positions via PIN diodes. A GUI (graphical user interface) enabled microcontroller controls the biasing current to change the switching state of

PIN diodes to exhibit frequency reconfiguration between four bands in LTE, UMTS and GSM channels. A novel monopole antenna [97] with PIN diodes is designed by Shah et al. for frequency reconfiguration between six frequencies involving two single frequencies 3.5 GHz, 4.5 GHz and two dual frequencies of 2.10, 4.15 GHz and 2.4, 5.2 GHz. In [98], Das et al. designed a CPW fed monopole antenna with Minkowaski fractal square ring on backside of monopole with a PIN diode and a metamaterial superstrate for enhancing gain and impedance bandwidth. The switching of PIN diode ON or OFF produces multiple resonant frequencies within frequency range from 1 – 10 GHz. A CPW fed flexible monopole antenna having two balanced arms with frequency selective surface placed behind the monopole is designed by Ibrahim et al. [100] for frequency reconfiguration. The loading of arms on monopole through PIN diodes produces frequency reconfiguration between 2.4, 3.5 and 4 GHz resonant frequencies with gain value more than 5 dBi in each band. An inset fed microstrip patch with underneath slot antenna [101] on ground plane having PIN diodes across slot and reflector is developed by Majid et al. for frequency reconfiguration. The overall antenna structure produces the six switchable frequencies with directional radiation pattern in the frequency range from 1.7 – 3.5 GHz. Trinh et al. suggested DTC controlled frequency reconfigurable antenna for frequency band from 470 – 700 MHz. The radiating element is comprised of folded monopole structure [102] with a digital tunable capacitor is mounted on the monopole. Five strip lines with r.f. inductor are placed to connect the DTC and control unit. The capacitance adjustment from 0.9 to 4.6 pf of DTC across thirty two states via digital control produces the frequency switching in white space frequency band. Jaume et al. [104] prototyped a multi-band reconfigurable antenna by using a non-resonant parallelepiped antenna element in conjugation with a MEMS based reconfigurable matching network of shunt tunable capacitor. The value of capacitance is selected from available 32 states via serial digital line exhibiting multi-band performance in 698 – 960 MHz and 1710 – 2690 MHz band.

2.2.2 Polarization Reconfigurable Antennas

As we know, the direction of current flow on antenna surface determine the polarization state of the radiated signal in the far-field of antenna. A polarization mismatch likely to occur at receiver's end, as complex propagation channel alter the polarization of the radiated beam. If polarization of incident beam is not matched with the polarization of receiving antenna results into the loss of signal or no signal is received. Maintaining a good polarization matching is needed in wireless system to avoid the above said. The application of any suitable

reconfiguration method like change in antenna structure, material properties and feed configuration has altered the way of current flows on the antenna geometry led to the polarization diversity. Thus polarization reconfigurable antennas not only mitigates the polarization mismatch but also enhances the channel capacity by suppressing multipath interference and also improves the link quality [67], [105–107].

Stimulating two adjacent modes with 90° phase difference simultaneously contributes to the creation of circular polarization, whereas stimulating the modes individually results in creation of linear polarization. Also, multi-mode stimulation is a useful method for reconfiguring antenna polarizations since it facilitates the achievements of circular polarization with a broad bandwidth because the frequency responses of the two modes overlap. These antennas are capable of switching from linear polarization (LP) to circular polarization (CP), between different orientation in LP, circular polarization with left and right hand rotation (LHCP, RHCP) and vice-versa [3], [108]. Generally two design strategies i.e. designing of reconfigurable radiator or realization of reconfigurable feed network can be adopted for polarization switching by utilizing tuning or switching elements. The polarization reconfigurable antennas are mainly used in indoor with multipath environment and satellite communication applications. The accomplishment of polarization diversity must be done carefully without much disturbances in frequency characteristics.

The first technique involves the introduction of RF switches in antenna structure and controlling their ON/ OFF state gives the different polarization behaviour. Sung [109] et al. designed a corner truncated square patch antenna for polarization diversity. The simultaneous loading or unloading of all triangular elements on patch via PIN diodes produces the linear polarization, while alternate loading of two diagonally placed triangular elements via PIN diodes generates circular polarization with left and right hand sense of rotation in the radiated beam. Sulakshana [110] et al. realised CPW fed based rectangular and circular shaped designs for polarization reconfiguration. Here, the main radiator is vertically segmented at symmetric placed location in horizontal direction and having two PIN diodes at center of each segment for bridging the gap. The simultaneous ON or OFF switching of PIN diodes produces the linear polarization in radiated beam and alternate switching of one diode at a time produces the LHCP and RHCP. Nishamol et al. designed a proximity [111] coupled antenna by etching X – shaped slot on cross shaped substrate and utilizing PASS (patch antenna with switchable slot) configuration for polarization diversity by putting two PIN diodes at the center of slot to control the behaviour of

current. The proper activation of PIN diodes produces vertical, horizontal linear polarization and RHCP in the resonating frequency bands. A CPW fed square-ring slot antenna [112] with four stubs of unequal length and widths protruded from upper and inner sections of ring suggested by Zhou et al. for polarization diversity. The loading of lower stubs produces the linear polarization in radiated beam, while loading of oppositely placed lower and upper stub via PIN diodes produces the LHCP, RHCP respectively in the beam. A square patch antenna with each edge is connected to ground plane through metallic vias [113] controlled by PIN diode and energized by diagonally placed feed network through aperture coupling is suggested by Qin et al. On activating the proper PIN diodes on antenna structure produces the polarization switching in vertical, horizontal and 45° direction for the 2.4 and 5.8 GHz resonant frequencies. Kim et al. [114], designed a circular patch antenna having a rectangular slot near the upper edge and fed by microstrip line with diode loaded matching stubs for polarization reconfiguration. The antenna can switch between linear (horizontal, vertical) and circular (LHCP, RHCP) states on loading of respective stubs on antenna geometry. Yadav et al. [115] prototyped a circular patch antenna with rectangular shaped DGS for resonant frequency of 5.5 GHz with linear polarization. The inclusion or exclusion of respective stubs of quarter wavelength on radiating patch via PIN diodes produces polarization reconfiguration between LP, LHCP and RHCP in the frequency range from 5.23 – 5.75 GHz.

Polarization reconfiguration can also be achieved through tunable feed networks. A multilayer antenna for polarization switching is designed by Aïssat et al. [116] comprises of a circular patch energized by diagonally slotted CPW feedline loaded with the PIN diodes below the radiating element. The switching of PIN diodes in feedline reconfigures the polarization state of resonating frequency between RHCP and LHCP. A circular slot antenna [117] fed by arrow shaped coupling strips with two PIN diodes at their ends is realized by Row et al. The activation of alternate PIN diodes generates the LHCP or RHCP, while linear polarization is obtained for simultaneously OFF state of both diodes in the resonating frequency. Lin et al. [118] designed a multilayer antenna structure with reconfigurable feed network for polarization diversity. The antenna is composed of square patch radiator in top layer, reconfigurable feed network and L – shaped probes with PIN diodes in the middle layer and biasing lines and DC battery in the bottom layer. The alternate activation of feed probes generates the beam with switchable LHCP and RHCP. Yang et al. [119] prototyped a polarization rotation artificial magnetic conductor (PRAMC) based multi polarized dipole antenna with RFIC switched network to realize the

polarization reconfiguration between LHCP, RHCP and 45° linear polarization. The SP3T and SPDT fed four dipole antennas are placed in plus – shaped configuration above on the PRAMC substrate. The activation of all diodes produces the 45° linear polarization and LHCP, RHCP in the radiated beam on energizing the alternate horizontal or vertical dipoles.

2.2.3 Pattern Reconfigurable Antennas

The arrangement of either electric or magnetic current on metallic structure determines the radiation pattern and also accounts for its magnitude and phase. The adaptability of the radiation pattern in terms of direction, shape or gain is desired without much changes in frequency and polarization of the antenna. Generally, any alteration in dominant current distribution on radiating surface by applying any of the different reconfiguration methods provides the reconfiguration in radiation pattern. The radiation pattern reconfigurable antennas are classified in three types i.e. direction switching, shape switching and radiation beam steering. The pattern reconfigurable antenna serves different purposes like increased reliability in communication link, object detection or tracking, increased coverage and enhanced channel capacity [120–123].

In pattern direction switching antennas, the main beam is switched in different directions but the shape of the pattern remains intact. Such an antenna involves tunable parasitic elements arranged symmetrically around the primary radiator and according to paired current, they act as reflector / director to guide the main beam in different directions. The input impedance matching is also not disturbed severely for different radiation modes, because of isolation between driven and parasitic elements, hence shape remains intact. The second type includes pattern shape switch antennas, which enhances the radiation coverage range by reconfiguring pattern shapes between unidirectional, omnidirectional, broadside and conical radiation patterns. The basic idea involves the activation of different modes corresponding to a particular pattern on the antenna radiator. Both methods change the radiation pattern in discrete manner with RF switching, while in the third category i.e. beam steering, the radiation patterns are steered in continuous manner by using reactive loading (varactor diode).

Kang et al. [124] designed a symmetrical vertical dipole antenna with two open wires and a pair of PIN diodes at each end of the wire. The alternate loading of one loop and open wire acts as director and produces switching of the main beam in two directions. A CPW fed step shaped two patches with four PIN diodes for pattern reconfiguration is realized by Zhang et al. [125].

Here, the activation of proper PIN diodes can switch the patches as reflector-radiator alternatively and give rise to the beam switching in opposite directions at the resonant frequencies. Qin et al. [126] suggested a square patch antenna having an embedded U-shaped slot with a pair of shorting posts connected at vertical or horizontal edges through PIN diodes. The unloaded antenna structure has boresight radiation pattern, while alternate loading of vertical or horizontal post via PIN diodes generates the conical radiation pattern with different orientations. Yong et al. [127] developed a center fed cross shaped patch with varactor diodes loaded with rectangular parasitic elements at each corner for a reconfigurable null scanning antenna. The identical frequency at all elements generates null at broadside in radiated pattern, while continuous change in matching frequency via varactor diodes tilt the null direction in continuous manner. Ren et al. [128] prototyped a novel pattern reconfigurable antenna composed of dipole and periodic H-shaped resonator (HSR) with PIN diodes between each HSR. The HSR acts as either director or reflector for the OFF or ON state of PIN diodes respectively, which in turn reconfigures the radiation pattern between end fire and broadside. Jusoh et al. [129] designed a two layered beam reconfigurable patch antenna by placing four parasitic circular elements around center fed circular patch antenna. The switching of PIN diode controlled shorting pins activates the appropriate parasitic element steers the direction of main beam in azimuthal planes 0°, 45° , 135° , 225° , and 315°, while 0° , 13° , 15° , 10° , and 12° in elevation plane. A five element linear array with Yagi microstrip and two parasitic strips having varactor diodes are realized by Xiao et al. [130]. The phase progressive input fed at each successive element of an array steers the main beam direction from -70° to + 70°. A combination of director-reflector for pattern reconfiguration is used by Alam et al. in his design [131]. Here, two radial sectors are placed on both sides of the center feeder at the top layer with a pair of stubs surrounding the radiator on a truncated ground plane. The activation of the radiator together with reflector and director in top & bottom layer respectively via PIN diodes produces the beam switching in 0°, 45°, 135° and 180° direction. Yang et al. [132] prototyped a pattern reconfigurable antenna based on a switchable feed network of symmetric stepped probes having PIN diodes. The in-phase and out-of-phase excitation through stepped probes gives the reconfiguration in between conical and broadside radiation pattern respectively.

2.2.4 Hybrid Reconfigurable Antennas

Hybrid or compound reconfiguration is an emerging research area that open new horizons for antenna applications in latest communication devices. In this case, a single device incorporates

two or more reconfigurable antenna characteristics without significantly altering their individual operations. Antenna parameters present a number of implementation strategy issues due to their interdependency and sensitivity.

2.2.4.1 Frequency – Polarization Reconfigurable Antennas

A type of smart antenna capable of altering its frequency and polarization characteristics dynamically to adapt to an ever changing communication environment and enhances the overall performance by providing multi-band operation, enhanced spectrum utilization, improved signal reliability, cost effectiveness, etc.

The four trapezoidal shaped radiating elements can be connected to a center fed square patch via eight varactor diodes and interconnected through capacitor is developed by Korosec et al. [133] for frequency and polarization diversity. The proper and asymmetric application of bias voltage to varactor diodes produces the continuous frequency tuning in L – band (890 – 1500 MHz) with polarization switching within and between linear and circular states. Hu et al. [134] prototyped a corner truncated square patch fed through cross slot coupling on the other side of the substrate for frequency and polarization switching. On switching both diodes OFF simultaneously from ON state, the antenna can switch resonant frequency from 2.416 GHz with LHCP to 2.464 GHz with RHCP. The design concept for frequency – pattern reconfiguration is slightly extended by Nguyen-Trong et al. [135] for frequency – polarization reconfiguration by replacing multiple vias on patch with single vias at the center and placing of varactor diodes enabled open stubs around diagonal fed square patch antenna. The continuous sweeping of biasing voltages across the horizontal or vertical stubs produces the frequency tuning from 2.4 – 3.6 GHz. While the equal biasing voltages produce the LP wave and alternate finite difference between voltages produces the LHCP or RHCP for the resonating frequency range. Similarly Qin et al. [136] realized frequency and polarization diversity in diagonal fed square patch antenna with loading / unloading of shorting posts on both vertical and horizontal sides via three switching elements. The loading of the shorting post on square patch via varactor diodes produces the continuous frequency switching from 1.35 – 2.25 GHz. The linear polarization with vertical or horizontal orientation is obtained on loading of either shorting post on square patch via PIN diodes in the above resonating band. While simultaneous loading of all shorting posts through PIN diodes on patch generates 1.35 – 1.9 GHz frequency band with linear polarization in 45° direction. Hu et al. in [137] designed a PIN diode controlled shorting posts

placed diagonally on patch for frequency switching in eight discrete bands within 1.7 – 2.8 GHz and four perturbation segments at each corner and their alternate or simultaneous loading via PIN diodes produces the LHCP, RHCP and LP respectively in the corresponding resonating frequency range.

Row et al. [138] designed a multi-layered antenna with a top layer composed of an annular slot ring on one side of substrate and tunable coupler with two open ended microstrip lines for feed network on other side of substrate. Also capacitors for frequency tuning are symmetrically placed below the slot along circumference and a reflector in the bottom layer. The activation of coupler modes in combination with a tunable capacitor generates the switchable frequencies in L – band with polarization diversity between two circular and one linear polarization. Babakhani et al. [139] realized frequency and polarization diversity patch antenna by tunable feed network. The patch antenna composed of two concentric circular patches joined at vertical and horizontal mid points via varactor diode and fed at two orthogonal positions from the external feed network. The alternate excitation signals at single port and activation of vertical or horizontal diodes produces the continuous tunable frequency from 1.17 – 1.58 GHz with vertical or horizontal linear polarization, while activating all PIN diodes and using signal of 90° phase difference at both ports produces the circular polarization with left or right hand rotation. Chun Ni et al. [140] developed a novel frequency and pattern agile antenna by utilizing a metasurface above the double slot antenna structure. The relative difference between antenna and metasurface gives the frequency tuning, while rotation of the metasurface relative to base antenna gives the polarization diversity between LP, LHCP and RHCP. Utilizing the liquid metal for reconfiguration in frequency and polarization in an antenna structure is also designed. Wang et al. [141] utilizing two dipoles having arms of liquid metal placed in cross configuration for frequency and polarization diversity. The shortened and lengthened arm's length by applying voltages produces the two independent resonating frequency bands with polarization switching from linear to circular in 0.8 – 3 GHz band. In [142] Liu et al. suggested a slot antenna with polydimethylsiloxane (PDMS) structure having five orthogonal microchannels located at different heights in PDMS structure. The suggested antenna structure has three different channel lengths to achieve frequency reconfiguration and polarization reconfiguration between linear and circular polarization through EGaIn liquid metal. The antenna exhibits linear polarization in frequency bands '2.03–2.28 GHz, 1.97–2.3 GHz, LHCP in 1.76–2.78 GHz, 1.8–3 GHz, 1.79 – 3.18 GHz' and RHCP in '1.96–2.75 GHz, 2.01–3.13 GHz, 1.86 – 3.13 GHz'.

Yang et al. suggested a flexible antenna design [143] for vehicle communication systems. Here, a square patch having two annular slots and four PIN diodes is placed on an appropriate position for achieving frequency and polarization reconfiguration in resonating bands. The activation or deactivation of PIN diodes produces resonating frequency 1.45 -1.47 GHz with linear polarization and 1.50-1.53 GHz with linear, LHCP and RHCP. Metamaterial inspired antenna design [144] is suggested by Lavanya et al. for frequency and polarization reconfiguration. The antenna design comprises a square patch having split ring resonator with PIN diodes and parasitic element. The proper activation or deactivation of diodes produces polarization and frequency switching in '2.4 GHz, 3.5 GHz' and '5.8 GHz' resonant frequencies.

2.2.4.2 Frequency – Pattern Reconfigurable Antennas

Frequency-pattern reconfigurable antennas can change their frequency and radiation pattern dynamically to adapt continuously changing communication conditions to improve signal quality and reliability by interference rejection.

A single turn square microstrip spiral patch fed by coaxial probe at edge of inner spiral with two tuning elements is suggested by Huff et al. [145] for compound reconfiguration of frequency and pattern. The antenna is capable of switching its resonating frequencies between 3.68 GHz and 6.02 GHz and broadside pattern reconfiguration in two directions at lower frequency. In [146], Nikolaou et al. etched an annular slot on one side of the square patch and printed a microstrip feed line with matching stubs on the other side of the substrate. The antenna can switch between 5.2, 5.8 and 6.4 GHz resonant frequencies by connecting / disconnecting stubs to feedline via PIN diodes and also controlling two diodes placed at 45° orientation on radiating element reconfigures the null direction. Rodrigue et al. [35] presented a novel pixel antenna design for frequency and pattern reconfiguration. Here, multi-size radiating elements are arranged in matrix configuration and twelve PIN diodes are utilized for interconnection among the radiating elements. The energizing of radiating elements by activation of proper PIN diodes produces the frequency reconfiguration L, S and C – frequency bands with beam steering in five directions with angular range upto 180°. Guo et al. realized a frequency-pattern reconfigurable antenna based on parasitic array [147]. The antenna configuration involves six rectangular radiating and PIN diode loaded parasitic elements, a circular patch with three rectangular strips in feeding structure and circular patch for ground plane with circular slots and rectangular strips. The proper activation of PIN diodes generates frequency reconfiguration

between 2.28 -2.58 GHz and 2.62 – 2.73 GHz with twelve different radiation patterns for the above resonating bands. Majid et al. [148] realized a slot antenna with embedded slits on the four edges at ground plane for frequency and pattern reconfiguration. The integration of two PIN diodes in slot feed line and their proper activation produces three switchable frequencies at 1.82 GHz, 1.93 GHz and 2.10 GHz, while three PIN diodes in each slit produces the switching of main beam in -15°, 0°, +15°direction. A dual band antenna consisting of square patch having shorting vias at the center with varactor diodes enabled open stubs for continuous tuning of frequency and pattern is designed by Trong et al. [149]. The continuous variation in bias voltage forces the antenna to switch from broadside pattern to omnidirectional radiation pattern for frequency tuning range from 2.68 – 3.51GHz. By extending the above design idea, Zainarray et al. [150], designed a two element array antenna with varactor diode loaded open stubs for frequency and pattern reconfiguration. The relative biasing between varactor diodes not only produces the continuous frequency tuning from 2.15 – 2.38 GHz, but also beam steering from -23° to + 23° through adjusting the phase difference between two elements obtained by optimizing the effective electrical length of patches. Patel et al. [151] simulated a multilayer antenna composed of three truncated corners microstrip patch antenna loaded with three split ring resonators (SRR) having RF-MEMS for frequency and pattern reconfiguration. On activating from none switch to four switch ON successively, the antenna can tune at 6.646, 6.685,6.708 and 6.761 GHz frequencies respectively and direction of main beam is shifted in different directions. A flexible and novel antenna geometry developed by Zhu et al. [152] for reconfigurability in frequency and pattern. The design has two switchable and symmetric radiating elements, where each element is composed of a circular monopole branch and hexagon open ring with extended branches. The radiating element with integrated PIN diodes is responsible for frequency switching in ‘1.9 GHz’ and ‘2.4 GHz’ band and selection of PIN diodes between feedline and radiating element accounts for the beam steering in two directions for each frequency. Singh et al. [153] prototyped a CPW fed ELC (electric-inductive-capacitive) resonator enclosed by a closed ring resonator (CRR) with four vertical metal strips surrounding it. The change in state of the PIN diode between ELC and CRR provides the frequency reconfiguration, while four PIN diodes between metal strips and ground plane gives the pattern diversity. An inset fed rectangular patch antenna having inverted U – shaped slot and single PIN diode [154] is suggested by Palsokar et al. The antenna has resonant frequency of 3.8 GHz with broadside radiation pattern tilted at -30°for the OFF state of diode, while activation of PIN diode produces dual 2.47GHz, 5.36 GHz resonant frequencies with

bidirectional radiation pattern tilted at +30°. Zhang et al. prototyped a liquid metal based antenna design for frequency and pattern reconfigurability [155]. The suggested patch antenna design consists of three elements of Yagi-Uda structure having slots in the middle of the director and reflector. Six microfluidic channels of polytetrafluoroethylene (PTFE) are filled with Galinstan and adhered to the front side of the patch. The air pumped positioning of Galinstan has led to shorting/opening of slots on the elements of patch produces the frequency and pattern diversity in the frequency range from 1.52 – 3.2 GHz. Li et al. fabricated an antenna structure [156] for continuous frequency tunable and controlled scanning of radiation pattern from 0° – 360° in 25.7° step through varactor and PIN diodes respectively. Firstly, four bending dipoles are designed to realize the omnidirectional radiation pattern and varactor diodes are placed for continuous frequency tuning from 2.2 – 2.52 GHz band. Now, double layer petal shaped parasitic elements with PIN diodes are placed around the antenna for radiation pattern diversity. An antenna design is prototyped by Ganesh et al. for achieving multiband and polarization diversity [157] with enhanced gain. Here, respective loading of two symmetrical rectangular split ring on half hexagonal shaped radiating patch via PIN diodes produces frequency reconfiguration between sub-6GHz and Wi-Fi 6E (3.3, 3.5, 5.1, 5.3, and 6.5 GHz) wireless standards and pattern diversity in 265°, 13°, 337° for 6.5 GHz, also placing a frequency reflector surface (FSS) below the radiating element improves gain by 2 – 4 dBi for each frequency.

2.2.4.3 Pattern – Polarization Reconfigurable Antennas

Similarly antennas can alter their polarization and pattern dynamically to adapt complex communication conditions. Also they enhance the performance of the antenna system by mitigating signal fading and multipath interference, high data rates, energy efficient and enhanced network coverage by beam steering in intended directions [158].

Liu et al. [159] developed a co-axial probe fed L – shaped strip within a square ring antenna and PIN diode enabled shorting walls at each edge of the patch for pattern and polarization reconfiguration. The alternate activation of diodes connects the respective shorting walls and edges, which in turn produces the broadside radiation pattern with vertical and horizontal polarization respectively, whereas conical radiation pattern is obtained on activation of all diodes. In [160], four rectangular patches are arranged in square configuration and fed from the tunable feed network is realized by Cao et al. for polarization and pattern diversity. Energizing all elements with signal of same magnitude and phase, a metamaterial antenna results with

linear polarization and conical beam. Whereas, signals of same amplitude and 90° successive phase difference are fed to each adjacent input which leads to a wide band antenna having circular polarization with broadside radiation pattern. A microstrip fed, two meandered strips lines placed orthogonally with truncated ground plane is designed by Raman et al. [161] for pattern and polarization switching. The alternate energizing of orthogonal strips produces the switchable linear polarization with omnidirectional radiation pattern in orthogonal planes. Gu et al. [162] prototyped a dual fed square patch antenna with electronically reconfigurable feed network and parasitic dipoles around the driven element for linear polarization diversity with vertical and horizontal orientation and radiation pattern switching from 0° to 360°respectively. Shaw et al. designed a square shaped antenna with switch loaded octagonal shaped ring [163] and fed with quad coaxial probes for polarization and pattern reconfiguration at 2.492 GHz. The antenna exhibits polarization switching between RHCP or LHCP on energizing antenna via ports having phase difference of 90° and simultaneously loading of octagonal ring gives switching in pattern beamwidth.

2.2.4.4 Frequency – Polarization – Pattern Reconfigurable Antennas

Here, antennas can change their frequency, polarization and pattern dynamically without much changing their other characteristics. Rodrigue et al. [164] prototyped a novel antenna design to achieve frequency-polarization-pattern reconfigurable antenna by using pixel method. Here, a multilayered antenna composed of a square patch as driven element at bottom layer and parasitic layer of 6 × 6 elements with 60PIN diodes over it. The proper activation of diodes configuration tunes the operating frequency above 25%, steers the main beam in ± 30° in E and H planes and switches in four polarization states i.e vertical LP, horizontal LP, LHCP and RHCP. In [165], Ge et al. realized a grounded CPW- fed cavity back antenna for reconfiguration in frequency, polarization and pattern. The two cross slots of same length are etched back to back and twelve pairs of PIN diodes are placed at respective positions on both sides of the substrate with SIW (surface integrated waveguide or metallized via) backed cavity. The activation of all diodes in alternate layers reconfigures the radiation pattern in opposite direction with switching in frequency and polarization state by controlling the ON/ OFF state of PIN diodes in other layers. Here, antenna can change their frequency, polarization and pattern dynamically without much changing their other characteristics.

2.3 Summary

The progress of wireless communication technology in recent years has revolutionized connectivity, which ultimately led to the exponential increase in wireless devices like IoT devices, smartphones and other smart gadgets. However, the manifold rise in wireless devices also presents multiple challenges like network congestion, signal interference, security threats, power consumption, higher operational cost, etc. in space and bandwidth constrained scenarios. In addition to being smaller and more effective than static antennas, multiband and reconfigurable antennas seemed to be the answer to the aforementioned problems. A brief discussion of the effects of growing numbers of wireless devices and services on hardware configuration and spectrum management and also different design methodologies, designs, and related difficulties for creating multi-band, reconfigurable antennas are presented.

In this chapter, selected antenna designs having single and compound adaptable characteristics like frequency, polarization, pattern, frequency–polarization, frequency–pattern, polarization–pattern and frequency–polarization–pattern were presented. The various mechanisms like electrical, optical, mechanical and material changes can be used to actuate reconfigurable antennas. In most of the reviewed articles, appropriate calculations were performed to determine the suitability of the diversity scheme in communication systems.

This chapter has discussed reconfigurable antenna designs and mainly focused on hybrid reconfigurable antenna designs. Here, two or all antenna characteristics are made reconfigurable by using electrical switching mechanism via PIN diodes, varactor diodes, RF-MEMS and etc. over other mechanisms, as it offers many advantages like creating simple planar design, low power consumption, low manufacturing cost, very high switching speed and concurrent working of several antenna in the system. Majority of the presented hybrid antennas can reconfigure at most two characteristics simultaneously using electrical switching. Although some novel work has been reported on frequency-polarization-pattern reconfigurable antennas, these antennas suffer from complex antenna structure, large number of switching elements and associated control circuitry. The exploration of many aspects, which were unexplored earlier, could lead to the development of reconfigurable antennas with very less number of switch elements as well as desired adaptive performance. The remaining part of the thesis will continue with description of application, domains, advantages, challenges and contribution towards designing reconfigurable antennas.

CHAPTER 3

TRIPLE BAND Y-SHAPED ANTENNA WITH SLIT FOR WLAN AND WIMAX APPLICATIONS

* A. Sharma, S. Khah and S. Rawat, "Design of slot loaded Y- Shaped Antenna for WLAN/Wi-Max Bands", *Scientia Iranica*, vol. 31, no. 17, pp. 1556 – 1566, 2022

TRIPLE BAND Y-SHAPED ANTENNA WITH SLIT FOR WLAN AND WIMAX APPLICATIONS

3.1 Introduction

Several wireless standards are extending or overlapping particular in short range radio links like Bluetooth, wireless fidelity (‘Wi-Fi’), wireless local area network (‘WLAN’) and worldwide interoperability for microwave access (‘WiMAX’) bands. To avail these services, mobile devices are equipped with Bluetooth/ Wi-Fi/ WiMAX modules for simultaneous functioning at numerous frequency bands [166–170]. This leads to the designing of antennas, which are compact, economically viable, wideband and capable of communicating in different wireless standards with good antenna performances for portable wireless communication devices. The appealing features of microstrip patch antenna includes low profile, inexpensive and easy to integrate with other devices makes it most appropriate candidate for above said applications. The federal communication commission (‘FCC’) specified the 2.4 – 2.484, 5.15 – 5.35 and 5.725 – 5.85 GHz spectrum for ‘WLAN’ and 2.5 – 2.69, 3.4 – 3.69 and 5.25 – 5.85 GHz for ‘WiMAX’ operation. A number of antenna designs with rigorous approaches such as loading of stub or slots on radiating/ ground element, bow-tie, metamaterial etc. have been discussed in literature [171–190] to achieve multi-band performance with overall reduced size and enhanced performances in WLAN/WiMAX applications. Multi-band antenna is useful for devices, in which a single antenna is operating at desired frequencies rather than having multiple antennas serving the same. Also, they can be used in internet of things (IoT) applications including Bluetooth, ‘WiMAX’, ‘WLAN’, ‘Industrial IoT’, medical body area network (‘MBAN’), Wireless body area network (‘WBAN’) and etc., which are operating from 2–5 ‘GHz’ [171].

Verma et al. [78] suggested a microstrip line fed inverted L-shaped monopole as radiating element with branched configuration of parasitic element near to the monopole and attached to the partial ground plane to generate triple resonant bands for WLAN/ WiMAX application. A narrowband coaxial probe fed ring antenna is designed on FR-4 substrate by Mathew et al. [172] to produce resonance in UMTS, WiMAX and WLAN band with asymmetrical V-shaped slits on the respective edges of the ring to produce circular polarization in the UMTS band. Two F-shaped slots of equal dimension are etched on left and right side of radiating element having modified ground structure is suggested by Gautam et al. [174] to generate 2–2.76, 3.04–4 and 5.2–6 GHz frequency bands. Liu et al. [175] prototyped a compound loop antenna consisting

of an outer rectangular ring having three splits, an inner rectangular ring with a single split and a parasitic metallic strip between these. The electric-magnetic coupling between rings generates a higher and lower frequency band and metallic strip is responsible for the middle band. A circular monopole patch antenna design with parasitic double T-shaped stubs and two inverted L-shaped stubs of unequal length behind the monopole patch on the partial ground plane is designed by Kumar et al. [178] to achieve four resonating frequencies of 2.5, 4.5, 5.7 and 7.7 GHz. Mathew et al. [179] proposed a coaxial probe fed sector shaped antenna with truncation at three corners. The truncation at respective corners produces three resonating frequencies of range '1.92 – 2.17' GHz for UMTS, '3.3–3.6' GHz for WiMAX and '5.1–5.3' GHz for ISM band.

A CPW fed asymmetric coplanar strip antenna designed by Li et al. [182] with reverse G-shaped slot and an U-shaped stub. In suggested antenna design, U-shaped stub is responsible for 2.4 GHz, asymmetric strip excites 5.2 GHz and reverse G – shaped slot produces the 3.5 and 5.8 GHz resonant frequencies respectively. Li et al. [183] suggested a CPW fed slot dipole antenna with two identical slot stubs with parasitic slots placed symmetrically along the arms of slot dipole antenna for generating three resonating frequency bands of range from 2.375 – 2.525 , 3.075 – 3.8 and 5.0 – 6.9 GHz respectively. Xu et al. in [184] proposed a CPW fed dual layer metallic structure composed of a square ring with S-shaped strip attached to the feed line and crooked U-shaped strips and three horizontal stripes on the other layer for generating triple resonating bands of range from 2.34 – 2.50, 3.07 – 3.82 and 5.13 – 5.89 GHz for WLAN/WiMAX applications. A bow-tie slot antenna and a thin strip line on it with rectangular tuning stub is designed by Yoon et al. [186] for producing three resonant frequencies of 2.4, 5.2 and 5.8 GHz in the 'WLAN' band. A cylindrical dielectric resonator antenna (CDRA) fed by modified microstrip line with vertical segment is prototyped by Sharma et al. [188] for producing multiband characteristics. The suggested antenna structure has five resonating frequencies ranging from '2.5 – 2.76 GHz, 3.38 – 3.54 GHz, 4.9 – 5.3 GHz, 5.5 – 5.61 GHz' and '5.78 -5.98 GHz' with broadside radiation pattern. Daniel et al. [189] developed an antenna for WiMAX and WLAN application by utilizing a ring monopole antenna in conjugation with ELC (Electric – Inductive – Capacitor) resonator and partial ground plane. The change in current direction on the suggested antenna by ELC metamaterial yields 3.74 and 5.1 GHz resonant frequencies. A dual band antenna using metamaterial based split ring structure with hexagonal complementary split ring resonator (HCSRR) and partial ground plane is designed

by Murugeshwari et al. [190] for ISM, WiMAX and WLAN band applications. The split ring excites the single resonant frequency from 3.44 – 5.84 GHz and HCSRR is responsible for 2.42 – 2.60 GHz frequency band.

The complex geometries, large size, and narrowband are some disadvantages of such structures. A modest and squeezed antenna design is discussed in this chapter to by-pass these shortcomings. The suggested antenna structure comprised of Y-shaped radiating element having horizontal, square and two hook shaped slits at opposite edges on partial ground plane to produce resonating frequencies in the WLAN/WiMAX band.

3.2 Antenna Design Configuration and Analysis

3.2.1 Design Procedure

The suggested antenna geometry is designed, optimized and analysed with full wave 'CST - Microwave studio'. Evolution process for final design is systematically explained by designing antenna designs from A–1 to A–4 as shown in figure 3.1

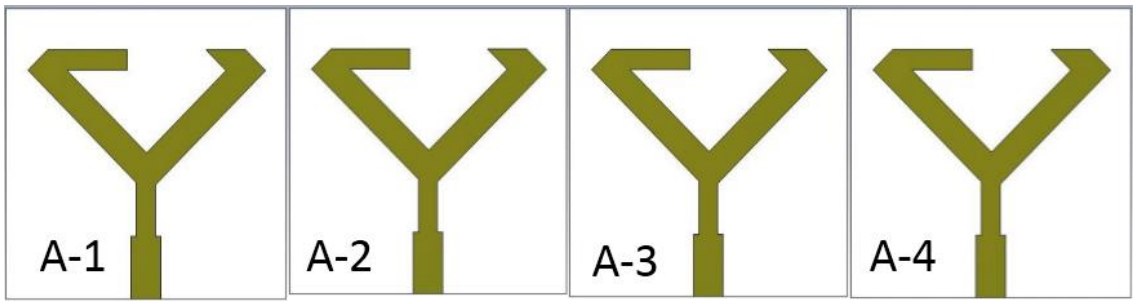

(a) Front side

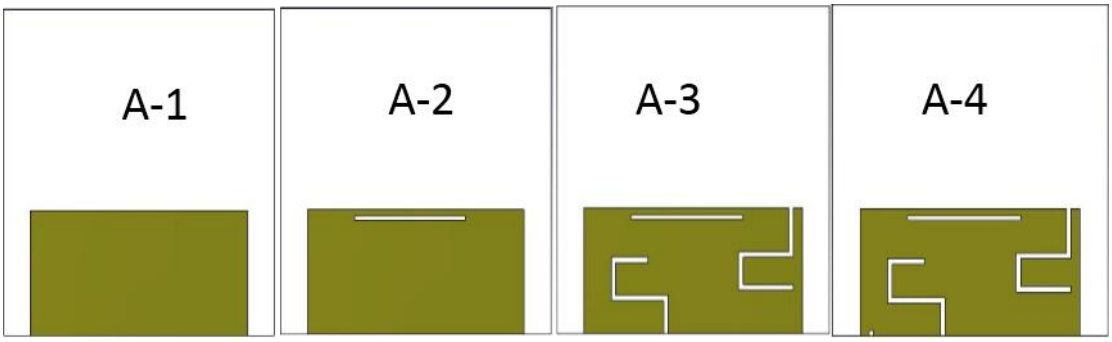

(b) Rear side

Figure 3.1 Evolution steps of proposed design

The proposed antenna structure is fed by a single microstrip feed line having two segments of varying lengths and widths to attain impedance matching of 50 Ω for all the resonating

frequency bands [191]. The parametric analysis and sweep are utilized to optimize antenna design and dimensions, which will be explained in the following sub-sections.

3.2.2 Ultra wideband (UWB) antenna design (A – 1)

In a number of UWB antenna designs [192-193], a combination of monopole radiating patch over partial ground plane is utilized for achieving compact, wideband antennas with stable radiation pattern. Here, a gap is devised between lower and upper edges of radiating patch and partial ground plane respectively to produce coupling capacitance. The coupling capacitance modifies the input impedance of the antenna and also helps in exciting closely spaced multiple harmonics of fundamental frequencies and their overlapping leads to wideband behaviour of the antenna structure [194]. Therefore, shape and design of ground plane is crucial to radiating structure as they determine the current flow. Any disturbance on ground plane modifies the current arrangement and ultimately the antenna performance.

The basic resonant frequency of antenna can be estimated by correlating antenna's area to that of a corresponding cylindrical monopole antenna of identical length and radius [194] is calculated from equation 3.1.

$$f_r = \frac{14.4}{L_p + L_g + g + R_p + R_g} GHz \qquad (3.1)$$

Where, L_p = Radiating patch length

L_g = Ground plane length

g = Gap

And R_p and R_g are the radius of cylindrical dipole corresponding to radiating and ground plane patch respectively as given by:

$$R_p = \frac{area\ of\ patch}{2\pi L_p \sqrt{\varepsilon_{re}}} = \frac{L_p W_p}{2\pi L_p \sqrt{\varepsilon_{re}}} \qquad (3.2)$$

$$R_g = \frac{area\ of\ ground}{2\pi L_g \sqrt{\varepsilon_{re}}} = \frac{L_g W_g}{2\pi L_g \sqrt{\varepsilon_{re}}} \qquad (3.3)$$

$$\varepsilon_{re} = \frac{\varepsilon_r + 1}{2} \qquad (3.4)$$

Where,

ε_r = Dielectric constant of substrate

ε_{re} = Approximate effective dielectric constant of air-substrate interface

In this design step, we start with a Y-shaped radiating patch with two arms of unequal length over partial ground plane with $h_g \times W_g$ mm^2 dimension as presented in figure 3.2. This asymmetry helps to achieve better impedance matching and also introduce multiple resonances to enhance the bandwidth. Together, the Y-shaped patch, the gap, and the ground plane work like the two arms of a dipole antenna. One arm is the monopole radiating patch and other arm is represented by mirror currents on the ground plane (due to image theory). Thus an analogous dipole antenna is formed by the gap (g), partial ground plane, and radiating patch. Since the radiation patterns and performance of planar printed monopole antennas typically resemble those of dipole antennas, they can be considered printed dipole antennas [195].

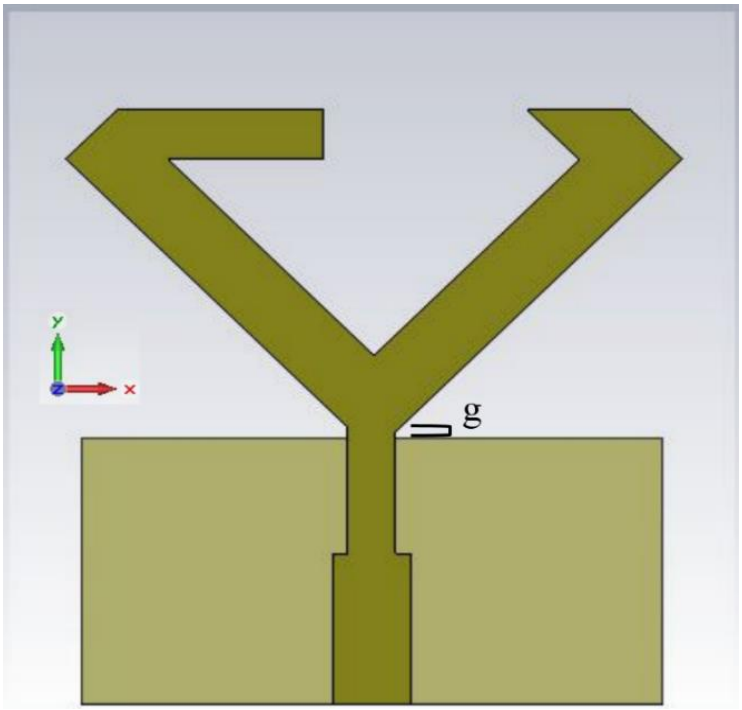

Figure 3.2 Suggested antenna A-1

For lowest cut off frequency, the radiating element length should be nearly equals to $\frac{1}{4}(\lambda_e)$, Where λ_e is effective wavelength. The ground element and radiating patch are optimized in simulation software for better impedance matching in the UWB. The value of lower cut off frequency is ≈ 2.97 GHz as approximated from equations 3.1 – 3.4 for 'L_p = 4.84 cm', 'L_g = 1.15 cm', 'g = 0.05 cm', 'R_p = 0.23 cm' and 'R_g = 0.02 cm'. It is observed from a simulated reflection coefficient plot against frequency that the antenna has resonating frequency band from 2.85 – 10.34 GHz, thus almost covers UWB, as shown in fig. 3.3.

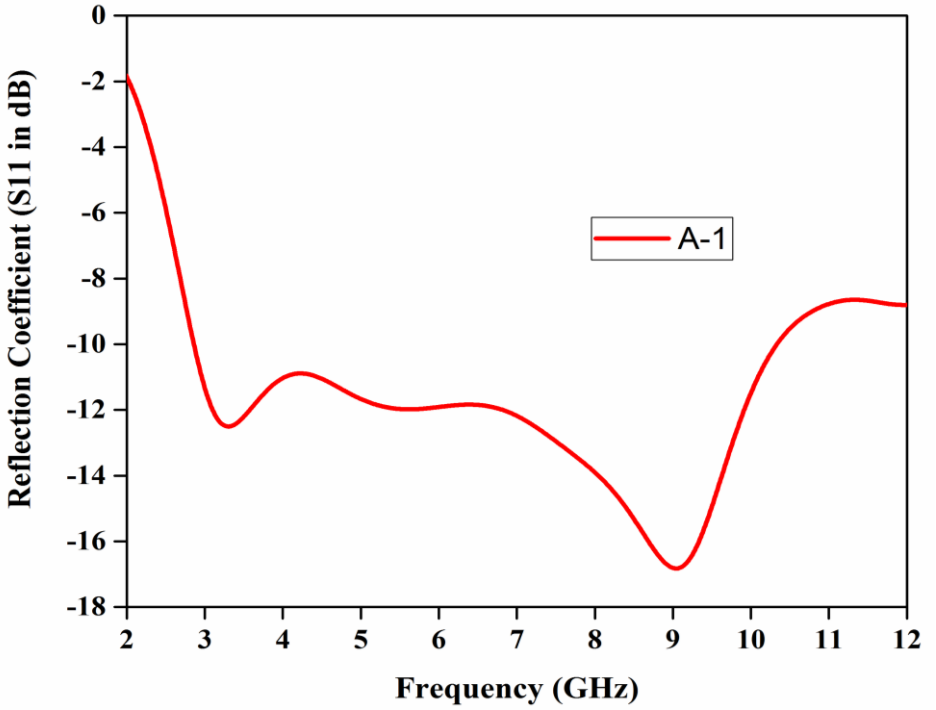

Figure 3.3 Simulated reflection coefficient vs frequency for antenna A-1

3.2.3 Wideband Antenna Design (A – 2)

As we know, the etching of slits on partial ground element is an effective technique to enhance the antenna performance by changes the surface current flow. When slits are introduced, they alter the natural path of current distribution on the ground plane, which directly affects the antenna's electromagnetic properties. These disruptions result in changes to the effective inductance and capacitance of the antenna structure. The geometry, length, and placement of the slits determine the degree to which these parameters are modified, thereby influencing the antenna's input impedance. This modification is critical because it allows the antenna impedance to be more closely matched with that of the microstrip feed line, typically 50 ohms.

Improved impedance matching leads to a reduction in reflected power and ensures that more energy from the feed line is efficiently transferred to the antenna for radiation [196–197]. Consequently, this enhances key performance metrics such as return loss, voltage standing wave ratio (VSWR), radiation efficiency, and bandwidth.

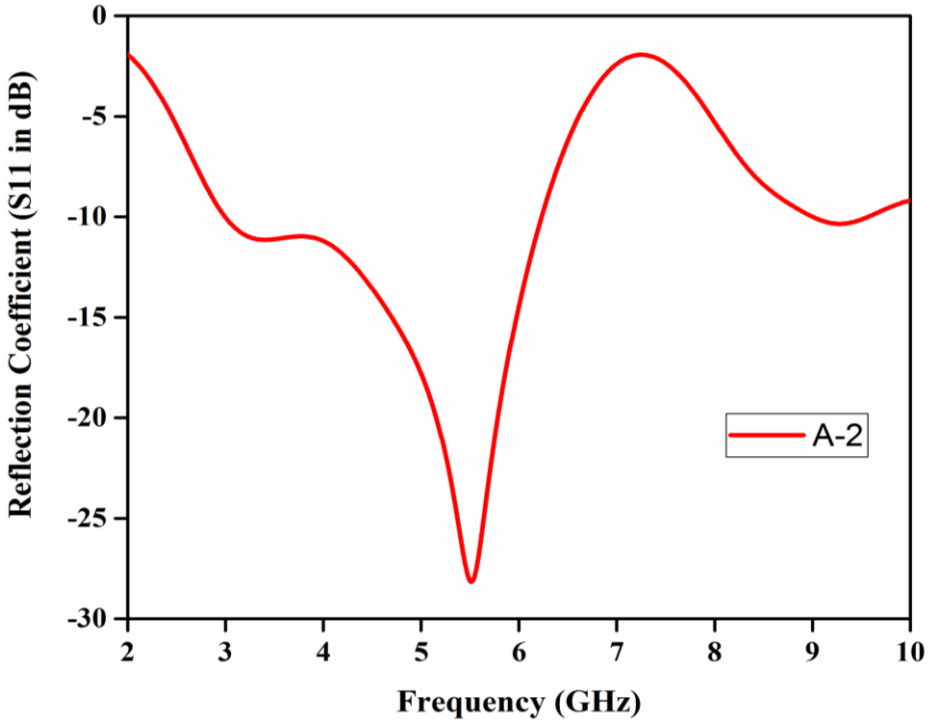

Figure 3.4 Simulated reflection coefficient (S11) vs frequency for antenna A-2

In this design step, a horizontal slit having length of '12.4 mm' and '0.4 mm' width is engraved on partial ground patch close to upper edge while keeping the other antenna dimensions intact as illustrated in figure 3.1(b). From reflection coefficient plot in figure 3.4, it is noticed that the antenna has single resonating band from 2.98–6.24 GHz with resonant frequency of '5.51 GHz'. Thus, a slit on the ground element modify the UWB antenna into a single wideband antenna. The resultant structure is termed as antenna A-2.

3.2.4 Multiple band Antenna design (A –3)

In this design step, the wideband antenna A-2 undergoes further modification to achieve triple-band operation. This transformation is accomplished by engraving two hook-shaped slits into the ground plane, originating from the respective side edges, as illustrated in Figure 3.5(b). These hook-shaped slits serve as additional resonant structures that introduce new current paths and localized resonances. By altering the current distribution and creating

specific reactive effects (inductance and capacitance), these slits help to generate and isolate multiple resonant modes within the desired frequency bands. The resulting structure, labelled as antenna A-3. The above mentioned is further evidenced from the plot of reflection coefficient against frequency for various vertical and horizontal slits as depicted in figure 3.6 (a)-(b). These plots clearly demonstrate how the introduction of the hook-shaped slits contributes to the emergence of multiple resonance dips, confirming the successful transformation from a wideband antenna to a triple-band antenna. This design approach highlights the usefulness of geometrical manipulation in ground plane engineering to tailor antenna performance for specific multi-band applications.

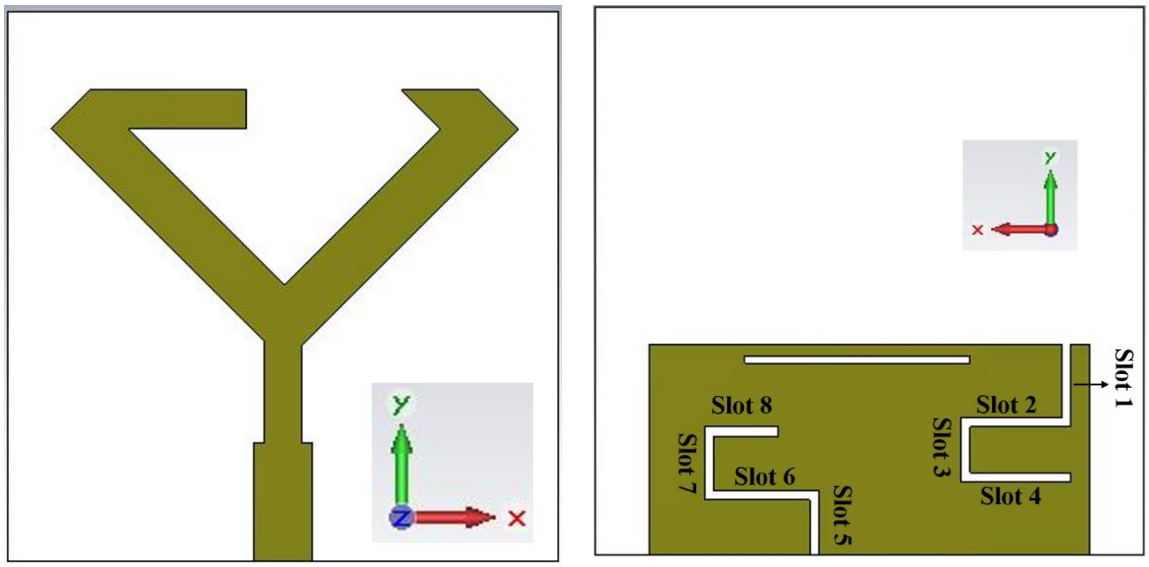

(a) Front side (b) Rear side

Figure 3.5 Proposed geometry of antenna A-3

From presented plot in figure 3.6(a), it is noticed that for vertical and horizontal slit on the partial ground plane from the upper edge that an additional second band of range from '2–3 GHz' starts appearing for respective slots from 1–4. The engraving of the second hook from the lower side of the partial ground plane by successive horizontal and vertical slits adjusts the second band within prescribed frequency range and also produces an additional band from '3–4 GHz' as shown in figure 3.6(b). Thus etching of two hooks on ground structure transforms the wide band antenna into a triple band antenna. The antenna has three resonating frequencies ranging from '2.54 – 2.74, 3.1– 4.4 and 4.6 – 6.1 GHz' with '2.64, 3.40' and '5.64 GHz' resonant frequencies.

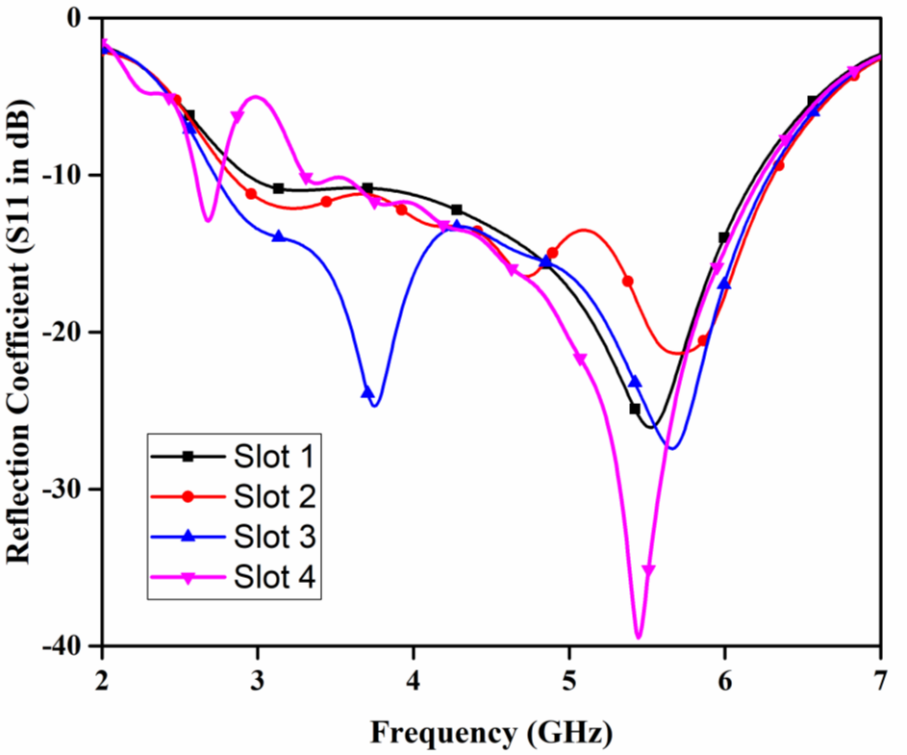

(a) First hook from upper edge

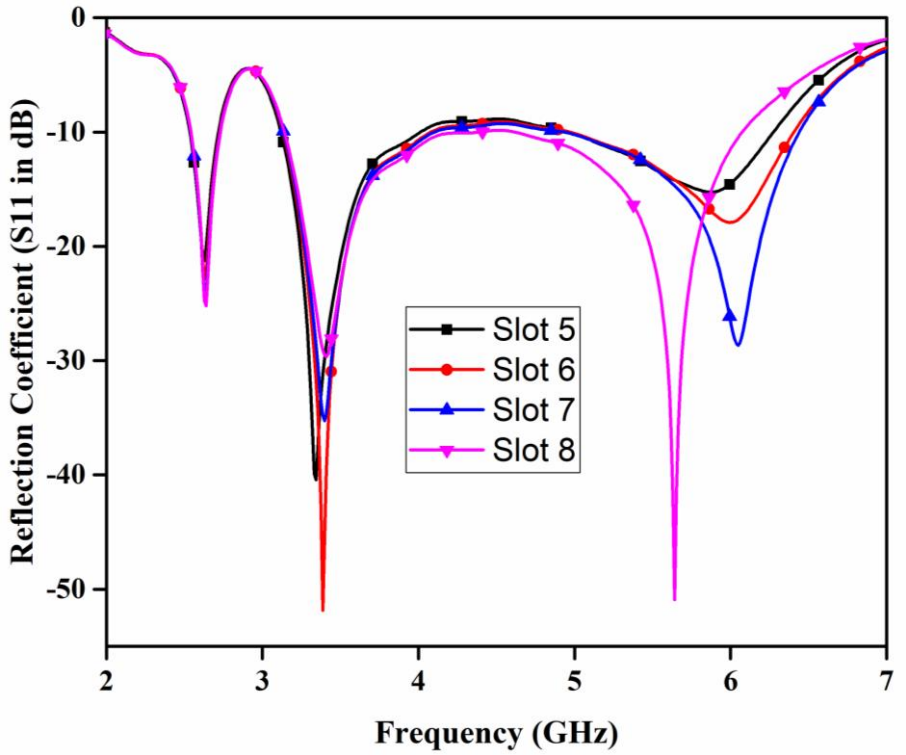

(b) Second hook from lower edge

Figure 3.6 Simulated reflection cofficient (S11) vs frequency for antenna A–3

3.2.5 Final Antenna Design A – 4

Although, the three resonating frequencies of antenna A-3 covers the notified frequency bands for WLAN and WiMAX. The range of these bands are quite large compared to the prescribed limit. A square slit of 0.5 mm is engraved on partial ground plane near to bottom hook without changing the other dimensons, squeeze the frequency bands with the prescribed limit as shown in figure 3.7 (b). The new antenna layout is labelled as A-4.

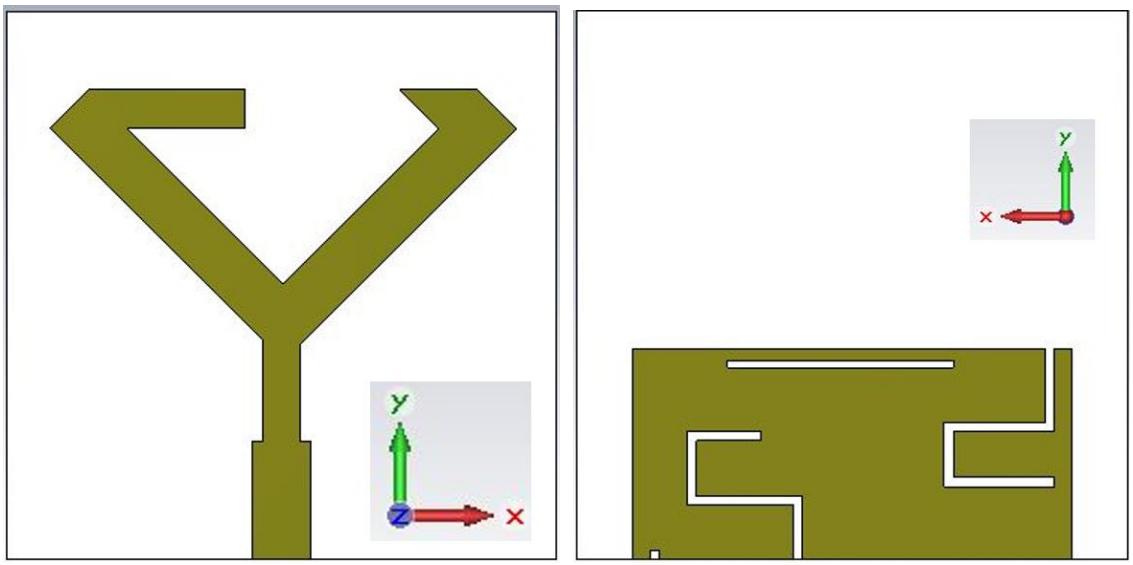

(a) Front side (b) Rear side

Figure 3.7 Final proposed antenna design A-4

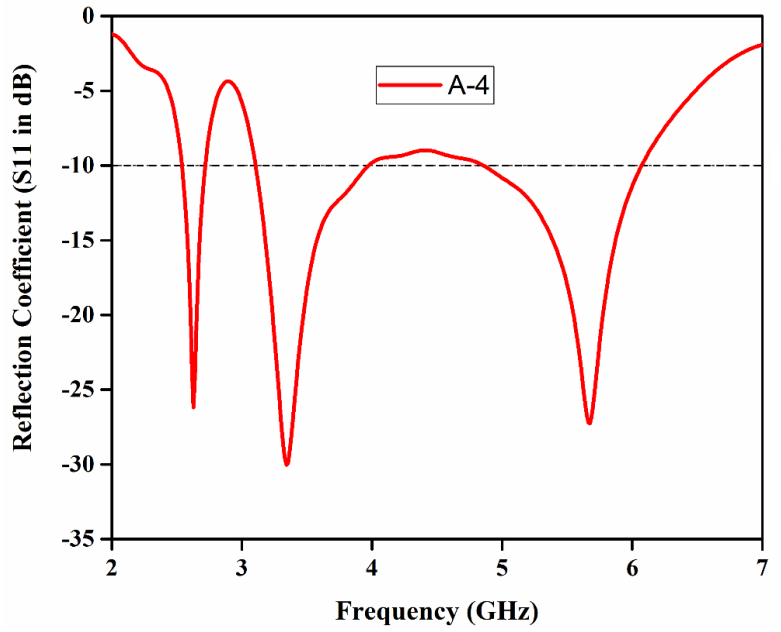

Figure 3.8 Simulated reflection coefficient (S11) vs frequency for antenna A-4

The simulated reflection coefficient vs frequency plot for antenna A– 4 presented in figure 3.8 supports the above stated. The new resonating band covers frequency range from '2.52 – 2.72, 3.1 – 3.94' and '4.86 – 6.1 GHz' with '2.63, 3.34' and '5.67 GHz' resonant frequency. A squeeze in the frequency bands are visible when compared with the resonating bands of antenna A–3. Although insignificant compression in the first and second band is observed, significant compression is obtained in the third band.

3.2.6 Surface Current Distribution

The surface current distribuitions of antenna A-4 at resonant frequencies '2.63, 3.34' and '5.67' GHz are illustrated in figure 3.9(i)–(ii) explains the working mechanism [7] and interdependence between resonant frequencies and antenna parameters. At the first resonant

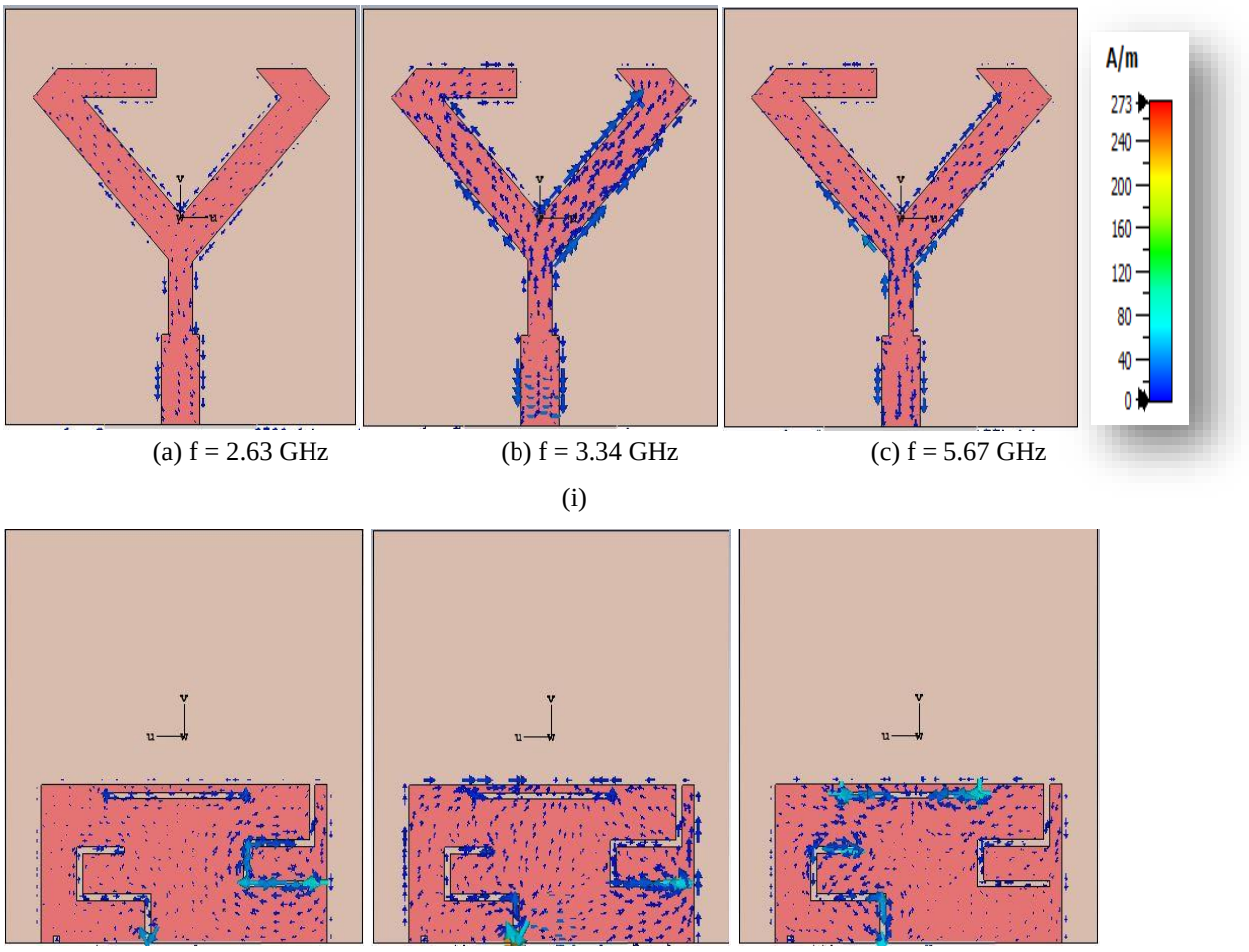

(a) f = 2.63 GHz (b) f = 3.34 GHz (c) f = 5.67 GHz

(i)

(d) f =2.63 (e) f =3.34 GHz (f) = 5.67 GHz

(ii)

Figure 3.9 Surface current distribution at resonant frequencies (i) front view (ii) rear view

frequency of 2.63 GHz, figures 3.9(a) & (d) show that the surface current is predominantly concentrated around the upper hook of the radiating element, with significantly weaker current observed across the remaining portions of the structure. This indicates that the upper hook plays a dominant role in determining the resonance at this frequency. While at '3.34' GHz, the surface current is more intensely concentrated along the shorter arm of the radiating element rather than the longer arm as depicted in figure 3.9 (b) & (e) . Additionally, there is noticeable current flow around the horizontal slit and both hook-shaped slots, suggesting their combined influence in enabling resonance at this intermediate frequency. At the highest observed resonant frequency of 5.67 GHz, figures 3.9(c) & (f) reveal that the surface current becomes more uniformly distributed across both arms of the radiating element, with a higher density of current around the horizontal slit and the lower hook on the ground plane. This pattern indicates that these features contribute significantly to the antenna's response at higher frequencies.

3.3 Final Antenna Design for WLAN/ WiMAX bands

Final antenna structure is presented in figure 3.10 (a)–(b), is fabricated on a '1.59 mm' thick 'FR-4' substrate with 'relative permittivity (ε_r)= 4.4' and 'loss tangent (tan δ) = 0.025'. The antenna has an overall volume of '30×30×1.59' mm^3. The optimized dimensions of antenna structure are tabulated in Table 3.1.

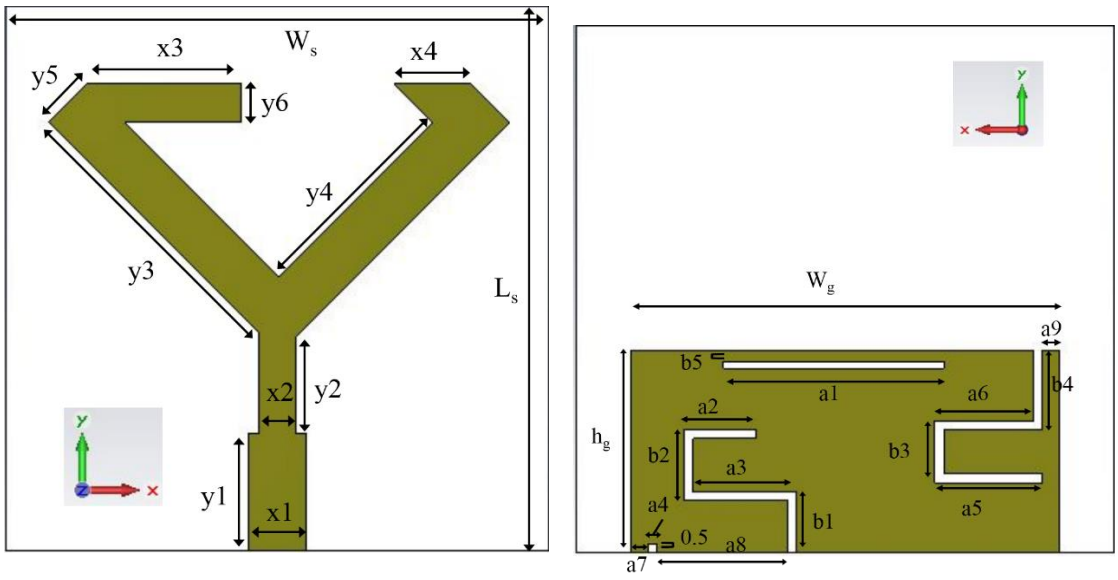

(a) (b)

Figure 3.10 Proposed antenna geometry (a) top side (b) bottom side

TABLE 3.1 Optimized dimensions of proposed antenna design

Parameters	**L_s**	**W_s**	**h_g**	**W_g**	**x1**	**x2**	**x3**	**x4**	**y1**	**y2**	**y3**	**y4**	**y5**	**y6**
Value (mm)	30	30	11.5	24	3.2	2	9	4.24	6.5	5.47	16.45	12	3	2.12
Parameters	**a1**	**a2**	**a3**	**a4**	**a5**	**a6**	**a7**	**a8**	**a9**	**b1**	**b2**	**b3**	**b4**	**b5**
Value (mm)	12.4	3	5.75	0.5	6	5.5	1	7.25	1	3.5	4	3.5	4.5	0.6

3.4 Simulated and Measured Result

The final optimized antenna design is prototyped on 'FR-4' substrate as displayed in figure 3.11 (a). The fabricated antenna is tested for reflection coefficient with Agilent (N5234A) vector network analyzer ('VNA') and beam pattern is observed in an anechoic chamber. The photograph of antenna under test is depicted with VNA and in an anechoic chamber in figure 3.11 (b) and (c) respectively.

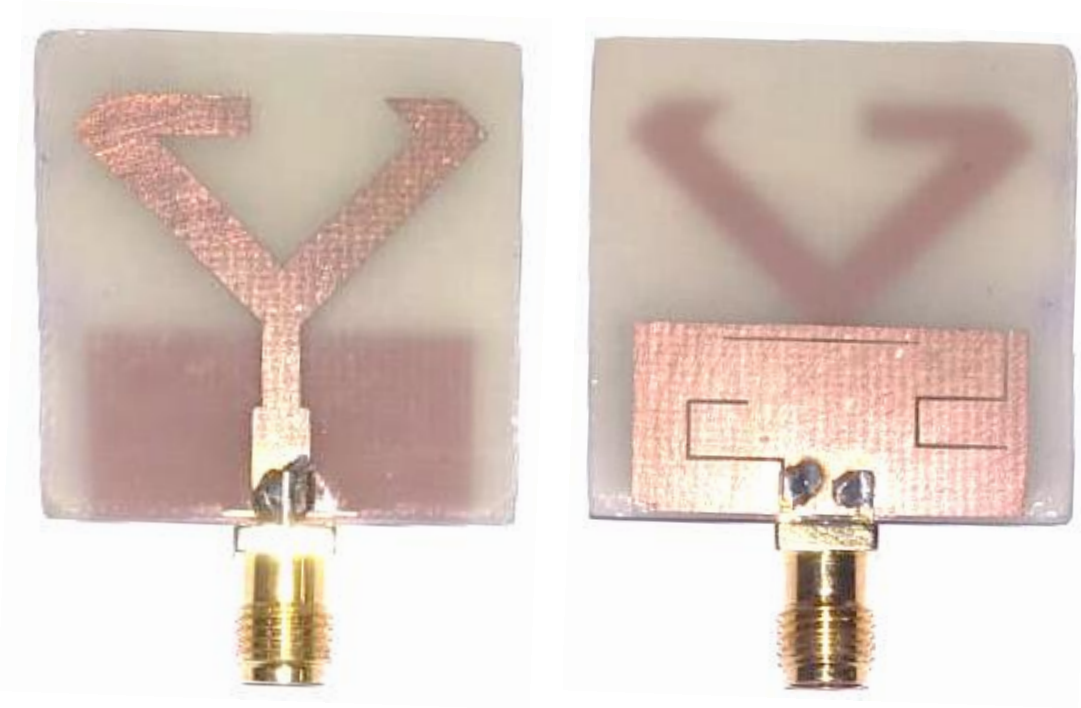

(a) Fabricated antenna with top and bottom view

(b) S_{11} measurement of prototyped antenna with VNA

(c) Fabricated antenna under measurement in anechoic chamber

Figure 3.11 Antenna measurement setup

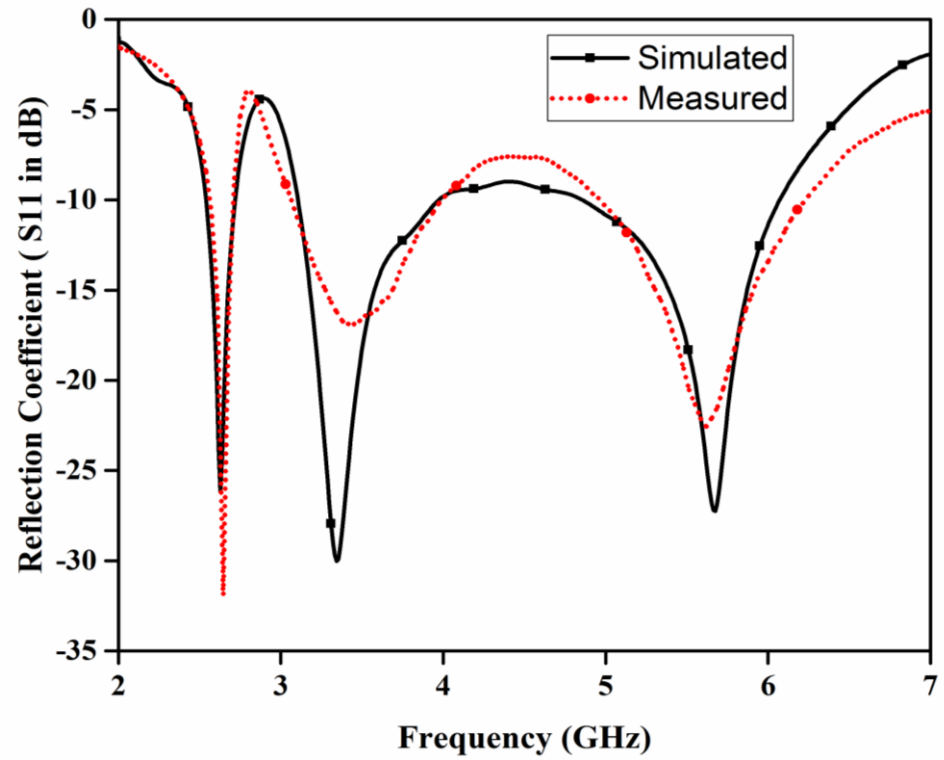

Figure 3.12 Simulated and measured reflection coefficient vs Frequency plot

The measured and simulated reflection coefficient of the fabricated design is presented in figure 3.12 shows very good matching of result with minor discrepancies. The -10 dB impedance

bandwidths of suggested design are ‘150 MHz’, ‘920 MHz’ and ‘1210 MHz’ in the frequency range of ‘2.55 – 2.70 GHz’, ‘3.06 – 3.98 GHz’ and ‘4.99 – 6.2 GHz’ respectively with resonant frequencies at ‘2.68’, ‘3.75’ and ‘5.72 GHz’.

The simulated and measured radiation pattern for ‘E-field’ (xz – plane) and ‘H – field’ (yz – plane) at ‘2.68’, ‘3.75’ and ‘5.72 GHz’ is presented in figure 3.13. Omnidirectional radiation pattern is observed for E- field at 2.68 GHz with bidirectional patterns are observed for remaining frequencies, while toroidal shaped radiation patterns are obtained in H-field for all three frequencies. The peak antenna gains of 0.5, 1.08 and 2.4 dBi for frequencies at 2.68, 3.75 and 5.72 GHz are obtained respectively from the gain plot as displayed in figure 3.14. Also, from total efficiency vs frequency plot in figure 3.15, it is observed that the total efficiency of designed antenna is lying between 50 – 80%, 58 – 74% for first and second resonant band respectively and also more than 70% for third resonant band. The simulated and measured results are tabulated in Table 3.2.

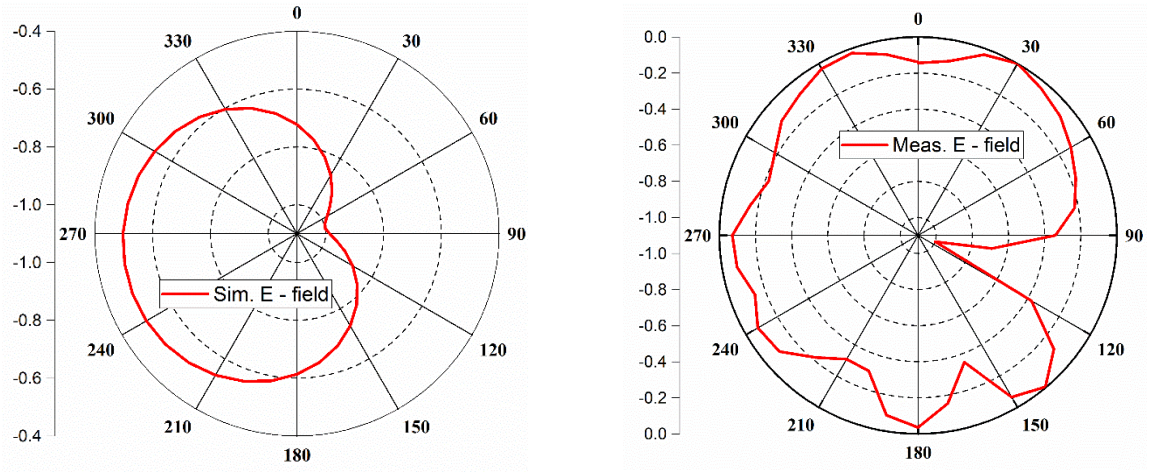

(a) f = 2.68 GHz

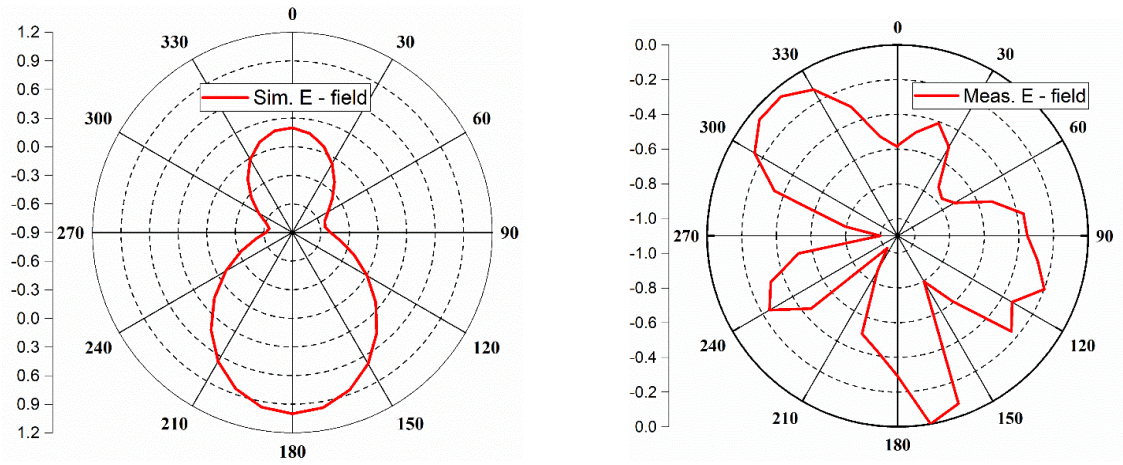

(b) f = 3.75 GHz

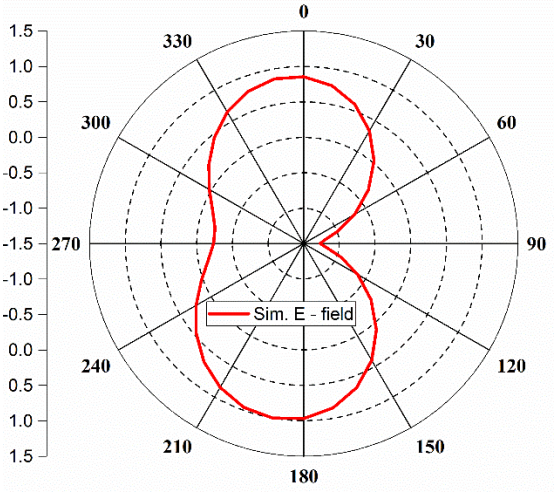

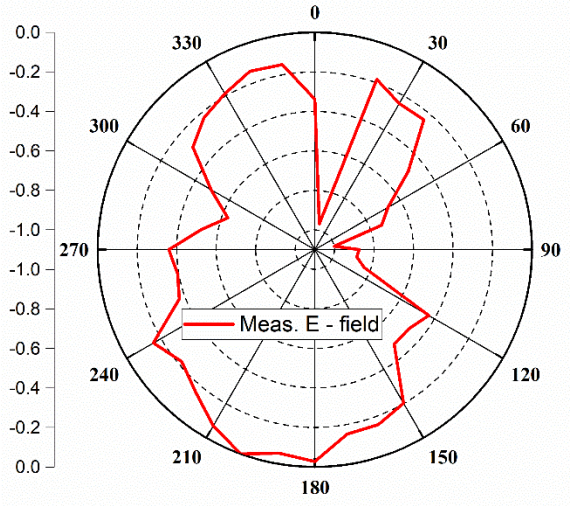

(c) f = 5.72 GHz

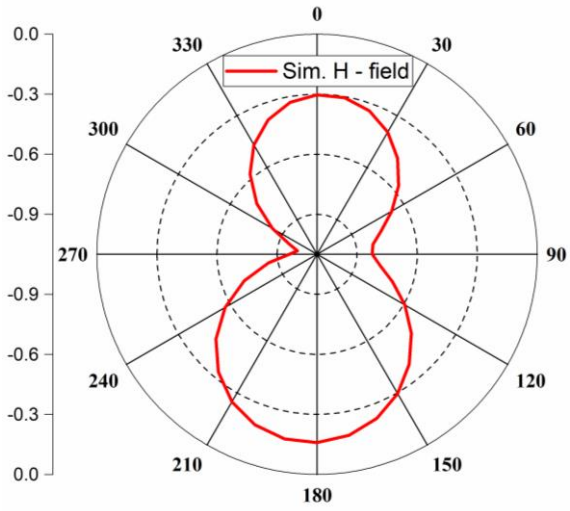

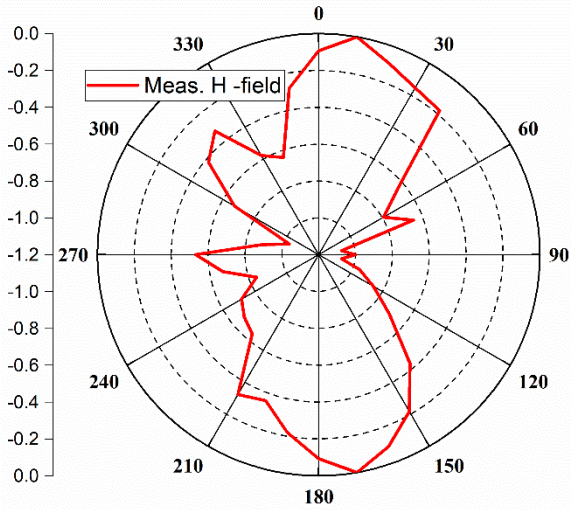

(d) f = 2.68 GHz

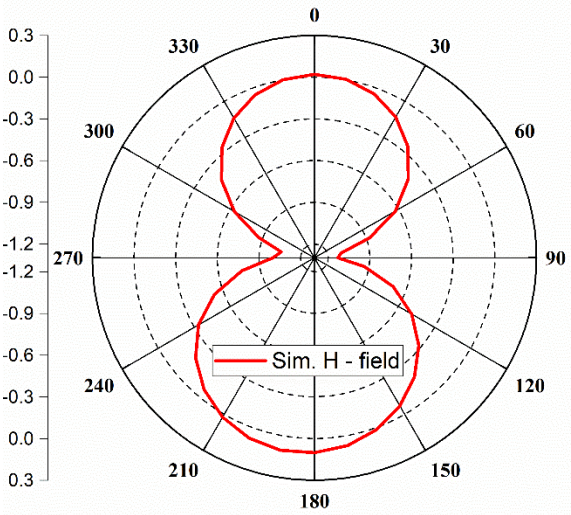

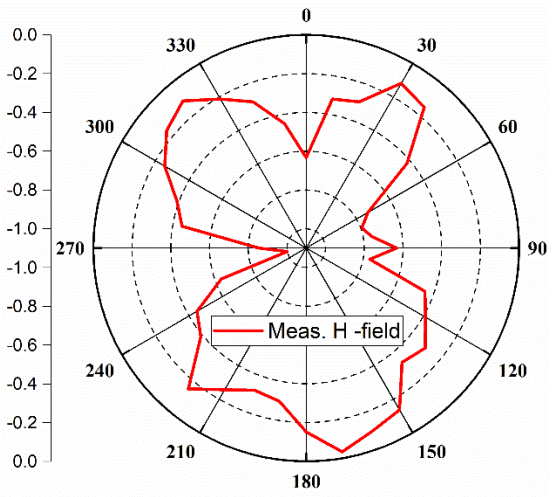

(e) f = 3.75 GHz

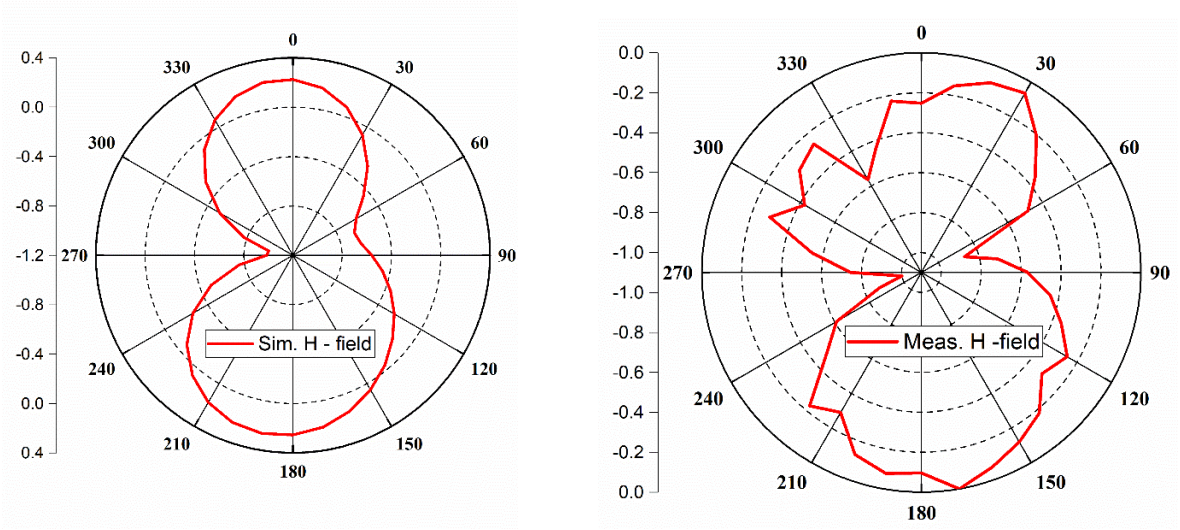

(f) f = 5.72 GHz

Figure 3.13 Simulated and measured radiation pattern for 2.68, 3.75 and 5.72 GHz

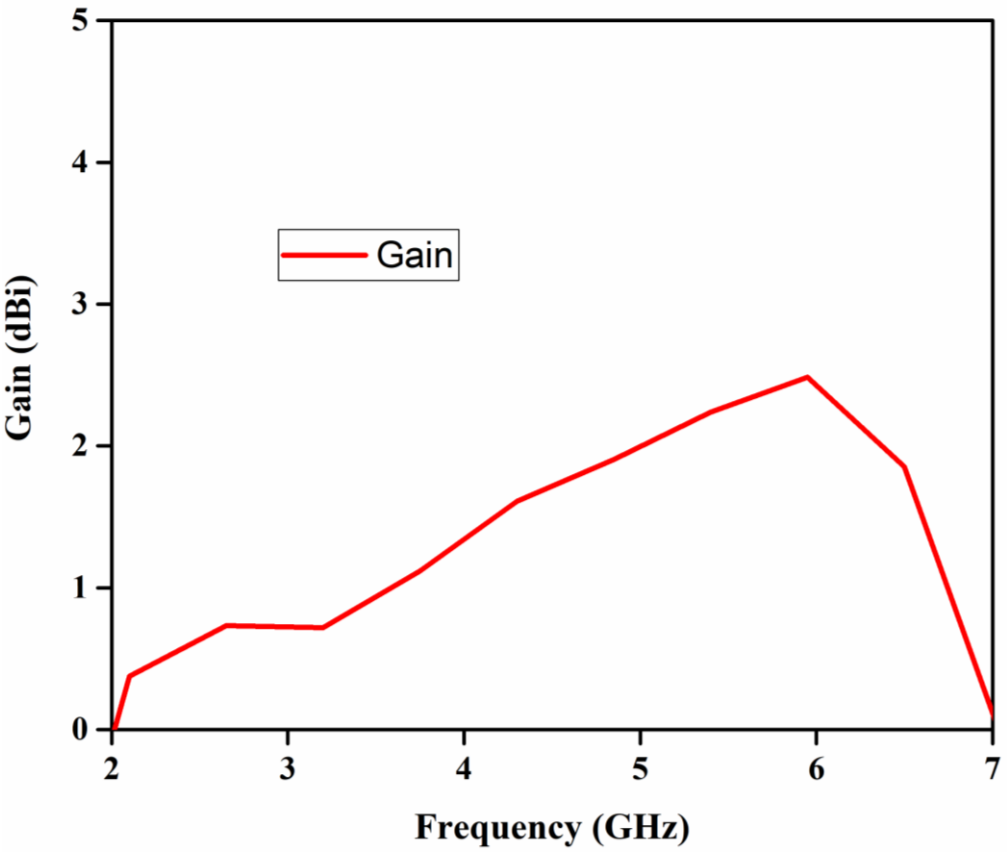

Figure 3.14 Gain vs frequency

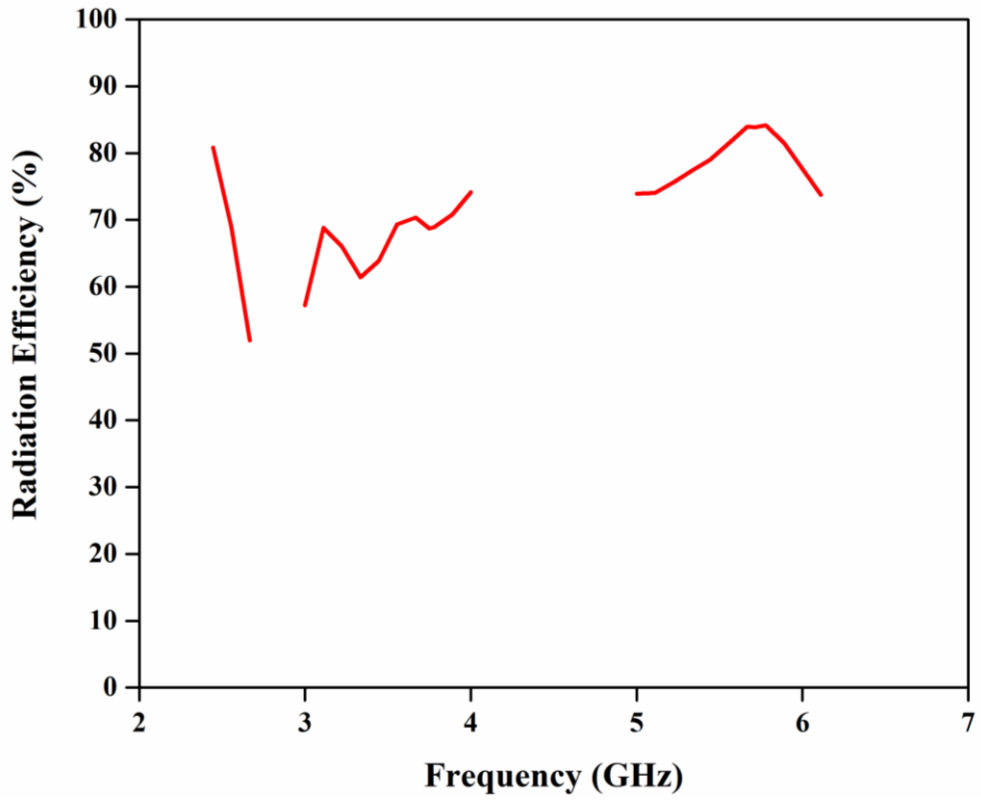

Figure 3.15 Total Efficiency vs frequency

Table 3.2 Summarized results of antenna

S. No.	Operating Band		BW		Meas. Reso. Frequency	Gain
	Simulated	Measured	Simulated	Measured		
	(GHz)		(GHz)		(GHz)	(dBi)
1	2.52 - 2.71	2.55- 2.70	0.19	0.15	2.68	0.5
2	3.11 – 4	3.06- 3.98	0.89	0.92	3.75	1.08
3	4.84 - 6.05	4.99 – 6.2	1.21	1.21	5.72	2.4

3.5 Comparison with Similar Antennas

Table 3.3 compares the measured outcomes of the suggested antenna design with earlier research. Comparing the presented antenna to other published designs, it is comparatively small, has a straightforward structure, and has many resonating bands with a respectable impedance bandwidth (IBW).

Table 3.3 Comparison of suggested antenna design with reported work

Reported Works	**Dimensions (mm)**	**Material**	**Frequency Bands (GHz)**	**Resonant Freq. (GHz)**	**BW (%)**
[172]	50×50×1.6	FR-4	2.08 - 2.17 3.47 - 3.54 5.325 - 5.675	2.12 3.5 5.6	4.2 2 6.2
[173]	40×54×1.6	FR-4	2 - 2.6 3.21 - 3.51 3.8 - 6.38	2.4 3.4 5.8	26 8.9 50.6
[176]	28.1×32×1.6	FR-4	1.5 - 2.2 4 - 4.3 6 - 7 8.2 - 10.68	1.85 4.15 6.5 9.5	40 7.23 15.4 26
[177]	30×35×1.6	FR-4	2.3 - 2.62 2.63 - 2.9 3.3 - 4.8 5 - 8.02	2.46 2.765 4.05 6.51	13 9.74 37 46.4
[179]	40×50×1.6	FR-4	1.92 - 2.16 3.5 - 3.68 5.16 - 5.36	2.06 3.56 5.2	11.2 5.14 3.9
[180]	35×45×1.5	Arlon AD255A	2.33 - 2.55 3.40 - 3.56	2.4 3.5	9.16 7.43

			4.26 - 8.11	5.8	66.4
[181]	26×36×1.6	ε_r = 3.5	2.38 - 2.82 3.32 - 3.88 5.13 - 6.53	2.6 3.6 5.83	16.9 15.6 6.86
[182]	35×19×1.6	FR-4	2.38 - 2.5 3.35 - 3.67 4.76 - 6.55	2.45 3.5 5.5	4.89 9.14 32.5
[183]	30×65×1.6	FR-4	2.375 - 2.525 3.075 - 3.8 5 - 6.9	2.45 3.5 5.2, 5.8	6.1 21.1 31.9
[185]	70×44×1.6	FR-4	2.35 - 2.77 5.47 - 6.10	2.5 5.8	16.4 10.9
Proposed Design	25.5×26×1.6	FR-4	2.55 - 2.7 3.06 - 3.98 4.99 - 6.2	2.68 3.75 5.72	5.6 26.67 21.53

3.6 Summary

This chapter presents the stepwise design process and detailed working mechanism of a microstrip line fed Y-shaped patch antenna having slits on ground patch to achieve multiple resonating bands in the frequency range from 2-6 GHz. The proposed design has resonating frequencies from 2.55 – 2.7, 3.06 – 3.98 and 4.99–6.2 GHz with fractional bandwidth of 5.6 %, 26.67 %, 21.53 % and 0.5, 1.08, 2.4 dBi gain respectively. The antenna design is appropriate for WLAN and WiMAX applications owing to its simplistic shape, small size, wideband, numerous bands, and steady radiation pattern.

CHAPTER 4

ANNULAR RINGS ANTENNA WITH FREQUENCY & POLARIZATION AGILITY

* A. Sharma, S. Khah and S. Rawat, “Annular rings antenna for WiMAX and WLAN application with frequency and polarization diversity”, Evergreen journal of Novel carbon resource sciences and green asia strategy, vol. 11, no. 4, pp. 3156 – 3163, 2024.

ANNULAR RINGS ANTENNA WITH FREQUENCY & POLARIZATION AGILITY

4.1 Introduction

In recent times, wireless communications are evolving rapidly and led to the development of various innovative services like GPS, Wi –Fi, GSM, WLAN, WiMAX, Bluetooth etc. to meet the end user requirement. Each application involves a unique frequency band with polarization and radiation characteristics, hence requiring a dedicated antenna [97], [110], [198–199]. So to avail these services, generally antennas with fixed properties like frequency, polarization and radiation pattern are integrated in a wireless system. The integration of multiple antennas in a single entity results in an expensive and bulky structure with increased complexity. Thus we need an efficient antenna system of smaller size, wide band, multifunctional and inexpensive to accommodate the needs of emerging wireless communication technologies. The reconfigurable antennas appeared as suitable candidates to address these issues. Reconfigurable antennas by utilizing adaptable and dynamically controlled geometries offer more functionalities over conventional antennas and deliver improved performances with same throughput as a multi–antenna system without enlarging its size [25], [32].

The reconfigurable antennas are broadly classified into two types on the basis of the number of reconfigurable parameters i.e. single and compound reconfigurable antennas. The single reconfigurable antenna is of frequency reconfigurable, polarization reconfigurable and pattern reconfigurable types. In literature, several antenna designs with single tunable parameters like frequency [200–203], pattern [125], [204–206] and polarization reconfigurable [112], [117], [207–208] have been reported. In the rapidly changing world, it is expected that reconfigurable antennas must possess the ability to alter multi-parameters. So compound reconfigurable antennas have received considerable attention in next generation wireless communication because of various attractive features which add more flexibility, diversity in the existing antenna system and enhance its performance in diverse communication environments. The compound reconfigurable antennas are further subdivided on the basis of integrated characteristics and are of following types like ‘frequency–polarization’, ‘frequency–pattern’, ‘polarization–pattern’ and ‘frequency–polarization–pattern’ reconfigurable antennas. Hybrid reconfigurable antennas have many advantages over the single reconfigurable antenna but pose significant challenges to antenna engineers in terms of implementing reconfigurability

functionality into the system to make it more efficient without severely degrading the antenna performance [33], [209].

The frequency and polarization diversity antenna has offered various advantages such as efficient spectrum utilization by frequency reuse, minimizing multipath fading with increased system capacity and may be used in next generation communication system like cognitive radio (CR), frequency hopped spread spectrum (FHSS) and software defined radios (SDR), which can be reconfigured for communicating using diverse protocols operating at different frequencies and polarizations. A number of antenna designs with frequency and polarization reconfigurability had fabricated successfully by employing PIN diodes, varactor diodes, MEMS switches and other methods [136–137], [139], [191], [210 – 216].

A diagonal fed square patch antenna with shorting post on vertical and horizontal sides for frequency and polarization diversity is designed by Qin et al. [136]. The loading of the shorting post on square patch via varactor diodes produces the continuous resonant frequency switching in 1.35–2.25 GHz frequency band. The loading of either vertical or horizontal shorting post via PIN diodes produces either vertical or horizontal linear polarization in the above band, while simultaneous loading of all shorting posts produces the resonating frequency band from 1.35–1.9 GHz with linear polarization in 45° direction. Trong et al. [210] designed a circular patch antenna fed at midpoint with switchable shorting post on its periphery that can be loaded on patch through PIN diodes for reconfiguration operations. The switching ON/ OFF of a set of PIN diodes creates a radiating slot and cavity of variable lengths with controllable location, which can produce the multiple resonance frequencies with linear polarization of different orientation angles. Hu et al. [137] designed a square radiating element antenna having PIN diode controlled shorting posts on patch and perturbation elements on its corner for frequency and polarization switching. The switching of shorting posts on square patch via PIN diodes gives the eight discrete resonant frequencies within 1.7–2.8 GHz and loading of alternate diagonal and all perturbation elements gives the LHCP, RHCP and linear polarization respectively for the resonating frequencies.

The switchable radiating elements with trimmed corner techniques are employed in [211–212] to achieve the frequency and polarization diversity. Anantha et al. in [211] designed a square patch antenna with trimmed corners and rectangular ring within square patch for reconfiguration operation. Activation of PIN diodes between patch and ring produces the frequency switching between 5.2 GHz and 5.8 GHz, while loading of either alternate diagonal

or all corners via PIN diodes produces either LHCP and RHCP or linear polarization respectively for each frequency band. A square patch having diagonally trimmed two corners with L-shaped radiating elements on both sides of the patch at upper portion is designed by George [212] for frequency and polarization switching. The loading or unloading of L-shaped elements via PIN diodes gives the frequency reconfiguration between GLONASS (global navigation satellite system), WLAN and WiMAX bands. On the other hand loading of truncated corners on patch via p-i-n diodes provides polarization reconfiguration in between linear and circular states. A rectangular monopole antenna was built by Liu et al. [213] with a reflector for frequency and polarization agility and two PIN diodes across the slotted ground plane. The simultaneous switching ON or OFF both diodes produces the linearly polarized radiation with resonant frequency reconfiguration between 2.35 GHz and 2.62 GHz respectively. Meanwhile, alternate switching of PIN diodes produces circular polarization in resonant frequency of 2.22 GHz with left and right hand orientation respectively. Liang et al. [214] suggested an antenna geometry for frequency and polarization agile operation by utilizing electronic band gap (EBG) structure. The EBG comprises two identical orthogonal metallic rectangular patches array with varactor diodes in each layer. The wideband CPW fed monopole antenna is upper positioned on EBG surface and adjusting the biasing of varactor diodes in each layer provides the LHCP and RHCP switching for each resonating frequency in 1.03–1.54 GHz band.

A tunable feed network is utilized for reconfiguration operations. Two concentric circular patch antennas joined at vertical and horizontal locations via varactor diodes and fed at two orthogonal positions designed by Babakhani et al. in [139]. The alternate activation of vertical or horizontal sets of diodes with excitation at single port produces the continuous varying resonating frequency from 1.17–1.58 GHz with vertical and horizontal linear polarizations respectively, while activating all the diodes and employing excitation at both ports with 90° phase difference results in circular polarization with left and right hand switching. Sedhaghara et al. [191] designed a concentric rings slot antenna with tunable stubs on both sides of the substrate. The loading or unloading of stubs on radiating elements and feed network via PIN diodes gives frequency and polarization diversity. The activation of the outer ring and tunable stubs produces 2.4 GHz resonant frequency with linear and circular polarization with left and right hand rotation. Similarly, excitation of the inner ring with alternate tuning stubs in the feed network produces a resonant frequency of 3.5 GHz having LHCP and RHCP. A circular patch with an outer circular ring fed at two ports by ‘open stub cascaded branch-line coupler’

(OSCBLC) feed network [215] is designed by Muthuvel et al. for frequency and polarization reconfiguration. The biasing of four varactor diodes between ring and patch produces continuous frequency tuning from '2–3' GHz and polarization switching in horizontal and vertical linear polarization via exciting one port at a time, also switching in left and right hand circular polarization via activating both ports with phase difference of ± 90°.

Ni et al. developed a metasurface based antenna for frequency and polarization diversity [140]. Here, a metasurface composed of sixty four identical patches is placed above on dual slot antenna and a metallic reflector placed behind this configuration. Relative adjustment between antenna, metasurface and reflector produces the resonant frequency reconfiguration in 8–11.2 GHz band, while the rotation of metasurface relative to the center of the slot antenna gives the linear, LHCP and RHCP in the resonating band.

The methods like switchable shorting posts, tunable radiating and feed network, trimmed corners, metasurface, EBG and etc. are utilized in above discussed antennas for frequency and polarization diversity. In this chapter, we primarily design a simple microstrip line fed reconfigurable annular rings antenna with slit etched on partial ground plane and PIN diodes on one ring for frequency and polarization diversity. The following sections of this chapter provide a systematic presentation and explanation of the design process and outcomes of the suggested antenna.

4.2 Antenna Design Specifications and Analysis

'Computer Simulation Technology−Microwave Studio (CST-MWS)' is utilized to simulate the proposed antenna arrangement. This section involves the systematic description of antenna design steps from Antenna–1 to Antenna–4 as shown in figure 4.1 along parametric analysis and organized explanations in terms of performances are provided in detail for better understanding the relationship between antenna dimensions, axial ratio and impedance bandwidth.

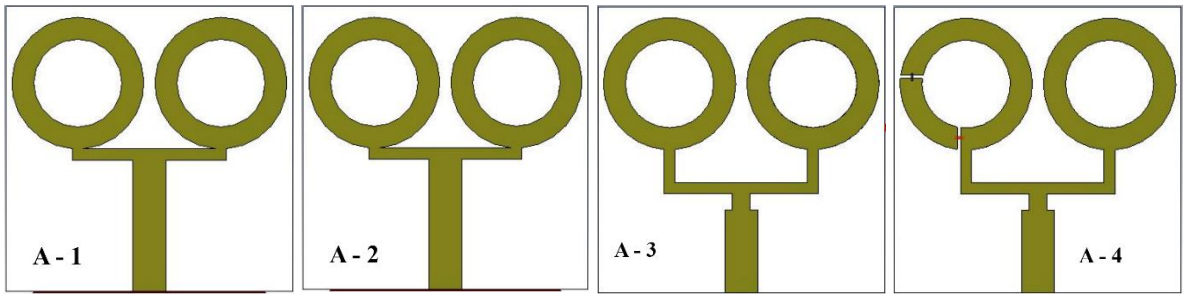

(a)

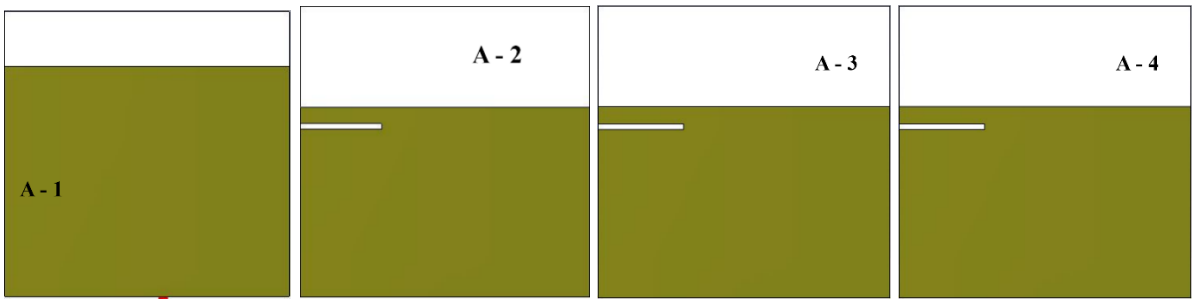

(b)

Figure 4.1 Evolution steps of proposed antenna deign (a) top view (b) rear view

4.2.1 Empirical Equations and Design Procedure to Narrowband Antenna – 1 (A – 1)

The proposed antenna design utilizes annular rings as the primary radiating elements, which significantly enhances its radiation characteristics. Unlike traditional antenna structures with a single outer edge, an annular ring features two distinct edges—an inner and an outer radius. This dual-edge configuration results in an increased number of discontinuities where the electric field can "fringe" or extend into the surrounding space, thereby generating stronger fringing fields. These intensified fringing fields contribute directly to improved radiation performance, making the annular ring-based design superior to those using simpler, single-edged radiating structures [217].

From the cavity model, the peripheries of a ring [218] are replaced by magnetic walls. This modelling approach assumes that there is no magnetic field component in the direction of wave propagation, which is a key characteristic of Transverse Magnetic (TM) modes. These modes are referred as TMnm modes, and describes the field distribution within the ring structure. The ability of the annular ring to support multiple TM modes further contributes to its versatile and enhanced radiation performance, making it a suitable candidate for modern multi-band or broadband antenna applications.

The average circumferential length of the ring is equated to wavelength in order to approach the resonance frequency of dominant mode (TM_{11}) for typical annular ring patch antennas [191], [219]. The following are the empirical equations.

$$\lambda = \pi(R_i + R_o) \qquad (4.1)$$

$$f = \frac{c}{\pi\,(R_i+R_o)\sqrt{\varepsilon_{eff}}} \qquad (4.2)$$

$$\varepsilon_{eff} = 1 + q(\varepsilon dr - 1) \qquad (4.3)$$

Where,

c = Speed of light

f = Frequency of dominant mode

λ = Wavelength of dominant mode

$\pi\ (R_i + R_o)$ = Mean circumference length

ε_{eff} = Effective dielectric constant

εdr = Relative permittivity

q = Correction factor for presence of different dielectric materials on both sides of antenna patch

Here, antenna geometry comprises of annular rings with rectangular ground is presented in figure 4.2. In this design step, dimensions of ground plane and radiating element are optimized for resonating frequencies covers WLAN band. The size of the rectangular ground plane is '26 × h3' mm^2, and Ri = 4 mm, Ro = 6 mm are the radius of inner and outer radius of annular ring. Antenna is fed by a W1 mm (3 mm) wide single microstrip feed line, which is divided into two sections of 1 mm width and respective length at height h1 mm as shown in below figure. From equations 4.1 – 4.3, the calculated value of resonant frequency is ≃ 5.82 GHz.

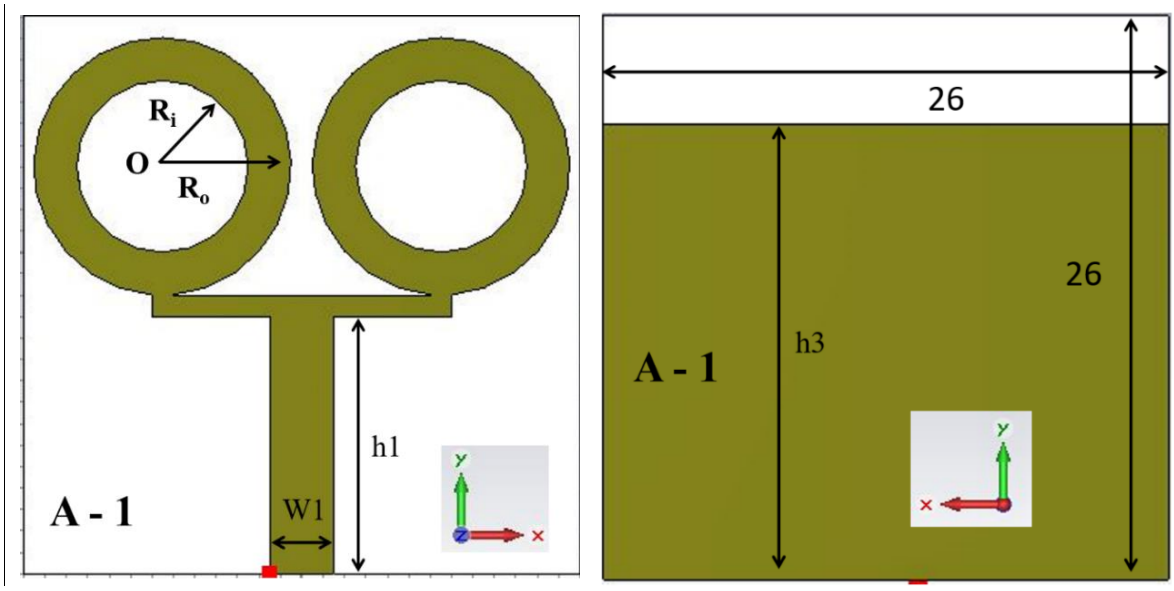

(a) (b)

Figure 4.2 Layout of suggested antenna (a) front view (b) rear view

The parametric study of ground plane height (h3) is carried out to study its impact on impedance bandwidth is presented in fig. 4.3. This investigation reveals a clear relationship

between the height of the ground plane and the resonant behaviour of the antenna. Specifically, as the value of h3 is increased, the entire resonant frequency band shifts toward the lower end of the frequency spectrum. This downward shift indicates that a larger ground plane height effectively increases the electrical length of the antenna, thereby lowering its natural resonant frequencies. At ground plane height h3 = 21 mm, the antenna has a single resonating frequency band from '5.25 – 5.38' GHz with resonant frequency '5.32' GHz is best impedance matched to -43 dB. The antenna has impedance bandwidth (IBW) of 130 MHz and fractional bandwidth of 2.4 %, hence design A – 1 is narrowband antenna. The optimized dimensions for antenna A–1 are as follows: $R_i = 4\ mm$, $R_o = 6\ mm$, $W_1 = 3\ mm$, $h_1 = 12\ mm$ and $h_3 = 21\ mm$.

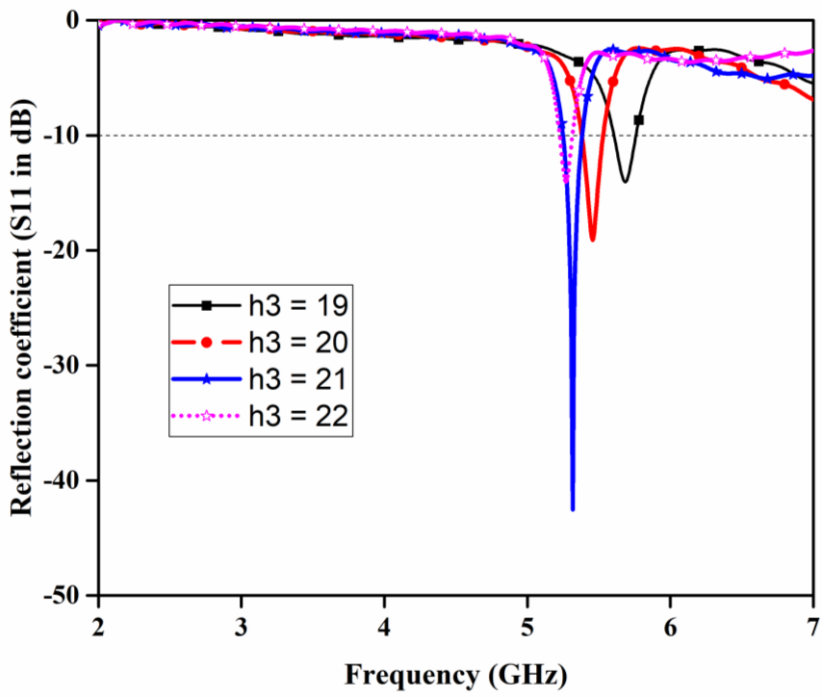

Figure 4.3 Simulated reflection coefficient vs frequency plot for different ground plane heights

4.2.2 Circularly Polarized Wide Band Antenna Design (A – 2)

It is well known that circular polarization (CP) can be achieved when two orthogonal electric field (E-field) components of equal amplitude are generated with a phase difference of 90 degrees (i.e., in quadrature) [76]. The originally linearly polarized antenna A-1 can be effectively transformed into a circularly polarized wideband antenna by etching a narrow slit of 0.5 mm width and one-quarter of the wavelength (λ/4) in length denoted as W4 mm on the partial ground plane from the left edge at a vertical height of h6 mm [220–221]. The introduction of this asymmetrical slit disturbs the current distribution on the ground plane in a

controlled manner, thereby facilitating the generation of the two required orthogonal E-field components with the necessary phase difference. In conjunction with this structural alteration, simultaneous optimization of the ground plane height is carried out to fine-tune the antenna's impedance characteristics and maintain broadband performance. The resultant antenna geometry is presented in figure 4.4 and labelled as antenna – 2 (A – 2).

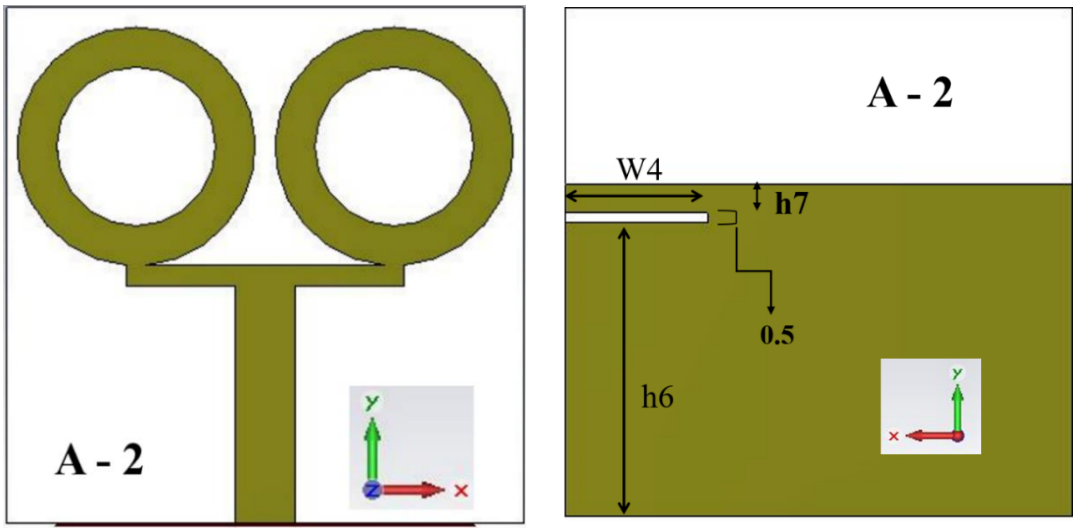

(a) Front side (b) Rear side

Figure 4.4 Design of simulated antenna structure (Antenna – 2)

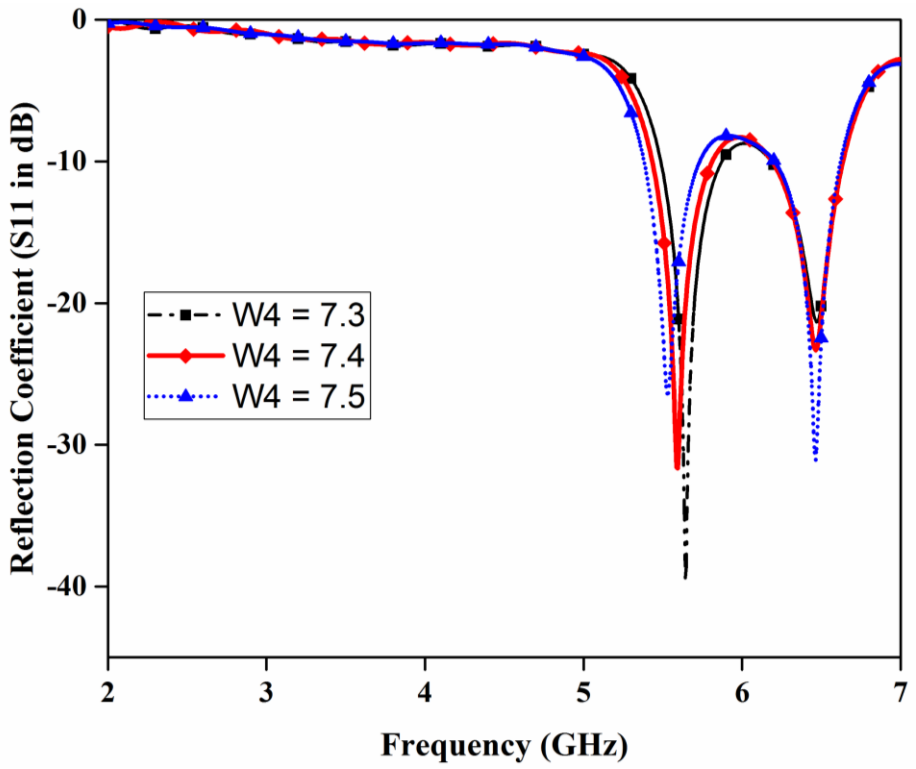

Figure 4.5 Effect of variation in slit length on reflection coefficient for A – 2

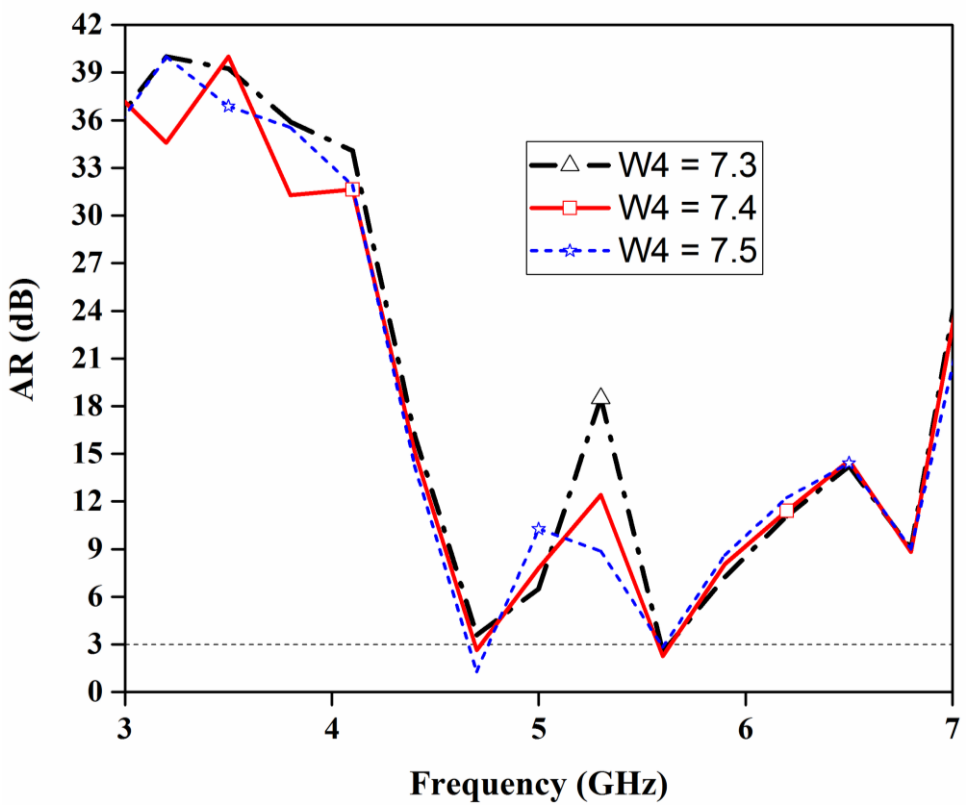

Figure 4.6 Effect of variation in slit length on AR bandwidth for A – 2

The impact of varying slit lengths on reflection coefficient and axial ratio against frequency is presented in figure 4.5 and 4.6 respectively for fixed ground plane height $h_3 = 17\ mm$ and corresponding result is tabulated in Table 4.1.

Table 4.1 Variation of slit length on IBW and ARBW

S. No.	Slit Length (W4) in mm	Resonating Frequencies (GHz)	Axial Ratio Bands (GHz)
1	7.3	5.38 – 5.74	5.59 – 5.61
		6.21 – 6.61	
2	7.4	5.43 – 5.82	5.58 – 5.63
		6.19 – 6.63	
3	7.5	5.48 – 5.88	5.59 – 5.63
		6.18 – 6.64	

It is observed that the introduction of a strategically etched slit into the ground plane of the antenna yields multiple performance enhancements. Primarily, the slit facilitates the generation of circular polarization within the existing resonating frequency band by altering the surface current distribution. In addition to this, the presence of the slit introduces a new resonant mode, effectively transforming the antenna from a single-band to a multi -band configuration. This occurs because the physical discontinuity introduced by the slit modifies the current path and electromagnetic field distribution, allowing the antenna to support an additional resonant frequency. As a result, not only is circular polarization achieved, but the impedance bandwidth (IBW) is also significantly improved across both bands. The best optimized value of slit length W4 = 7.4 mm is selected, because 50 MHz axial ratio bandwidth is obtained in comparison to other lengths, although impedance matching at resonant frequency is not matched good. At slit length of W4 = 7.4 mm, the dual resonating bands cover the frequency range from '5.43 – 5.82 GHz', '6.19 – 6.63 GHz' with 5.6 and 6.5 GHz resonant frequencies respectively and also exhibit circular polarization with axial ratio band from '5.58 – 5.63 GHz'. The optimized dimensions are given as: $R_i = 4\ mm, R_o = 6\ mm, W_1 = 3\ mm, W_4 = 7.4\ mm, h_1 = 12\ mm, h_3 = 17\ mm, h_6 = 15\ mm$ and $h_7 = 1.5\ mm$

The etching of slit on partial ground plane has led to quasi-symmetrical antenna structure. The slit is positioned near the upper edge of the ground plane, just beneath the right annular ring, acts as a perturbation that influences the surface current distribution. It alters the surface current vector primarily in the horizontal direction, effectively changing the current path length along this axis, while leaving the vertical component largely unaffected. This deliberate disturbance leads to the splitting of the antenna's fundamental mode, TM11, into two orthogonal degenerate modes of equal amplitude but with a 90° phase difference—an essential condition for generating circular polarization in the radiated wave [110], [191]. The above mention is further verified from the dispersal of surface current vector on antenna structure at 5.6 GHz as depicted in figure 4.7 for different phase angles. The surface current vector undergoes directional changes near the etched slit, forming a rotational motion in an anti-clockwise manner. This rotating current vector indicates the presence of left-hand circular polarization (LHCP) [222]. Additionally, it is observed that the surface current vectors at phase angles of 0° and 180°, as well as at 90° and 270°, are equal in magnitude but opposite in direction—meaning they are 180° out of phase. This phase relationship further confirms the successful generation of LHCP in the proposed antenna design [223].

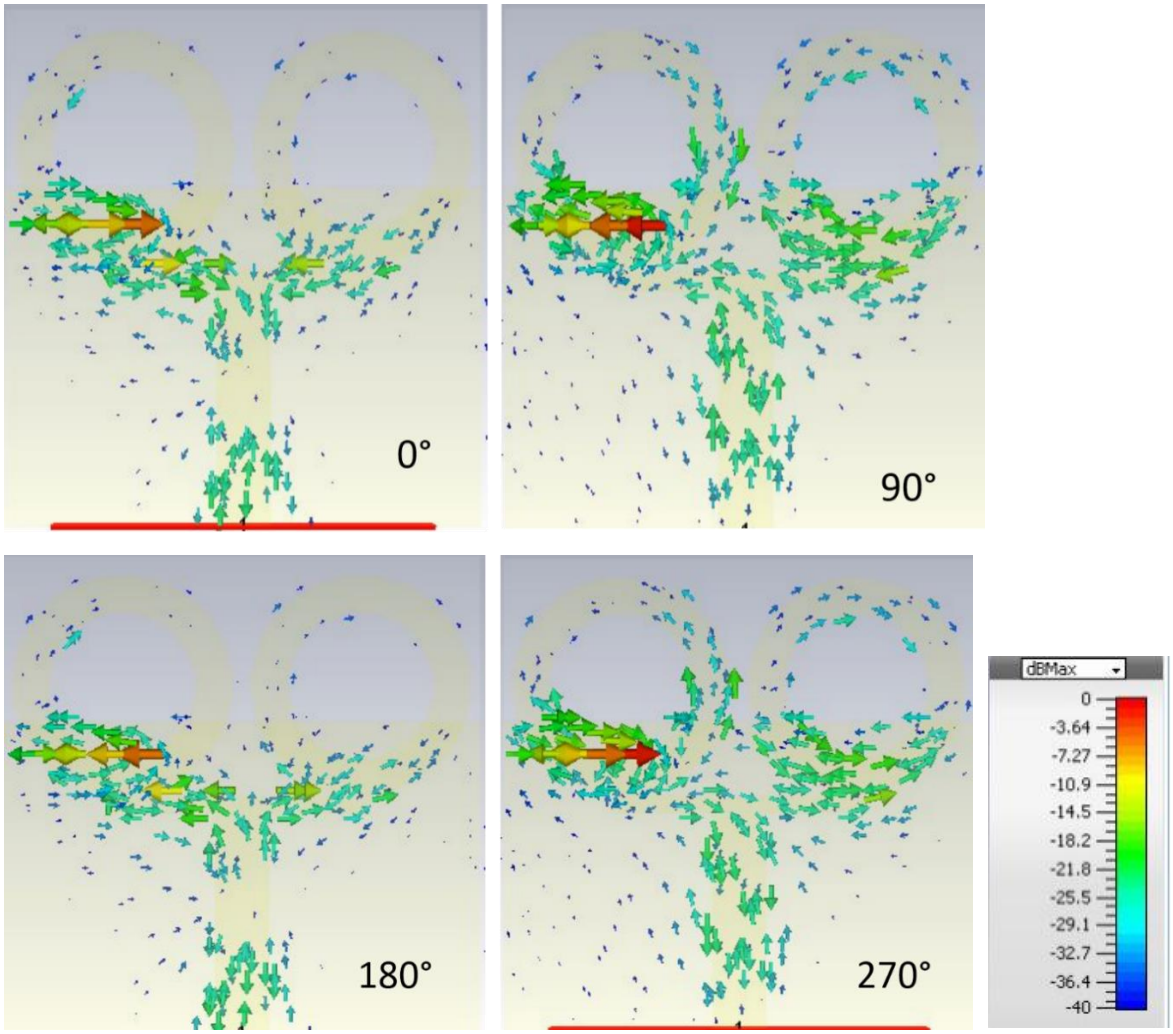

Figure 4.7 Surface current distribution of antenna A – 2 at 5.6 GHz

4.2.3 Single Band Antenna Design (A – 3) with Circular polarization

The resonating frequency band from 6.19 – 6.63 GHz of design A - 2 is suppressed in this design step by modifying the microstrip feed line. Here, the 3 mm wide feed line is segmented into two sections of optimized lengths and widths as presented below. This segmentation serves a dual purpose in refining the antenna's performance. Firstly, by adjusting the physical dimensions of the feed line, the modified structure effectively suppresses unwanted higher-order resonant frequency bands. These higher bands, which may lead to undesired radiation or interference, are eliminated or significantly reduced, allowing the antenna to focus its operation within a more controlled frequency spectrum. Secondly, this segmentation impacts the primary operational band—specifically, the WLAN band—by compressing or "squeezing" its bandwidth. This narrowing helps in precisely targeting the desired frequency range for WLAN applications, improving selectivity and efficiency. Additionally, the modification influences the polarization characteristics of the antenna. The original design, which supported circular

polarization, is altered by the segmented feed structure in such a way that the balance and quadrature phase relationship between orthogonal electric field components are disrupted. As a result, the polarization state transitions from circular to linear. The circular polarization is again restored in the WLAN band by changing horizontal slit length value to 7.65 mm. The resultant antenna design with front and rear view is shown in figure 4.8 and labelled as antenna – 3 (A – 3). The optimized dimensions are as follows: $R_i = 4\,mm$, $R_o = 6\,mm$, $W_1 = 3\,mm, W_2 = 6.2\,mm$, $W_3 = 1.6\,mm$, $W_4 = 7.65\,mm, h_1 = 7.5\,mm$, $h_2 = 4\,mm$, $h_3 = 17\,mm$, $h_4 = 1.5\,mm$, $h_6 = 15\,mm$ and $h_7 = 1.5\,mm$.

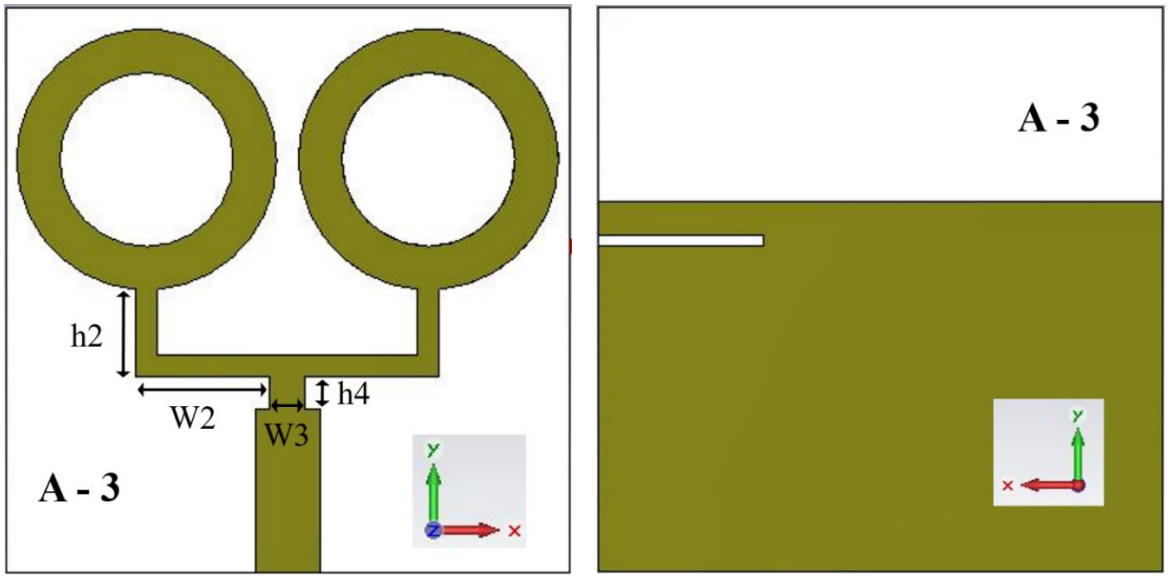

(a) Front side (b) Rear side

Figure 4.8 Layout of antenna – 3 (A – 3)

From simulated reflection coefficient plot against frequency as shown in fig. 4.9, it is observed that a single resonating frequency band covers the frequency range from '5.24 – 5.53 GHz' with resonant frequency at '5.38 GHz' is best impedance matched to -22 dB. The simulated design also exhibits circular polarization in 5.28–5.33 GHz band with ARBW of 50 MHz as observed from axial ration plot in figure 4.10. Thus modification in feed line and minor adjustment of slot length shifts the resonating band and axial ratio bands towards the lower frequency side with impedance and axial ratio bandwidths are conserved.

4.2.4 Reconfigurable Antenna Design – 4 (A – 4)

Antenna A – 3 can be transformed into a reconfigurable antenna by forming an arc of suitable length through etching of vertical and horizontal slits at appropriate locations on the left ring.

The truncated ring and arc can be connected to form a complete ring via two PIN diodes placed over the slits. Thus reconfiguration in frequency and polarization is achieved in the suggested antenna through loading or unloading of arc on left ring. The description of PIN diode will be presented in subsequent section 4.3. The resultant antenna is labelled as A-4 as displayed in figure 4.11 (a) – (b) with front and back side respectively.

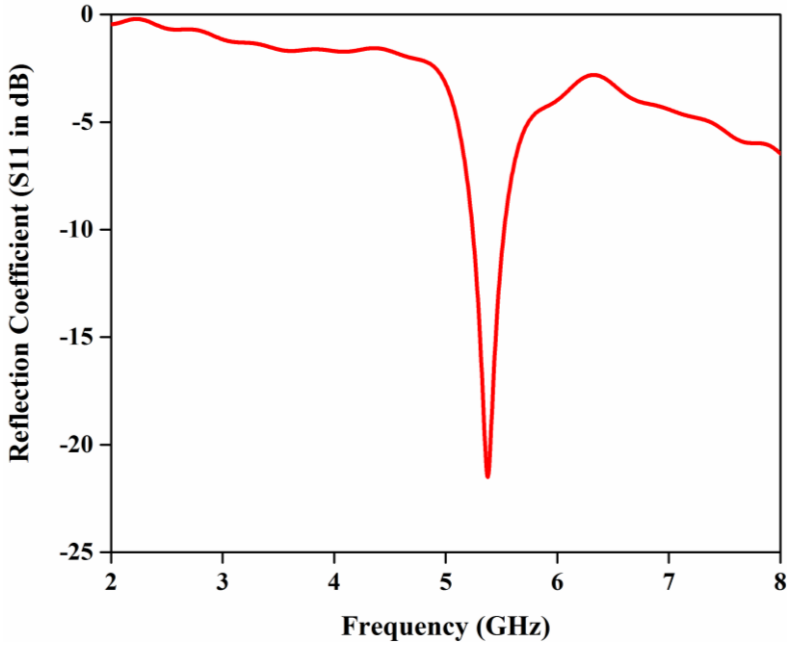

Figure 4.9 Simulated reflection coefficient plot against frequency

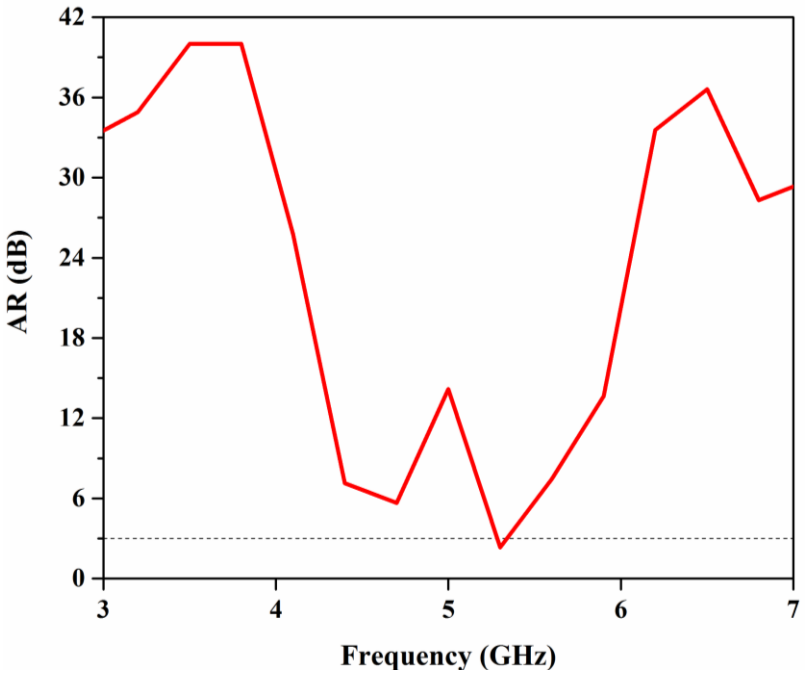

Figure 4.10 AR vs frequency

Figure 4.12 and 4.13 displayed the plot of reflection coefficient and axial ratio against frequency respectively for antenna design A–4. It is noticed from the plot that activating both PIN diodes simultaneously completes the left ring and produces a single resonating band of frequency range from 5.24 – 5.52 GHz and circular polarization of ARBW of 30 MHz at resonant frequency of 5.3 GHz. On the other hand, dual band behaviour with linear polarization in the later band is exhibited by the same antenna structure on switching both PIN diodes simultaneously OFF. The resonating frequencies for OFF state are ranging from 3.21 – 3.54, 5.21 – 5.42 GHz and cover WiMAX and WLAN band respectively.

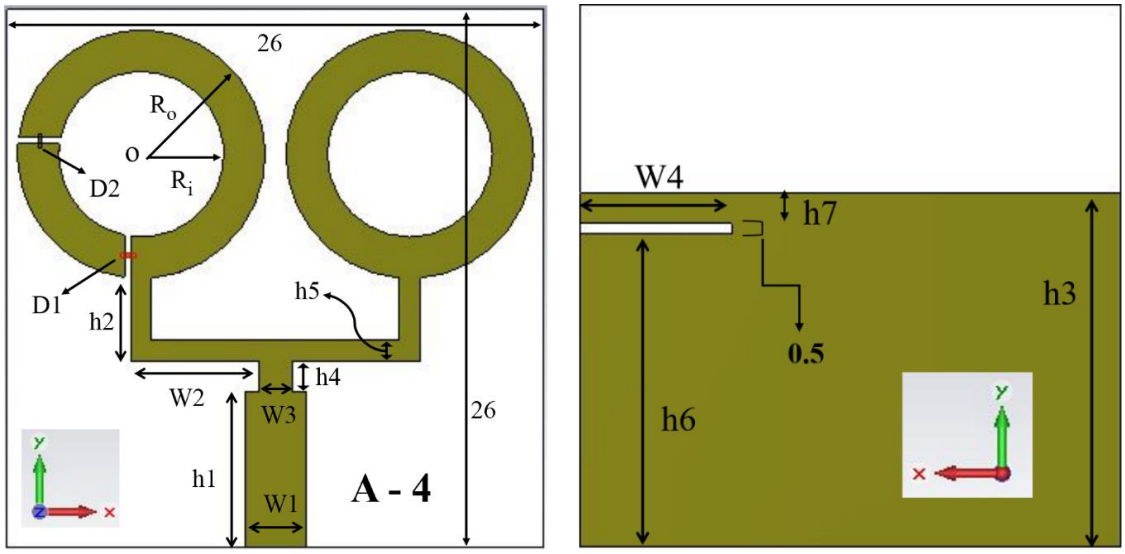

(a) Front side (b) Back side

Figure 4.11 Proposed reconfigurable antenna design A-4

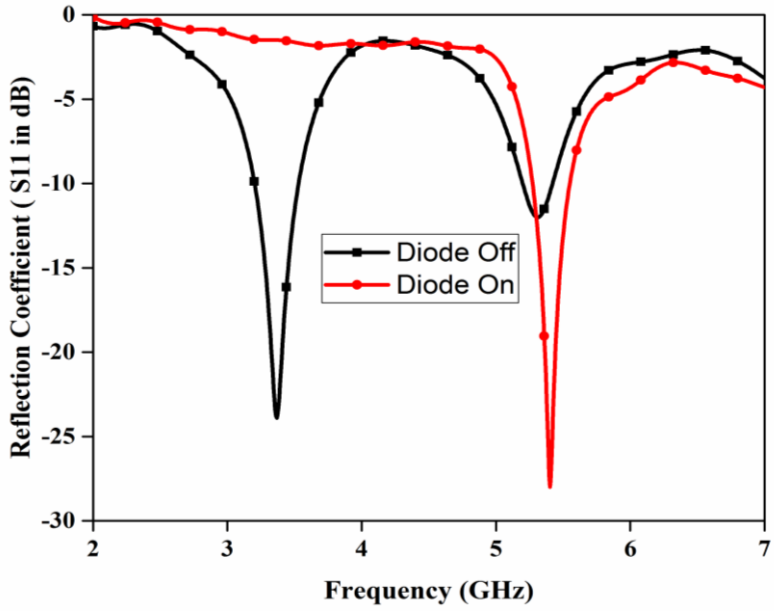

Figure 4.12 Simulated reflection coefficient vs frequency plot for ON / OFF state of PIN diodes

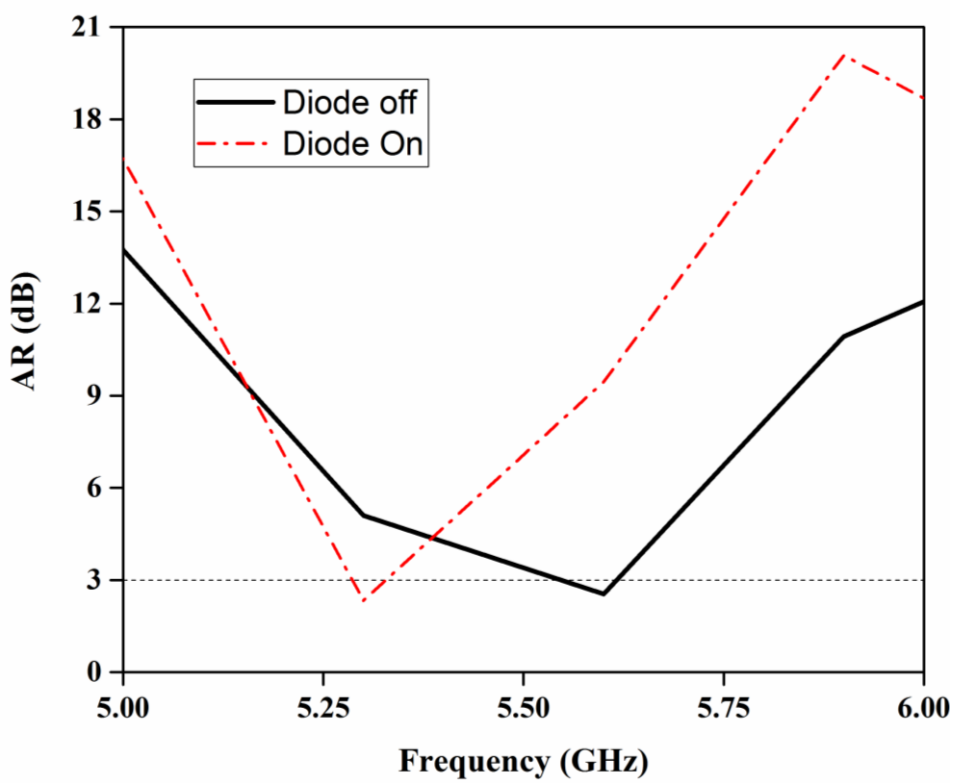

Figure 4.13 AR vs frequency for ON and OFF states of both diodes

4.2.4.1 Principle of Reconfiguration Operation

(i) **Frequency Reconfiguration:** It is known that the effective electrical length of an antenna design defines its operating frequency and related bandwidth. Any change in electrical length of antenna by removing or adding in antenna element via various means like electrically, optically or mechanically translates the resonating frequency to a new value [224]. In the present design, this principle is exploited by incorporating PIN diodes to dynamically include or remove an arc segment on the annular ring. The state of these diodes controls whether the arc is electrically connected to the ring or isolated, thereby redirecting the surface current flow within the antenna. This redirection effectively alters the antenna's electrical length, enabling frequency reconfiguration between the WiMAX and WLAN bands. The underlying mechanism of this frequency tuning is illustrated through surface current distribution plots at the respective resonant frequencies, as shown in Figure 4.14.

When the diodes are in the OFF state (non-conducting), the arc is disconnected, and the surface current is primarily concentrated near the slit and partially below thefeed

lines, resulting in a resonant frequency of 5.37 GHz as depicted in Figure 4.14(a). This corresponds to the antenna operating predominantly within the WLAN band. Upon forward biasing diodes D1 and D2, they behave like short circuits, electrically joining the arc to the radiating ring and thus completing the circular path. This connection allows the surface current to flow over a longer path on the left ring and below the feed lines, as shown in Figure 4.14(b), which introduces an additional resonance at 3.36 GHz corresponding to the WiMAX band, alongside the existing WLAN resonance.

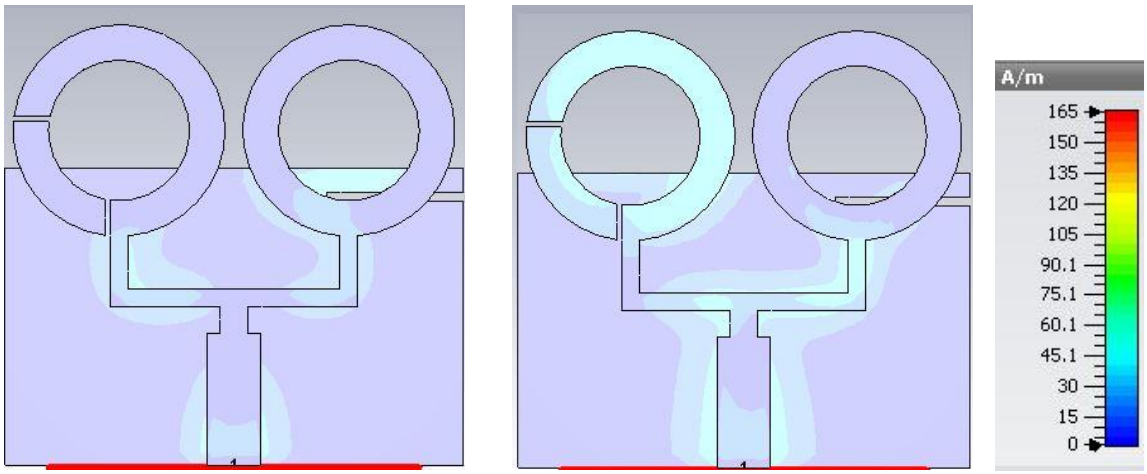

(a) f = 5. 37 GHz diodes OFF (b) f = 3.36 GHz diodes OFF

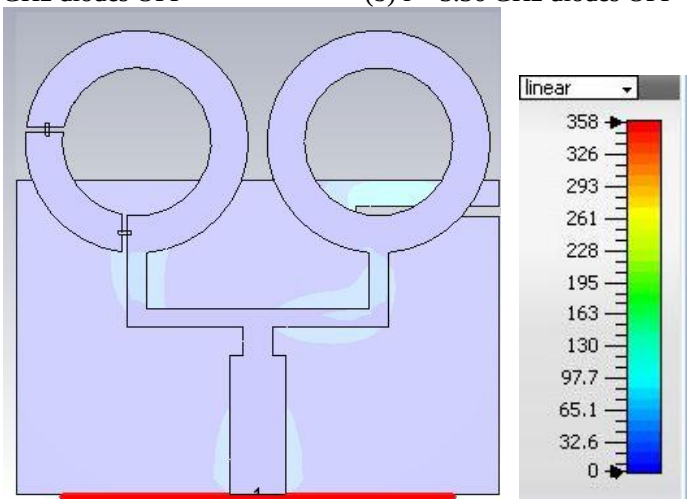

(c) f= 5.37 GHz diodes ON

Figure 4.14 Surface current distribution at resonant frequencies for ON / OFF state of diodes

Further, Figure 4.14(c) illustrates that with the diodes ON and the arc connected, the surface current density near the same locations becomes more concentrated. This increase

in current density enhances the impedance matching of the antenna at the new resonant frequency, improving the antenna's efficiency and overall performance. In summary, the clever use of PIN diodes to control the inclusion of the arc segment enables effective and flexible frequency reconfiguration, making the antenna suitable for multi-band wireless applications by switching between WiMAX and WLAN operating bands dynamically.

(ii) Polarization Diversity: The activation or deactivation of both PIN diodes plays a crucial role in controlling the polarization characteristics of the antenna. When both diodes are forward biased, they connect specific sections of the antenna structure, creating a quasi-symmetrical geometry. This quasi-symmetry enables the antenna to generate two orthogonal electric field components of equal amplitude. In this state, the antenna radiates circularly polarized waves within its resonant frequency band, enhancing signal robustness and reducing multipath fading effects, which are beneficial for many wireless communication applications. This operating principle is consistent with the detailed explanation provided earlier in Section 4.2.2.

Conversely, when the PIN diodes are reverse biased, the electrical connection is broken, disrupting the quasi-symmetrical configuration. This structural asymmetry alters the surface current distribution such that the necessary phase relationship between orthogonal electric field components is lost. As a result, the antenna no longer supports circular polarization and instead radiates linearly polarized waves within the same frequency bands. Therefore, by simply switching both PIN diodes ON or OFF simultaneously, the antenna achieves a dynamic polarization reconfiguration between circular and linear polarization states specifically within the WLAN frequency band.

4.3 Antenna Design with Biasing Pads

The final antenna design with optimized dimensions are presented in figure 4.15 and Table 4.2 respectively. For independent biasing of PIN diodes, two biasing pads of size 2×1 mm^2 are printed at 0.8 mm distance from the inner edge of ring and two 47 nH surface mount inductors are placed in series with each dc feed line to choke the radio frequency signals [225] as shown below.

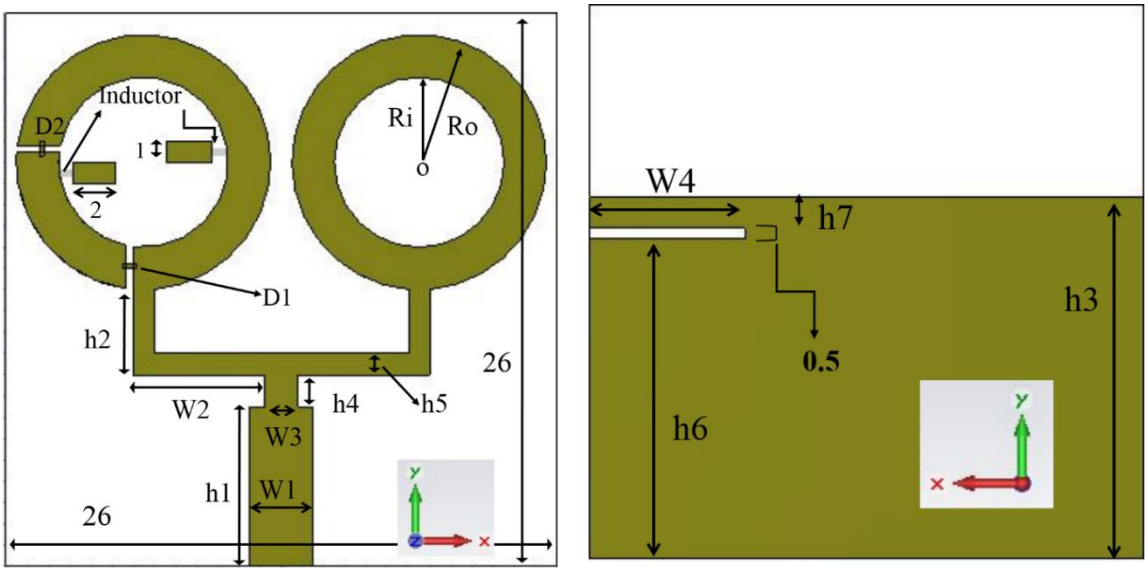

(a) (b)

Figure 4.15 Final antenna design with biasing pads (a) front side (b) rear side

Table 4.2 Optimized dimensions of final antenna design

Parameters	**h1**	**h2**	**h3**	**h4**	**h5**	**h6**	**h7**	**W1**	**W2**	**W3**	**W4**	**R_o**	**R_i**
Value (mm)	7.5	4	17	1.5	1	15	1.5	3	6.2	1.6	7.65	6	4

4.4 Measured Results and Analysis

The final optimized antenna design is realized on '1.6 mm' thick 'FR – 4' dielectric substrate with dielectric constant of '4.4' and loss tangent of '0.025' as shown in figure 4.16. The Alpha's planar surface mountable DGS 6474 PIN diode [226] having very low value of capacitance (0.02 pF) and resistance (4 Ω) is utilized for switching purposes.

The equivalent circuit model of PIN diode for ON/ OFF switching state is presented in figure 4.17. In forward biasing, it includes a 4Ω resistance in series with 0.2 nH inductor, while in reverse biasing, the equivalent model includes a 0.2 nH inductor in series with shunt combination of resistor (15 kΩ) and capacitor (0.02 pF). A DC bias of + 1.5 V from the battery is applied to the PIN diode for forward biasing. The reflection coefficient (S_{11}) of suggested antenna structure are measured with Agilent N5234A Vector Network Analyzer (VNA) and normalized radiation pattern in an anechoic chamber as displayed in figure 4.18 (a)–(b) respectively.

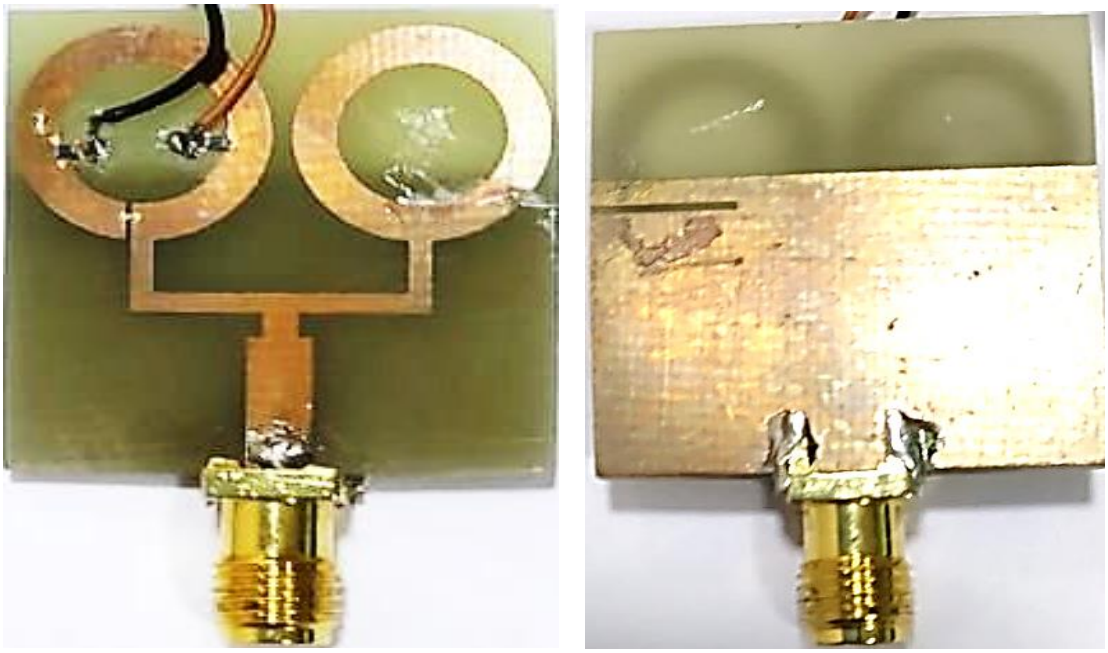

(a) (b)

Figure 4.16 Printed antenna (a) radiating side (b) ground plane side

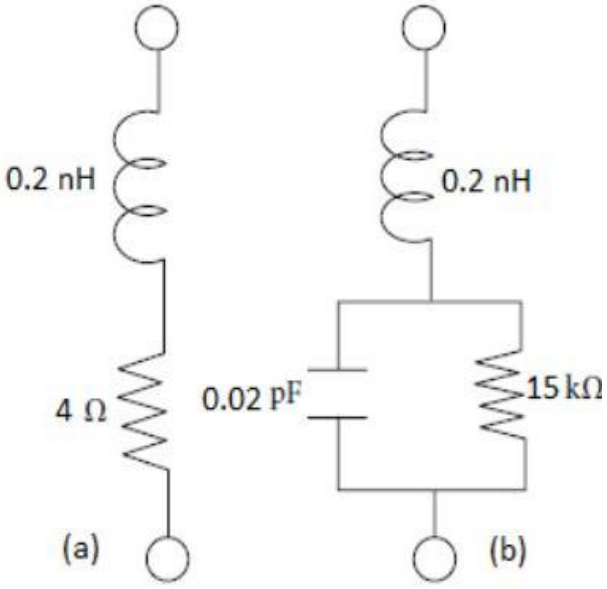

Figure 4.17 RF equivalent circuit of p-i-n diode (DSG6474) (a) forward biased (b) reverse biased

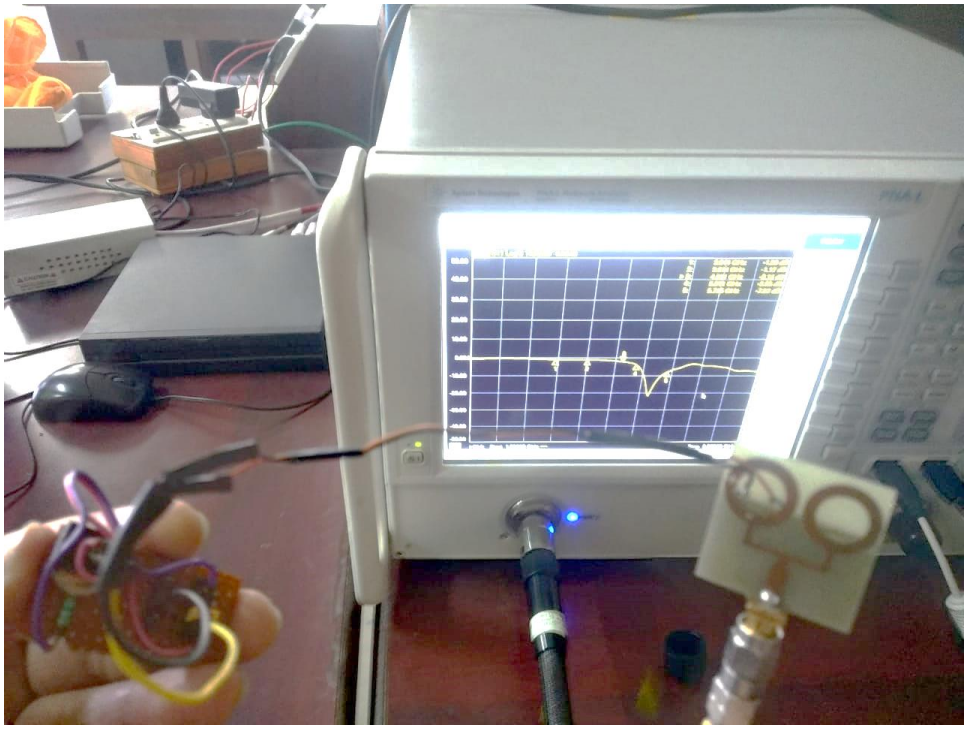

(a)

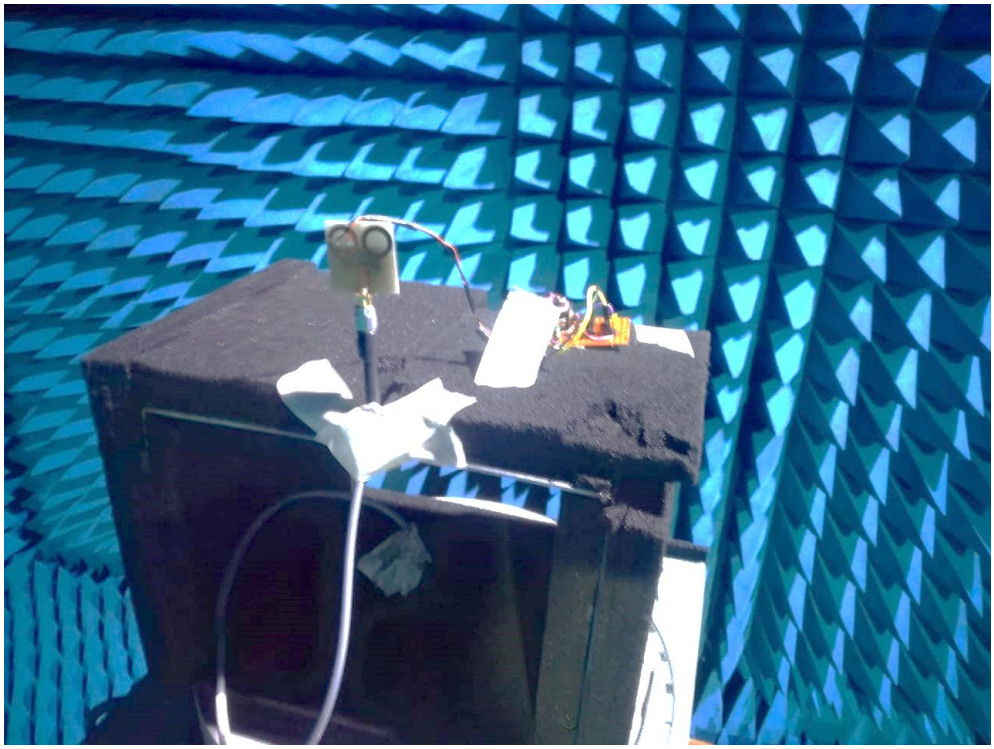

(b)

Figure 4.18 Fabricated antenna under measurement (a) VNA (b) anechoic Chamber

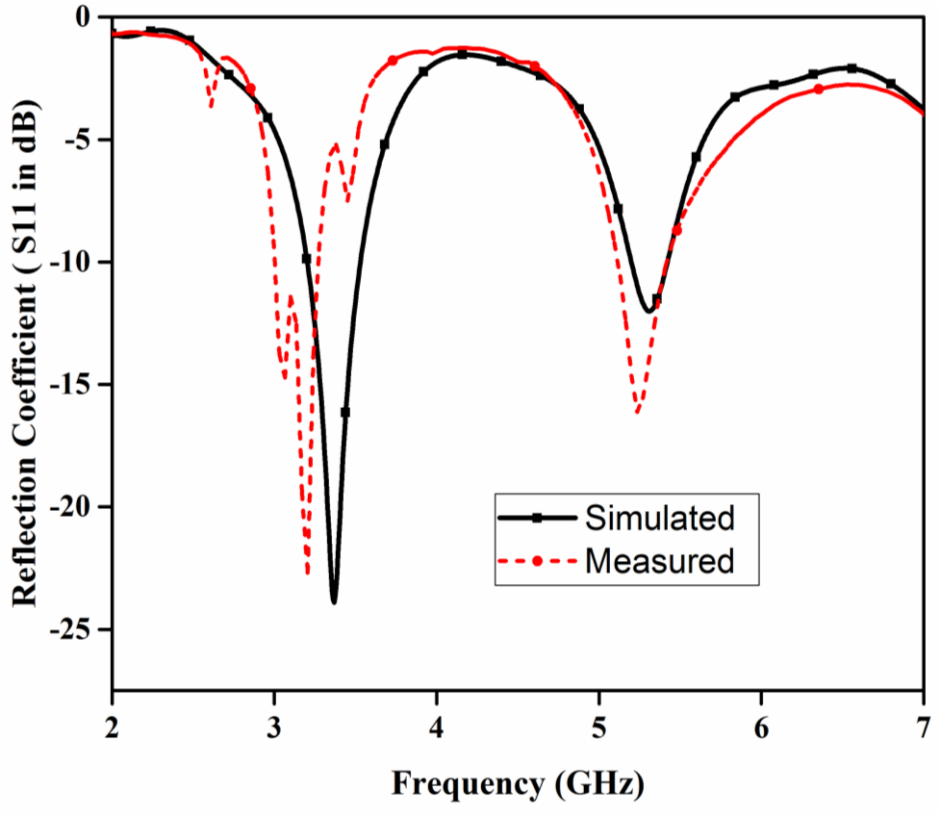

(a) Diode Off

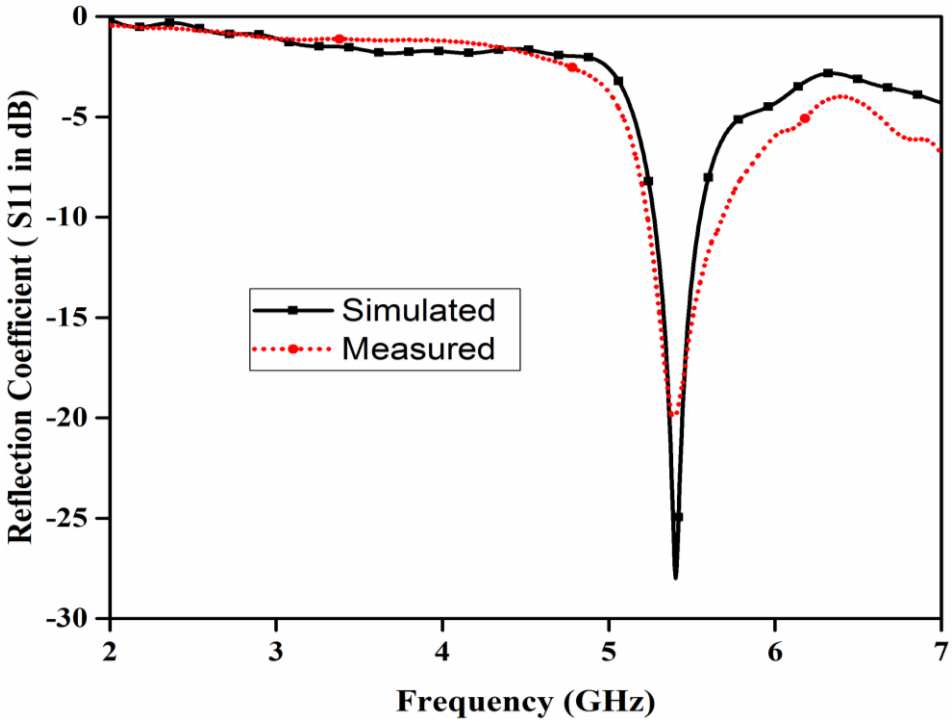

(b) Diode ON

Figure 4.19 Simulated and measured reflection coefficient plot

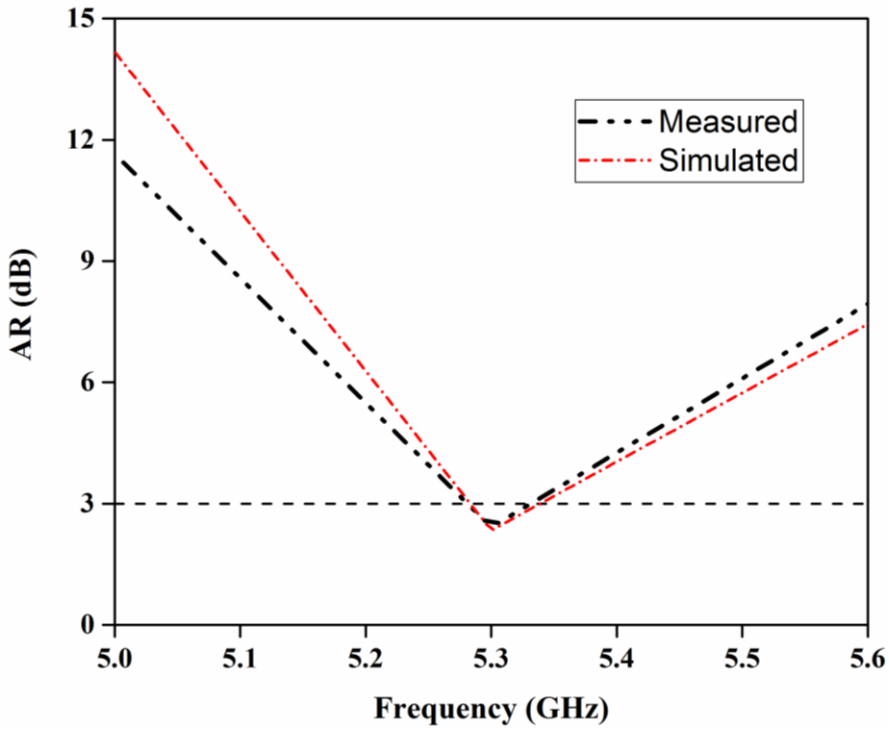

Figure 4.20 AR vs frequency for ON state of both diodes

In the first scenario, when reverse bias is applied to both PIN diodes i.e. both diodes are switched OFF, as a result arc is not connected to the ring because diodes behave as open circuited. The resonating behavior of given configuration has dual bands as shown in figure 4.19 (a) and covering 3.0 – 3.28 GHz, 5.13 – 5.42 GHz frequency bands for S11 ≤ -10 dB with resonant frequencies at 3.21 GHz, 5.24 GHz respectively.The simultaneously forward biasing of PIN diodes completed the left ring by connecting arc to radiating structure, thus producing a single resonating frequency band of range from 5.24 – 5.68 GHz with resonant frequency of 5.38 GHz is matched to -28 dB as displayed in figure 4.19 (b). The measured results have very good agreement with the simulated reflection coefficient and have only minor deviation in the lower frequency band. The minor mismatch in results is attributed due to fabrication tolerance, measurement environment etc.

Also, antenna exhibits the circular polarization in WLAN band for ON state of diodes with axial ratio band from 5.29–5.32 GHz with ARBW of 290 MHz as depicted in figure 4.20. Thus, reconfiguration in frequency and polarization is attained in the suggested design via switching diodes ON or OFF simultaneously. The gain plot against frequency in the boresight direction is shown in figure 4.21, confirms the gain variation from 0.9–2.34 dBi for switching states PIN diodes. The total efficiency of suggested antenna is lying between 60-70%, 50 – 55% in 3.0 – 3. 28 GHz, 5.13 – 5.42 GHz resonating bands respectively for OFF state of PIN diodes and

also total efficiency is more than 50% in 5.24 – 5.68 GHz for ON state of PIN diodes as depicted in figure 4.22. The simulated and measured results are tabulated in Table 4.3.

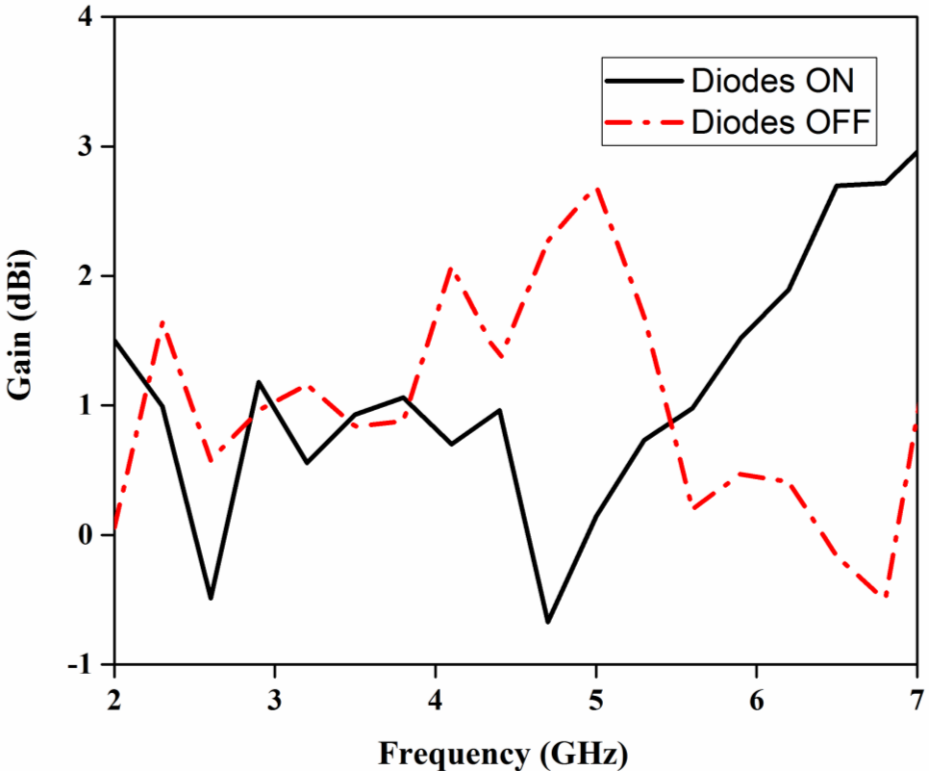

Figure 4.21 Gain vs frequency plot for ON/OFF states of diodes

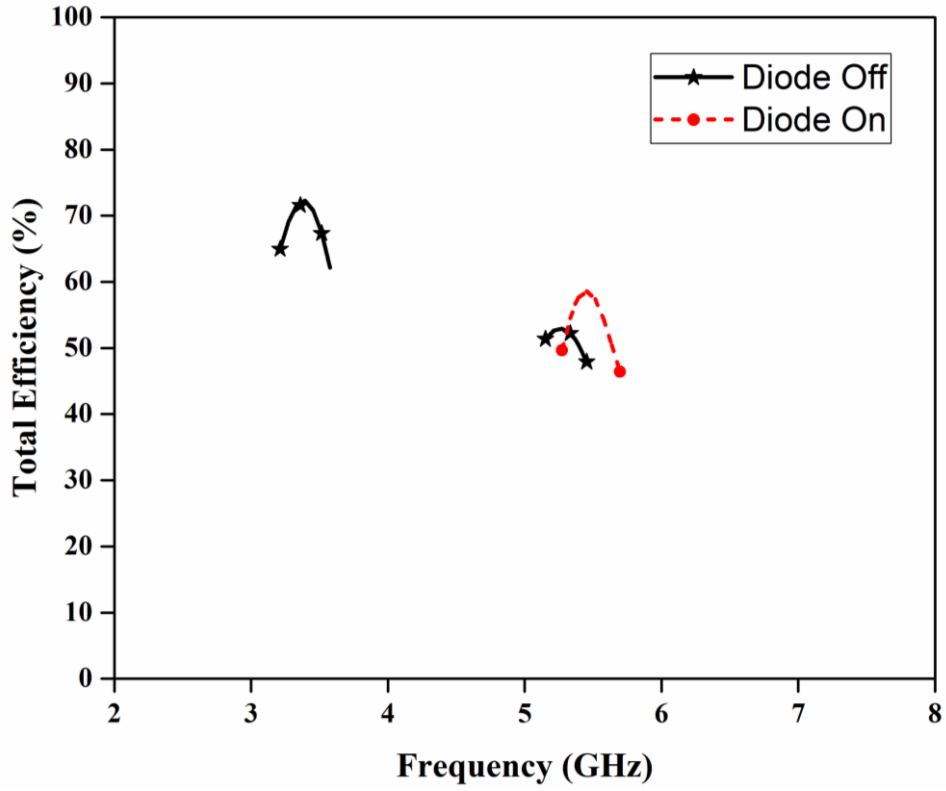

Figure 4.22 Total efficiency vs frequency plot for ON/OFF states of diodes

Table 4.3 Diode states and antenna operations

S. No.	Diodes State	Sim. Freq. Band (GHz)	Meas. Freq. Band (GHz)	ARBW (GHz)	Gain (dBi)
1	ON	5.27 – 5.55	5.24 – 5.68	0.029 (5.29 -5.32)	0.91
2	OFF	3.21 – 3.54	3.0 – 3.28	--	1.15
		5.21 – 5.42	5.13 -5.42	--	1.90

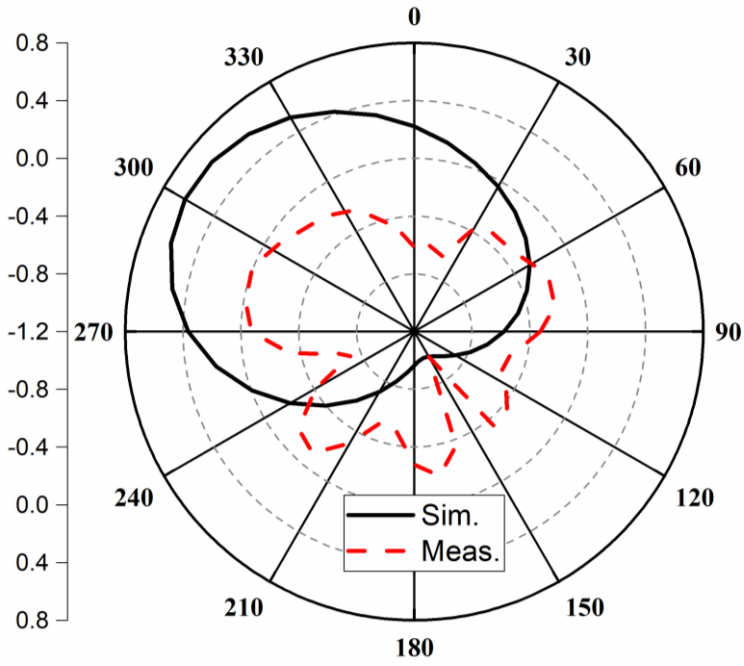

(a) E-field pattern at f = 3.17 GHz for diodes OFF

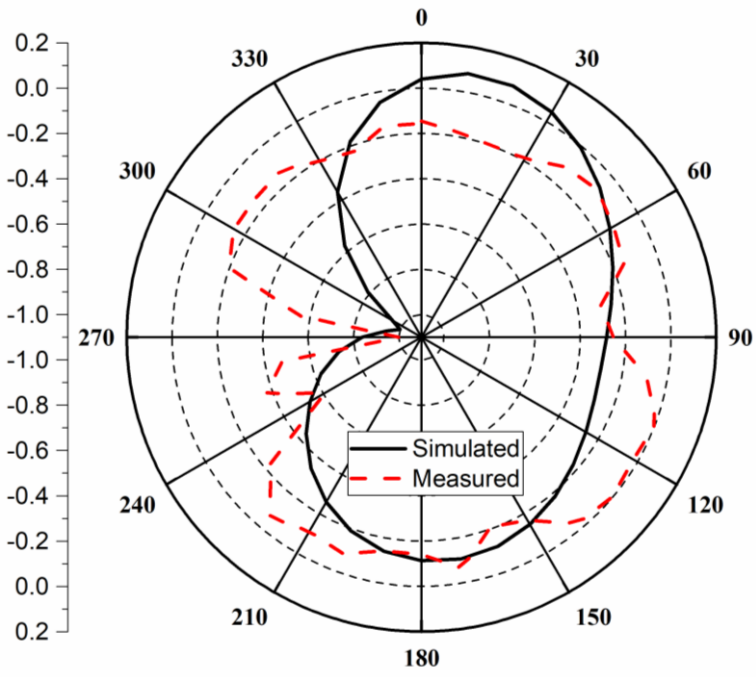

(b) E-field pattern at f = 5.3 GHz for diodes OFF

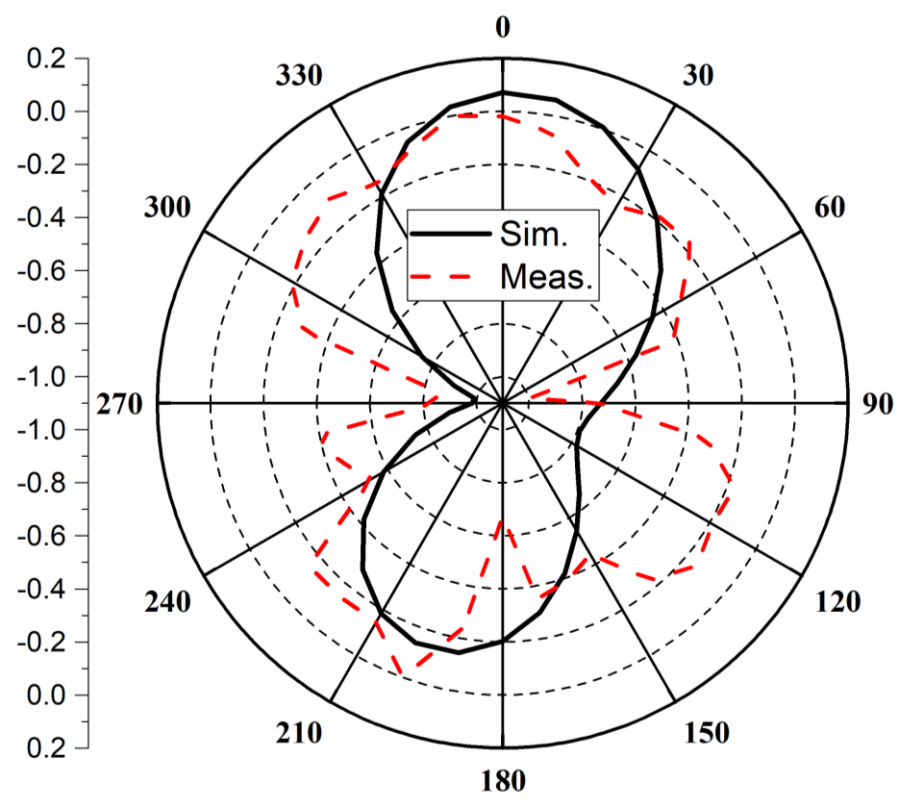

(c) E-field pattern at f = 5.3 GHz for diodes ON

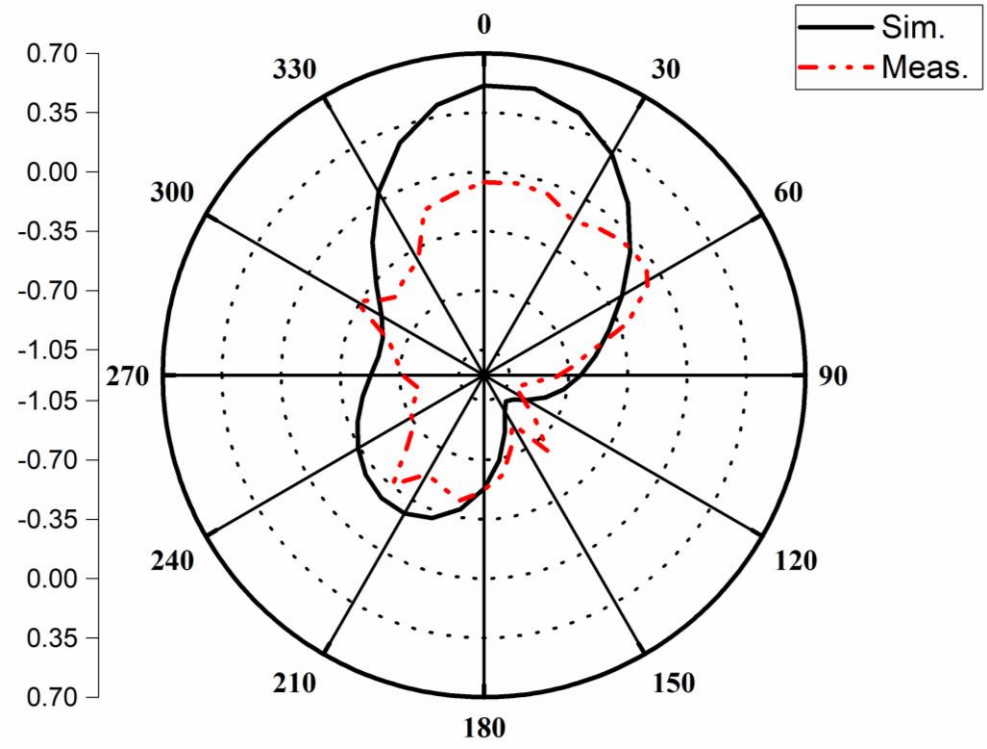

(d) H-field pattern at 3.17 GHz for diodes OFF

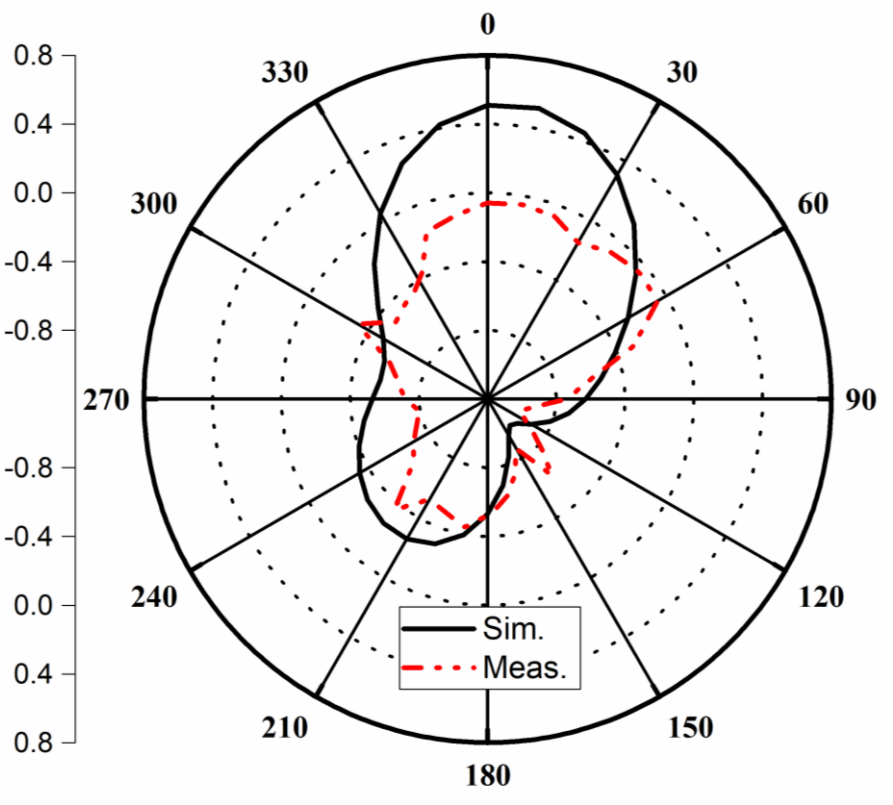

(e) H-field pattern at 5.3 GHz for diodes OFF

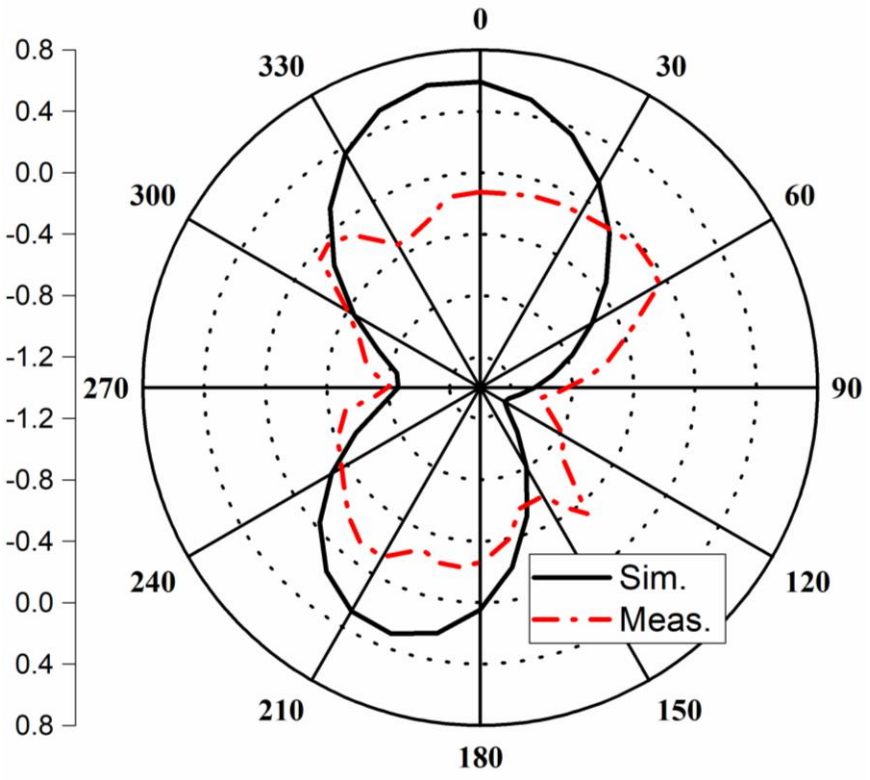

(f) H – field pattern at 5.3 GHz for diodes ON

Figure 4.23 Simulated and measured radiation pattern for switching states of PIN diodes in antenna structure at 3.17,5.3 GHz

Figure 4.23 presents the 2D simulated and measured normalized radiation pattern of antenna geometry in *xoz* and *yoz* planes at '3.17', '5.3 GHz'. The measured antenna's radiation patterns are almost alike with minor discrepancies, which may be due to the measurement arrangement and rotating table shakings. The E – field radiation pattern is unidirectional at both frequencies for OFF state and bidirectional radiation pattern is witnessed for the ON state of diodes. While in the H- field, almost omnidirectional radiation patterns are observed for both frequencies irrespective of switching states.

4.5 Performance Comparison with Similar Antennas

The performance of suggested antenna design has been compared with previously reported frequency and polarization reconfigurable antenna designs and tabulated in Table 4.4. In comparison to other designs, the suggested antenna has a simple design, completely planar, small in size, utilizes fewer PIN diodes for switching which also requires less power (≈ 40 mW) and simple feed network. Also, it adds more flexibility, freedom to select different working modes for various applications as required by the users in a crowded WiMAX/ WLAN environment and provides satisfactory antenna performances.

Table 4.4 Performance analysis of proposed antenna with earlier reported designs

Ref.	**Antenna Dim. (mm^3)**	**Substrate Material**	**No. of Diodes**	**Resonant Freq. (GHz)**	**Polarization Reconfiguration**
[136]	70×70×3.175	RT duroid 5880	4 PIN 8 Varactor	Discrete frequencies in 1.35 – 2.25	Horizontal, vertical and 45° Linear Polarization
[137]	120×120× 3.175	Rogers 5880	16 PIN	Eight discrete frequencies in 1.83-2.65	LP, LHCP and RHCP
[139]	150×150× 3.05	Arlon AD 450	4 Varactor Diodes	Discrete operating frequencies in 1.17 – 1.58	LP, LHCP and RHCP
[140]	80×80×32	Rogers RO4003C		Continuous in 8 – 11.2	LP, LHCP and RHCP

[191]	× ×1.6	FR-4	5 PIN	2.4 GHz 3.5 GHz	LP, LHCP and RHCP LHCP, RHCP
[211]	× ×0.8	RT duroid 5880	8 PIN	5.2 5.8	LP, LHCP, RHCP LP, LHCP, RHCP
[216]	60×65×1.6	FR-4	2 PIN diodes	2.41 3.4 4.18	LP LHCP, RHCP LP
Propos--ed Design	26× 26 ×1.6	FR-4	2 PIN	3.21 5.38	LP LP, LHCP

4.6 Summary

The construction of frequency-polarization reconfigurable antennas using the fewest possible PIN diodes was the focus of this chapter. Simulation and supplementary test findings from the prototype measurement are used to demonstrate the antenna design and analysis. The conceptualized idea is realized with simple electronic control without any reflecting surface to achieve multi-state reconfigurability. Here, annular rings have a microstrip antenna design having an arc on the left ring and horizontal slit etched on partial ground plane. The loading or unloading of arc on ring through switching of PIN diodes ON or OFF simultaneously, realizes the frequency reconfiguration between single and dual resonating frequency bands with frequency ranges from 5.24 – 5.68 GHz and 3 – 3.28, 5.13 – 5.42 GHz respectively. Also, polarization reconfiguration between circular and linear state respectively in WLAN band with axial ratio bandwidth of 290 MHz. The developed antenna's potential is studied and compared to other similar reported antennas to unearth advantages and disadvantages. The suggested antenna is of planar, small size with simple reconfiguration network makes it highly suitable for communication operations in next generation wireless systems.

CHAPTER 5

OPEN ANNULAR RING SHAPED PATCH ANTENNA WITH FREQUENCY, POLARIZATION & PATTERN RECONFIGURATION

---

* A. Sharma, S. Khah and S. Rawat, "An open annular ring antenna for WiMAX /WLAN band with frequency, polarization and pattern diversity", accepted in in Physica Scripta.
doi: https://iopscience.iop.org/article/10.1088/1402-4896/aded45

OPEN ANNULAR RING SHAPED PATCH ANTENNA WITH FREQUENCY, POLARIZATION & PATTERN RECONFIGURATION

5.1 Introduction

In the preceding chapter, we discussed that research and innovation in wireless communication developed numerous applications with unique frequency, polarization and pattern to meet the end user requirements. To avail these services, multiple antennas with fixed characteristics are integrated in a single entity have led to a complex, bulky and expensive system. Thus we need a low cost, smaller size, wideband and efficient antenna design with multiple functions and capabilities for emerging mobile technologies. The planar antennas with multiple reconfigurable characteristics have appeared as suitable candidates to address these issues for different applications in wireless, mobile and satellite communication [25], [33], [97], [227].

Briefly reconfigurable antennas, their classification and advantages are presented in the previous chapter. Because of flexibility and diversity features, the compound reconfigurable antennas can enhance the performance of a system in a diverse communication environment and are preferred in next generation wireless communication systems. There are two methods by which compound reconfiguration is implemented successfully in a single device without much affecting its individual operations. In the first method, individual reconfigurable elements are joined together by different means to form hybrid reconfigurable antenna, while in the second method or pixel technique, the radiating surface is sub-divided into small sections or pixels and interconnected by RF switches. The activation of proper switch configuration reshapes the radiating surface of the antenna for different individual reconfiguration operations [36]. In literature, several antenna designs with compound reconfiguration implemented in a single entity by both methods are reported.

Li et al. [228] proposed a configuration of microstrip patch, ground plane with bottom monopole and PIN diodes for frequency and pattern reconfiguration. The grouping of bottom monopole and upper patch through PIN diodes is responsible for 2.21 – 2.79 GHz band with omnidirectional radiation pattern, while activating the PIN diodes between bottom monopole and ground plane produces the unidirectional radiation pattern in 5.27 – 5.56 GHz and finally the dual mode simultaneously for switched OFF state of all diodes. Slot based antenna designs

with loaded PIN diodes across the slots on radiating patch with reconfigurable feed networks are designed for frequency and pattern reconfiguration. In [146] Nikolaou et al. designed PIN diodes loaded an annular ring slot antenna with a reconfigurable matching network on opposite sides of the substrate. The association or separation of stubs on microstrip feed line via PIN diodes generates the reconfiguration in 5.2 GHz, 5.8 GHz and 6.4 GHz resonant frequencies, while switching of PIN diodes across the annular slot antenna shifts the null position in radiation pattern within 150° of antenna plane. Han et al. [229] proposed a PIN diode loaded symmetric sickle shaped slot antenna on FR – 4 substrate and fed by a fork-shaped microstrip feed line. microstrip feed line. The switching of PIN diodes on the slot is responsible for frequency switching in '3.4 – 3.8 GHz' and '3.7 – 4.2 GHz' band and PIN diodes in the feed line steers the radiation pattern in 20° and 25° direction for each band. A microstrip line fed rectangular patch antenna with two horizontal slots and pair of PIN diodes across slots is designed by Selvam et al. [230] for frequency and pattern reconfiguration. The change in state of PIN diodes across slits is responsible for frequency agility between '4.5 GHz, 4.8 GHz, 5.2 GHz and 5.8 GHz' and radiation pattern tilt of '-30°', '0°', '+30°'. A single turn spiral antenna layout is proposed by Huff et al. in [145] for frequency and pattern switching. The design can be reconfigured in two frequency bands with pattern diversity in lower frequency band and non- reconfigurable radiation pattern at higher frequency. Singh et al. in [153] suggested a novel CPW fed closed ring resonator ('CRR') with enclosed ELC ('Electric-inductive-capacitive') resonator and four metal strips of asymmetric length on both sides of CRR along horizontal axes. The switching of PIN diodes between CRR and ELC resonator is responsible for reconfiguring multiple resonant frequencies within 1–5 GHz, while the connection of metal strips and ground plane via PIN diodes steers the omnidirectional radiation pattern to bi-directional and unidirectional end fire radiation pattern. Rodrigo et al. [36] designed a multi-size pixel antenna with twelve r.f. switches for achieving reconfiguration in frequency and radiation pattern.

Cao et al. [160] suggested a reconfigurable feed network based antenna design for pattern and polarization diversity. Here, four rectangular elements are arranged in square design and energized by a four-way power divider. A metamaterial antenna with conical beam pattern and linear polarization is achieved, when all elements are energized by sources with equal amplitude and phase, while all sources of same amplitude and progressive phase difference of 90° for each adjacent output results in wideband radiated wave having broadside radiation pattern with circular polarization. Raman et al. [161] suggested a microstrip fed, symmetric

truncated meandered monopole antennas placed side by side with a partial ground plane for reconfiguration in pattern and polarization. The alternate activation of monopole via PIN diodes produces the reconfiguration in radiation pattern and polarization in orthogonal planes at resonant frequency 2.4 GHz. Rodrigo et al. [164] designed a patch antenna with parasitic pixel layer of '6 × 6' elements and '60' PIN diodes between each pair of adjacent pixels for frequency switching, steers the radiation pattern in ±30° in antenna planes and reconfiguration in horizontal, vertical, RHCP and LHCP. In [165], a cavity backed antenna with back to back cross shaped slots having 48 PIN diodes is prototyped by Ge et al. for frequency, polarization and pattern reconfiguration. The activation of all switching elements on alternate layers generates the radiation pattern in opposite direction, while switching of PIN diodes in remaining layer produces three resonant frequencies of 2.29, 2.33 and 2.38 GHz with linear polarization and two frequencies of 2.31 and 2.35 GHz with circular polarizations.

However, most of the above reported designs have limitations in terms of huge size, large number of switching elements, complex feed network, increased power consumption, multilayered and less flexible etc. In [164–165], both designs utilize a huge number of PIN diodes to achieve all reconfiguration operations, so they have limitations in terms of complex feed network and tuning operations. In this chapter, an innovative open annular ring antenna design with two stubs of unequal lengths having two PIN diodes for loading / unloading on the partial ground plane gives rise to switching in frequency, pattern and polarization. The design development of the proposed structure along with parametric study and results are explained systematically in the upcoming sections of the chapter.

5.2 Antenna Design Configuration and Analysis

The proposed antenna is designed and optimized in 'CST – Microwave studio' software. The final design configuration is printed on inexpensive on 1.6 mm thick, inexpensive FR-4 substrate with dielectric constant of 4.4 and loss tangent has value of 0.025. In the subsequent sections, the systematic description of antenna design along with parametric analysis has been performed to optimize the antenna layout and for understanding of the interdependence between antenna dimensions and antenna characteristics in terms of impedance and axial ratio bandwidths. The evolution of final antenna geometry is systematically explained in five design steps from antenna-1 (A-1) to antenna-5 (A-5) as shown in figure 5.1 and their organized explanation in terms of antenna performances are provided in detail.

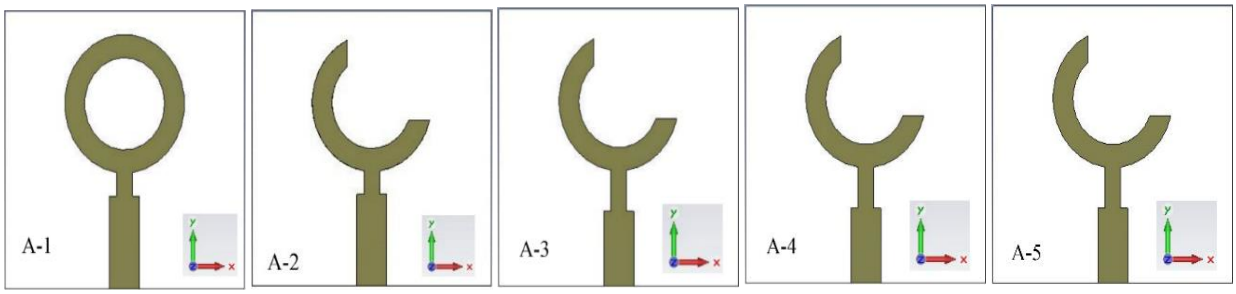

(a) Front side

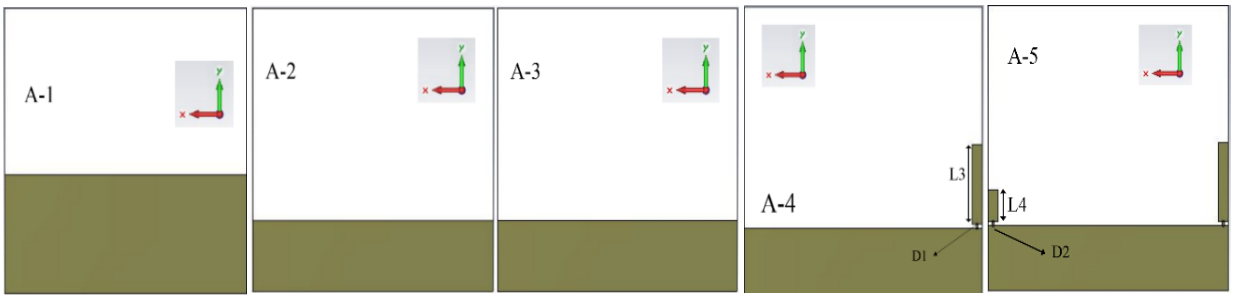

(b) Rear side

Figure 5.1 Evolution design steps of the proposed antenna design

5.2.1 Designing of Wideband antenna (A – 1) and Empirical formulas

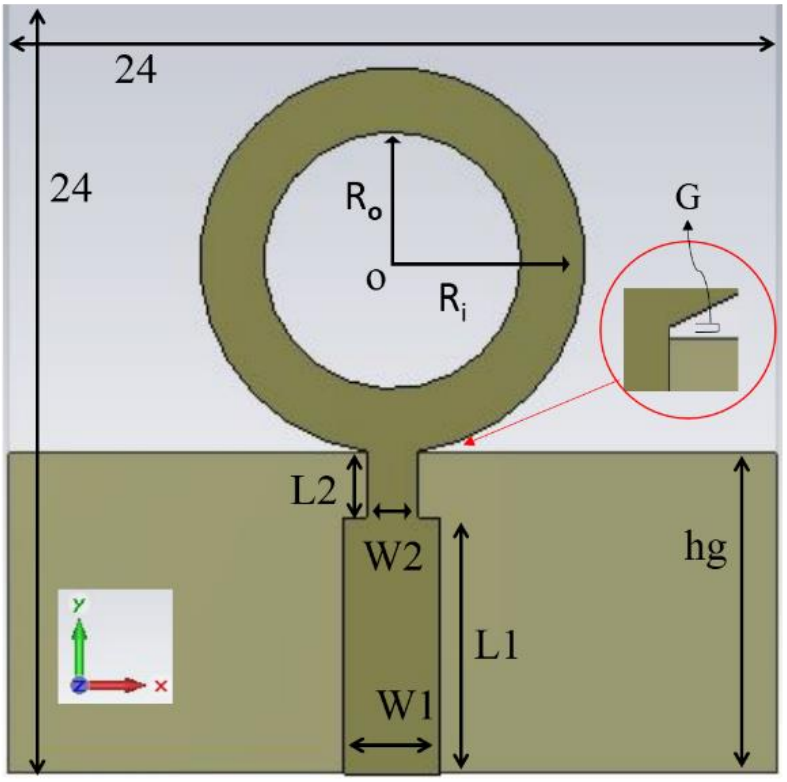

Figure 5.2 Proposed antenna design (A – 1)

In the first design step, an annular ring is selected as a radiating element over other available shapes, because more fringing fields are emitted at inner and outer edges at respective radii resulting in larger bandwidth and higher radiation performance [217]. It has been reported that the gap between radiating patch and partial ground plane in wide band antenna geometry exhibits coupling capacitance [52], [194]. The coupling capacitance is critical in generating wide band behaviour in the antenna. Hence, ground element plays a crucial role in antenna structure and any modification on it disturbs the current arrangement and ultimately the radiation characteristics.

The suggested antenna design comprises an annular ring with partial ground plane having a gap (G) between lower side of radiating element and upper outline of partial ground plane as displayed in figure 5.2 and labelled as antenna - 1 (A – 1). The antenna structure is fed by single microstrip feed line of two sections with varying lengths L1, L2 and widths W1, W2 respectively. The first section from the lower edge is matched to 50 Ω and next section is equated to the antenna impedance. The calculated value of resonant frequency from equations 4.1 – 4.3 is ≈ 5.82 GHz for inner and outer radius value of 4 mm and 6 mm respectively. The ground plane height (hg) and feed height (L1) are simultaneously optimized by parametric operations to obtain the almost UWB frequency response.

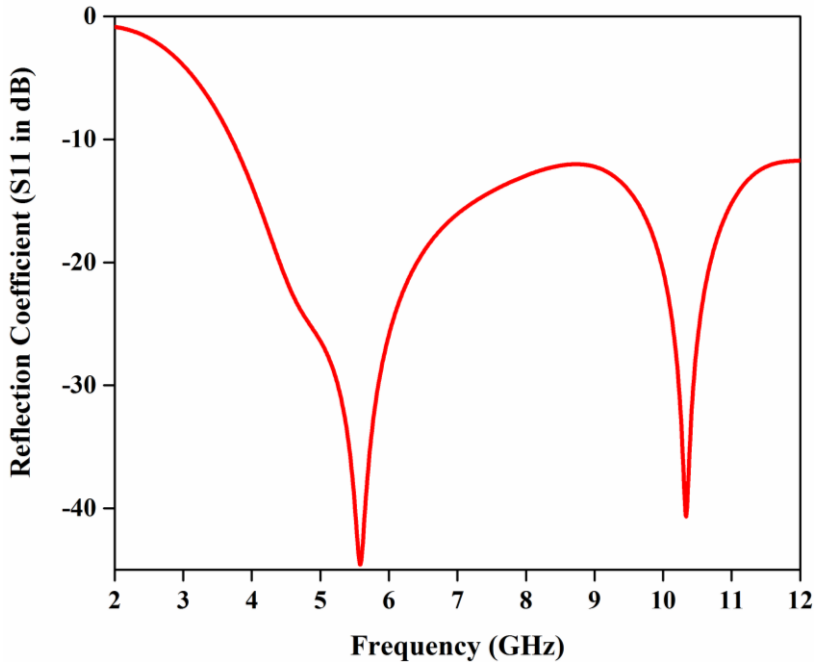

Figure 5. 3 Simulated reflection coefficient of proposed design A – 1

The simulated reflection coefficient against frequency is presented in figure 5.3, which depicts the dual resonating bands with 5.59, 10.39 GHz resonant frequencies lies in the UWB

frequency range from 3.7–12 'GHz. The optimized dimensions of the design A–1 are as follows: $L_1 = 8\,mm$, $L_2 = 2.05\,mm$, $W_1 = 3\,mm$, $W_2 = 1.6\,mm$, $G = 0.5\,mm$ and $hg = 10\,mm$.

5.2.2 Designing of Dual Band Antenna (A-2) with circular Polarization

As we know, two electric field vectors same in magnitude and 90° in phase produces circular polarization (CP) in the radiated field [195]. In this design step, the removal of arc approximately quarter wavelength long from annular ring and adjusting the ground plane height modifies the design A – 1 into open ended ring antenna – 2 (A – 2) as shown in figure 5.4. The above modification transforms the linearly polarized UWB antenna into a dual (WiMAX and WLAN) band antenna with linear and circular polarizations in 'WiMAX' and 'WLAN' bands respectively.

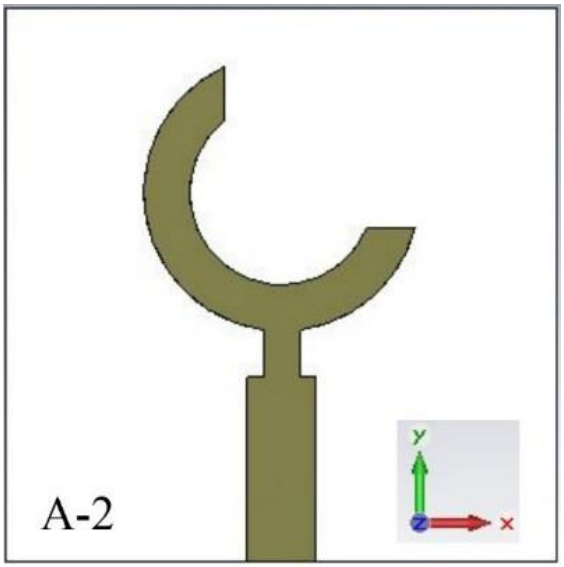

(a)

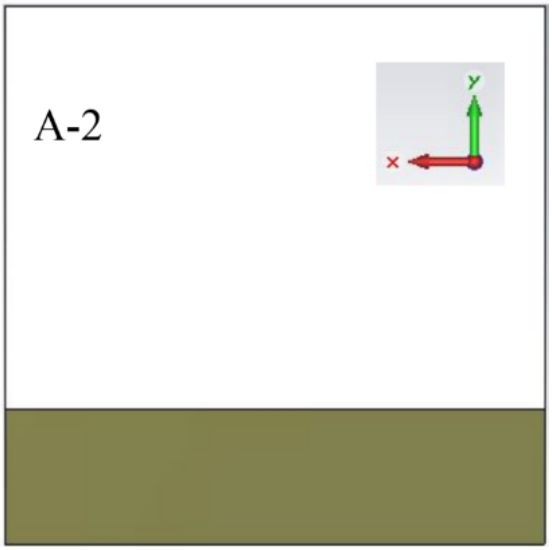

(b)

Figure 5.4 Proposed Antenna Geometry of A-2 (a) Front side (b) Back side

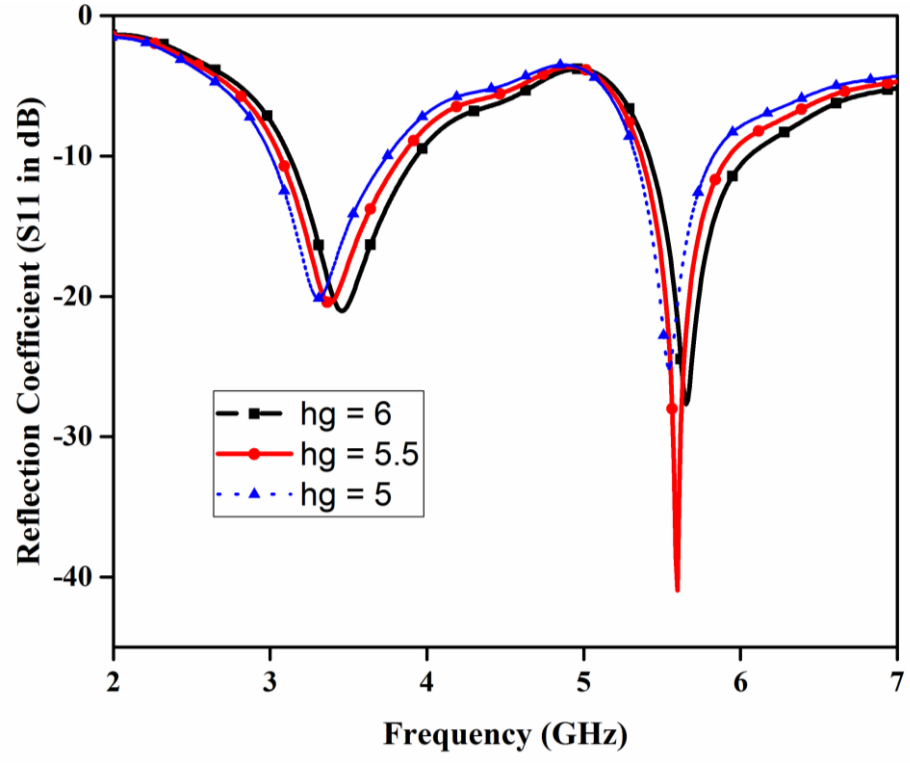

(a) Reflection coefficient vs frequency for different ground plane heights in A – 2

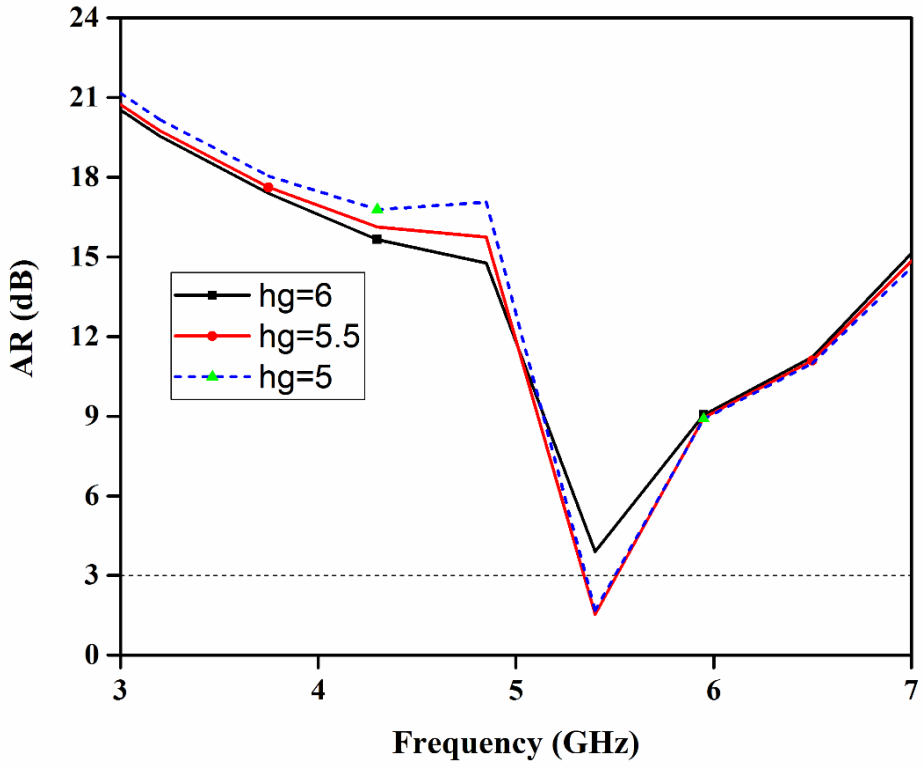

(b) Axial ratio vs frequency for different ground plane heights in A - 2

Figure 5.5 Simulated plot of proposed antenna design A – 2

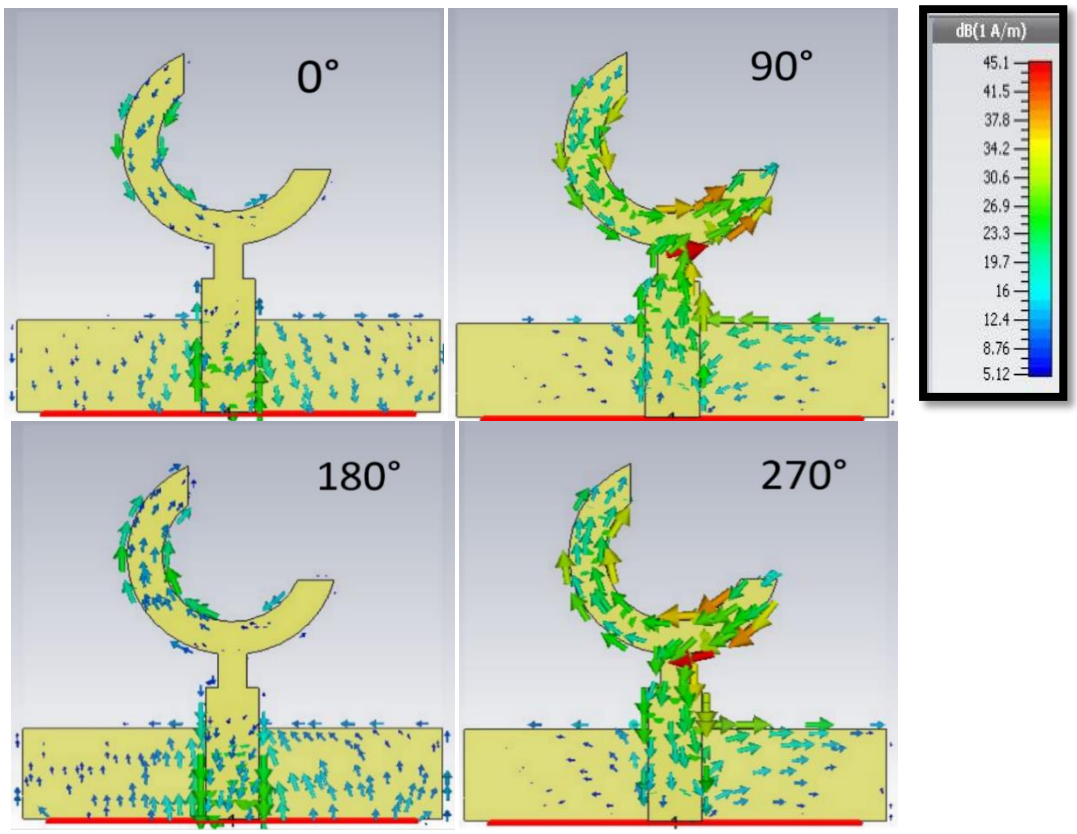

Figure 5.6 Surface current distribution at 5.4 GHz of proposed design at different phase angles

For fixed feed height , the parametric analysis of ground plane height on resonating frequency and axial ratio bands are presented in figure 5.5(a)–(b) respectively. From the plot, it was observed that the change in ground plane height to new value either 5 or 5.5 mm modifies the UWB antenna into circularly polarized dual band antenna. From available hg = 5 and 5.5 mm, we select ground plane height hg = 5.5 mm because at this ground plane height the impedance matching is very good in WLAN band with ARBW is slightly more than in comparison to other values of ground plane height. Thus at hg = 5.5 mm, the antenna design has two resonating frequency bands covering the frequency ranges from '3.06–3.83 GHz' , '5.37–5.93 GHz' with circular polarization in the 'WLAN' band with 170 MHz axial ratio bandwidth extended in 5.34 – 5.51 GHz.

The mechanism behind the generation of circular polarization (CP) in this antenna design is rooted in the interplay of capacitive and inductive effects introduced by the asymmetrically shaped arcs on the radiating patch. These asymmetries cause the dominant resonant mode to split into two orthogonal resonant modes of equal magnitudes with phase difference of 90°. This behaviour is clearly evidenced in the surface current distribution plots at the resonant frequency, as shown in Figure 5.6. The figure helps visualize how the surface currents behave

across the structure. Specifically, the longer arc of the radiating patch and the upper end of the ground plane support surface currents flowing in the same direction, forming a strong vertical current component. Conversely, on the shorter arc, the surface current flows in the opposite direction relative to the current on the ground plane, leading to partial cancellation of their contributions. This cancellation results from the inductive nature of the shorter arc. Due to this behaviour, the longer arc becomes capacitive, producing an electric field (E-field) component that is phase-advanced, while the shorter arc, exhibiting inductive behaviour, generates an E-field that lags in phase[110], [198]. This capacitive–inductive interaction between the arcs results in the required quadrature (90°) phase difference between the two orthogonal E-field components. Also, surface current vectors are equal in magnitude and opposite in phase for 0° and 180°, for 90° and 270°, also rotates in clockwise direction giving rise to right hand circular polarization (RHCP).

The horizontal and vertical truncations of the annular ring are combined with precise adjustments to the ground plane height (hg), significantly influence the electrical behavior of the antenna. These changes redirect the flow of surface current to specific regions of the patch, effectively modifying the antenna's electrical length. This redefinition of current paths shifts the frequency response from an ultra-wideband (UWB) nature to a more selective dual-band response that is capable of covering distinct communication bands (e.g., WiMAX and WLAN). After extensive simulation and optimization steps, the final optimized design was achieved by removing a radiating patch segment of 8.5 mm in length and setting the ground plane height to hg = 5.5 mm. All other geometrical parameters were kept constant.

5.2.3 Circularly Polarized Modified Dual Band Antenna A – 3

The proposed antenna A – 2 has a limitation that the starting edges of axial ratio and resonating frequency band are not coinciding or the starting edge of axial ratio is not contained within the resonating frequency band. This limitation can be eleminated in this design step by optimizing the feed length (L1) via parameteric study and keeping the other parameters unchanged. The modified antenna is presented in figure 5.7 and lablled as antenna – 3 (A – 3).

The parametric operation for optimization of feed length L1 is carried out and its impact on S11and axial ratio are plotted in figure 5.8 and 5.9 respectively. From both plots, it was observed that resonating frequency bands are shifted towards the lower frequency side and engulfs the axial ratio band within it. We select the best optimized feed length L1 = 6.5 mm,

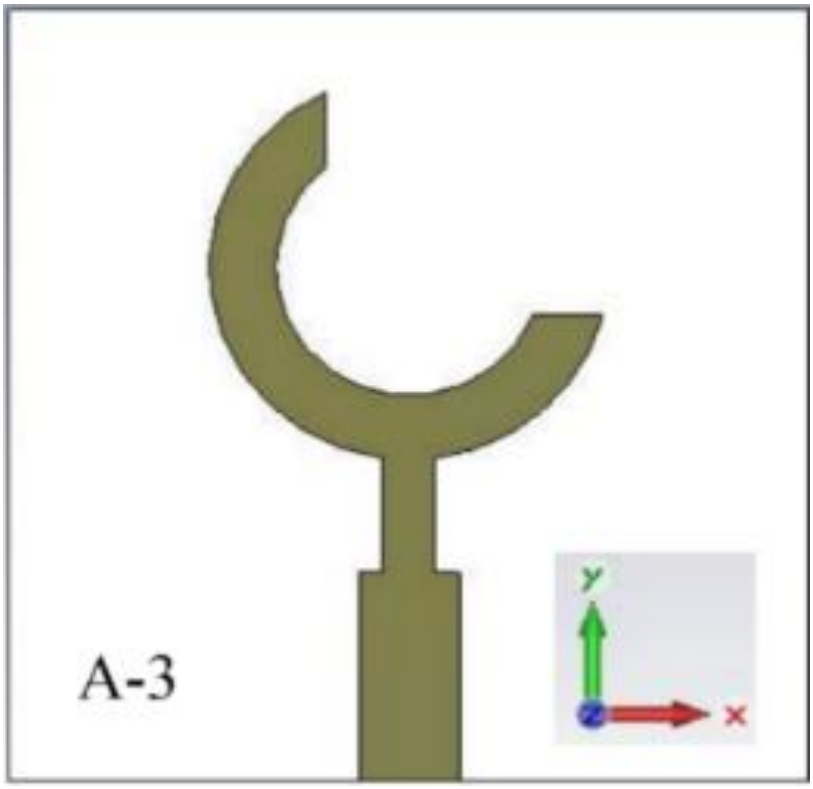

Figure 5.7 Proposed antenna geometry (A – 3)

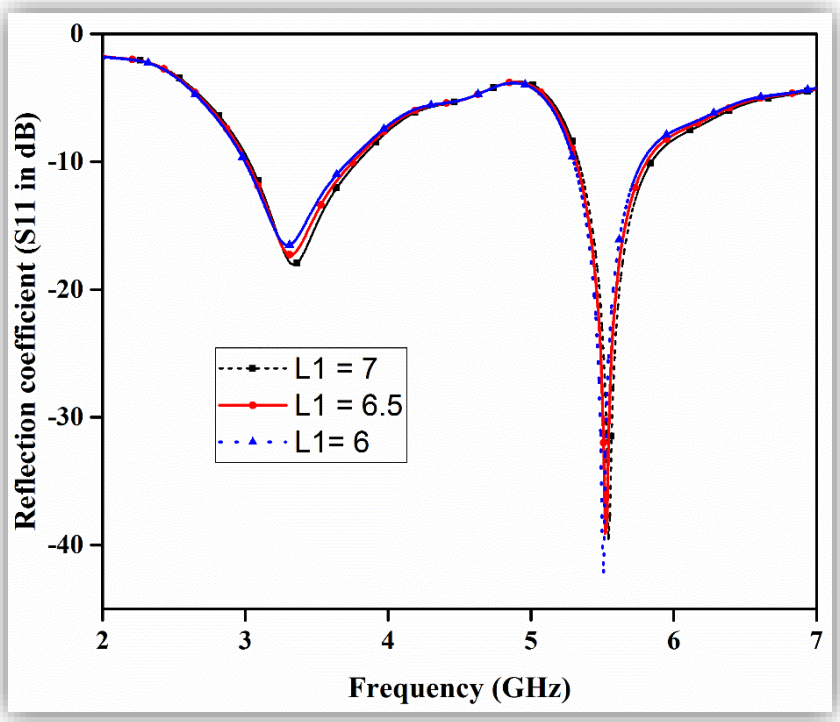

Figure 5.8 Reflection coefficient vs frequency for different feed lengths in A - 3

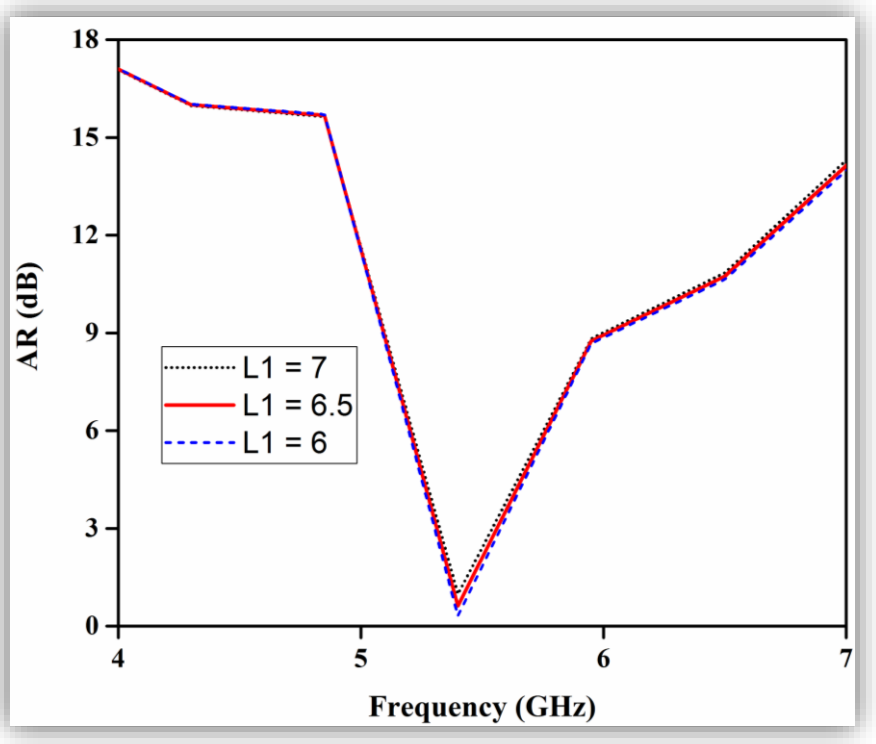

Figure 5.9 AR vs frequency for different feed lengths in A – 3

better ARBW and impedance matching is obtained at L1 = 6 mm in comparison to other values. Because at this feed length, the first resonating band lies quite away from the prescribed limit of WiMAX band. So at L1 = 6.5 mm, the impedance bandwidth (IBW) of 750, 500 MHz are extended in the frequency range '3–3.75 GHz' and '5.31–5.81 GHz' respectively. Also circular polarization in the WLAN band with enhanced ARBW of 240 MHz (5.32–5.56 GHz) is also observed. The optimized dimensions of design A – 3 are as follows: are $L_1 = 6.5\ mm$, $L_2 = 3.55\ mm$, $W_1 = 3\ mm$, $W_2 = 1.6\ mm$ and $hg = 5.5\ mm$.

5.2.4 Stub loaded frequency and Polarization Reconfigurable Antenna – 4 (A–4)

The circularly polarized dual-band antenna, referred to as Antenna A–3, which is originally designed to operate within the WiMAX and WLAN frequency bands, is further enhanced in functionality by introducing reconfigurability in both frequency and polarization. This is achieved through the loading or unloading of 1 mm wide and L3 mm long, I – shaped stub on the partial ground plane through PIN diode (D1) as shown in figure 5.10. When the diode is forward-biased (ON state), the stub becomes an active part of the ground plane, influencing the surface current distribution and introducing a perturbation that alters the electromagnetic behaviour of the antenna. This change modifies the effective electrical length and resonant

conditions of the antenna, leading to a shift in the operating frequency and a potential change in the polarization characteristics. Conversely, when the diode is reverse-biased (OFF state), the stub is electrically isolated from the ground plane, returning the antenna to its original configuration similar to that of A–3. This switching mechanism enables the antenna to alternate between different functional states —effectively providing reconfigurability in both frequency (shifting between WiMAX and WLAN bands) and polarization switching between linear and circular polarization modes. The newly resulting structure, after the addition of the PIN-controlled I-shaped stub, is referred to as Antenna A–4.

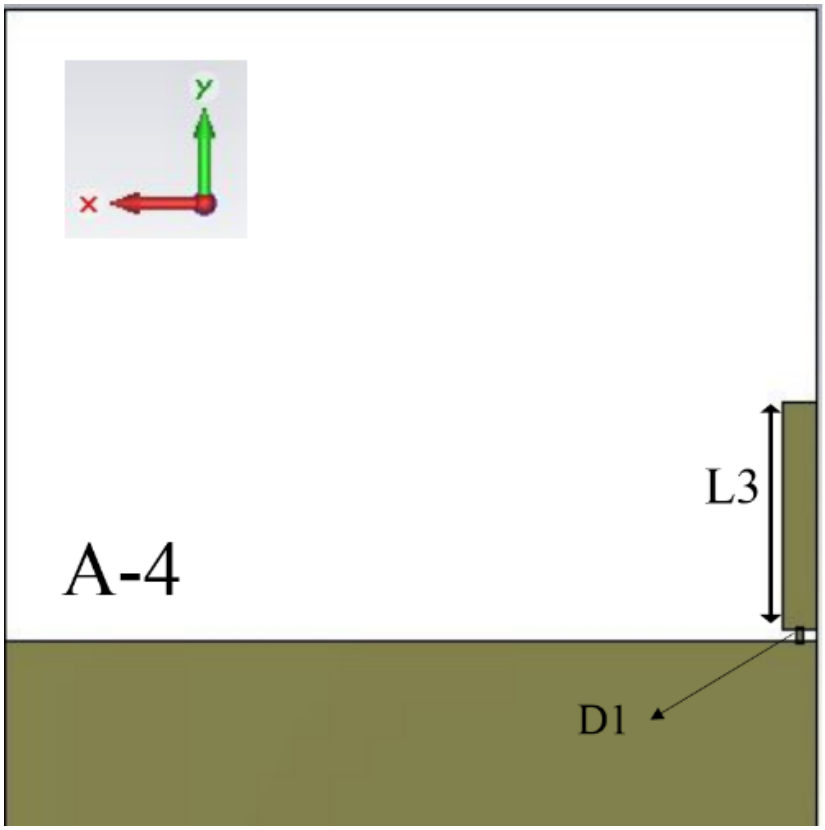

Figure 5.10 Rear view of suggested antenna design A-4

The forward biasing of D1 loaded I – shaped stub on the partial ground plane, which in turn varies the effective electrical length of antenna, thus translating circularly polarized dual band antenna into a single band antenna with linear polarization. While on reverse biasing, design A–4 has the same characteristics as that of design A – 3 but having enhanced values. The surface current distribution at respective frequencies further concreted the above said.

The effect of stub lengths (L3) on impedance bands are carried out through parametric analysis and corresponding reflection coefficient and axial ratio results are displayed in figure 5.11 and

5.12 respectively. From S11 plots, it is noticed that the resonating behavior of the antenna remains the same with negligible variations in IBW for different stub lengths and both switching states of PIN diode. The best optimized value of L3 is set to 6.6 mm, because axial ratio bandwidth (ARBW) reaches maximum value at this stub height as depicted in figure 5.12. Hence at L3 = 6.6 mm, antenna has impedance bandwidth (IBW) of 400 MHz in resonating band from 5.30 – 5.70 GHz for the ON state of diode D1. Similarly for the OFF state of PIN diode, the antenna has two resonating frequencies from '3.03–3.73', '5.33–5.81 GHz' with resonant frequencies at '3.32 GHz' and '5.52 GHz' respectively. The proposed design has linear polarization when the stub is loaded on the ground plane and unloading of stub produces the circular polarization with ARBW of 170 MHZ extended in 5.34 – 5.51 GHz band. The axial ratio plot in figure 5.13 further confirms the reconfiguration between linear and circular polarization state of the antenna on switching PIN diode ON / OFF respectively. Thus, the presence of stub changes antenna behaviour from dual band to single band with slight shift and shrink in the resonating frequency bands and ARBW as well.

To understand the frequency reconfiguration mechanism in A-4, surface current distribution at frequencies '3.32' and '5.4 GHz' are displayed in figure 5.14. At 3.32 'GHz' for the OFF state of diode D1, the surface current is more distributed on annular ring and around the feed line as shown in figure 5.14 (a). The activation of diode, withdrew the surface current from the truncated ring and partially redistributed on stub and upper side of the ground patch as displayed in figure 5.14 (b) thus suppressing the WiMAX band. While surface current distribution at '5.4 GHz' remains the same for both switching states of PIN diode as depicted in figure 5.14(c)–(d).

Also from the plotted 2D radiation pattern at '5.4 GHz' for switching states of PIN diode as shown in figure 5.15. It is noticed that the main beam direction is slightly shifted its orientation from -85° to -90° as the diode changes its state from OFF to ON. Thus we concluded that the loading or unloading of stub on a partial ground plane via PIN diode successfully exhibited the frequency, polarization reconfiguration operation with very small pattern diversity. The optimized dimensions of A – 4 are as follows: are $L_1 = 6.5\,mm$, $L_2 = 3.55\,mm$, $L_3 = 6.6\,mm$, $W_1 = 3\,mm$, $W_2 = 1.6\,mm$ and $hg = 5.5\,mm$.

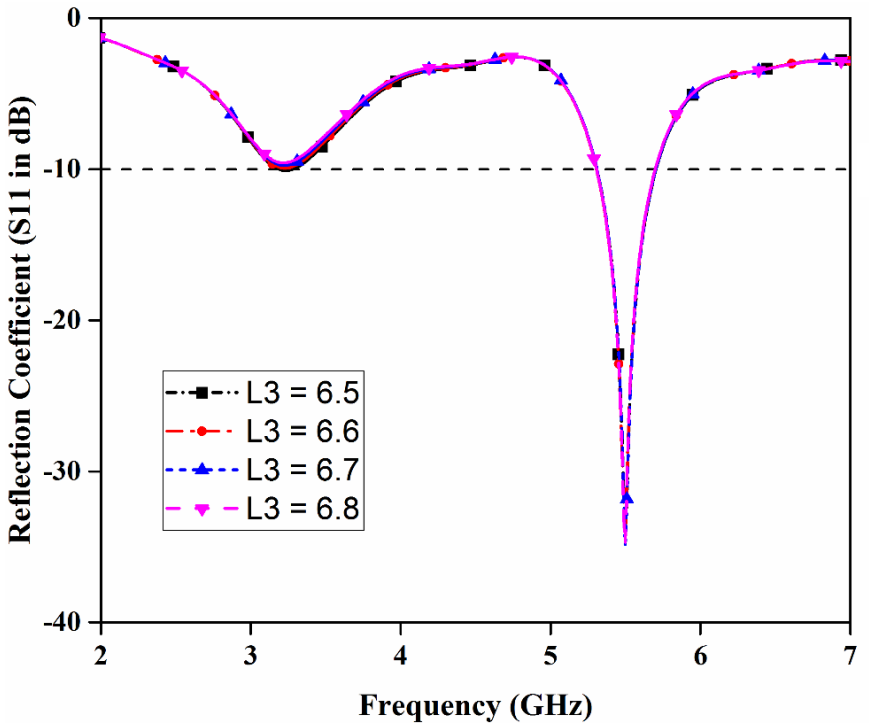

(a)

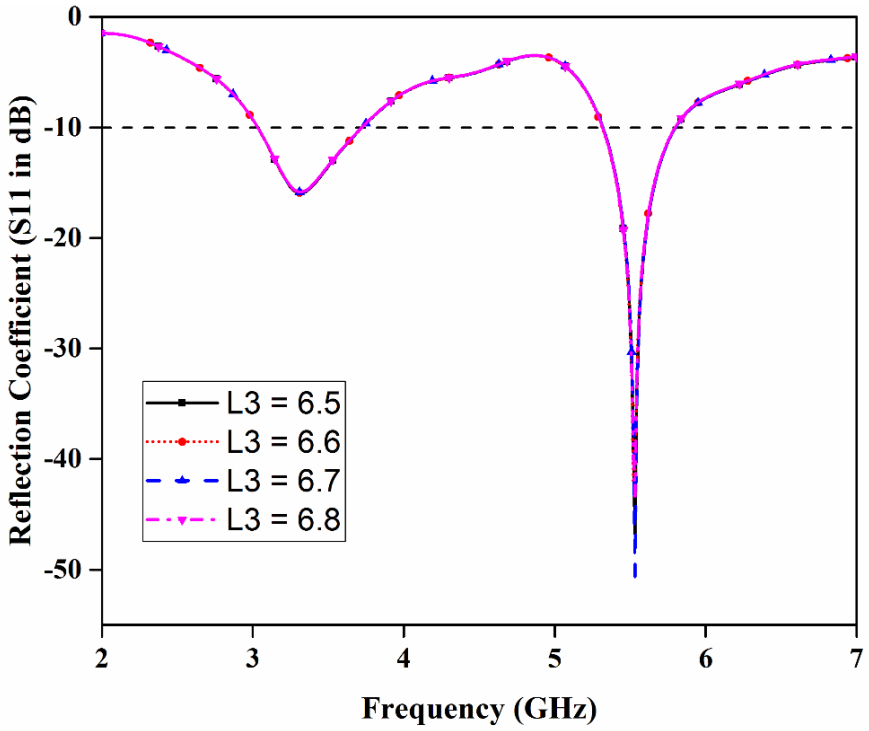

(b)

Figure 5.11 Reflection coefficient for A-4 (a) diode ON (b) diode OFF

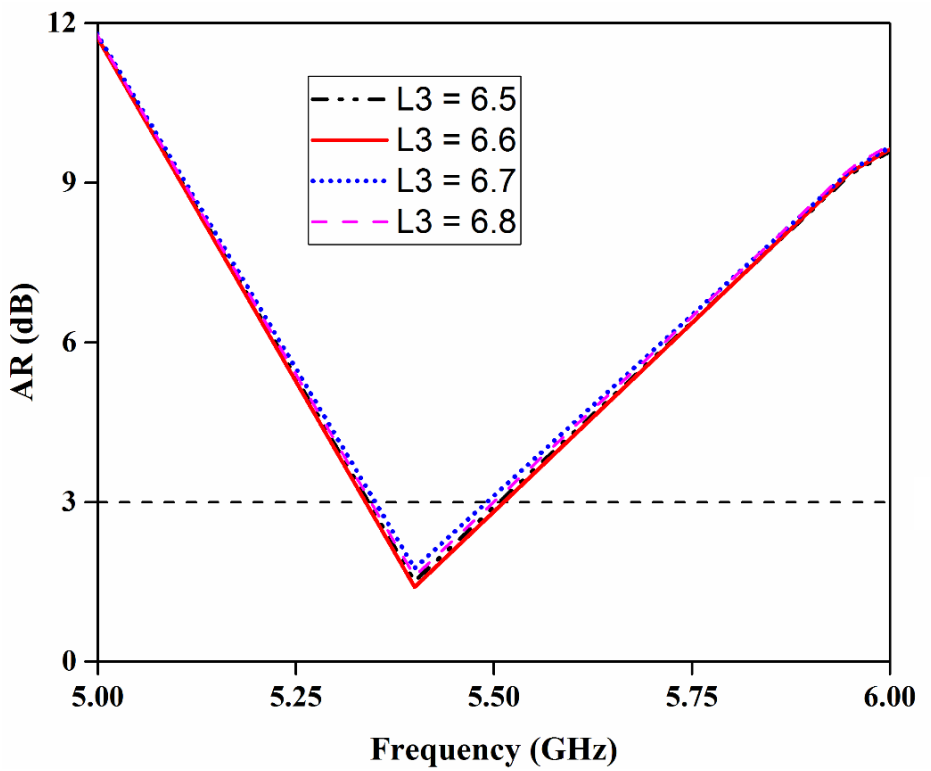

Figure 5.12 Simulated AR vs frequency plot for OFF state

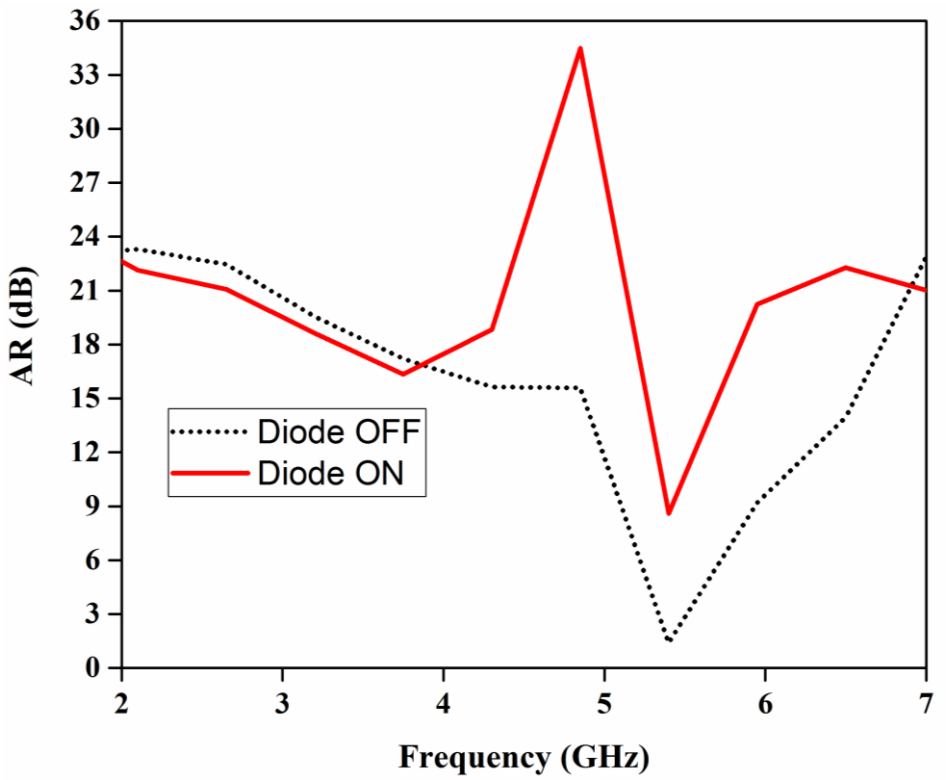

Figure 5.13 AR plot for ON or OFF states of proposed antenna A – 4

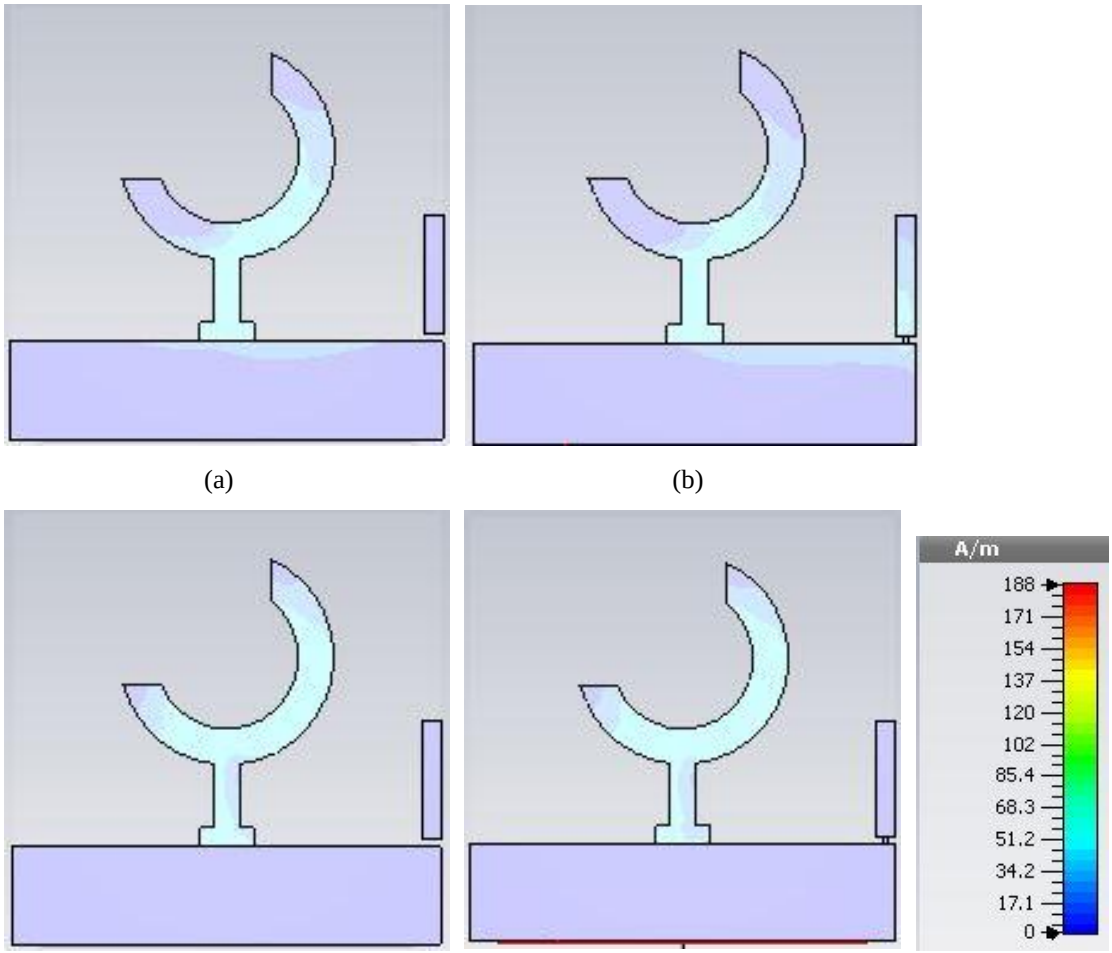

(a) (b)

(c) (d)

Figure 5.14 Simulated surface current distribution (a) f = 3.32 GHz diode OFF (b) f = 3.32 GHz diode ON (c) f = 5.4 GHz diode OFF (d) f = 5.4 GHz diode ON

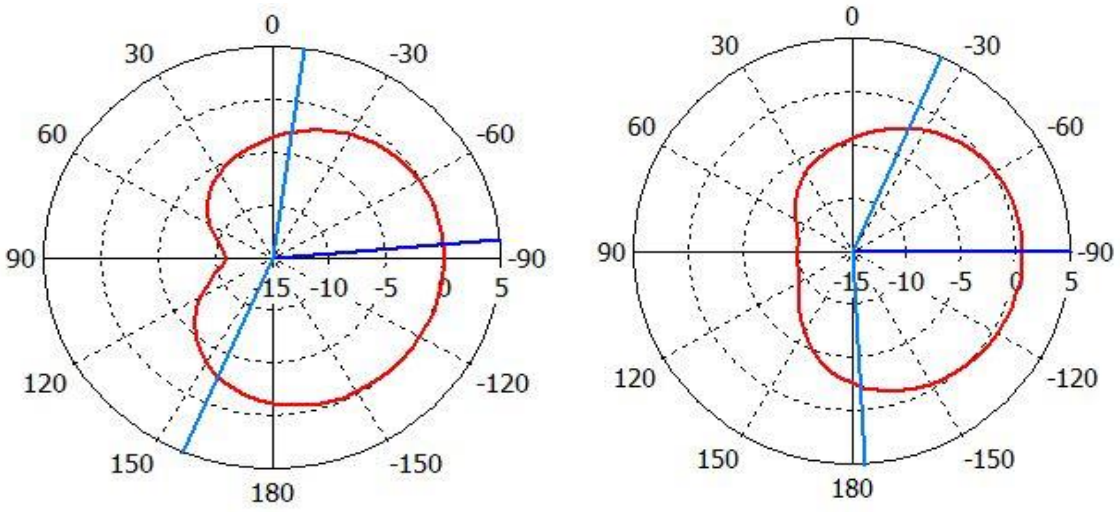

(a) Diode OFF (b) Diode ON

Figure 5.15 Normalized E-field radiation pattern at 5.4 GHz

5.2.5 Designing of Frequency, Pattern and Polarization reconfigurable Antenna–5 (A–5)

As we know that any alteration in the current dispersal on radiating structure gives the pattern diversity [60]. Here in this design step, the inclusion or exclusion of another I – shaped stub of length L4 on a partial ground plane through PIN diode D2, worked as a reflector and changed the effective electrical length of the ground element to realize the pattern switching. Because of this element, the current has to cover the extra distance which leads to path difference that produces the phase difference in excitation current results in pattern tilting [153], [230–231] in the modified antenna geometry. The modified antenna structure with asymmetric stubs is as depicted in figure 5.16 and labelled as antenna–5 (A–5).

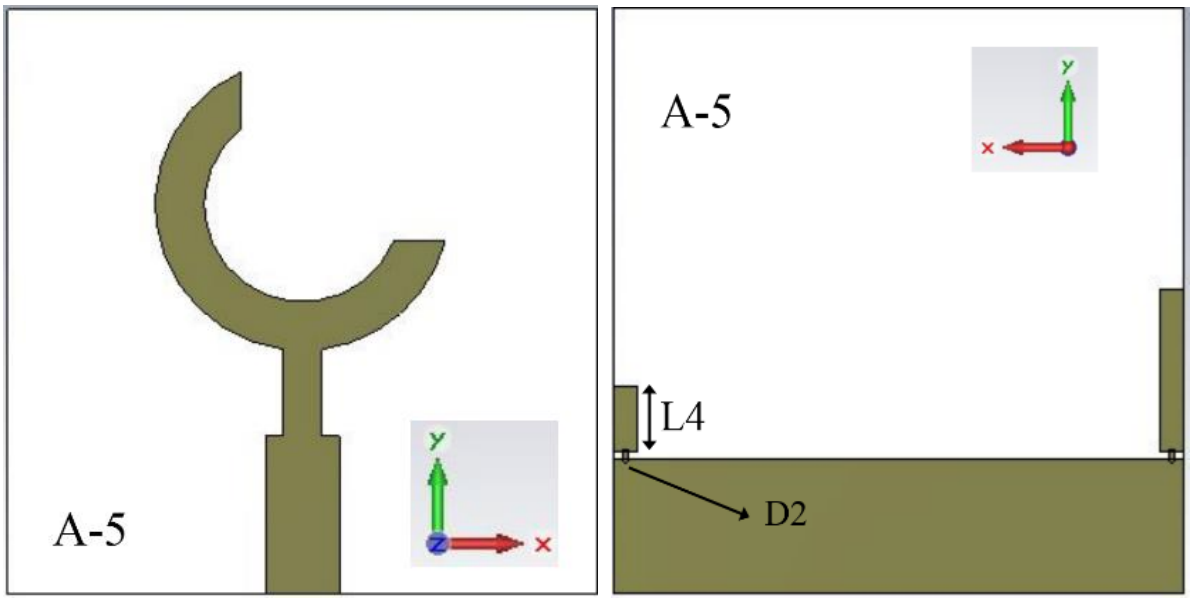

(a) Front View (b) Rear View

Figure 5.16 Layout of proposed antenna -5 (A-5)

After running several parametric processes, the optimized value of stub length L4 is set equals to 2.7 mm, as satisfactory IBW, ARBW and pattern steering in different angles are obtained. At this stub length, the simulated reflection coefficient, axial ratio, gain, radiation efficiency and 2D, 3D radiation pattern are presented in figures 5.17–5.21 respectively for all possible states of PIN diodes and corresponding outcomes are summarized in Table 5.1. The antenna has single and dual resonant band for state II, IV, I, III respectively, circular polarization in state I. The antenna gain is ranging from 0.5 – 3 dBi with total efficiency more than 50% for all four states as depicted in figure 5.20 and 5.21 respectively.

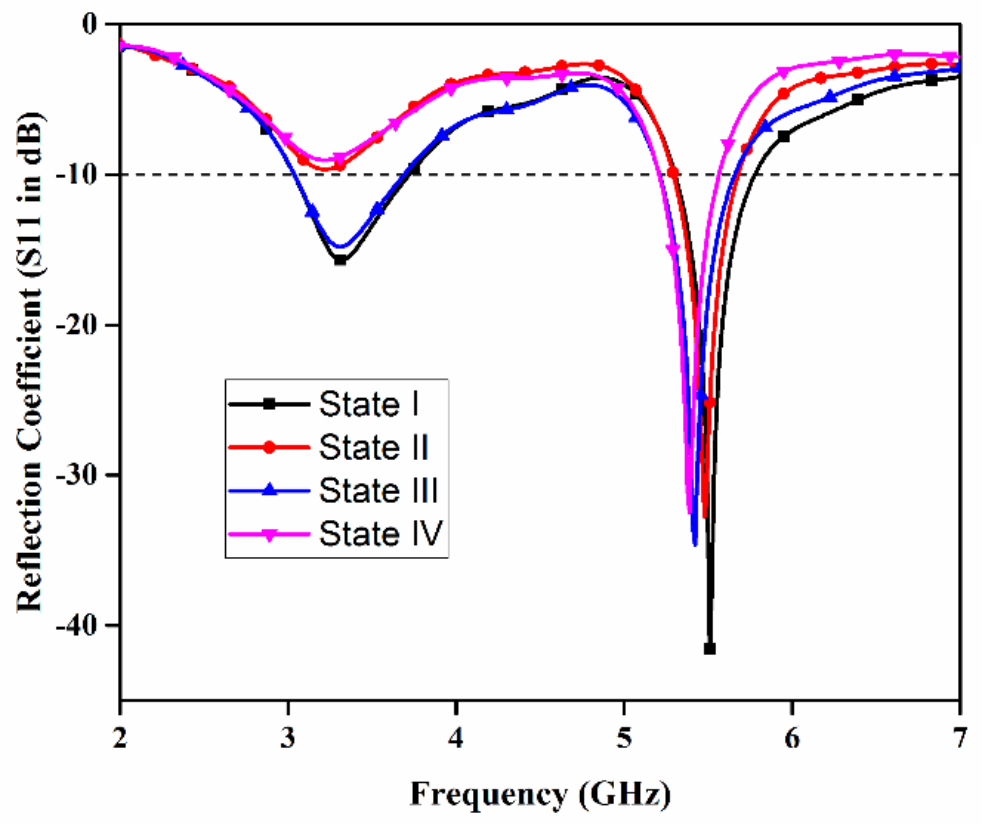

Figure 5.17 Simulated reflection coefficient for proposed antenna A – 5

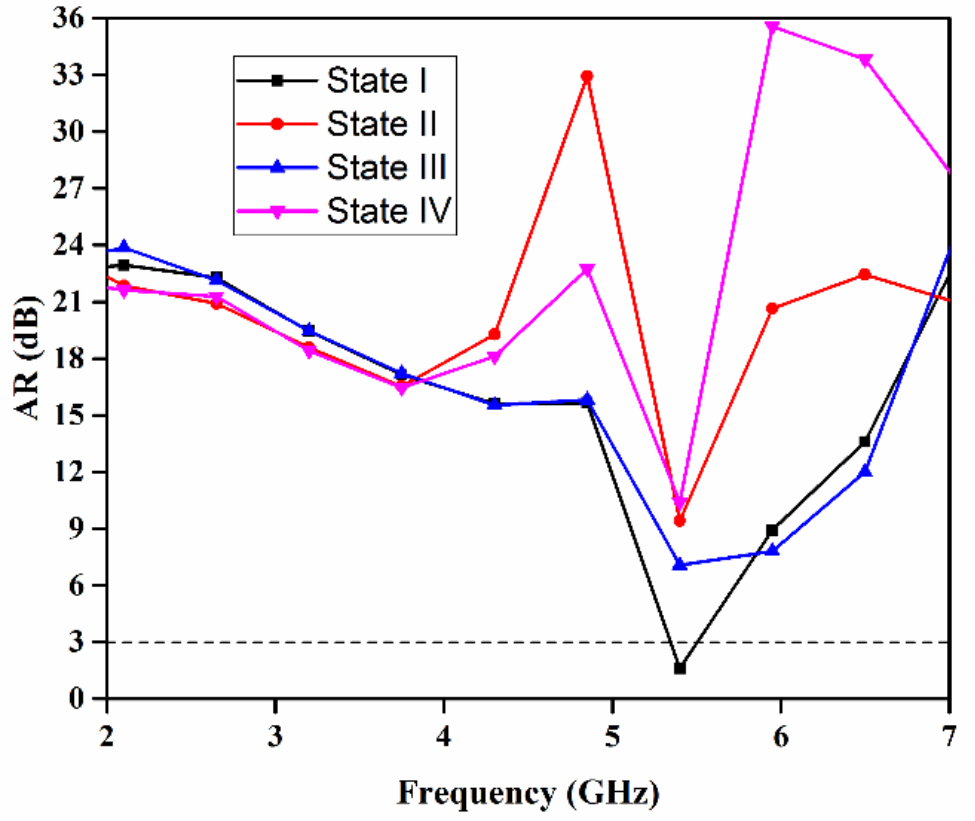

Figure 5.18 Simulated AR vs frequency for proposed antenna A – 5

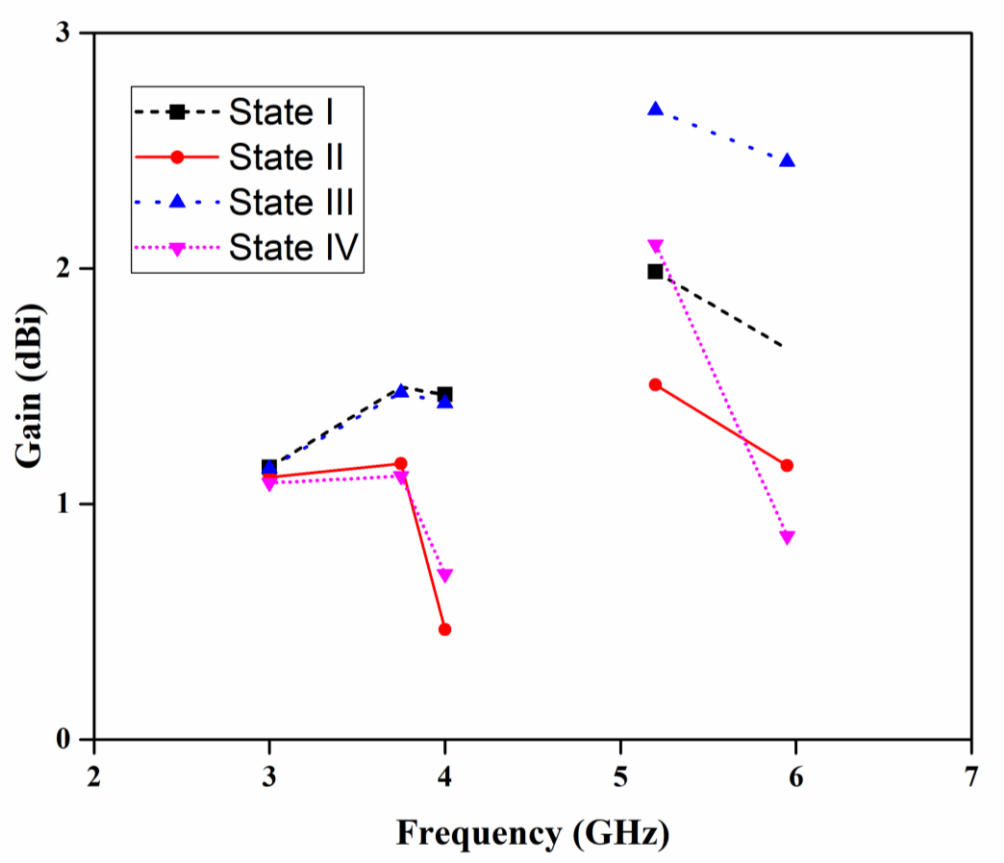

Figure 5.19 Gain vs frequency plot for proposed antenna A – 5

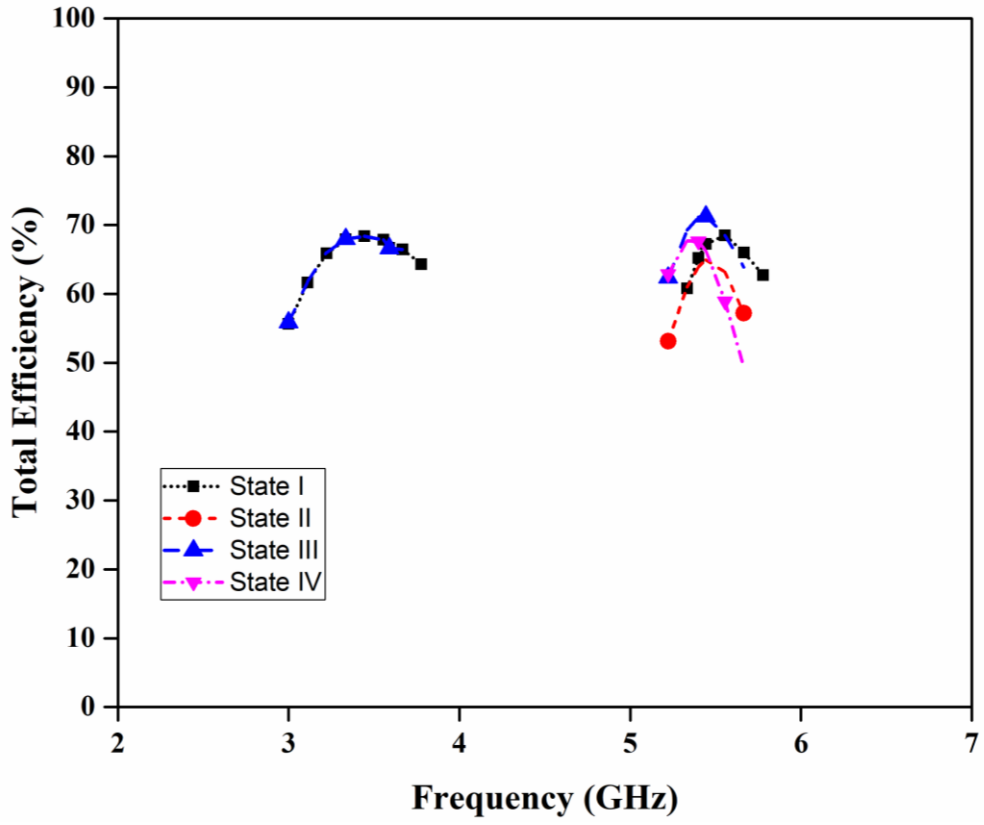

Figure 5.20 Total Efficiency vs frequency plot for proposed antenna A – 5

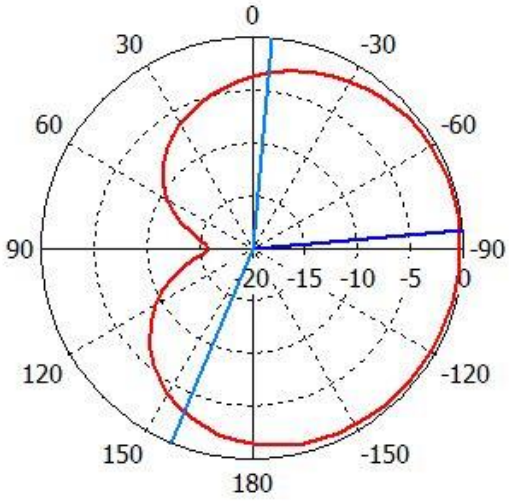

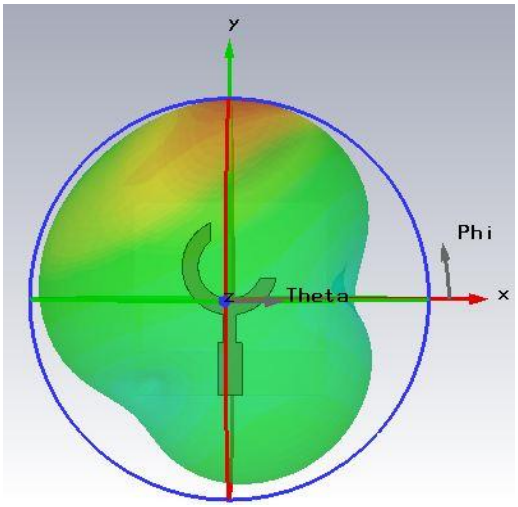

(a) Both diodes OFF

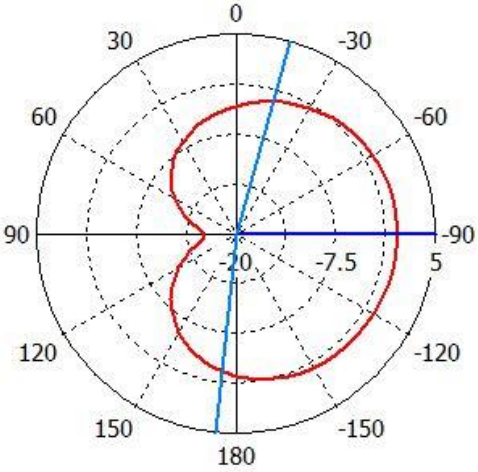

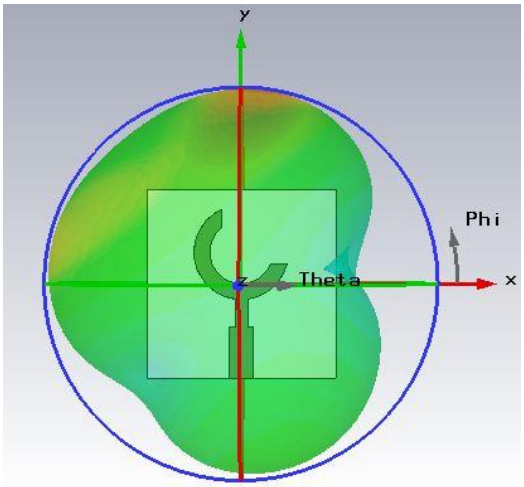

(b) Diode D1 ON

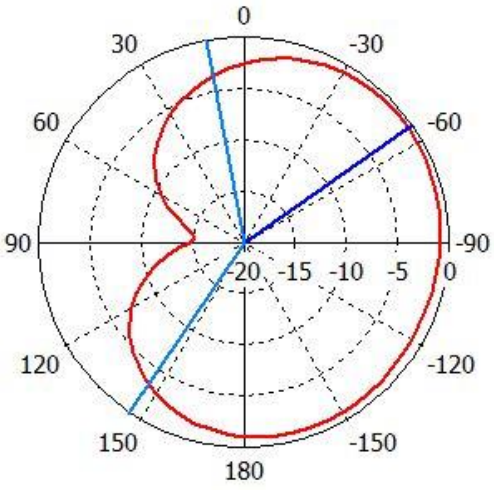

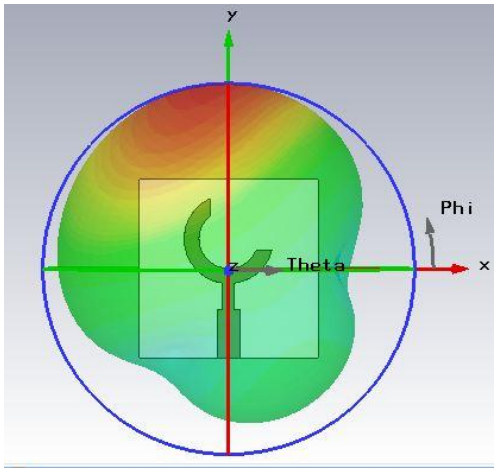

(c) Diode D2 ON

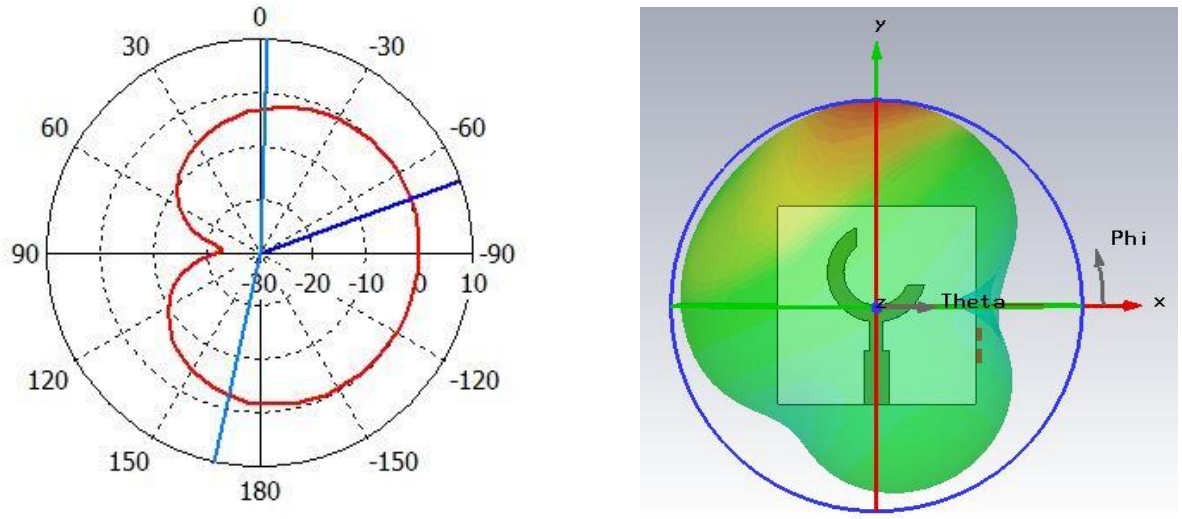

(d) Both Diodes ON

Figure 5.21 Simulated 2D and 3D radiation pattern at 5.4 GHz for different states of PIN diode

Table 5.1 Operation States of Antenna A-5

State	PIN Diodes		Reso. Freq. Band (GHz)	Reso. Freq. (GHz)	ARBW (GHz)	Pol.	Main Lobe Direction at 5.4 GHz (°)
	D1	D2					
I	OFF	OFF	3.03 – 3.72	3.31		LP	
			5.30 – 5.78	5.51	0.20 (5.33 – 5.53)	CP	-85
II	ON	OFF	5.29 – 5.68	5.48		LP	-90
III	OFF	ON	3.02 – 3.68	3.31		LP	
			5.21 – 5.65	5.41		LP	-55
IV	ON	ON	5.21 – 5.56	5.38		LP	-70

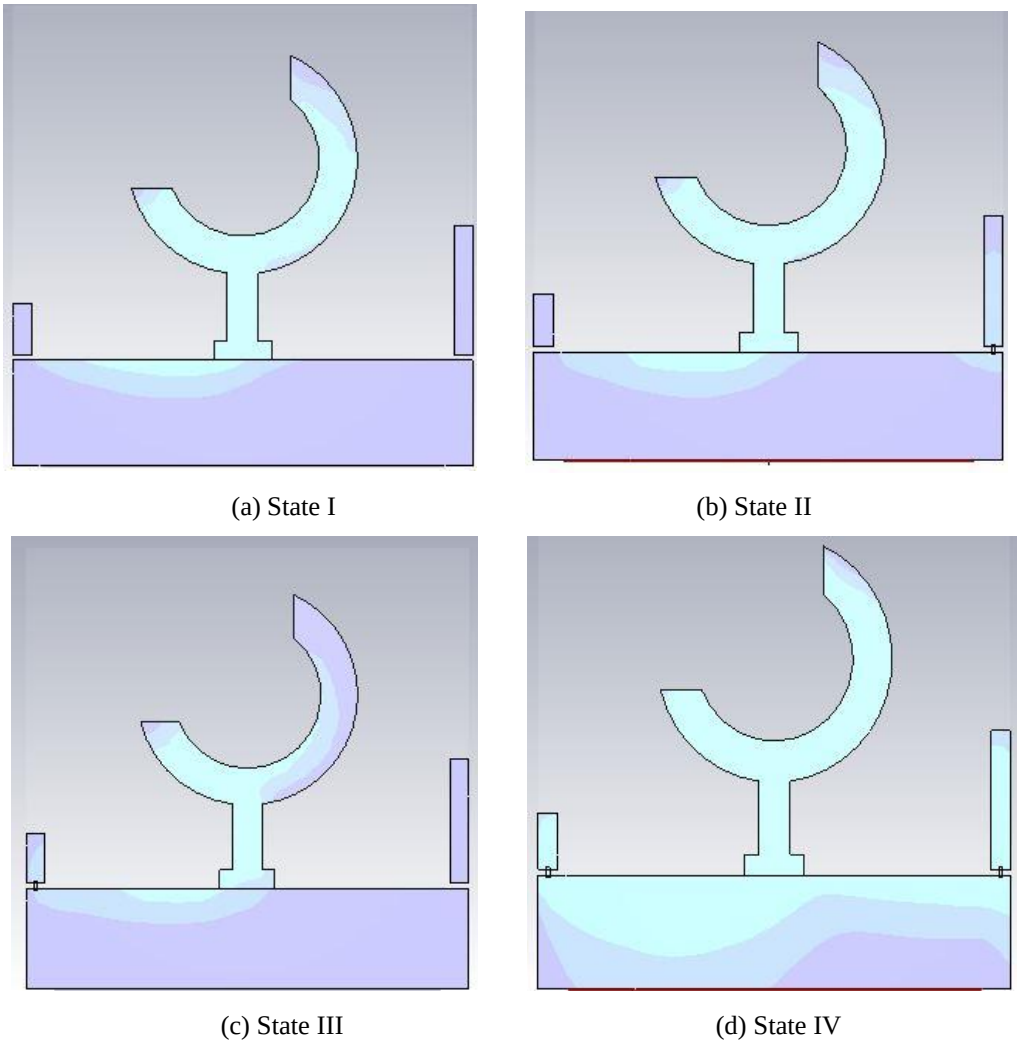

(a) State I (b) State II

(c) State III (d) State IV

Figure 5.22 Surface current distribution at 5.4 GHz for states I – IV

The depicted surface current dispersal at 5.4 GHz in figure 5.22 explains the pattern reconfiguration mechanism for various states of PIN diodes. In state I, surface current is mainly concentrated on open annular ring with small amount of current on upper edge of partial ground plane towards the shorter stub provides the direction of main beam towards -85° direction. The forward biasing of diode D1 in state II connects the longer stub to partial ground patch and act as reflector by redirecting the small amount of surface current from annular ring and redistribute on itself, while most of the surface current concentrated on the radiating patch. This arrangement minutely shifts the direction of main beam in -90° direction. While deactivating the diode D1 and activating the diode D2 in state III connects the short stub to partial ground plane,which in turn redistribute the current on smaller arc and smaller stub produces the switching in main beam direction towards -55° angle. The activation of both diodes in state IV connects both stubs with partial ground plane. This arrangement redistributes the considerable amount of surface currents on both stubs, partial ground plane and truncated

annular ring shifts the direction of main beam to -70° orientation. Thus suggested antenna A – 5 successfully exhibited the 'frequency', 'polarization and pattern' reconfiguration operations by governing the switching states of PIN diodes.

5.3 Final Reconfigurable Antenna Design with Inductance Pad and Lumped Elements

To realize the reconfiguration operation, two PIN diodes D1, D2 with DC biasing circuit are embedded on the ground plane side. The DC biasing circuit includes three inductor pads of 2×1 mm^2 size placed at 0.8 mm distance from edges, three 47 nH RF chokes to isolate the RF signal from biasing lines and 1.5 V DC battery as displayed in figure 5.23 for driving Alpha's PIN diode (DGS 6474) [226]. The final antenna design with optimized dimensions is presented in figure 5.23 and Table 5.2 respectively.

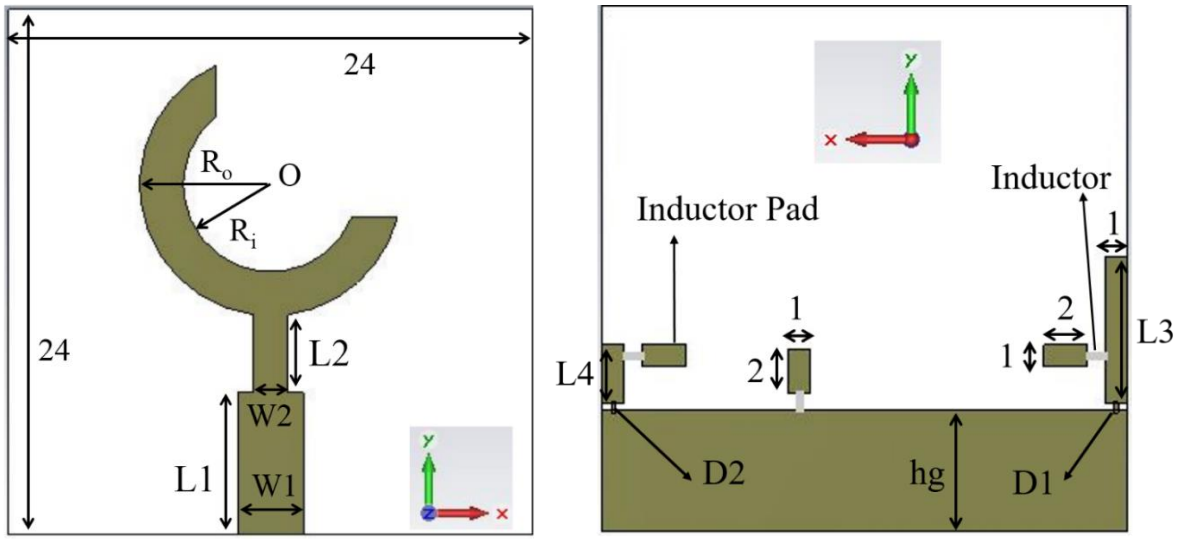

(a) (b)

Figure 5.23 Final antenna layout (a) Front side (b) Rear side

Table 5.2 Optimized dimensions of antenna layout

Parameters	hg	L1	L2	L3	L4	W1	W2	R_o	R_i
Value (mm)	5.5	6.5	3.55	6.7	2.7	3	1.6	6	4

5.4 Measured Results and Analysis

The final optimized antenna design is printed on inexpensive '1.6 mm' thick 'FR–4' substrate as shown in figure 5.24. For the validation of reconfigurability operations at all four states, the

prototyped antenna is measured with 'Vector Network Analyzer' for S_{11} parameter and radiation pattern in microwave chamber as displayed in figure 5.25.

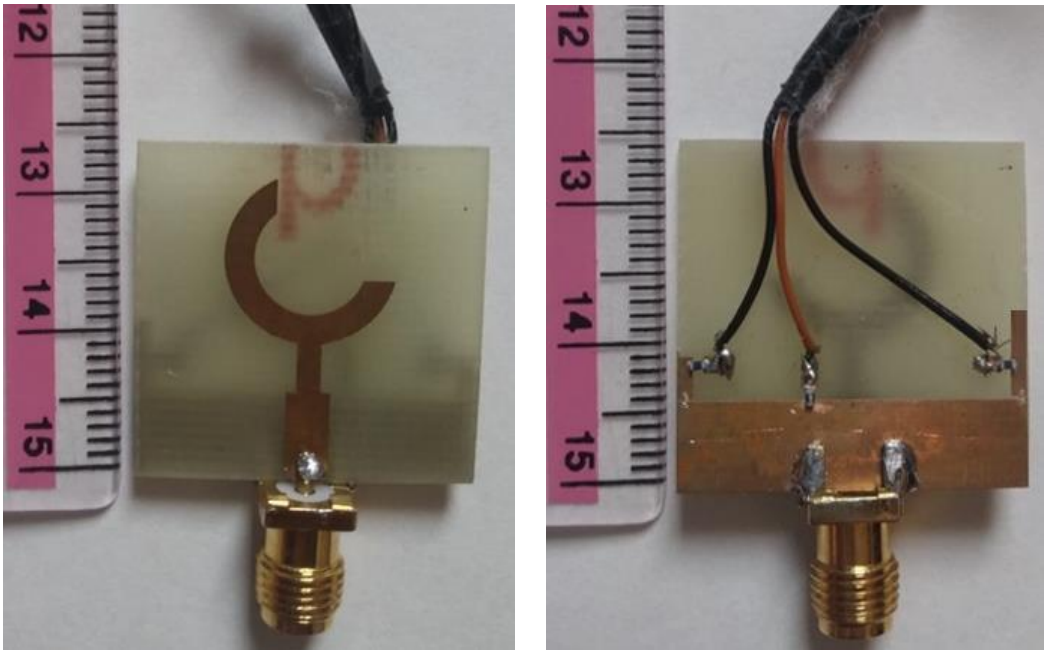

(a) Front view (b) Rear view

Figure 5.24 Fabricated Antenna

The simulated and measured -10 dB impedance bandwidth of the antenna for all possible four states of PIN diodes are displayed in figure 5.26. It is noticed from the reflection coefficient plot that the measured resonance bands are in good agreement with simulated bands in the higher frequency band with minor variations in lower frequency ranges. A number of factors, including fabrication tolerance, biasing wires, soldering, DC power supply, and measuring environment, may be responsible for the little discrepancy between the simulated and measured results. The realized ARBW of the design as a function of frequency is displayed in figure 5.27 that depicts the circular polarization characteristics with ARBW of 160 MHz. Antenna gain for resonating frequency bands varies from 1.25 – 2.35 dBi for all states of PIN diodes.

The 2D simulated and measured normalized radiation patterns in the *xoz* and *yoz* planes at 5.4 GHz and 3.38 GHz are depicted in figure 5.28–5.30 respectively. The measured radiation patterns for E and H –plane are in agreement with simulated radiation patterns at all frequencies. The E- field radiation patterns are directional radiation pattern for both resonant frequencies. The simulated and measured results for different states are tabulated in Table 5.3.

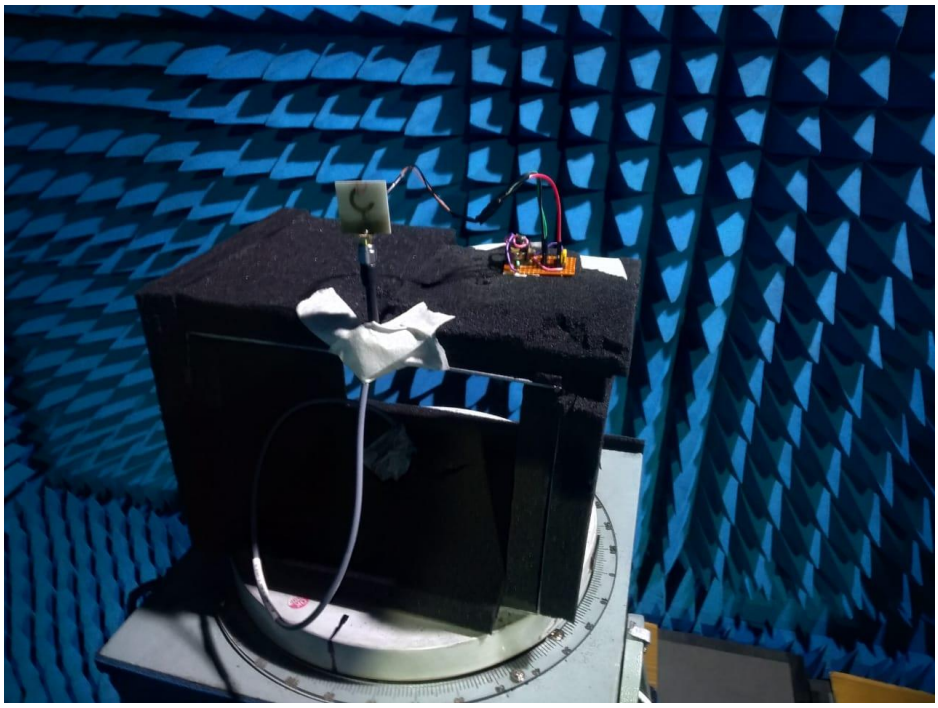

Figure 5.25 AUT (Antenna under test) in anechoic chamber

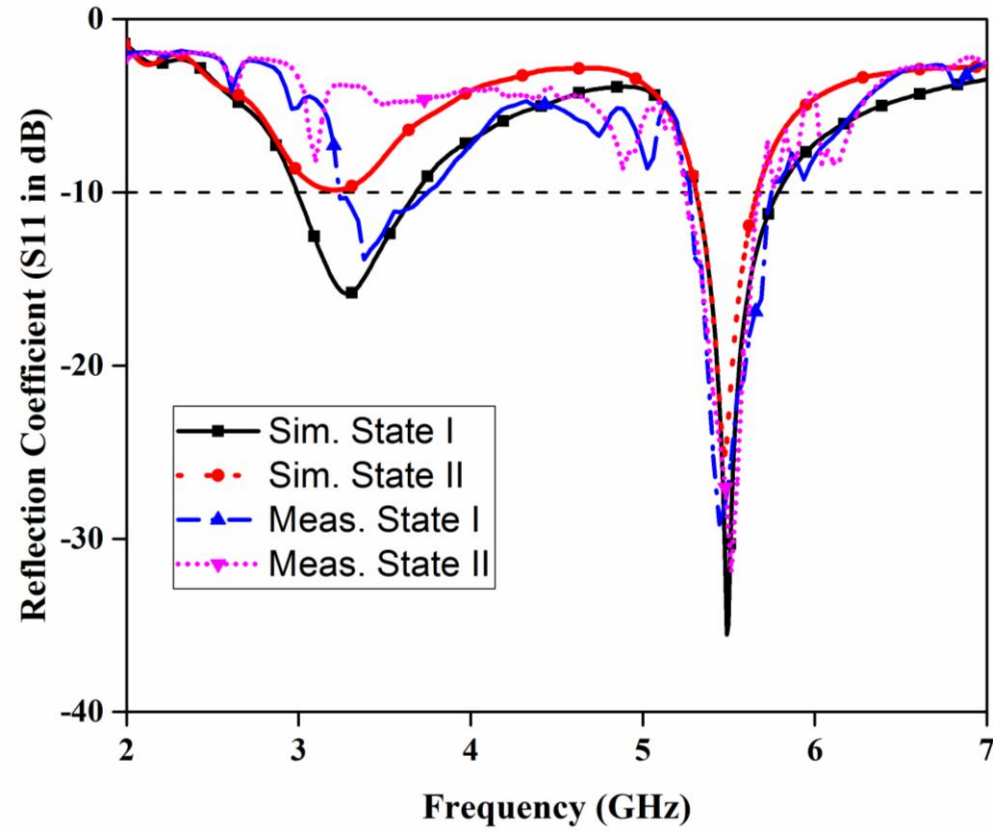

(a)

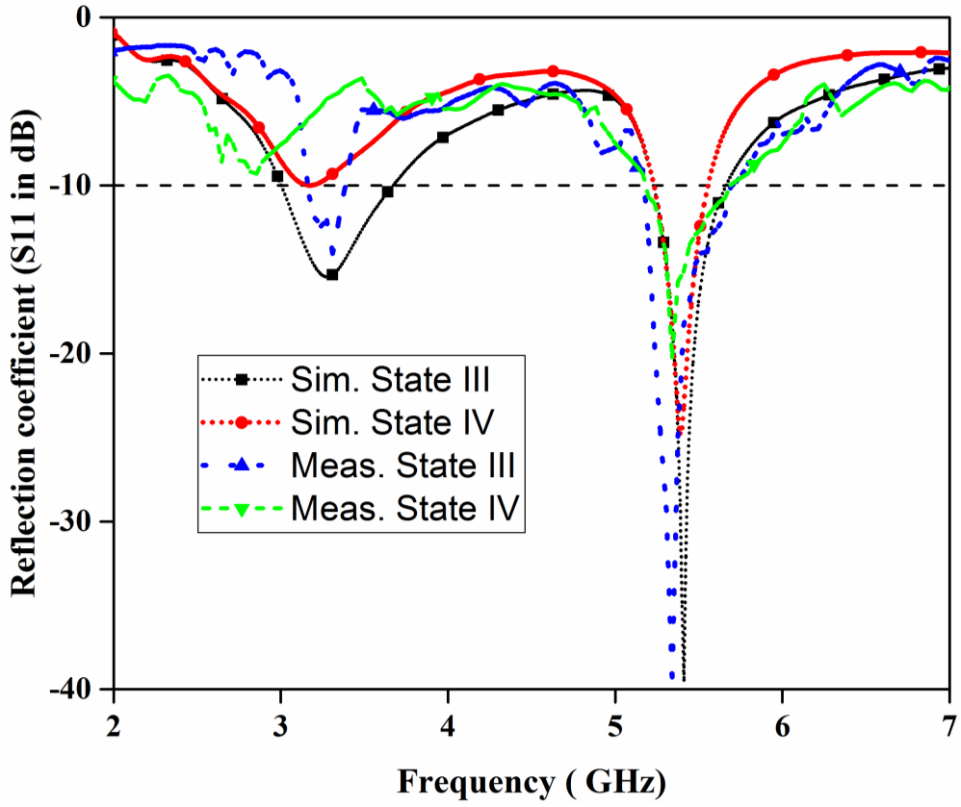

(b)

Figure 5.26 Measured and simulated reflection coefficient of fabricated antenna design

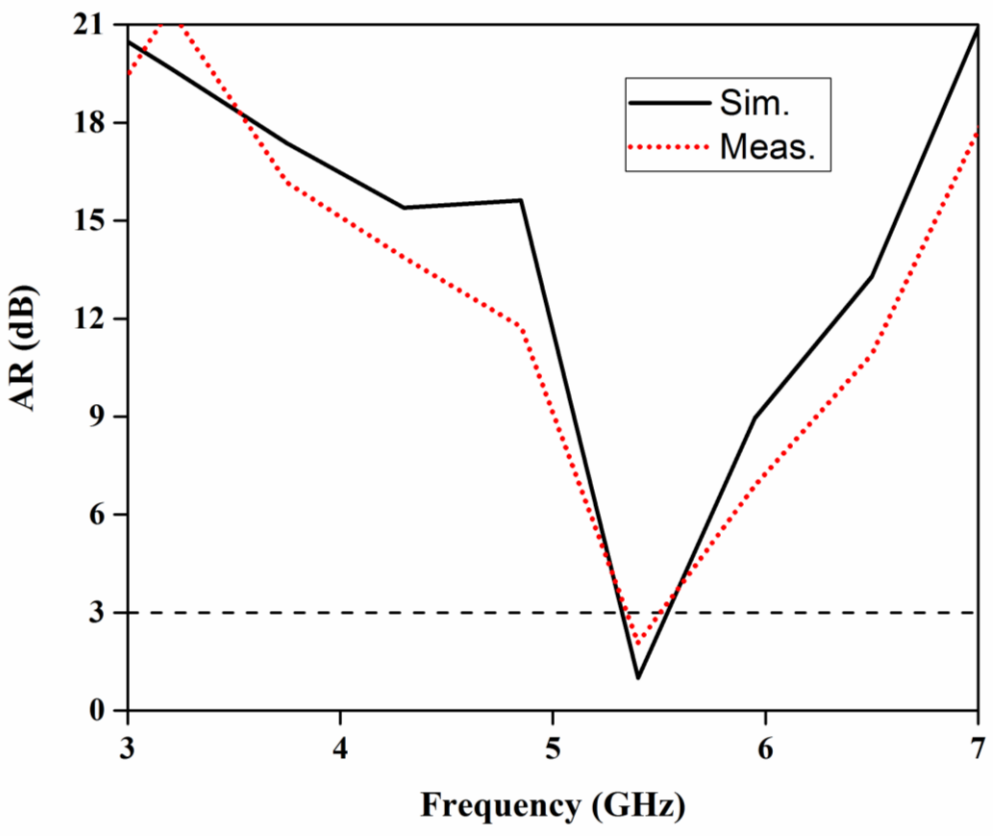

Figure 5.27 AR vs frequency plot for state I

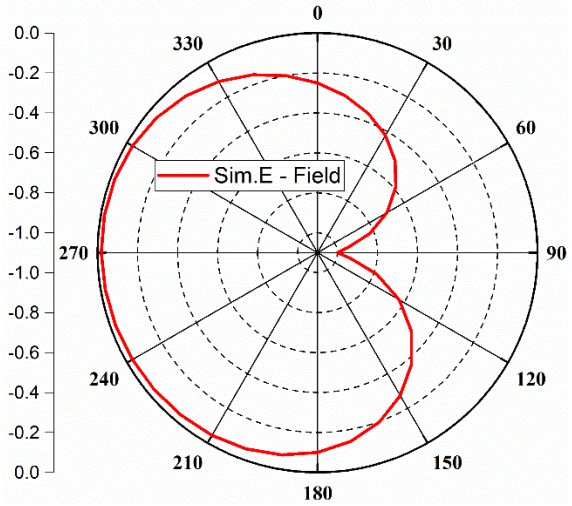

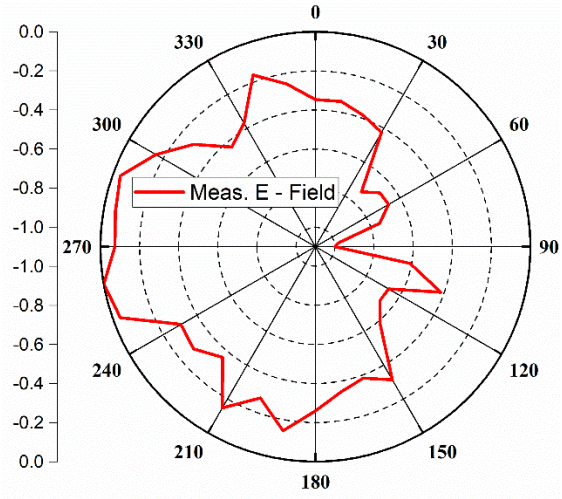

(a) State I

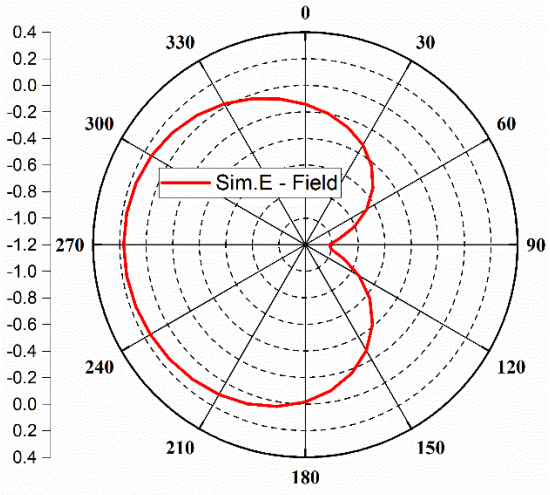

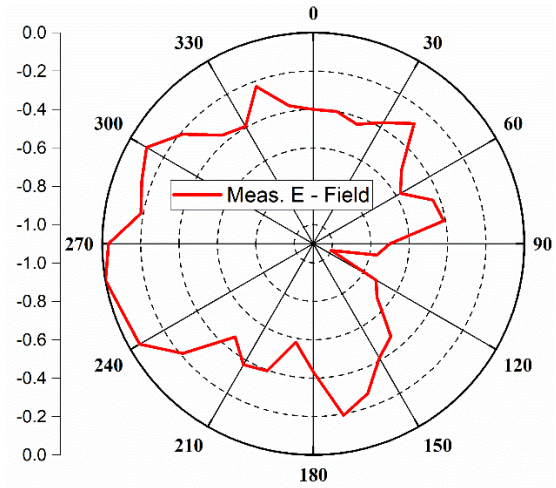

(b) State II

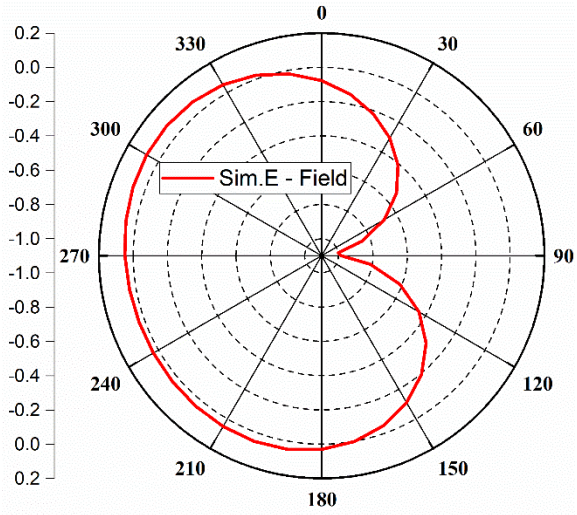

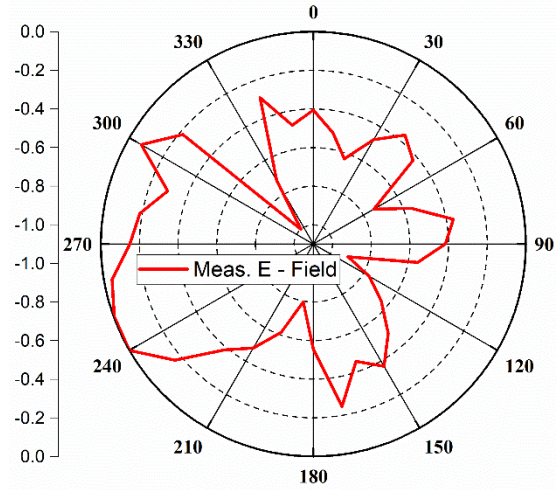

(c) State III

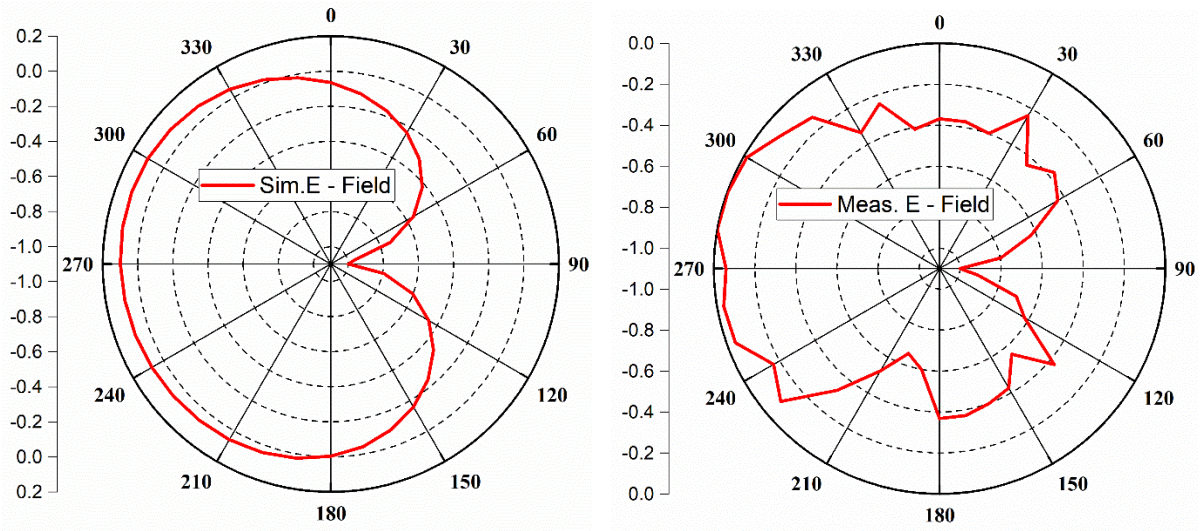

(d) State IV

Figure 5.28 Simulated and measured E- field radiation pattern at 5.4 GHz

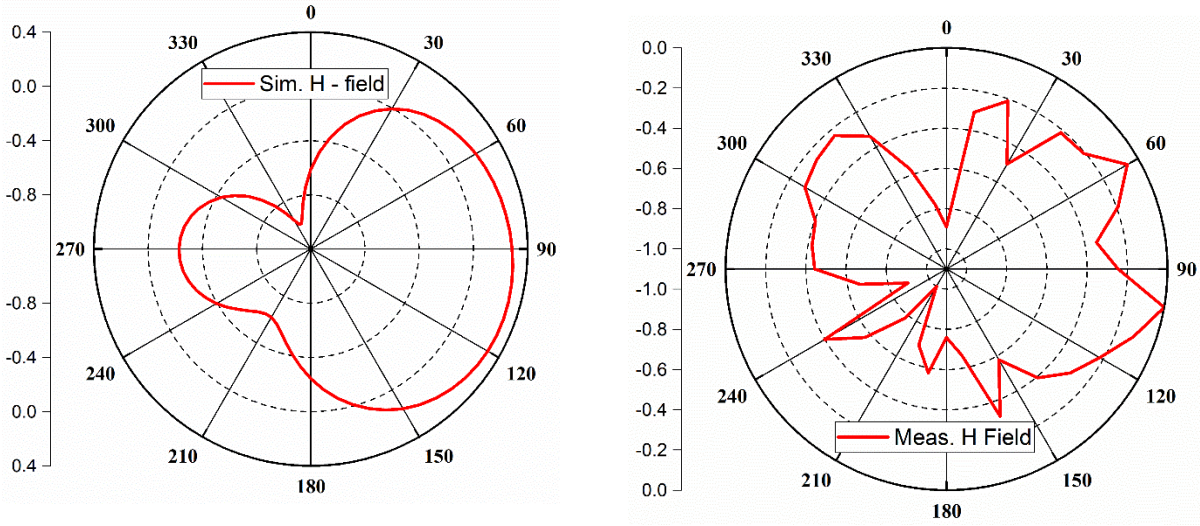

(a) State I

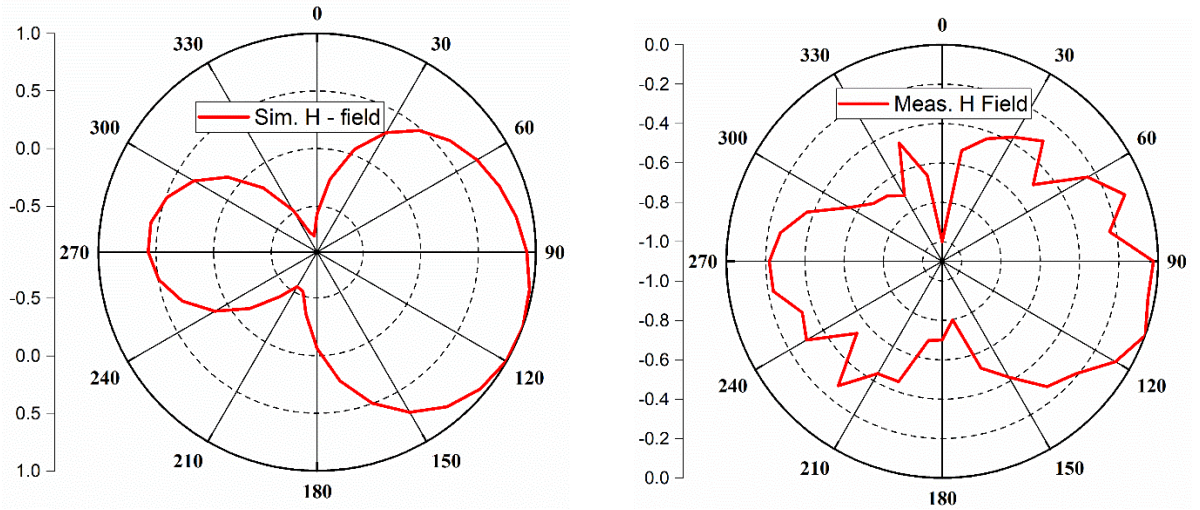

(b) State II

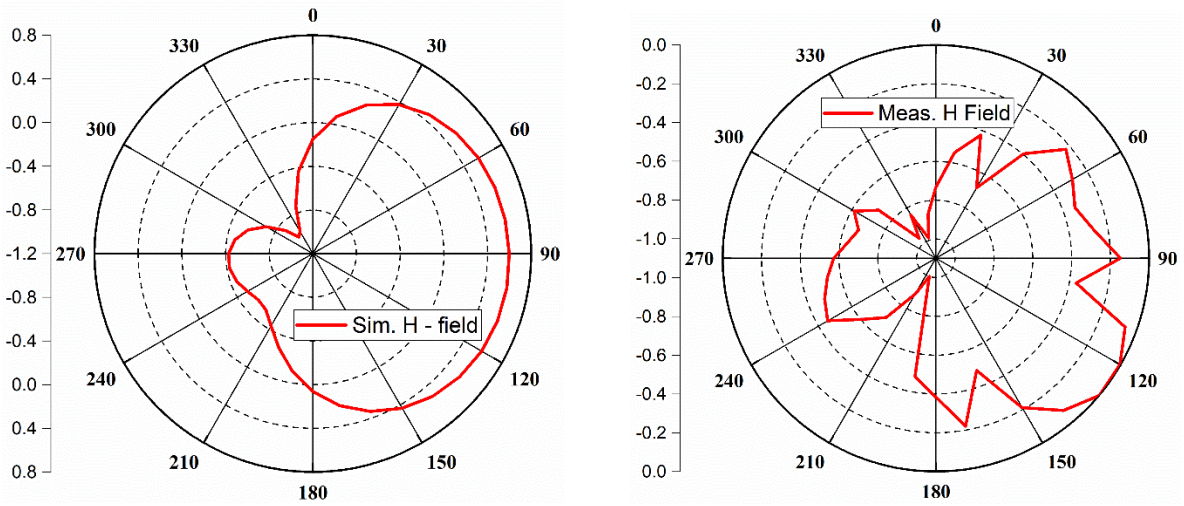

(c) State III

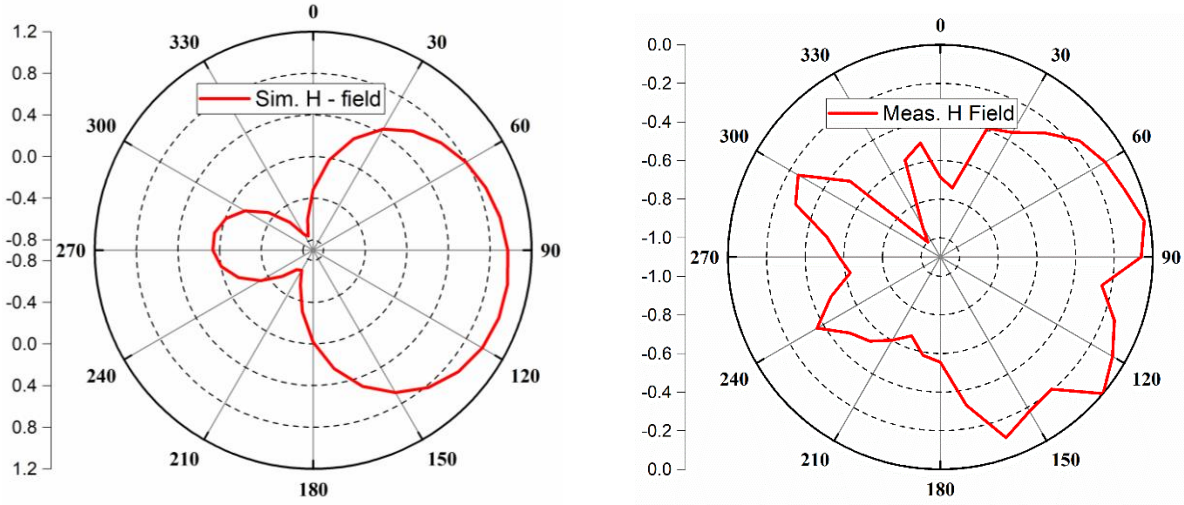

(d) State IV

Figure 5.29 Simulated and measured H- field radiation pattern at 5.4 Hz

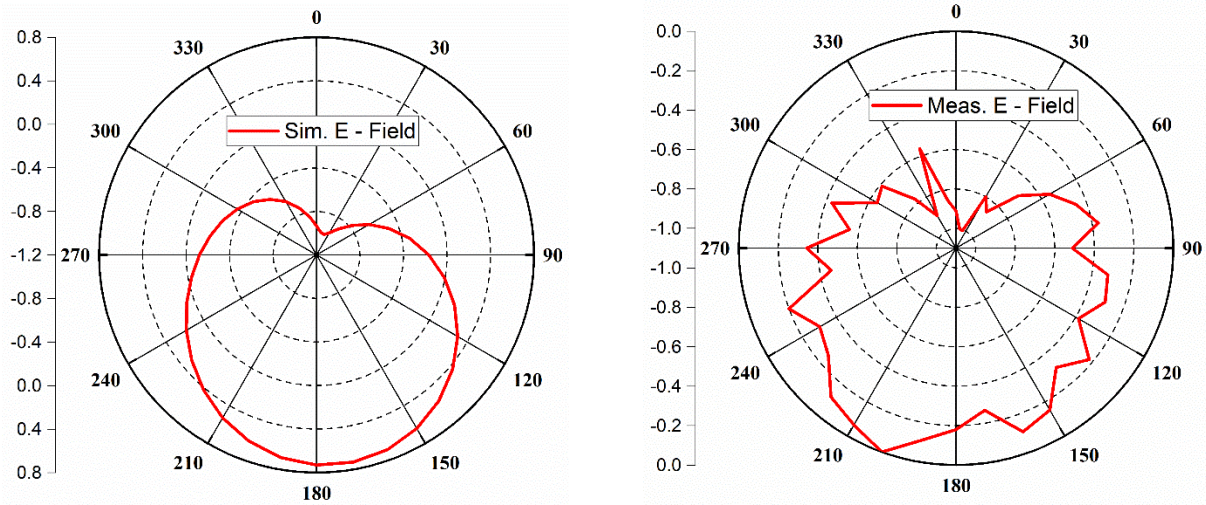

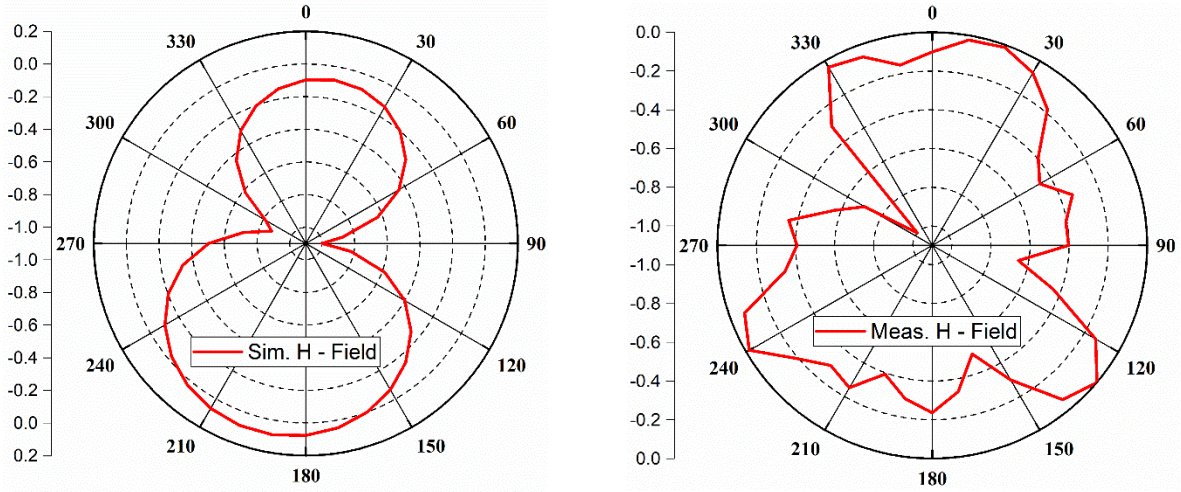

Figure 5.30 Simulated and Measured E - Field, H – field radiation pattern at 3.38 GHz

Table 5.3 Measure antenna characteristics for different states

State	Sim. Reso. Bands (GHz)	Meas. Reso. Bands (GHz)	Sim. Reso. Freq. (GHz)	Meas. Reso. Freq. (GHz)	Sim. ARBW (GHz)	Meas. ARBW (GHz)	Gain
I	3.03 – 3.72 5.30 -5.79	3.23 – 3.76 5.29 – 5.74	3.32 5.51	3.38 5.45	0.20 (5.33 – 5.53)	0.16 (5.35 – 5.49)	1.4 1.61
II	5.29 – 5.68	5.25 – 5.68	5.48	5.51			1.27
III	3.04 – 3.70 5.21 – 5.67	3.16 – 3.39 5.18 – 5.70	3.33 5.41	3.24 5.38			1.25 2.37
IV	5.21 – 5.56	5.19 – 5.68	5.38	5.34			2.53

The comparison of proposed antennas with other reported hybrid reconfigurable antennas is carried out and presented in Table 5.4. The suggested antenna is compact in size, simple design,

least complex biasing network and fewer PIN diodes successfully exhibited all the three reconfiguration characteristics.

Table 5.4 Comparison of hybrid reconfigurable Antennas

Ref.	**Ant. Type**	**Size (mm)**	**Substrate**	**No. of Switching Elements**	**Reconfiguration Type**
[136]	Patch Antenna	70×34×3.175	RT/Duroid 5880	4 PIN 8Varactors	Freq. – Two bands 1.35 – 2.25 GHz 1.35 – 1.9 GHz Pol. – Vertical / Horizontal LP in first band 45° direction LP in second band
[140]	Patch with Metasurface	80×80×32	RO4003C		Freq. – Continuous 8 – 11.2 GHz Pol. – LP, LHCP, RHCP
[146]	Slot Antenna	50×50×h h = 0.635 μm	Rogers RO3006	4 PIN Diodes	Freq. – Three central frequencies at 5.2, 5.8, 6.4 GHz Pattern –Null direction between 0° to 50°
[160]	Patch Antenna	100×100×5	$\varepsilon_{r2} = 3.5$ $\varepsilon_{r1} = 2.2$	12 copper strips	Freq. – 2.1 GHz central freq. with 2.1% fractional BW Second band 1.55 – 2.37 GHz with 41% fractional BW Pattern – Conical in first Band

					Broadside in second band
[164]	Patch and pixel parasitic layer	240×120×3 (Patch) 240×120×3 (Pixel layer)	RO4003	60 PIN diodes	Freq. – Discrete, ± 25% of central frequency of driven element Pol. – Two linear pol., LHCP, RHCP Pattern – ± 30° in E & H planes
[165]	Cavity backed slot antenna	136×124× 1.575	Rogers 5870	48 PIN diodes	Freq. – 20 different states Pol. – Two LP, LHCP, RHCP Pattern – ± Z– direction
[228]	Patch Antenna	80×46×1.5	Rogers RO4350	5 PIN Diodes	Freq. – Two bands 2.21 – 2.79 GHz 5.27 – 5.56 GHz Pattern – Omnidirectional uni-directional
Proposed Design	Patch antenna	24×24×1.6	FR - 4	2 PIN diodes	Freq. – WiMAX, WLAN bands Pol. – LP, CP in WLAN band Pattern – Max. 35° shift

5.5 Summary

The multiple reconfigurable characteristics are realized in the proposed antenna design with single feed excitation by utilizing simple electronic switching. Here, a novel wideband antenna design consisted of a truncated annular ring as a radiating patch and two asymmetric I-shaped

stubs on a partial ground plane. The loading or unloading of stubs on ground patch via two PIN diodes realizes frequency, polarization and pattern reconfigurability in the suggested design. Together with simulation and test findings from prototype measurements, the antenna design and analysis are provided. The loading of long stub and both stubs on the ground plane transforms the dual band antenna having resonating frequencies from 3–4 GHz, 5–6 GHz to single band antenna with resonating frequency lies within 5–6 GHz band. The antenna without any loaded stub exhibits circular polarization in the WLAN band with axial ratio bandwidth of 160 MHz. The loading of either or both stub on it realizes the polarization switching from circular to linear state in the WLAN band and it also steers the main beam orientation from -55° to -90°, thus achieving the pattern reconfiguration. The proposed antenna has simple, planar and reconfigurable characteristics with the least number of PIN diodes, hence can found application in the next generation wireless communication devices.

CHAPTER 6

CONCLUSION & FUTURE SCOPE

CONCLUSION & FUTURE SCOPE

6.1 Conclusions

In the modern world, wireless communication greatly influences daily human life where data transfer, connectivity, navigation, audio-visual communication and so on are important aspects nowadays. The revolutionary services and application has led to the unprecedented growth in wireless industry, but also presents the challenges in spectrum management and hardware implementation in front of regulatory bodies and designers at the same time.

Antenna is vital and frontier component in wireless communication systems for receiving or transmitting signals in the form of electromagnetic wave. Multi-standard portable devices are in high demand as a result of the extensive use of wireless communication in many applications. Such antennas that can function across many frequency bands are practically necessary to facilitate multi-standard functioning in mobile devices. Generally, conventional antennas with fixed performances in terms of frequency, pattern and polarization are used for a variety of services, which turns the communication system into an expensive, bulky and complex structure with limiting its performances in fast changing communication scenarios. To address these issues, multiband and reconfigurable antennas have appeared as potential candidates to address the above issues due to their lucrative features like low profile, compact size, inexpensive construction, lightweight and easy integration with other microwave devices. Hence, the present and futuristic applications of multi-band and reconfigurable antennas over conventional antennas necessitates and motivates to this research work.

A detailed and comprehensive literature survey on electric tunable reconfigurable antennas was presented in Chapter 2, prior to the discussion of prototyped antenna designs. Also, it provides an insight into reconfigurable antenna types from single to multiple characteristics, design methods, applications etc. The recent developments and various aspects were reported in this manuscript to ascertain the research area.

A wideband ‘Y – shaped’ microstrip antenna with slits on the partial ground plane is discussed in Chapter 3 for multi-band applications. Initially, an UWB antenna is achieved by ensuring a small gap between upper and lower edges of the partial ground plane and radiating element respectively. The above designed structure is modified into triple (Wi-Fi, WiMAX and WLAN) band antennas by etching two hook shaped, single horizontal and vertical slits on a partial

ground plane at appropriate locations. Although, a triple resonating band antenna is prototyped successfully but can't exploit its full potential because a separate radiating element is needed for transmission or reception of signal at each frequency.

The limitations of multi-band antennas and to fulfill the requirements of emerging advanced communication systems led to the development of reconfigurable antennas. The reconfigurable antennas also enhances the channel capacity, link robustness and also reduce the interference by considerable amount among adjacent wireless networks. One could refer to the communication systems with reconfigurable antennas as early prototypes of intelligent and self-organizing networks. The profile reduction, performance steadiness throughout the many reconfiguration phases and firm gain characteristics are fundamental norms for designing reconfigurable antennas. Two hybrid reconfigurable annular ring antenna designs based on integration of reconfigurable elements concept are developed and presented in Chapter 4 and Chapter 5 respectively with detailed procedure and explanations.

In Chapter 4, antenna geometry of annular rings for frequency and polarization agility has been discussed. First, two annular rings with a partial ground plane fed from the microstrip line are designed for the WLAN band. The CP characteristics in the WLAN band is obtained by extruding a slit of suitable length below one ring, which divides the dominant mode in two degenerate modes of same amplitude and 90° phase difference and IBW of the resonating band is also enhances. To realize frequency and polarization reconfigurability, a switchable arc of suitable length is implemented on the left ring via PIN diodes. The simultaneous control of PIN diodes between ON / OFF states transforms the circularly polarized single (WLAN) band antenna into dual WiMAX and WLAN band antennas with linear polarization. The fractional impedance bandwidth of 8.30 % with 0.03 GHz ARBW for ON state and 8.33 %, 5.47 % in WiMAX, WLAN band respectively for OFF state are obtained that demonstrates the wideband behavior in resonating bands.

Chapter 5 is aimed to enhance the radiation coverage with operation impedance and axial ratio bandwidths of an antenna design for indoor or outdoor applications. Based on the same principle of Chapter 3, an UWB annular ring antenna with two resonating bands is initially designed. The optimization of the ground plane in combination with truncated radiating elements results in an asymmetric open ring antenna with two resonating bands that covers the prescribed frequency range for WiMAX and WLAN band with circular polarization in the later band. The loading or unloading of I–shaped stubs of unequal lengths on partial ground element

through two p-i-n diodes realizes reconfiguration in antenna characteristics. The application of stubs provides frequency reconfiguration from dual to single band, polarization switching among CP, LP in WLAN band and direction switching of main beam upto 35° while maintaining the shape of radiation pattern almost the same. The fractional bandwidth is above 5 % for all resonating band with 15.68 %, 9.66 % in WiMAX and WLAN band respectively, which establishes the wideband behavior, also 0.16 GHz ARBW is achieved in later band for the OFF state of PIN diodes.

6.2 Future Scope

The accomplished research work in this manuscript presented some innovative antenna designs to address few challenges in the evolution of reconfigurable antennas. However, more efforts would be put in reconfigurable antennas, as some research areas still remain unexplored and could find applications in emerging next generation communication systems. Some of the suggested potential areas are discussed below.

(a) Frequency-Polarization-Pattern Reconfigurable Array: The array antennas give us more flexibility to operate the system as per the requirement with few limitations. The work reported in the present manuscript printed can be extended and optimized to realize an antenna array with enhanced antenna performances in wide range of reconfigurability and diversity functions.

(b) Green Energy Harvester: Nowadays, capability to accumulate power from adjacent wireless networks or dedicated devices is being utilized to wirelessly charge the devices. This innovative technique has potential to eliminates the need for batteries and also enhance the lifespan of electrical systems. The outcomes of this manuscript suggested that the use of reconfigurable antennas will surge the amount of energy transfer between the power transmitter and receiver, reduces the charging time by directing the beam in intended direction and also data throughput in the same device.

(c) Tuning Range Enhancement: At present, the adjustable bandwidth or frequency range of the antenna is greatly influenced and restricted by the tunable components. The use of sophisticated tuning elements in near future might be extended the tunable frequency range or bandwidth without any change in antenna structure.

(d) Automatic Control: The incorporation of software based digital control circuit instead of analog circuit on antenna geometry may be subdue their effect on antenna characteristics and improves the antenna efficiency by speed up the antenna operations. Though, the original reconfigurability and modest volume of antenna's profile should be preserved.

(e) Future Application Scenario: Reconfigurable antennas in mobile gadgets, interconnected services for 'Internet of Things' operations, massive 'MIMO' operations, 'CR', device-to-device communication, diversity applications and etc. will all become much more necessary when 5G communication is implemented in the near future. In order to connect future upper mm-wave 5G services with current 3G/4G microwave frequency ranges, standardized devices may find that reconfigurable antennas are a reasonably simple solution. Additionally, upcoming biomedical applications, wearable gadgets and military applications may be made possible by reconfigurable antennas based on low loss malleable materials with adjustable characteristics. Reconfigurable antennas would provide more functionality and flexibility while also making it simpler to run many services concurrently.

REFERENCES

[1] D. V. Thiel, "Stand on standards [antenna types standards]," *IEEE Antennas and Propagation Magazine*, vol. 46, no. 2, pp. 120–121, Apr. 2004, doi: 10.1109/MAP.2004.1305559.

[2] K.-F. Lee and K.-F. Tong, "Microstrip Patch Antennas—Basic Characteristics and Some Recent Advances," *Proceedings of the IEEE*, vol. 100, no. 7, pp. 2169–2180, Jul. 2012, doi: 10.1109/JPROC.2012.2183829.

[3] C. A. Balanis, *Antenna Theory: Analysis and Design*. John Wiley & Sons, 2015.

[4] Y.-B. Jung, A. V. Shishlov, and S.-O. Park, "Cassegrain Antenna With Hybrid Beam Steering Scheme for Mobile Satellite Communications," *IEEE Transactions on Antennas and Propagation*, vol. 57, no. 5, pp. 1367–1372, May 2009, doi: 10.1109/TAP.2009.2016706.

[5] M. A. Abou-Khousa, M. T. Ghasr, S. Kharkovsky, D. Pommerenke, and R. Zoughi, "Modulated Elliptical Slot Antenna for Electric Field Mapping and Microwave Imaging," *IEEE Transactions on Antennas and Propagation*, vol. 59, no. 3, pp. 733–741, Mar. 2011, doi: 10.1109/TAP.2010.2103024.

[6] M. T. Islam, M. S. Alam, N. Misran, M. Ismail, and B. Yatim, "Development of high gain multiband antenna with centre-offset copper strip-based periodic structure," *Microwave and Optical Technology Letters*, vol. 57, no. 7, pp. 1608–1614, 2015, doi: 10.1002/mop.29161.

[7] Q. Luo *et al.*, "Design and Analysis of a Reflectarray Using Slot Antenna Elements for Ka-band SatCom," *IEEE Transactions on Antennas and Propagation*, vol. 63, no. 4, pp. 1365–1374, Apr. 2015, doi: 10.1109/TAP.2015.2401393.

[8] P. Singh *et al.*, "Fractal and Periodical Biological Antennas: Hidden Topologies in DNA, Wasps and Retina in the Eye," in *Soft Computing Applications*, K. Ray, M. Pant, and A. Bandyopadhyay, Eds., Singapore: Springer, 2018, pp. 113–130. doi: 10.1007/978-981-10-8049-4_6.

[9] G. M. Roy, B. K. Kanuajia, S. Dwari, S. Kumar, and H. Song, "2–18 GHz wide band co-design integrated LNA with active antenna for mobile communication technologies," *Analog Integr Circ Sig Process*, vol. 96, no. 1, pp. 39–52, Jul. 2018, doi: 10.1007/s10470-018-1211-8.

[10] G. Deschamps and W. Sichak, "Microstrip Microwave Antennas," *Proceedings of the Third Symposium on the USAF Antenna Research and Development Program, Oct*, pp. 18–22, 1953.

[11] A. Alexiou and M. Haardt, “Smart antenna technologies for future wireless systems: trends and challenges,” *IEEE Communications Magazine*, vol. 42, no. 9, pp. 90–97, Sep. 2004, doi: 10.1109/MCOM.2004.1336725.

[12] Y. Rahmat-Samii and A. C. Densmore, “Technology Trends and Challenges of Antennas for Satellite Communication Systems,” *IEEE Transactions on Antennas and Propagation*, vol. 63, no. 4, pp. 1191–1204, Apr. 2015, doi: 10.1109/TAP.2014.2366784.

[13] J. Anguera *et al.*, “Reconfigurable Multiband Operation for Wireless Devices Embedding Antenna Boosters,” *Electronics*, vol. 10, no. 7, Art. no. 7, Jan. 2021, doi: 10.3390/electronics10070808.

[14] S. Borisov and A. Shishlov, “Antennas for Satcom-on-the-Move, Review,” in *2014 International Conference on Engineering and Telecommunication*, Nov. 2014, pp. 3–7. doi: 10.1109/EnT.2014.12.

[15] J. T. Bernhard, *Reconfigurable Antennas*. Morgan & Claypool Publishers, 2007.

[16] R. L. Haupt and M. Lanagan, “Reconfigurable Antennas,” *IEEE Antennas and Propagation Magazine*, vol. 55, no. 1, pp. 49–61, Feb. 2013, doi: 10.1109/MAP.2013.6474484.

[17] J. Kountouriotis, D. Piazza, K. R. Dandekar, M. D’Amico, and C. Guardiani, “Performance analysis of a reconfigurable antenna system for MIMO communications,” in *Proceedings of the 5th European Conference on Antennas and Propagation (EUCAP)*, Apr. 2011, pp. 543–547. Accessed: Mar. 07, 2025. [Online]. Available: https://ieeexplore.ieee.org/abstract/document/5782487

[18] A. Grau, H. Jafarkhani, and F. De Flaviis, “A reconfigurable multiple-input multiple-output communication system,” *IEEE Transactions on Wireless Communications*, vol. 7, no. 5, pp. 1719–1733, May 2008, doi: 10.1109/TWC.2008.060905.

[19] R. Bahl, N. Gulati, K. R. Dandekar, and D. Jaggard, “Impact of pattern reconfigurable antennas on Interference Alignment over measured channels,” in *2012 IEEE Globecom Workshops*, Dec. 2012, pp. 557–562. doi: 10.1109/GLOCOMW.2012.6477634.

[20] R. Wang *et al.*, “Capacity and Performance Analysis for Adaptive Multi-Beam Directional Networking,” in *MILCOM 2006 - 2006 IEEE Military Communications conference*, Oct. 2006, pp. 1–7. doi: 10.1109/MILCOM.2006.302366.

[21] K. Wanuga, N. Gulati, H. Saarnisaari, and K. R. Dandekar, “Online learning for spectrum sensing and reconfigurable antenna control,” in *2014 9th International Conference on Cognitive Radio Oriented Wireless Networks and Communications (CROWNCOM)*, Jun. 2014, pp. 508–513. doi: 10.4108/icst.crowncom.2014.255737.

[22] P. Mookiah, J. Kountouriotis, R. Dorsey, B. Shishkin, and K. R. Dandekar, "Securing wireless links at the physical layer through reconfigurable antennas," in *2010 IEEE Antennas and Propagation Society International Symposium*, Toronto, ON: IEEE, Jul. 2010, pp. 1–4. doi: 10.1109/APS.2010.5561248.

[23] N. Gulati, R. Greenstadt, K. R. Dandekar, and J. M. Walsh, "GMM Based Semi-Supervised Learning for Channel-Based Authentication Scheme," in *2013 IEEE 78th Vehicular Technology Conference (VTC Fall)*, Sep. 2013, pp. 1–6. doi: 10.1109/VTCFall.2013.6692216.

[24] D. H. Schaubert, F. G. Farrar, S. T. Hayes, and A. R. Sindoris, "Frequency-agile, polarization diverse microstrip antennas and frequency scanned arrays," US4367474A, Jan. 04, 1983 Accessed: Mar. 07, 2025. [Online]. Available: https://patents.google.com/patent/US4367474A/en

[25] N. Haider, D. Caratelli, and A. G. Yarovoy, "Recent Developments in Reconfigurable and Multiband Antenna Technology," *International Journal of Antennas and Propagation*, vol. 2013, no. 1, p. 869170, 2013, doi: 10.1155/2013/869170.

[26] M. S. Alam, "Reconfigurable antennas with single and multiple reconfigurability functions for wireless communications," Jan. 2019, doi: 10.14264/uql.2019.69.

[27] N. Behdad and K. Sarabandi, "A varactor-tuned dual-band slot antenna," *IEEE Transactions on Antennas and Propagation*, vol. 54, no. 2, pp. 401–408, Feb. 2006, doi: 10.1109/TAP.2005.863373.

[28] L. Hinsz and B. D. Braaten, "A Frequency Reconfigurable Transmitter Antenna With Autonomous Switching Capabilities," *IEEE Transactions on Antennas and Propagation*, vol. 62, no. 7, pp. 3809–3813, Jul. 2014, doi: 10.1109/TAP.2014.2316298.

[29] E. García, A. Andújar and J. Anguera, "Overview of Reconfigurable Antenna Systems for IoT Devices," *Electronics*, vol. 13, no. 3988, 2024, doi: https://doi.org/10.3390/electronics13203988.

[30] C. Qi, Y. Cui, and R. Li, "Multi-polarization reconfigurable omnidirectional antenna," in *2017 International Symposium on Antennas and Propagation (ISAP)*, Oct. 2017, pp. 1–2. doi: 10.1109/ISANP.2017.8228743.

[31] S.-L. S. Yang and K.-M. Luk, "Design of a wide-band L-probe patch antenna for pattern reconfiguration or diversity applications," *IEEE Transactions on Antennas and Propagation*, vol. 54, no. 2, pp. 433–438, Feb. 2006, doi: 10.1109/TAP.2005.863376.

[32] A. Bondarik and D. Sjöberg, "Investigation of reconfigurability for a stacked microstrip patch antenna pattern targeting 5G applications," in *2015 IEEE-APS Topical Conference on Antennas and Propagation in Wireless Communications (APWC)*, Sep. 2015, pp. 1202–1205. doi: 10.1109/APWC.2015.7300200.

[33] J. Costantine, Y. Tawk, S. E. Barbin, and C. G. Christodoulou, “Reconfigurable Antennas: Design and Applications,” *Proceedings of the IEEE*, vol. 103, no. 3, pp. 424–437, Mar. 2015, doi: 10.1109/JPROC.2015.2396000.

[34] C. G. Christodoulou, Y. Tawk, S. A. Lane, and S. R. Erwin, “Reconfigurable Antennas for Wireless and Space Applications,” *Proceedings of the IEEE*, vol. 100, no. 7, pp. 2250–2261, Jul. 2012, doi: 10.1109/JPROC.2012.2188249.

[35] E. Motovilova and S. Y. Huang, “A Review on Reconfigurable Liquid Dielectric Antennas,” *Materials*, vol. 13, no. 8, Art. no. 8, Jan. 2020, doi: 10.3390/ma13081863.

[36] D. Rodrigo and L. Jofre, “Frequency and Radiation Pattern Reconfigurability of a Multi-Size Pixel Antenna,” *IEEE Transactions on Antennas and Propagation*, vol. 60, no. 5, pp. 2219–2225, May 2012, doi: 10.1109/TAP.2012.2189739.

[37] A. Petosa, “An Overview of Tuning Techniques for Frequency-Agile Antennas,” *IEEE Antennas and Propagation Magazine*, vol. 54, no. 5, pp. 271–296, Oct. 2012, doi: 10.1109/MAP.2012.6348178.

[38] P. Yaghmaee, O. H. Karabey, B. Bates, C. Fumeaux, and R. Jakoby, “Electrically Tuned Microwave Devices Using Liquid Crystal Technology,” *International Journal of Antennas and Propagation*, vol. 2013, no. 1, p. 824214, 2013, doi: 10.1155/2013/824214.

[39] L. Wei, “Reconfigurable Antennas for Emerging Wireless Communication Systems,” Ph. D Thesis, Deptt. of Electronic Engineering, City University of Hong Kong, 2016.

[40] D. Wang and C. H. Chan, “Multiband Antenna for WiFi and WiGig Communications,” *IEEE Antennas and Wireless Propagation Letters*, vol. 15, pp. 309–312, 2016, doi: 10.1109/LAWP.2015.2443013.

[41] W. Lee *et al.*, “Low-Profile Multiband Ferrite Antenna for Telematics Applications,” *IEEE Transactions on Magnetics*, vol. 52, no. 7, pp. 1–4, Jul. 2016, doi: 10.1109/TMAG.2016.2535381.

[42] D. Guo, K. He, Y. Zhang, and M. Song, “A Multiband Dual-Polarized Omnidirectional Antenna for Indoor Wireless Communication Systems,” *IEEE Antennas and Wireless Propagation Letters*, vol. 16, pp. 290–293, 2017, doi: 10.1109/LAWP.2016.2573840.

[43] Y. Cui, L. Yang, B. Liu, and R. Li, “Multiband planar antenna for LTE/GSM/UMTS and WLAN/WiMAX handsets,” *IET Microwaves, Antennas & Propagation*, vol. 10, no. 5, pp. 502–506, 2016, doi: 10.1049/iet-map.2015.0545.

[44] Y. F. Cao, S. W. Cheung, and T. I. Yuk, “A Multiband Slot Antenna for GPS/WiMAX/WLAN Systems,” *IEEE Transactions on Antennas and Propagation*, vol. 63, no. 3, pp. 952–958, Mar. 2015, doi: 10.1109/TAP.2015.2389219.

[45] S. S. Hong, J. Mehlman, and S. Katti, “Picasso: flexible RF and spectrum slicing,” *SIGCOMM Comput. Commun. Rev.*, vol. 42, no. 4, pp. 37–48, Aug. 2012, doi: 10.1145/2377677.2377683.

[46] S. Yang, C. Zhang, H. K. Pan, A. E. Fathy, and V. K. Nair, "Frequency-Reconfigurable Antennas for Multiradio Wireless Platforms," *IEEE Microwave Magazine*, vol. 10, no. 1, pp. 66–83, Feb. 2009, doi: 10.1109/MMM.2008.930677.

[47] N. Tasouji, J. Nourinia, C. Ghobadi, and F. Tofigh, "A Novel Printed UWB Slot Antenna With Reconfigurable Band-Notch Characteristics," *IEEE Antennas and Wireless Propagation Letters*, vol. 12, pp. 922–925, 2013, doi: 10.1109/LAWP.2013.2273452.

[48] J. Xu, D. Shen, X. Zhang, and K. Wu, "A Compact Disc UltrawideBand (UWB) Antenna With Quintuple Band Rejections," *IEEE Antennas and Wireless Propagation Letters*, vol. 11, pp. 1517–1520, 2012, doi: 10.1109/LAWP.2012.2234075.

D. Zhao, L. Lan, Y. Han, F. Liang, Q. Zhang, and B.-Z. Wang, "Optically Controlled Reconfigurable Band-Notched UWB Antenna for Cognitive Radio Applications," *IEEE Photonics Technology Letters*, vol. 26, no. 21, pp. 2173–2176, Nov. 2014, doi: 10.1109/LPT.2014.2349961.

[49] Y. Cai, Y. J. Guo, and T. S. Bird, "A Frequency Reconfigurable Printed Yagi-Uda Dipole Antenna for Cognitive Radio Applications," *IEEE Transactions on Antennas and Propagation*, vol. 60, no. 6, pp. 2905–2912, Jun. 2012, doi: 10.1109/TAP.2012.2194654.

[51] A. Mansoul, F. Ghanem, M. R. Hamid, and M. Trabelsi, "A Selective Frequency-Reconfigurable Antenna for Cognitive Radio Applications," *IEEE Antennas and Wireless Propagation Letters*, vol. 13, pp. 515–518, 2014, doi: 10.1109/LAWP.2014.2311114.

[52] T. Aboufoul, A. Alomainy, and C. Parini, "Reconfiguring UWB Monopole Antenna for Cognitive Radio Applications Using GaAs FET Switches," *IEEE Antennas and Wireless Propagation Letters*, vol. 11, pp. 392–394, 2012, doi: 10.1109/LAWP.2012.2193551.

[53] https://www.telecomhall.net/t/how-many-antennas-are-used-in-a-smartphone/10458/2

[54] I. F. Akyildiz, W.-Y. Lee, M. C. Vuran, and S. Mohanty, "NeXt generation/dynamic spectrum access/cognitive radio wireless networks: A survey," *Computer Networks*, vol. 50, no. 13, pp. 2127–2159, Sep. 2006, doi: 10.1016/j.comnet.2006.05.001.

[55] S. V. S. Nair and M. J. Ammann, "Reconfigurable Antenna With Elevation and Azimuth Beam Switching," *IEEE Antennas and Wireless Propagation Letters*, vol. 9, pp. 367–370, 2010, doi: 10.1109/LAWP.2010.2049332.

[56] Y. Tanabe, H. Wong, S. Kim, J. S. Ho, and A. S. Y. Poon, "Beam focused slot antenna for microchip implants," in *2012 International Symposium on Antennas and Propagation (ISAP)*, Oct. 2012, pp. 467–470. Accessed: Mar. 07, 2025. [Online]. Available: https://ieeexplore.ieee.org/abstract/document/6393953

[57] L. Ge, K. M. Luk, and S. Chen, “360° Beam-Steering Reconfigurable Wideband Substrate Integrated Waveguide Horn Antenna,” *IEEE Transactions on Antennas and Propagation*, vol. 64, no. 12, pp. 5005–5011, Dec. 2016, doi: 10.1109/TAP.2016.2617820.

[58] S. Yong and J. T. Bernhard, “Reconfigurable Null Scanning Antenna With Three Dimensional Null Steer,” *IEEE Transactions on Antennas and Propagation*, vol. 61, no. 3, pp. 1063–1070, Mar. 2013, doi: 10.1109/TAP.2012.2227101.

[59] A. Pal, A. Mehta, D. Mirshekar-Syahkal, and H. Nakano, “A Twelve-Beam Steering Low-Profile Patch Antenna With Shorting Vias for Vehicular Applications,” *IEEE Transactions on Antennas and Propagation*, vol. 65, no. 8, pp. 3905–3912, Aug. 2017, doi: 10.1109/TAP.2017.2715367.

[60] S. Yong and J. T. Bernhard, “A Pattern Reconfigurable Null Scanning Antenna,” *IEEE Transactions on Antennas and Propagation*, vol. 60, no. 10, pp. 4538–4544, Oct. 2012, doi: 10.1109/TAP.2012.2207336.

[61] L. Zhang, Q. Wu, and T. A. Denidni, “Electronically Radiation Pattern Steerable Antennas Using Active Frequency Selective Surfaces,” *IEEE Transactions on Antennas and Propagation*, vol. 61, no. 12, pp. 6000–6007, Dec. 2013, doi: 10.1109/TAP.2013.2282921.

[62] R. Mehmood and J. W. Wallace, “MIMO Capacity Enhancement Using Parasitic Reconfigurable Aperture Antennas (RECAPs),” *IEEE Transactions on Antennas and Propagation*, vol. 60, no. 2, pp. 665–673, Feb. 2012, doi: 10.1109/TAP.2011.2173445.

[63] M. D. Migliore, D. Pinchera, and F. Schettino, “Improving Channel Capacity Using Adaptive MIMO Antennas,” *IEEE Transactions on Antennas and Propagation*, vol. 54, no. 11, pp. 3481–3489, Nov. 2006, doi: 10.1109/TAP.2007.884302.

[64] F. Fazel, A. Grau, H. Jafarkhani, and F. D. Flaviis, “Space-time-state block coded mimo communication systems using reconfigurable antennas,” *IEEE Transactions on Wireless Communications*, vol. 8, no. 12, pp. 6019–6029, Dec. 2009, doi: 10.1109/TWC.2009.12.080876.

[65] D. Piazza, N. J. Kirsch, A. Forenza, R. W. Heath, and K. R. Dandekar, “Design and Evaluation of a Reconfigurable Antenna Array for MIMO Systems,” *IEEE Transactions on Antennas and Propagation*, vol. 56, no. 3, pp. 869–881, Mar. 2008, doi: 10.1109/TAP.2008.916908.

[66] B. A. Cetiner, H. Jafarkhani, J.-Y. Qian, H. J. Yoo, A. Grau, and F. De Flaviis, “Multifunctional reconfigurable MEMS integrated antennas for adaptive MIMO systems,” *IEEE Communications Magazine*, vol. 42, no. 12, pp. 62–70, Dec. 2004, doi: 10.1109/MCOM.2004.1367557.

[67] A. Maltsev, E. Perahia, R. Maslennikov, A. Sevastyanov, A. Lomayev, and A. Khoryaev, "Impact of Polarization Characteristics on 60-GHz Indoor Radio Communication Systems," *IEEE Antennas and Wireless Propagation Letters*, vol. 9, pp. 413–416, 2010, doi: 10.1109/LAWP.2010.2048410.

[68] A. Grau, J. Romeu, M. J. Lee, S. Blanch, L. Jofre, and F. D. Flaviis, "A dual-linearly-polarized MEMS-reconfigurable antenna for narrowband MIMO communication systems," *IEEE Transactions on Antennas and Propagation*, vol. 58, no. 1, pp. 4-17, 2010, doi: 10.1109/TAP.2009.2036197

[69] W. Lin and H. Wong, "Multipolarization-Reconfigurable Circular Patch Antenna With L-Shaped Probes," *IEEE Antennas and Wireless Propagation Letters*, vol. 16, pp. 1549–1552, 2017, doi: 10.1109/LAWP.2017.2648862.

[70] H. Wong, W. Lin, L. Huitema, and E. Arnaud, "Multi-Polarization Reconfigurable Antenna for Wireless Biomedical System," *IEEE Transactions on Biomedical Circuits and Systems*, vol. 11, no. 3, pp. 652–660, Jun. 2017, doi: 10.1109/TBCAS.2016.2636872.

[71] T. J. Jung, I.-J. Hyeon, C.-W. Baek, and S. Lim, "Circular/Linear Polarization Reconfigurable Antenna on Simplified RF-MEMS Packaging Platform in K-Band," *IEEE Transactions on Antennas and Propagation*, vol. 60, no. 11, pp. 5039–5045, Nov. 2012, doi: 10.1109/TAP.2012.2207662.

[72] C. T. Rodenbeck, M.-Y. Li, and K. Chang, "Circular-polarized reconfigurable grating antenna for low-cost Millimeter-wave beam-steering," *IEEE Transactions on Antennas and Propagation*, vol. 52, no. 10, pp. 2759–2764, Oct. 2004, doi: 10.1109/TAP.2004.834367.

[73] J. Perruisseau-Carrier, "Versatile reconfiguration of radiation patterns, frequency and polarization: A discussion on the potential of controllable reflectarrays for software-defined and cognitive radio systems," in *2010 IEEE International Microwave Workshop Series on RF Front-ends for Software Defined and Cognitive Radio Solutions (IMWS)*, Feb. 2010, pp. 1–4. doi: 10.1109/IMWS.2010.5440982.

[74] D. Rodrigo, J. Romeu, and L. Jofre, "Interference rejection using frequency and pattern reconfigurable antennas," in *Proceedings of the 2012 IEEE International Symposium on Antennas and Propagation*, Jul. 2012, pp. 1–2. doi: 10.1109/APS.2012.6347994.

[75] Y. Siriwardhana, G. Gür, M. Ylianttila, and M. Liyanage, "The role of 5G for digital healthcare against COVID-19 pandemic: Opportunities and challenges," *ICT Express*, vol. 7, no. 2, pp. 244–252, Jun. 2021, doi: 10.1016/j.icte.2020.10.002.

[76] B. Y. Toh, R. Cahill, and V. F. Fusco, "Understanding and measuring circular polarization," *IEEE Transactions on Education*, vol. 46, no. 3, pp. 313–318, Aug. 2003, doi: 10.1109/TE.2003.813519.

[77] TRAI, "White Paper Enabling 5G in India," p. 70, 2019, [Online]. Available: https://trai.gov.in/sites/default/files/White_Paper_22022019_0.pdf

[78] S. Verma and P. Kumar, "Compact triple-band antenna for WiMAX and WLAN applications," *Electronics Letters*, vol. 50, no. 7, pp. 484–486, 2014, doi: 10.1049/el.2013.4313.

[79] K. Vyas, A. K. Sharma, and P. K. Singhal, "Design And Analysis Of Two Novel CPW-Fed Dual Band-Notched UWB Antennas With Modified Ground Structures," *PIER C*, vol. 49, pp. 159–170, 2014, doi: 10.2528/PIERC14031710.

[80] P. Kumar, M. M. M. Pai, and T. Ali, "Design And Analysis Of Multiple Antenna Structures For Ultrawide Bandwidth," *TRE*, vol. 80, no. 6, 2021, doi: 10.1615/TelecomRadEng.2021038819.

[81] A. K. Arya, S. J. Kim, and S. Kim, "A Dual-Band Antenna For LTE-R and 5G Lower Frequency Operations," *PIER Letters*, vol. 88, pp. 113–119, 2020, doi: 10.2528/PIERL19081502.

[82] J. Anguera, A. Andujar, G. Mestre, J. Rahola, and J. Juntunen, "Design of Multiband Antenna Systems for Wireless Devices Using Antenna Boosters [Application Notes]," *IEEE Microwave Magazine*, vol. 20, no. 12, pp. 102–114, Dec. 2019, doi: 10.1109/MMM.2019.2941662.

[83] O. Benkhadda *et al.*, "A miniaturized reconfigurable antenna for modern wireless applications with broadband and multi-band capabilities," *Progress In Electromagnetics Research M*, vol. 127, pp. 93–101, 2024, doi:10.2528/PIERM24042801

[84] J.-H. Lim, G.-T. Back, Y.-I. Ko, C.-W. Song, and T.-Y. Yun, "A Reconfigurable PIFA Using a Switchable PIN-Diode and a Fine-Tuning Varactor for USPCS/WCDMA/m-WiMAX/WLAN," *IEEE Transactions on Antennas and Propagation*, vol. 58, no. 7, pp. 2404–2411, Jul. 2010, doi: 10.1109/TAP.2010.2048849.

[85] C. W. Jung, Y. J. Kim, Y. E. Kim, and F. De Flaviis, "Macro-micro frequency tuning antenna for reconfigurable wireless communication systems," *Electronics Letters*, vol. 43, no. 4, pp. 201–202, Feb. 2007, doi: 10.1049/el:20073906.

[86] B. A. Cetiner, G. Roqueta Crusats, L. Jofre, and N. Biyikli, "RF MEMS Integrated Frequency Reconfigurable Annular Slot Antenna," *IEEE Transactions on Antennas and Propagation*, vol. 58, no. 3, pp. 626–632, Mar. 2010, doi: 10.1109/TAP.2009.2039300.

[87] Y. Tawk, A. R. Albrecht, S. Hemmady, G. Balakrishnan, and C. G. Christodoulou, "Optically Pumped Frequency Reconfigurable Antenna Design," *IEEE Antennas and Wireless Propagation Letters*, vol.9, pp. 280–283, 2010, doi:10.1109/LAWP.2010.2047373.

[88] L. Ge and K.-M. Luk, "Frequency-Reconfigurable Low-Profile Circular Monopolar Patch Antenna," *IEEE Transactions on Antennas and Propagation*, vol. 62, no. 7, pp. 3443–3449, Jul. 2014, doi: 10.1109/TAP.2014.2318077.

[89] C. Y. Rhee, J. H. Kim, W. J. Jung, T. Park, B. Lee, and C. W. Jung, "Frequency-Reconfigurable Antenna for Broadband Airborne Applications," *IEEE Antennas and Wireless Propagation Letters*, vol. 13, pp. 189–192, 2014, doi: 10.1109/LAWP.2014.2301036.

[90] S. Pendharker, R. K. Shevgaonkar, and A. N. Chandorkar, "Optically Controlled Frequency-Reconfigurable Microstrip Antenna With Low Photoconductivity," *IEEE Antennas and Wireless Propagation Letters*, vol. 13, pp. 99–102, 2014, doi: 10.1109/LAWP.2013.2296621.

[91] S. Danesh, S. K. A. Rahim, M. Abedian, and M. R. Hamid, "A Compact Frequency-Reconfigurable Dielectric Resonator Antenna for LTE/WWAN and WLAN Applications," *IEEE Antennas and Wireless Propagation Letters*, vol. 14, pp. 486–489, 2015, doi: 10.1109/LAWP.2014.2369411.

[92] T. Li, H. Zhai, X. Wang, L. Li, and C. Liang, "Frequency-Reconfigurable Bow-Tie Antenna for Bluetooth, WiMAX, and WLAN Applications," *IEEE Antennas and Wireless Propagation Letters*, vol. 14, pp. 171–174, 2015, doi: 10.1109/LAWP.2014.2359199.

[93] N. Nguyen-Trong, A. Piotrowski, and C. Fumeaux, "A Frequency-Reconfigurable Dual-Band Low-Profile Monopolar Antenna," *IEEE Transactions on Antennas and Propagation*, vol. 65, no. 7, pp. 3336–3343, Jul. 2017, doi: 10.1109/TAP.2017.2702664.

[94] I. H. Idris, M. R. Hamid, K. Kamardin, and M. K. A. Rahim, "A multi to wideband frequency reconfigurable antenna," *International Journal of RF and Microwave Computer-Aided Engineering*, vol. 28, no. 4, p. e21216, 2018, doi: 10.1002/mmce.21216.

[95] M. D. Wright, W. Baron, J. Miller, J. Tuss, D. Zeppettella, and M. Ali, "MEMS Reconfigurable Broadband Patch Antenna for Conformal Applications," *IEEE Transactions on Antennas and Propagation*, vol. 66, no. 6, pp. 2770–2778, Jun. 2018, doi: 10.1109/TAP.2018.2819818.

[96] Y. Tawk, A. El-Amine, S. Saab, J. Costantine, F. Ayoub, and C. G. Christodoulou, "A Software-Defined Frequency-Reconfigurable Meandered Printed Monopole," *IEEE Antennas and Wireless Propagation Letters*, vol. 17, no. 2, pp. 327–330, Feb. 2018, doi: 10.1109/LAWP.2017.2788461.

[97] I. A. Shah *et al.*, "Design and analysis of a hexa-band frequency reconfigurable antenna for wireless communication," *AEU - International Journal of Electronics and Communications*, vol. 98, pp. 80–88, Jan. 2019, doi: 10.1016/j.aeue.2018.10.012.

[98] S. Das, A. Gupta, and S. Sahu, "Metamaterial based fractal-ground loaded frequency-reconfigurable monopole-antenna with gain-bandwidth enhancement," *AEU - International Journal of Electronics and Communications*, vol. 132, p. 153593, Apr. 2021, doi: 10.1016/j.aeue.2020.153593.

[99] P. Rakesh Kumar, P. Sunitha, and M. V. S. Prasad, “Compact Reconfigurable Patch Antenna for Wirelesss Applications,” *PIER C*, vol. 138, pp. 161–174, 2023, doi: 10.2528/PIERC23090102.

[100] A.A. Ibrahim, H.A. Mohamed, M.A. Abdelghany and E. Tammam, “Flexible and frequency reconfigurable CPW-fed monopole antenna with frequency selective surface for IoT applications,” *Scientific Reports,* vol. 13, 8409, 2023, Doi: 10.1038/s41598-023-34917-y

[101] H.A. Majid, M.K.A. Rahim, M.R. Hamid and M.F. Ismail, “Frequency reconfigurable Microstrip Patch-Slot Antenna with Directional Radiation Pattern”, *PIER M*, vol. 144, pp. 319–328, 2014, doi: 10.2528/PIER13102901

[102] L.-H. Trinh, F. Ferrero, “Multiband Frequency Tuneable Antennas for Selection Combining Strategy in White Space Applications,” *Appl. Sci.*, vol. 12, no. 11062, 2022, doi: doi.org/10.3390/app122111062

[103] F. A. Asadallah, A. Eid, G. Shehadeh, J. Costantine, Y. Tawk and E. M. Tentzeris, “Digital Reconfiguration of a Single Arm 3-D Bowtie Antenna,” *IEEE Transactions on Antennas and Propagation*, vol. 69, no. 7, pp. 4188, 2021.

[104] J.Anguera, A. Andujar, J. L. Leiva, C. Schepens, R Gaddi, S. Kahng, “Multiband Antenna Operation with a Non-Resonant Element Using a Reconfigurable Matching Network, ” *in proceedings of 12th European Conference on Antennas and Propagation (EuCAP 2018),* 2018

[105] M. Boti, L. Dussopt and J. M. Laheurte, “Circularly polarized antenna with switchable polarization sense”, *Electronics Letters*, vol. 36, pp. 1518–1519, 2000, doi: 10.1049/el:20001098.

[106] T. Nakamura and T. Fukusako, “Broadband Design of Circularly Polarized Microstrip Patch Antenna Using Artificial Ground Structure With Rectangular Unit Cells,” *IEEE Transactions on Antennas and Propagation*, vol. 59, no. 6, pp. 2103–2110, Jun. 2011, doi: 10.1109/TAP.2011.2143656.

[107] A. Bhattacharjee, S. Dwari, and M. K. Mandal, “Polarization-Reconfigurable Compact Monopole Antenna With Wide Effective Bandwidth,” *IEEE Antennas and Wireless Propagation Letters*, vol. 18, no. 5, pp. 1041–1045, May 2019, doi: 10.1109/LAWP.2019.2908661.

[108] J. M. Kovitz, H. Rajagopalan, and Y. Rahmat-Samii, “Design and Implementation of Broadband MEMS RHCP/LHCP Reconfigurable Arrays Using Rotated E-Shaped Patch Elements,” *IEEE Transactions on Antennas and Propagation*, vol. 63, no. 6, pp. 2497–2507, Jun. 2015, doi: 10.1109/TAP.2015.2417892.

[109] Y. J. Sung, T. U. Jang, and Y.-S. Kim, “A reconfigurable microstrip antenna for switchable polarization,” *IEEE Microwave and Wireless Components Letters*, vol. 14, no. 11, pp. 534–536, Nov. 2004, doi: 10.1109/LMWC.2004.837061.

[110] C. Sulakshana and L. Anjaneyulu, “Reconfigurable antennas with frequency, polarization, and pattern diversities for multi-radio wireless applications”, *International Journal of Microwave and Wireless Technologies*, vol. 9, no. 1, pp. 121–132, 2017, doi: 10.1017/S1759078715000926.

[111] M. S. Nishamol, V. P. Sarin, D. Tony, C. K. Aanandan, P. Mohanan, and K. Vasudevan, “An Electronically Reconfigurable Microstrip Antenna With Switchable Slots for Polarization Diversity,” *IEEE Transactions on Antennas and Propagation*, vol. 59, no. 9, pp. 3424–3427, Sep. 2011, doi: 10.1109/TAP.2011.2161446.

[112] S.G. Zhou, G.L. Huang, H.Y. Liu, A.S. Lin and C.Y.D. Sim, “A CPW-Fed Square-Ring Slot Antenna With Reconfigurable Polarization”, *IEEE Access*, vol. 6, pp. 16473 – 16483, 2018. doi: 10.1109/ACCESS.2018.2815609.

[113] P.-Y. Qin, Y. J. Guo, and C. Ding, “A Dual-Band Polarization Reconfigurable Antenna for WLAN Systems,” *IEEE Transactions on Antennas and Propagation*, vol. 61, no. 11, pp. 5706–5713, Nov. 2013, doi: 10.1109/TAP.2013.2279219.

[114] B. Kim, B. Pan, S. Nikolaou, Y.-S. Kim, J. Papapolymerou, and M. M. Tentzeris, “A Novel Single-Feed Circular Microstrip Antenna With Reconfigurable Polarization Capability,” *IEEE Transactions on Antennas and Propagation*, vol. 56, no. 3, pp. 630–638, Mar. 2008, doi: 10.1109/TAP.2008.916894.

[115] A. Yadav and R.P. Yadav, “Quarter wavelength parasitic stub loaded polarization reconfigurable patch antenna”, *Electromagnetics*, vol. 41, pp. 459-467, 2021. doi: 10.1080/02726343.2021.2003026

[116] H. Aissat, L. Cirio, M. Grzeskowiak, J.-M. Laheurte, and O. Picon, “Reconfigurable circularly polarized antenna for short-range communication systems,” *IEEE Transactions on Microwave Theory and Techniques*, vol. 54, no. 6, pp. 2856–2863, Jun. 2006, doi: 10.1109/TMTT.2006.875454.

[117] J.-S. Row, W.-L. Liu, and T.-R. Chen, “Circular Polarization and Polarization Reconfigurable Designs for Annular Slot Antennas,” *IEEE Transactions on Antennas and Propagation*, vol. 60, no. 12, pp. 5998–6002, Dec. 2012, doi: 10.1109/TAP.2012.2211556.

[118] W. Lin and H. Wong, “Wideband Circular-Polarization Reconfigurable Antenna With L-Shaped Feeding Probes,” *IEEE Antennas and Wireless Propagation Letters*, vol. 16, pp. 2114–2117, 2017, doi: 10.1109/LAWP.2017.2699289.

[119] W. Yang, W. Che, H. Jin, W. Feng, and Q. Xue, “A Polarization-Reconfigurable Dipole Antenna Using Polarization Rotation AMC Structure,” *IEEE Transactions on Antennas and Propagation*, vol. 63, no. 12, pp. 5305–5315, Dec. 2015, doi: 10.1109/TAP.2015.2490250.

[120] S.-H. Chen, J.-S. Row, and K.-L. Wong, “Reconfigurable Square-Ring Patch Antenna With Pattern Diversity,” *IEEE Transactions on Antennas and Propagation*, vol. 55, no. 2, pp. 472–475, Feb. 2007, doi: 10.1109/TAP.2006.889950.

[121] G. Jin, M. Li, D. Liu, and G. Zeng, “A Simple Four-Beam Reconfigurable Antenna Based on Monopole,” *IEEE Access*, vol. 6, pp. 30309–30316, 2018, doi: 10.1109/ACCESS.2018.2845552.

[122] M. Kaur, H. Shankar Singh, and M. Agarwal, “A compact two-state pattern reconfigurable antenna for 5G Sub-6 GHz cellular applications,” *AEU - International Journal of Electronics and Communications*, vol. 162, p. 154577, Apr. 2023, doi: 10.1016/j.aeue.2023.154577.

[123] S.-L. Chen, P.-Y. Qin, W. Lin, and Y. J. Guo, “Pattern-Reconfigurable Antenna With Five Switchable Beams in Elevation Plane,” *IEEE Antennas and Wireless Propagation Letters*, vol. 17, no. 3, pp. 454–457, Mar. 2018, doi: 10.1109/LAWP.2018.2794990.

[124] W. Kang, S. Lee, and K. Kim, “Design of symmetric beam pattern reconfigurable antenna,” *Electronics Letters*, vol. 46, no. 23, pp. 1536–1537, Nov. 2010, doi: 10.1049/el.2010.2527.

[125] G.-M. Zhang, J.-S. Hong, G. Song, and B.-Z. Wang, “Design and analysis of a compact wideband pattern-reconfigurable antenna with alternate reflector and radiator,” *IET Microwaves, Antennas & Propagation*, vol. 6, no. 15, pp. 1629–1635, Dec. 2012, doi: 10.1049/iet-map.2012.0005.

[126] P.-Y. Qin, Y. J. Guo, A. R. Weily, and C.-H. Liang, “A Pattern Reconfigurable U-Slot Antenna and Its Applications in MIMO Systems,” *IEEE Transactions on Antennas and Propagation*, vol. 60, no. 2, pp. 516–528, Feb. 2012, doi: 10.1109/TAP.2011.2173439.

[127] S. Yong, S. and J.T. Bernhard, “A Pattern Reconfigurable Null Scanning Antenna”, *IEEE Transactions on Antennas and Propagation,* vol. 60, no. 10, pp. 4538 – 4544, 2012, doi: 10.1109/TAP.2012.2207336.

[128] J. Ren, X. Yang, J. Yin, and Y. Yin, “A Novel Antenna with Reconfigurable Patterns Using H-Shaped Structures,” *IEEE Antennas and Wireless Propagation Letters*, vol. 14, pp. 915–918, Dec. 2015, doi: 10.1109/LAWP.2014.2387292.

[129] M. Jusoh, T. Sabapathy, M. F. Jamlos, and M. R. Kamarudin, “Reconfigurable Four-Parasitic-Elements Patch Antenna for High-Gain Beam Switching Application,” *IEEE Antennas and Wireless Propagation Letters*, vol. 13, pp. 79–82, 2014, doi: 10.1109/LAWP.2013.2296491

[130] S. Xiao, C. Zheng, M. Li, J. Xiong, and B.-Z. Wang, “Varactor-Loaded Pattern Reconfigurable Array for Wide-Angle Scanning With Low Gain Fluctuation,” *IEEE Transactions on Antennas and Propagation*, vol. 63, no. 5, pp. 2364–2369, May 2015, doi: 10.1109/TAP.2015.2410311.

[131] M. S. Alam and A. M. Abbosh, “Wideband Pattern-Reconfigurable Antenna Using Pair of Radial Radiators on Truncated Ground With Switchable Director and Reflector,” *IEEE Antennas and Wireless Propagation Letters*, vol. 16, pp. 24–28, 2017, doi: 10.1109/LAWP.2016.2552492.

[132] X. Yang, H. Lin, H. Gu, L. Ge, and X. Zeng, “Broadband Pattern Diversity Patch Antenna With Switchable Feeding Network,” *IEEE Access*, vol. 6, pp. 69612–69619, 2018, doi: 10.1109/ACCESS.2018.2877426.

[133] T. Korošec, P. Ritoša, and M. Vidmar, “Varactor-tuned microstrip-patch antenna with frequency and polarisation agility,” *Electronics Letters*, vol. 42, no. 18, pp. 1015–1017, Aug. 2006, doi: 10.1049/el:20061699.

[134] C.-H. Hu, T.-R. Chen, J.-F. Wu, and J.-S. Row, “Reconfigurable microstrip antenna with polarisation diversity and frequency agility,” *Electronics Letters*, vol. 43, no. 24, pp. 1329–1330, Nov. 2007, doi: 10.1049/el:20071614.

[135] N. Nguyen-Trong, L. Hall, and C. Fumeaux, “A Frequency- and Polarization-Reconfigurable Stub-Loaded Microstrip Patch Antenna,” *IEEE Transactions on Antennas and Propagation*, vol. 63, no. 11, pp. 5235–5240, Nov. 2015, doi: 10.1109/TAP.2015.2477846.

[136] P.-Y. Qin, Y. J. Guo, Y. Cai, E. Dutkiewicz, and C.-H. Liang, “A Reconfigurable Antenna With Frequency and Polarization Agility,” *IEEE Antennas and Wireless Propagation Letters*, vol. 10, pp. 1373–1376, 2011, doi: 10.1109/LAWP.2011.2178226.

[137] J. Hu and Z.-C. Hao, “Design of a Frequency and Polarization Reconfigurable Patch Antenna With a Stable Gain,” *IEEE Access*, vol. 6, pp. 68169–68175, 2018, doi: 10.1109/ACCESS.2018.2879498.

[138] J.-S. Row and C.-J. Shih, “Polarization-Diversity Ring Slot Antenna With Frequency Agility,” *IEEE Transactions on Antennas and Propagation*, vol. 60, no. 8, pp. 3953–3957, Aug. 2012, doi: 10.1109/TAP.2012.2201114.

[139] B. Babakhani and S. Sharma, “Wideband Frequency Tunable Concentric Circular Microstrip Patch Antenna with Simultaneous Polarization Reconfiguration,” *IEEE Antennas and Propagation Magazine*, vol. 57, no. 2, pp. 203–216, Apr. 2015, doi: 10.1109/MAP.2015.2414666.

[140] C. Ni, M. S. Chen, Z. X. Zhang, and X. L. Wu, “Design of Frequency-and Polarization-Reconfigurable Antenna Based on the Polarization Conversion Metasurface,” *IEEE Antennas and Wireless Propagation Letters*, vol. 17, no. 1, pp. 78–81, Jan. 2018, doi: 10.1109/LAWP.2017.2775444.

[141] M. Wang, M. R. Khan, M. D. Dickey, and J. J. Adams, “A Compound Frequency- and Polarization- Reconfigurable Crossed Dipole Using Multidirectional Spreading of Liquid Metal,” *IEEE Antennas and Wireless Propagation Letters*, vol. 16, pp. 79–82, 2017, doi: 10.1109/LAWP.2016.2556983.

[142] Y. Liu, Q. Wang, Y. Jia, and P. Zhu, “A Frequency- and Polarization-Reconfigurable Slot Antenna Using Liquid Metal,” *IEEE Transactions on Antennas and Propagation*, vol. 68, no. 11, pp. 7630–7635, Nov. 2020, doi: 10.1109/TAP.2020.2993110.

[143] J. Yang, J. Li, S. Zhou, D. Li, and G. Yang, “A Polarization and Frequency Reconfigurable Microstrip Antenna for Vehicular Communication System Application,” *IEEE Transactions on Vehicular Technology*, vol. 72, no. 1, pp. 623–631, Jan. 2023, doi: 10.1109/TVT.2022.3202973.

[144] V. Lavanya, C. Rimmya, R.K. Rabin Kanisha and M. Ganesh Madhan, “A novel miniaturized metamaterial inspired frequency reconfigurable antenna with

switchable polarization for sub 6 GHz band," *Phys. Scr.*, vol. 99, no. 12, p. 125501, Oct. 2024, doi: 10.1088/1402-4896/ad8992.

[145] G. H. Huff, J. Feng, S. Zhang, and J. T. Bernhard, "A novel radiation pattern and frequency reconfigurable single turn square spiral microstrip antenna," *IEEE Microwave and Wireless Components Letters*, vol. 13, no. 2, pp. 57–59, Feb. 2003, doi: 10.1109/LMWC.2003.808714.

[146] S. Nikolaou *et al.*, "Pattern and frequency reconfigurable annular slot antenna using PIN diodes," *IEEE Transactions on Antennas and Propagation*, vol. 54, no. 2, pp. 439–448, Feb. 2006, doi: 10.1109/TAP.2005.863398.

[147] T. Guo, W. Leng, A. Wang, J. Li, and Q. Zhang, "A Novel Planar Parasitic Array Antenna With Frequency- and Pattern-Reconfigurable Characteristics," *IEEE Antennas and Wireless Propagation Letters*, vol. 13, pp. 1569–1572, 2014, doi: 10.1109/LAWP.2014.2345776.

[148] H. A. Majid, M. K. A. Rahim, M. R. Hamid, and M. F. Ismail, "Frequency and Pattern Reconfigurable Slot Antenna," *IEEE Transactions on Antennas and Propagation*, vol. 62, no. 10, pp. 5339–5343, Oct. 2014, doi: 10.1109/TAP.2014.2342237.

[149] N. Nguyen-Trong, L. Hall, and C. Fumeaux, "A Frequency- and Pattern-Reconfigurable Center-Shorted Microstrip Antenna," *IEEE Antennas and Wireless Propagation Letters*, vol. 15, pp. 1955–1958, 2016, doi: 10.1109/LAWP.2016.2544943.

[150] S. N. M. Zainarry, N. Nguyen-Trong, and C. Fumeaux, "A Frequency- and Pattern-Reconfigurable Two-Element Array Antenna," *IEEE Antennas and Wireless Propagation Letters*, vol. 17, no. 4, pp. 617–620, Apr. 2018, doi: 10.1109/LAWP.2018.2806355.

[151] S. K. Patel, C. Argyropoulos, and Y. P. Kosta, "Pattern controlled and frequency tunable microstrip antenna loaded with multiple split ring resonators," *IET Microwaves, Antennas & Propagation*, vol. 12, no. 3, pp. 390–394, 2018, doi: 10.1049/iet-map.2017.0319.

[152] Z. Zhu, P. Wang, S. You, and P. Gao, "A Flexible Frequency And Pattern Reconfigurable Antenna For Wireless Systems," *PIER Letters*, vol. 76, pp. 63–70, 2018, doi: 10.2528/PIERL18040401.

[153] G. Singh, B. K. Kanaujia, V. K. Pandey, D. Gangwar, and S. Kumar, "Pattern and frequency reconfigurable antenna with diode loaded ELC resonator," *International Journal of Microwave and Wireless Technologies*, vol. 12, no. 2, pp. 163–175, Mar. 2020, doi: 10.1017/S1759078719001077.

[154] A. A. Palsokar and S. L. Lahudkar, “Frequency and pattern reconfigurable rectangular patch antenna using single PIN diode,” *AEU - International Journal of Electronics and Communications*, vol. 125, p. 153370, Oct. 2020, doi: 10.1016/j.aeue.2020.153370.

[155] Y. Zhang, S. Lin, Z. Yang, B. Li, J. Cui, and J. Jiao, “A pattern- and frequency-reconfigurable antenna using liquid metal,” *Microwave and Optical Technology Letters*, vol. 63, no. 5, pp. 1499–1506, 2021, doi: 10.1002/mop.32767.

[156] J.-F. Li, B. Wu, J.-Q. Zhou, K.-X. Guo, H.-R. Zu, and T. Su, “Frequency and Pattern Reconfigurable Antenna Using Double Layer Petal Shaped Parasitic Structure,” *IEEE Transactions on Circuits and Systems II: Express Briefs*, vol. 71, no. 4, pp. 1934–1938, Apr. 2024, doi: 10.1109/TCSII.2023.3329659.

[157] M. Ganesh, N. S. Raghava, T. Sabapathy, and Y. Sharma, “A Gain-Enhanced Multiband Frequency and Pattern Reconfigurable Antenna for Wi-Fi 6E and 5G New Radio Wireless Standards,” *International Journal of Communication Systems*, vol. 38, no. 4, p. e6011, 2025, doi: 10.1002/dac.6011.

[158] V. Suryapaga and V. V. Khairnar, “Review on Multifunctional Pattern and Polarization Reconfigurable Antennas,” *IEEE Access*, vol. 12, pp. 90218–90251, 2024, doi: 10.1109/ACCESS.2024.3420426.

[159] W.-L. Liu, T.-R. Chen, S.-H. Chen, and J.-S. Row, “Reconfigurable microstrip antenna with pattern and polarisation diversities,” *Electronics Letters*, vol. 43, no. 2, pp. 77–78, Jan. 2007, doi: 10.1049/el:20073373.

[160] W. Cao, B. Zhang, A. Liu, T. Yu, D. Guo, and K. Pan, “A Reconfigurable Microstrip Antenna With Radiation Pattern Selectivity and Polarization Diversity,” *IEEE Antennas and Wireless Propagation Letters*, vol. 11, pp. 453–456, 2012, doi: 10.1109/LAWP.2012.2193549.

[161] S. Raman, P. Mohanan, N. Timmons, and J. Morrison, “Microstrip-Fed Pattern- and Polarization- Reconfigurable Compact Truncated Monopole Antenna,” *IEEE Antennas and Wireless Propagation Letters*, vol. 12, pp. 710–713, 2013, doi: 10.1109/LAWP.2013.2263983.

[162] C. Gu *et al.*, “Compact Smart Antenna With Electronic Beam-Switching and Reconfigurable Polarizations,” *IEEE Transactions on Antennas and Propagation*, vol. 63, no. 12, pp. 5325–5333, Dec. 2015, doi: 10.1109/TAP.2015.2490239.

[163] M. Shaw and Y. K. Choukiker, “Reconfigurable polarization and pattern microstrip antenna for IRNSS band applications,” *AEU - International Journal of Electronics and Communications*, vol. 160, p. 154501, Feb. 2023, doi: 10.1016/j.aeue.2022.154501.

[164] D. Rodrigo, B. A. Cetiner, and L. Jofre, “Frequency, Radiation Pattern and Polarization Reconfigurable Antenna Using a Parasitic Pixel Layer,” *IEEE Transactions on Antennas and Propagation*, vol. 62, no. 6, pp. 3422–3427, Jun. 2014, doi: 10.1109/TAP.2014.2314464.

[165] L. Ge, Y. Li, J. Wang, and C.-Y.-D. Sim, “A Low-Profile Reconfigurable Cavity-Backed Slot Antenna With Frequency, Polarization, and Radiation Pattern Agility,” *IEEE Transactions on Antennas and Propagation*, vol. 65, no. 5, pp. 2182–2189, May 2017, doi: 10.1109/TAP.2017.2681432.

[166] H. Zhai, Z. Ma, Y. Han, and C. Liang, “A Compact Printed Antenna for Triple-Band WLAN/WiMAX Applications,” *IEEE Antennas and Wireless Propagation Letters*, vol. 12, pp. 65–68, 2013, doi: 10.1109/LAWP.2013.2238881.

[167] X. Q. Zhang, Y. C. Jiao, and W. H. Wang, “Compact wide tri-band slot antenna for WLAN/WiMAX applications,” *Electronics Letters*, vol. 48, no. 2, pp. 64–65, Jan. 2012, doi: 10.1049/el.2011.3376.

[168] N. Hassan *et al.*, “Design of dual-band microstrip patch antenna with right-angle triangular aperture slot for energy transfer application,” *International Journal of RF and Microwave Computer-Aided Engineering*, vol. 29, no. 1, p. e21666, 2019, doi: 10.1002/mmce.21666.

[169] A. Yadav, S. Agrawal, and R. P. Yadav, “SRR and S-shape slot loaded triple band notched UWB antenna,” *AEU - International Journal of Electronics and Communications*, vol. 79, pp. 192–198, Sep. 2017, doi: 10.1016/j.aeue.2017.06.003.

[170] T. Ali, M. S. Aw, R. C. Biradar, A. Andújar, and J. Anguera, “A miniaturized slotted ground structure UWB antenna for multiband applications,” *Microwave and Optical Technology Letters*, vol. 60, no. 8, pp. 2060–2068, 2018, doi: 10.1002/mop.31298.

[171] S. Painam, V. S. Anumala, and M. Gatram, “Triple-Band Antenna for IoT and 5G Applications using Metasurfaces and Polygon Slot,” in *2021 IEEE Indian Conference on Antennas and Propagation (InCAP)*, Dec. 2021, pp. 416–419. doi: 10.1109/InCAP52216.2021.9726409.

[172] S. Mathew, M. Ameen, M. p. Jayakrishnan, P. Mohanan, and K. Vasudevan, “Compact dual polarised V slit, stub and slot embedded circular patch antenna for UMTS/WiMAX/WLAN applications,” *Electronics Letters*, vol. 52, no. 17, pp. 1425–1426, 2016, doi: 10.1049/el.2016.1996.

[173] A. Kunwar, A. K. Gautam, B. K. Kanaujia, and K. Rambabu, “Circularly polarized D-shaped slot antenna for wireless applications,” *International Journal of RF and Microwave Computer-Aided Engineering*, vol. 29, no. 1, p. e21498, 2019, doi: 10.1002/mmce.21498.

[174] A. K. Gautam, L. Kumar, B. K. Kanaujia, and K. Rambabu, “Design of Compact F-Shaped Slot Triple-Band Antenna for WLAN/WiMAX Applications,” *IEEE Transactions on Antennas and Propagation*, vol. 64, no. 3, pp. 1101–1105, Mar. 2016, doi: 10.1109/TAP.2015.2513099.

[175] F. Liu, K. Xu, P. Zhao, L. Dong, and G. Wang, “Uniplanar dual-band printed compound loop antenna for WLAN/WiMAX applications,” *Electronics Letters*, vol. 53, no. 16, pp. 1083–1084, 2017, doi: 10.1049/el.2017.1543.

[176] P. Singh and R. Aggarwal, "Design of ultra wideband antenna with triple band notch for minimum EMI," *Microwave and Optical Technology Letters*, vol. 58, no. 7, pp. 1521–1525, 2016, doi: 10.1002/mop.29851.

[177] S. Saxena, B. K. Kanaujia, S. Dwari, S. Kumar, and R. Tiwari, "A compact microstrip fed dual polarised multiband antenna for IEEE 802.11 a/b/g/n/ac/ax applications," *AEU - International Journal of Electronics and Communications*, vol. 72, pp. 95–103, Feb. 2017, doi: 10.1016/j.aeue.2016.11.024.

[178] A. Kumar, J. K. Deegwal, and M. M. Sharma, "Design of multi-polarised quad-band planar antenna with parasitic multistubs for multiband wireless communication," *IET Microwaves, Antennas & Propagation*, vol. 12, no. 5, pp. 718–726, 2018, doi: 10.1049/iet-map.2017.0526.

[179] S. Mathew, R. Anitha, U. Deepak, C. K. Aanandan, P. Mohanan, and K. Vasudevan, "A Compact Tri-Band Dual-Polarized Corner-Truncated Sectoral Patch Antenna," *IEEE Transactions on Antennas and Propagation*, vol. 63, no. 12, pp. 5842–5845, Dec. 2015, doi: 10.1109/TAP.2015.2479216.

[180] T. Wu, X.-W. Shi, P. Li, and H. Bai, "Tri-band microstrip-fed monopole antenna with dual-polarisation characteristics for WLAN and WiMAX applications," *Electronics Letters*, vol. 49, no. 25, pp. 1597–1598, 2013, doi: 10.1049/el.2013.3230.

[181] Q.-Y. Zhang and Q.-X. Chu, "Triple-band dual rectangular ring printed monopole antenna for WLAN/WiMAX applications," *Microwave and Optical Technology Letters*, vol. 51, no. 12, pp. 2845–2848, 2009, doi: 10.1002/mop.24773.

[182] B. Li, Z.-H. Yan, and T.-L. Zhang, "Triple-Band Slot Antenna With U-Shaped Open Stub Fed By Asymmetric Coplanar Strip For WLAN/WiMAX Applications," *PIER Letters*, vol. 37, pp. 123–131, 2013, doi: 10.2528/PIERL12122601.

[183] J. Li, J. Guo, B. He, A. Zhang, and Q. H. Liu, "Tri-Band CPW-Fed Stub-Loaded Slot Antenna Design for WLAN/WiMAX Applications," *Frequenz*, vol. 70, no. 11–12, pp. 521–526, Nov. 2016, doi: 10.1515/freq-2015-0261.

[184] Y. Xu, Y.-C. Jiao, and Y.-C. Luan, "Compact CPW-fed printed monopole antenna with triple-band characteristics for WLAN/WiMAX applications," *Electronics Letters*, vol. 48, no. 24, pp. 1519–1520, Nov. 2012, doi: 10.1049/el.2012.3255.

[185] H. Li, Q. Zheng, J. Ding, and C. Guo, "Dual-band planar antenna loaded with CRLH unit cell for WLAN/WiMAX application," *IET Microwaves, Antennas & Propagation*, vol. 12, no. 1, pp. 132–136, 2018, doi: 10.1049/iet-map.2016.1133.

[186] J. H. Yoon and Y. C. Lee, "Modified bow-tie slot antenna for the 2.4/5.2/5.8 GHz WLAN bands with a rectangular tuning stub," *Microwave and Optical Technology Letters*, vol. 53, no. 1, pp. 126–130, 2011, doi: 10.1002/mop.25647.

[187] B. R. R and S. K. Pandey, "Printed CPW-fed dual-band antenna using square closed-ring and square split-ring resonator," *Appl. Phys. A*, vol. 126, no. 8, p. 626, Jul. 2020, doi: 10.1007/s00339-020-03791-0.

[188] A. Sharma, P. Ranjan, and R. k. Gangwar, “Multiband cylindrical dielectric resonator antenna for WLAN/WiMAX application,” *Electronics Letters*, vol. 53, no. 3, pp. 132–134, 2017, doi: 10.1049/el.2016.3548.

[189] R. S. Daniel, R. Pandeeswari, and S. Raghavan, “Dual-band monopole antenna loaded with ELC metamaterial resonator for WiMAX and WLAN applications,” *Appl. Phys. A*, vol. 124, no. 8, p. 570, Jul. 2018, doi: 10.1007/s00339-018-1985-7.

[190] B. Murugeshwari, R.S. Daniel and S. Raghavan “A compact dual band antenna based on metamaterial-inspired split ring structure and hexagonal complementary split-ring resonator for ISM /WiMAX/ WLAN applications”, *Applied Physics A 125*, 628, 2019, doi: 10.1007/s00339-019-2925-x

[191] A. Sedghara and Z. Atlasbaf, “A novel single-feed reconfigurable antenna for polarization and frequency diversity,” *International Journal of Microwave and Wireless Technologies*, vol. 9, no. 5, pp. 1155–1161, Jun. 2017, doi: 10.1017/S1759078716001240.

[192] M. G. N. Alsath and M. Kanagasabai, “Compact UWB Monopole Antenna for Automotive Communications,” *IEEE Transactions on Antennas and Propagation*, vol. 63, no. 9, pp. 4204–4208, Sep. 2015, doi: 10.1109/TAP.2015.2447006.

[193] H.-W. Liu, C.-H. Ku, T.-S. Wang, and C.-F. Yang, “Compact Monopole Antenna With Band-Notched Characteristic for UWB Applications,” *IEEE Antennas and Wireless Propagation Letters*, vol. 9, pp. 397–400, 2010, doi: 10.1109/LAWP.2010.2049633.

[194] K. G. Thomas and M. Sreenivasan, “A Simple Ultrawideband Planar Rectangular Printed Antenna With Band Dispensation,” *IEEE Transactions on Antennas and Propagation*, vol. 58, no. 1, pp. 27–34, Jan. 2010, doi: 10.1109/TAP.2009.2036279.

[195] G. Kumar and K. P. Ray, *Broadband Microstrip Antennas*. Artech House, 2003.

[196] L. H. Weng, Y.-C. Guo, X.-W. Shi, and X.-Q. Chen, “An Overview On Defected Ground Structure,” *PIER B*, vol. 7, pp. 173–189, 2008, doi: 10.2528/PIERB08031401.

[197] M.K. Khandelwal, B.K. Kanaujia and S. Kumar, “Defected Ground Structure: Fundamentals, Analysis, and Applications in Modern Wireless Trends”, *International Journal of Antennas and Propagation, v*olume 2017, Article ID 2018527, 2017, doi: 10.1155/2017/2018527.

[198] T. Jhajharia, V. Tiwari, and D. Bhatnagar, “Polarisation reconfigurable dual-band circularly polarised patch antenna with defected ground plane for C-band wireless applications,” *IET Microwaves, Antennas & Propagation*, vol. 13, no. 14, pp. 2551–2558, 2019, doi: 10.1049/iet-map.2018.6214.

[199] A. H. Shah and V. Thangasamy, “Wideband and Reduced Size Micro-Strip on-Body Antenna for Wimax and Long Term Evolution (LTE)”, Accessed: Mar. 08, 2025. [Online]. Available: https://www.academia.edu/download/34757332/164.pdf

[200] H. A. Majid, M. K. Abdul Rahim, M. R. Hamid, N. A. Murad, and M. F. Ismail, "Frequency-Reconfigurable Microstrip Patch-Slot Antenna," *IEEE Antennas and Wireless Propagation Letters*, vol. 12, pp. 218–220, 2013, doi: 10.1109/LAWP.2013.2245293.

[201] M. Kelley, C. Koo, H. McQuilken, B. Lawrence, S. Li, A. Han and G. Huff, " Frequency reconfigurable patch antenna using liquid metal as switching mechanism", *Electron. Lett*., vol. 49, no. 22, pp. 1370–1371, 2013, doi: 10.1049/el.2013.2930.

[202] J.-S. Row and T.-Y. Lin, "Frequency-Reconfigurable Coplanar Patch Antenna With Conical Radiation," *IEEE Antennas and Wireless Propagation Letters*, vol. 9, pp. 1088–1091, 2010, doi: 10.1109/LAWP.2010.2093118.

[203] S.-L. S. Yang, A. A. Kishk, and K.-F. Lee, "Frequency Reconfigurable U-Slot Microstrip Patch Antenna," *IEEE Antennas and Wireless Propagation Letters*, vol. 7, pp. 127–129, 2008, doi: 10.1109/LAWP.2008.921330.

[204] S.-H. Chen, J.-S. Row, and K.-L. Wong, "Reconfigurable Square-Ring Patch Antenna With Pattern Diversity," *IEEE Transactions on Antennas and Propagation*, vol. 55, no. 2, pp. 472–475, Feb. 2007, doi: 10.1109/TAP.2006.889950.

[205] W. S. Kang, J. A. Park, and Y. J. Yoon, "Simple reconfigurable antenna with radiation pattern," *Electronics Letters*, vol. 44, no. 3, pp. 182–183, Jan. 2008, doi: 10.1049/el:20082994.

[206] S. Zhang, G. H. Huff, J. Feng, and J. T. Bernhard, "A pattern reconfigurable microstrip parasitic array," *IEEE Transactions on Antennas and Propagation*, vol. 52, no. 10, pp. 2773–2776, Oct. 2004, doi: 10.1109/TAP.2004.834372.

[207] X.-X. Yang, B.-C. Shao, F. Yang, A. Z. Elsherbeni, and B. Gong, "A Polarization Reconfigurable Patch Antenna With Loop Slots on the Ground Plane," *IEEE Antennas and Wireless Propagation Letters*, vol. 11, pp. 69–72, 2012, doi: 10.1109/LAWP.2011.2182595.

[208] H.L. Zhu, S.W. Cheung, X.H. Liu and T.I. Yuk, "Design of polarization reconfigurable antenna using metasurface", *IEEE Trans. Antennas Propag*., vol. 62, no. 6, pp. 2891–2898, 2014, doi: 10.1109/TAP.2014.2310209

[209] B. Rohrdantz, C. Luong, and A. F. Jacob, "A frequency and polarization reconfigurable patch antenna at K-band," in *2014 44th European Microwave Conference*, Oct. 2014, pp. 49–52. doi: 10.1109/EuMC.2014.6986366.

[210] N. Nguyen-Trong, A. Piotrowski, L. Hall, and C. Fumeaux, "A Frequency- and Polarization-Reconfigurable Circular Cavity Antenna," *IEEE Antennas and Wireless Propagation Letters*, vol. 16, pp. 999–1002, 2017, doi: 10.1109/LAWP.2016.2616128.

[211] B. Anantha, L. Merugu, and P. V. D. Somasekhar Rao, "A novel single feed frequency and polarization reconfigurable microstrip patch antenna," *AEU - International Journal of Electronics and Communications*, vol. 72, pp. 8–16, Feb. 2017, doi: 10.1016/j.aeue.2016.11.012.

[212] U. George and F. Lili, "A simple frequency and polarization reconfigurable antenna," *Electromagnetics*, vol. 40, no. 6, pp. 435–444, Aug. 2020, doi: 10.1080/02726343.2020.1811940.

[213] J. Liu, J. Li, and R. Xu, "Design of very simple frequency and polarisation reconfigurable antenna with finite ground structure," *Electronics Letters*, vol. 54, no. 4, pp. 187–188, 2018, doi: 10.1049/el.2017.4364.

[214] B. Liang, B. Sanz-Izquierdo, E. A. Parker, and J. C. Batchelor, "A Frequency and Polarization Reconfigurable Circularly Polarized Antenna Using Active EBG Structure for Satellite Navigation," *IEEE Transactions on Antennas and Propagation*, vol. 63, no. 1, pp. 33–40, Jan. 2015, doi: 10.1109/TAP.2014.2367537.

[215] S. K. Muthuvel and Y. K. Choukiker, "Wideband Frequency Agile and Polarization Reconfigurable Antenna for Wireless Applications," *IETE Journal of Research*, vol. 69, no. 3, pp. 1529–1538, Apr. 2023, doi: 10.1080/03772063.2020.1871421.

[216] D. V. Niture, P. A. Govind, and S. P. Mahajan, "Frequency and polarisation reconfigurable square ring antenna for wireless application," in *2016 IEEE Region 10 Conference (TENCON)*, Nov. 2016, pp. 1302–1306. doi: 10.1109/TENCON.2016.7848223.

[217] S. Rawat and K. K. Sharma, "Annular ring microstrip patch antenna with finite ground plane for ultra-wideband applications," *International Journal of Microwave and Wireless Technologies*, vol. 7, no. 2, pp. 179–184, Apr. 2015, doi: 10.1017/S1759078714000592.

[218] S. I. Latif and L. Shafai, "Polarization Characteristics of Multiband Loaded Microstrip Annular Ring Antennas," *IEEE Transactions on Antennas and Propagation*, vol. 57, no. 9, pp. 2788–2793, Sep. 2009, doi: 10.1109/TAP.2009.2027354.

[219] K. Jhamb, L. Li, and K. Rambabu, "Frequency adjustable microstrip annular ring patch antenna with multi-band characteristics," *IET Microwaves, Antennas & Propagation*, vol. 5, no. 12, pp. 1471–1478, Sep. 2011, doi: 10.1049/iet-map.2010.0571.

[220] M. M. Sharma, A. Kumar, S. Yadav, and Y. Ranga, "An Ultra-wideband Printed Monopole Antenna with Dual Band-Notched Characteristics Using DGS and SRR," *Procedia Technology*, vol. 6, pp. 778–783, Jan. 2012, doi: 10.1016/j.protcy.2012.10.094.

[221] R. Agrawal, B. Kalra, S. Shrimal, M. M. Sharma, and Jaiverdhan, "Defective ground structure loaded polarization reconfigurable ring-shaped patch antenna for multiband applications," *Electromagnetics*, vol. 45, no. 3, pp. 241–256, Apr. 2025, doi: 10.1080/02726343.2025.2456199.

[222] T. Jhajharia, V. Tiwari, D. Yadav, S. Rawat, and D. Bhatnagar, "Wideband circularly polarised antenna with an asymmetric meandered-shaped monopole and defected ground structure for wireless communication," *IET Microwaves, Antennas & Propagation*, vol. 12, no. 9, pp. 1554–1558, 2018, doi: 10.1049/iet-map.2018.0092.

[223] M. S. Ellis, Z. Zhao, J. Wu, X. Ding, Z. Nie, and Q.-H. Liu, "A Novel Simple and Compact Microstrip-Fed Circularly Polarized Wide Slot Antenna With Wide Axial Ratio Bandwidth for C-Band Applications," *IEEE Transactions on Antennas and Propagation*, vol. 64, no. 4, pp. 1552–1555, Apr. 2016, doi: 10.1109/TAP.2016.2526076.

[224] J. T. Bernhard, "Reconfigurable antennas and apertures: state of the art and future outlook," in *Smart Structures and Materials 2003: Smart Electronics, MEMS, BioMEMS, and Nanotechnology*, SPIE, Jul. 2003, pp. 1–9. doi: 10.1117/12.497433.

[225] D. Yadav, M. P. Abegaonkar, S. K. Koul, V. N. Tiwari, and D. Bhatnagar, "A Novel Frequency Reconfigurable Monopole Antenna With Switchable Characteristics Between Band-Notched Uwb And Wlan Applications," *PIER C*, vol. 77, pp. 145–153, 2017, doi: 10.2528/PIERC17062203.

[226] Data sheet Available at https://www.alphalnd.com/datasheets/Planar and mesa PIN diodes (DSG6405-000, DSG6474-000, DSM63000 series).pdf

[227] M. Zhang, G. Xu and R. Gao, "Reconfigurable Antennas for Wireless Communication: Design Mechanism, State of the Art, Challenges, and Future Perspectives," *International Journal of Antennas and Propagation*, 3046393, 2024, doi: 10.1155/2024/3046393

[228] P. K. Li, Z. H. Shao, Q. Wang, and Y. J. Cheng, "Frequency- and Pattern-Reconfigurable Antenna for Multistandard Wireless Applications," *IEEE Antennas and Wireless Propagation Letters*, vol. 14, pp. 333–336, 2015, doi: 10.1109/LAWP.2014.2359196.

[229] L. Han, C. Wang, W. Zhang, R. Ma, and Q. Zeng, "Design of Frequency- and Pattern-Reconfigurable Wideband Slot Antenna," *International Journal of Antennas and Propagation*, vol. 2018, no. 1, p. 3678018, 2018, doi: 10.1155/2018/3678018.

[230] Y. P. Selvam *et al.*, "A Low-Profile Frequency- and Pattern-Reconfigurable Antenna," *IEEE Antennas and Wireless Propagation Letters*, vol. 16, pp. 3047–3050, 2017, doi: 10.1109/LAWP.2017.2759960.

[231] S. Koley, L. Murmu, and B. Pal, "A Pattern Reconfigurable Antenna For Wlan And Wimax Systems," *PIER C*, vol. 66, pp. 183–190, 2016, doi: 10.2528/PIERC16052306.